



**UNIVERSIDAD NACIONAL AUTÓNOMA DE MÉXICO**  
**DOCTORADO EN CIENCIAS BIOMÉDICAS**  
**INSTITUTO DE QUÍMICA**

“Selección y caracterización bioquímica de péptidos derivados de la hidrólisis enzimática de las globulinas de amaranto (*Amaranthus hypochondriacus*) y su evaluación antiviral contra el *Virus del enrollamiento de la hoja amarilla del tomate (TYLCV)*”

**TESIS**

QUE PARA OPTAR POR EL GRADO DE:  
**DOCTOR EN CIENCIAS**

Presenta:

**JOSÉ SILVESTRE MENDOZA FIGUEROA**

Director de tesis:

**Dr. MANUEL SORIANO GARCÍA**

Instituto de Química, UNAM

Comité tutor:

**Dr. ABEL MORENO CÁRCAMO**

Instituto de Química, UNAM

**Dr. CARLOS KUBLI GARFIAS**

Instituto de Investigaciones Biomédicas, UNAM

Ciudad de México, noviembre de 2018



Universidad Nacional  
Autónoma de México

Dirección General de Bibliotecas de la UNAM

**Biblioteca Central**



**UNAM – Dirección General de Bibliotecas**  
**Tesis Digitales**  
**Restricciones de uso**

**DERECHOS RESERVADOS ©**  
**PROHIBIDA SU REPRODUCCIÓN TOTAL O PARCIAL**

Todo el material contenido en esta tesis esta protegido por la Ley Federal del Derecho de Autor (LFDA) de los Estados Unidos Mexicanos (México).

El uso de imágenes, fragmentos de videos, y demás material que sea objeto de protección de los derechos de autor, será exclusivamente para fines educativos e informativos y deberá citar la fuente donde la obtuvo mencionando el autor o autores. Cualquier uso distinto como el lucro, reproducción, edición o modificación, será perseguido y sancionado por el respectivo titular de los Derechos de Autor.

**Selección y caracterización bioquímica de péptidos derivados de la hidrólisis enzimática de las globulinas de amaranto (*Amaranthus hypochondriacus*) y su evaluación antiviral contra el *Virus del enrollamiento de la hoja amarilla del tomate* (TYLCV).**

**José Silvestre Mendoza Figueroa**

*Grupo de Agroquímica Molecular, Depto. De Química de Biomacromoléculas,  
Instituto de Química*

**Tesis Doctoral**

*Programa de Doctorado en Ciencias Biomédicas*

**Universidad Nacional Autónoma de México**

Ciudad Universitaria, 2018

Asesor:

**Dr. Manuel Soriano García**, Instituto de Química, UNAM

Comité tutorial:

**Dr. Abel Moreno Cárcamo**, Instituto de Química, UNAM

**Dr. Carlos Kubli Garfias**, Inst. de Inv. Biomédicas, UNAM

Colaboradores externos:

**Dr. Jesús Méndez Lozano**, Instituto Politécnico Nacional,  
CIIDIR Unidad Sinaloa.

**Professor Anders Kvarnheden**, Swedish University of  
Agricultural Sciences.

**El presente trabajo fue realizado en:**

***Grupo de Agroquímica Molecular,***

Depto. De Química de Biomacromoléculas,  
Instituto de Química, UNAM, México.

***Laboratorio de Virología Molecular de Plantas,***

Depto. De Biotecnología Agrícola,  
CIIDIR-Sinaloa, IPN, Guasave, México

***Plant Virology group, Plant Biology Department***

Swedish University of Agricultural Sciences,  
Uppsala, Sweden.

***Laboratorio de Fitopatología,***

Escuela Nacional de Ciencias Biológicas,  
IPN, Ciudad de México.

# Índice

	<i>Página</i>
Agradecimientos	i
Dedicatoria	ii
Índice de figuras	iii
Índice de cuadros	iv
<b>Resumen</b>	1
<b><i>Abstract</i></b>	2
<b><i>Sammanfattning</i></b>	3
<b>1.0 Introducción</b>	4
<b>2.0 Antecedentes</b>	7
2.1 Cereales y pseudocereales como fuente de moléculas bioactivas.	7
2.2 El amaranto	7
2.2.1 Perfil bioquímico de la semilla y la planta	8
2.2.2 Aplicaciones nutraceuticas.	9
2.2.3 Aplicaciones agrícolas del amaranto	10
2.3 El tomate, biología y cultivo	11
2.3.1 Generalidades agrobiológicas del tomate.	11
2.3.2 Enfermedades del cultivo del tomate	12
2.4 Virus del enchinamiento amarillo de la hoja del tomate, TYLCV	14
2.4.1 Clasificación y diversidad	14
2.4.2 Genoma y replicación	15
2.4.3 Biología de la infección.	17
2.4.4 Respuesta inmunológica de la planta ante la infección por TYLCV.	20
2.5 Estrategias para el manejo de la enfermedad del enchinamiento de la hoja amarilla del tomate.	21
2.5.1 Estrategias biológicas para el manejo de la enfermedad.	21
2.5.2 Control de geminivirus basado en proteínas y péptidos	23
2.5.3 Propuesta para el control químico directo de TYLCV	25
<b>Justificación e hipótesis</b>	27

<b>Objetivos generales y específicos</b>	28
<b>3.0 Materiales y métodos</b>	29
3.1 Obtención, purificación y aislamiento de péptidos bioactivos de globulinas y albúminas de amaranto.	29
3.2 Selección de péptidos con capacidad de interacción química hacia el OriRep de TYLCV.	30
3.3 Secuenciación e identificación de secuencias de los péptidos purificados	30
3.4 Inhibición de síntesis in vitro de DNA.	31
3.5 Pruebas biológicas	32
3.5.1 Actividad biológica del extracto de péptidos en plantas de tomate y maíz.	32
3.5.1.1 Efecto del extracto de péptidos sobre el crecimiento de tomate e inducción de defensa primaria.	32
3.5.1.2 Efecto del extracto de péptidos en la inducción de defensa en plantas de tomate contra TYLCV.	33
3.5.1.3 Efecto del extracto de péptidos en el desarrollo de tizón foliar en maíz.	34
3.5.2 Actividad antiviral en <i>Nicotiana benthamiana</i> y <i>Solanum lycopersicum</i>	35
3.5.3 Evaluación in vivo de la tasa replicativa del virus.	35
3.5.4 Translocación del péptido en las células.	36
3.6 Interacción de AmPep1- OriRep mediante espectroscopia Raman	37
<b>4.0 Resultados y discusión</b>	39
4.1 Péptidos bioactivos derivados de globulinas de amaranto.	39
4.2 Selección y purificación de péptidos con afinidad hacia el OriRep de TYLCV.	46
4.3 Actividad antiviral de AmPep1	49
4.4 Estudio de la interacción molecular entre AmPep1 y OriRep mediante espectroscopia Raman y modelado teórico.	52
4.5 Transporte del péptido en el tejido vegetal.	60
<b>5.0 Conclusiones</b>	63
<b>6.0 Referencias</b>	64

## AGRADECIMIENTOS

- El autor de esta tesis extiende su más sincero agradecimiento al Dr. Manuel Soriano García, quien me asesoró y motivó para desarrollar este trabajo, orientándome a buscar horizontes cada vez más grandes.
- De la misma manera se hace un extenso agradecimiento a los miembros de mi comité tutorial Dr. Abel Moreno y Dr. Carlos Kubli, quien fueron una excelente guía en mi camino como doctorante.
- De manera especial agradezco al Dr. Jesús Méndez Lozano y al Dr. Anders Kvarnheden, quienes confiaron en mi sin conocerme y me extendieron la mano para poder desenvolverme en el mundo de los virus de plantas, sin duda alguna siempre estaré infinitamente agradecido por el apoyo y consejos que obtuve de su parte. ¡Muchas Gracias! y Tack så mycket!
- Agradezco a los Doctores: Dr. Edgar Rodríguez Negrete, Dr. Oswaldo Valdés López y Dr. José Manuel Saniger Blesa, quienes fueron parte medular para mi desarrollo profesional durante este trabajo al orientarme en técnicas y metodologías para el desarrollo de esta tesis.
- Agradezco sinceramente al Dr. Isaac Juan Luna Romero y a los miembros de la academia de Fitopatología de la Escuela Nacional de Ciencias Biológicas del IPN por darme de la oportunidad de desempeñarme como docente y poder transmitir los conocimientos adquiridos en mi formación doctoral, así como sus valiosos consejos en el área de la Fitopatología.
- Agradezco al Instituto de Química y al departamento de Química de Biomacromoléculas por todas las facilidades brindadas para el desarrollo de esta tesis.
- Agradezco también al departamento de Biología Vegetal (*Plant Biology*) de la Universidad de Ciencias Agrícolas de Suecia (*Swedish University of Agricultural Sciences*) y al departamento de Biotecnología Agrícola del Centro Interdisciplinario de Investigación para el Desarrollo Integral Regional-Sinaloa del IPN y al Laboratorio Universitario de Caracterización Espectroscópica del Instituto de Ciencias y Tecnología Aplicada de la UNAM por todas las facilidades técnicas brindadas para el desarrollo del trabajo.
- Se recibió la beca doctoral por parte del CONACyT con registro: 363126
- El proyecto fue financiado con recursos del Programa de Innovación, Investigación, Desarrollo Tecnológico y Educación (PIDETEC) Componente de Recursos Genéticos Agrícolas, SAGARPA/COFUPRO 2014 Registro: A/GTO/RGAG-2014-003.
- El autor agradece a los miembros del comité sinodal por su tiempo en la revisión de esta tesis.



Dedicatoria

Con esta frase le dedico a mis padres el amor que me dieron hacia el campo:

***“La tierra es para quien la trabaja”***

*Emiliano Zapata*

<b>Índice de figuras</b>	<b>Página</b>
<b>Figura 1.</b> Mapa genómico de TYLCV clona LV2015SATom. Acs: KU836749.1 aislado Sinaloa	16
<b>Figura 2.</b> Síntomas de la enfermedad causad por TYLCV (aislado Sinaloa) en plantas de tomate Rio Grande bajo condiciones de invernadero de producción	19
<b>Figura 3.</b> Efecto de los péptidos derivados del hidrolizado de globulina de amaranto en la promoción de crecimiento e inducción de especies reactivas de oxígeno en tomate.	41
<b>Figura 4.</b> Efecto de inducción de defensa del extracto de péptidos en tomate sobre el desarrollo de la enfermedad por TYLCV.	43
<b>Figura 5.</b> El hidrolizado de glubulinas de amaranto induce respuesta preventiva contra manchado foliar por <i>Helminthosporium</i> sp. en maíz.	45
<b>Figura 6.</b> Cálculo de la constante de afinidad entre el péptido AmPep1 y el oligonucleótido OriRepTYLCV mediante resonancia de plasmón localizada en superficie (LSRP) utilizando nanopartículas de oro.	48
<b>Figura 7.</b> Actividad antiviral de AmPep1 sobre TYLCV en plantas de tomate.	50
<b>Figura 8.</b> El péptido AmPep1 disminuye la síntesis de intermediarios replicativos virales de TYLCV en <i>N. benthamiana</i> .	51
<b>Figura 9.</b> Modelo experimental y teórico de la interacción entre AmPep1 y OriRepTYLCV utilizando espectroscopía Raman y modelado molecular	59
<b>Figura 10.</b> Translocación del péptido AmPep1 en células de <i>N. benthamiana</i> .	61

<b>Índice de cuadros</b>	<b>Página</b>
<b>Cuadro 1.</b> Potenciales aplicaciones de las proteínas de amaranto en el área agrícola.	11
<b>Cuadro 2.</b> Principales agentes fitopatógenos (microorganismos y virus) que afectan el cultivo de tomate.	13
<b>Cuadro 3.</b> Función de genes y proteínas de TYLCV.	16
<b>Cuadro 4.</b> Asignación de bandas del espectro Raman del oligonucleótido OriRepTYLCV, del péptido AmPep1 y de la matriz de interacción de ambas biomoléculas.	54

## RESUMEN

Las enfermedades de las plantas pueden ocasionar pérdidas en la producción de cultivos o pérdidas económicas de grandes dimensiones en industrias dependientes de material vegetal. Una de las patologías de mayor importancia son los virus, el *Virus del enrollamiento de la hoja amarilla del tomate*, TYLCV (del inglés: *Tomato yellow leaf curl virus*) es uno de los virus de mayor relevancia fitosanitaria a nivel mundial, ya que afecta a un amplio rango de hospedantes comerciales, como es el tomate, tomatillo, chile, frijol, soja. Hasta el momento no se conoce una formulación agroquímica que ayude a mitigar la enfermedad causada por dicho virus una vez que esta se encuentra instalada. Previamente se ha reportado el uso de péptidos y proteínas como agentes correctivos de la enfermedad a nivel de controlar el ciclo replicativo del virus, sin embargo, estos necesitan ser expresados en líneas transgénicas para su aplicación en campo. Utilizando los principios de diseño y/o selección racional de agroquímicos; en esta tesis se presenta el uso de semilla de amaranto como una fuente de péptidos bioactivos con actividad antiviral contra TYLCV. La primera evaluación consistió en estudiar si el extracto peptídico derivado de la hidrólisis enzimática de globulinas de amaranto era capaz de inducir actividad protectora contra la infección por TYLCV en tomate (*Solanum lycopersicum*). En los resultados se observó que el tratamiento con dicho extracto en dos variedades comerciales (Bola y Maya) induce protección contra la virosis por la activación de genes relacionados a defensa como la enzima fenilalanina amonio liasa (PAL) además de inducir promoción de crecimiento en dicha especie vegetal. Por otro lado, dicho extracto mostró la misma actividad de inducción de defensa al prevenir el desarrollo de manchado foliar en maíz causado por *Helminthosporium* sp. Posteriormente se procedió a la búsqueda de péptidos en el extracto los cuales tuvieran afinidad hacia la secuencia que forma la estructura de tallo y asa (horquilla) presente en el origen de replicación de TYLCV, los péptidos se seleccionaron mediante resonancia de plasmón localizada en superficie (LSRP) y se obtuvo un péptido denominado AmPep1 el cual demostró tener alta afinidad ( $k_d=1.4 \times 10^{-2} \mu\text{M}$ ) hacia el blanco viral en estudio. Dicho péptido mostró actividad antiviral curativa en plantas de *Nicotiana benthamiana* y tomate infectadas con el TYLCV al ser aplicado exógenamente, así como actividad antiviral curativa en plantas de *N. benthamiana* infectadas con el *Virus de la vena amarilla del chile Huasteco* (PHYVV). Al estudiar su potencial mecanismo de acción mediante la técnica “2-steps-qPCR” se comprobó que el péptido reduce la síntesis de intermediarios replicativos como el DNA sentido viral (VS) y por consiguiente la síntesis del DNA sentido complementario (CS) de TYLCV, lo que indicó que al ser un péptido seleccionado hacia el origen de replicación del virus este interfiere negativamente con la replicación de TYLCV, atenuando el desarrollo de la enfermedad. En un ensayo de interacción molecular mediante espectroscopia Raman y modelado teórico se deduce que el péptido se une a la horquilla de origen de replicación viral mediante puentes de hidrógeno e interacciones Pi en la región 3', la cual es la zona donde la proteína iniciadora de la replicación viral (Rep) lleva a cabo el inicio de este proceso, por lo tanto, se concluye que el péptido AmPep1 afecta directamente la síntesis de DNA viral en la planta generando actividad antiviral contra TYLCV.

## ABSTRACT

Plant diseases can cause losses in crop production or large economic losses in industries dependent on plant material. One of the most important diseases are viruses. *Tomato yellow leaf curl virus* TYLCV, is one of the most relevant phytosanitary viruses worldwide, since it affects a wide range of commercial hosts, such as tomato, tomatillo, pepper, bean, soybean. So far, an agrochemical formulation which helps mitigate the disease caused by the virus once it is installed is not known. Previously, the use of peptides and proteins as corrective agents of the disease has been reported to control the replicative cycle of the virus, however, these need to be expressed in transgenic lines for field application. Using the principles of design and / or rational selection of agrochemicals; this thesis presents the use of amaranth seed as a source of bioactive peptides with antiviral activity against TYLCV. The first evaluation was to study whether the peptide extract derived from the enzymatic hydrolysis of amaranth globulins was able to induce protective activity against TYLCV infection in tomato (*Solanum lycopersicum*). In the results it was observed that the treatment with this extract in two tomato commercial varieties (Bola and Maya) induced protection against the viral disease by the activation of defense-related genes such as the enzyme phenylalanine ammonia lyase (PAL) as well as inducing growth promotion in these vegetable species. On the other hand, this extract showed the same activity of defense induction by preventing the development of leaf blight in corn leaves caused by *Helminthosporium* sp. Subsequently we proceeded to search for peptides in the extract which had affinity to the sequence that forms the structure of stem and loop (hairpin) present in the origin of replication of TYLCV, the peptides were selected by localized surface resonance plasmon (LSRP) and a peptide called AmPep1 was selected, this peptide showed high affinity ( $k_d = 1.4 \times 10^{-2} \mu\text{M}$ ) towards the viral target under study. AmPep1 peptide showed curative antiviral activity in *Nicotiana benthamiana* and tomato plants infected with the TYLCV when it was applied exogenously, as well as curative antiviral activity in *N. benthamiana* plants infected with the *Pepper Huasteco yellow vein virus* (PHYVV). By studying its potential mechanism of action using the technique "2-steps-qPCR" it was found that the peptide reduces the synthesis of replicative intermediates such as viral sense DNA (VS) and consequently the synthesis of complementary sense DNA (CS) of TYLCV, which indicated that being a peptide selected towards the origin of replication of the virus this negatively interferes with the replication of TYLCV, attenuating the development of the disease. In a molecular interaction assay using Raman spectroscopy and theoretical modeling, it was deduced that the peptide binds to the hairpin of origin of viral replication by forming hydrogen bonds and Pi interactions in the -3' region, which is the area where the viral replication initiation protein (Rep) performs the beginning of this process, therefore, it is concluded that the peptide AmPep1 directly affects viral DNA synthesis in the plant, generating antiviral activity against TYLCV.

## SAMMANFATTNING

Växtsjukdomar kan förorsaka minskade skördar och stora ekonomiska förluster i industrier som är beroende av växtmaterial. En av de viktigaste patogenerna är virus. *Tomato yellow leaf curl virus*, TYLCV, är ett av de virus som har störst fyto-sanitär betydelse i världen, eftersom det påverkar ett brett spektrum av kommersiella värdväxter såsom tomat, tomatillo, chili, bönor och sojabönor. Hittills finns det inget känt lantbrukskemiskt preparat som kan hjälpa till att lindra sjukdomen som orsakas av viruset när det har etablerat sig i värdväxten. Det har tidigare rapporterats att peptider och proteiner, när de används som behandling mot sjukdomen, kan reglera förökningscykeln hos viruset; dock måste dessa uttryckas i transgena linjer för att användas i fält. Genom tillämpning av principer för design och/eller rationellt urval av lantbrukskemikalier presenterar denna avhandling användning av amarantfrö som en källa till bioaktiva peptider med antiviral aktivitet mot TYLCV. Till att börja med undersöktes om peptidextrakt framställt genom enzymatisk hydrolys av amarantglobuliner kunde inducera skyddsaktivitet mot TYLCV-infektion i tomat (*Solanum lycopersicum*). Resultaten visade att behandling med detta extrakt i två kommersiella varianter av tomat (Bola och Maya) inducerade skydd mot virussjukdom genom aktivering av försvarsrelaterade gener såsom enzymet fenylalanin-ammoniaklyas (PAL) och främjade tillväxt i dessa växtarter. Dessutom visade extraktet samma försvarsinducerande aktivitet genom att förebygga utveckling av mjöldagg på majsblad orsakad av *Helminthosporium* sp. I nästa steg övergick vi till att leta i extraktet efter peptider som hade affinitet till den sekvens som bildar en hårnålsloop i startpunkten för replikation i TYLCV. Dessa peptider identifierades genom lokaliserad yt-plasmonresonans (LSRP) och en peptid kallad AmPep1 valdes ut som uppvisade hög affinitet ( $k_d = 1.4 \times 10^{-2} \mu\text{M}$ ) till målsekvensen som studerades. AmPep1-peptiden uppvisade läkande antiviral aktivitet i *Nicotiana benthamiana* och tomatplantor infekterade med TYLCV när den applicerades exogent, liksom läkande antiviral aktivitet i *N. benthamiana* infekterad med *Pepper Huasteco yellow vein virus* (PHYVV). Genom att studera dess potentiella verksamma mekanism med tekniken "2-steps-qPCR" upptäcktes att peptiden reducerar syntesen av mellanprodukter i replikationen såsom DNA viral mening (VS) och följaktligen syntesen av DNA av komplementär (CS) hos TYCLV, vilket indikerar att den, till följd av sin affinitet till replikationsstarten, verkar genom negativ interferens med replikationen av TYLCV och därigenom dämpar sjukdomsförloppet. I en molekylär interaktions-assay med användning av Raman-spektroskopi och teoretisk modellering, kunde slutsatsen dras att peptiden binder till hårnålsstrukturen i replikationsstarten genom att forma vätebindningar och Pi-interaktion i 3'-regionen, vilket är det område där virusets Rep-protein påbörjar replikationsprocessen. Därför dras slutsatsen att peptiden AmPep1 direkt påverkar syntesen av viralt DNA i växten, vilket genererar antiviral aktivitet mot TYLCV.

## 1. INTRODUCCIÓN

El mejoramiento en la calidad agroalimentaria de los cultivos (e.g. la resistencia al estrés biótico) viene acompañado de una serie de cuidados al sistema agrícola de producción. Por ejemplo, la nutrición vegetal, la prevención de enfermedades y plagas, ente otros (Zadoks J. 2003). El ser humano desde que comenzó con la domesticación de cultivos ha buscado una gran variedad de estrategias que ayuden a mantener a la planta en una homeostasis con el medio ambiente, ya sea mediante la aplicación de extractos vegetales repelentes de insectos, mezclas salinas con acción fungicida, agroquímicos tipo plaguicidas, insecticidas, bactericidas, fungicidas, nematocidas o inductores de defensa vegetal así como hormonas de origen natural o sintético (Jeschke P. 2016; Urech P. A. 1999; Zadoks J. C. y Waibel H. 2000; Zadoks J. 2003).

El control de las enfermedades y plagas en los cultivos es de suma importancia, ya que si éstas no son controladas pueden generar pérdidas parciales o totales en la producción agrícola, perdidas económicas totales, e inclusive derivar en hambrunas a nivel regional, continental o mundial (Vurro M. *et al* 2010; Pinstруп Andersen P. 2001; Turner R. 2005). Actualmente, se ha desarrollado una estrategia de control químico directo para casi todos los grupos microbianos que generan enfermedades, sin embargo, un grupo faltante son los virus (Sanfaçon H. 2017; Rybicki E. P. 2015). Estos agentes patógenos pueden ser transmitidos mecánicamente mediante herramientas de cultivo o bien mediante insectos o arácnidos que se alimentan de la planta (vectores) (Sacristan S. *et al* 2011; Whitfield A. E. *et al* 2015), aunque se han desarrollado un buen número de agroquímicos de tipo insecticida y acaricida, los organismos vectores han generado resistencia por el uso desmedido de estas moléculas (Sudo M. *et al* 2018). Sin embargo, cuando la enfermedad viral se ha instalado, hasta el momento ha sido difícil erradicarla mediante un control químico correctivo, aun cuando su vector haya sido eliminado (Nicaise V. 2014; Rybicki E. P. 2015).

En el desarrollo de productos antivirales es importante considerar el correcto diseño o elección de la molécula (s), debido a que muchos de los virus se alojan en tejidos profundos

de la planta (e.g. haces vasculares) o bien en estructuras celulares como el núcleo, lo que puede complicar la correcta translocación tisular de una molécula potencial con actividad antiviral (Smith C. y Gilberson L. 2018; Li X. y Song B. 2017).

Para el correcto desarrollo de un producto viricida se propone considerar los siguientes factores:

- Blanco viral. Definido como el o los sitios moleculares del virus (genoma o proteínas virales) que interactuarán directamente con el compuesto antiviral. Es preferible sea(n) muy definido y lo más conservado posible entre especies virales con la finalidad disminuir la susceptibilidad de mutaciones del blanco con una consecuente generación de resistencia al tratamiento, en el diseño actual de agroquímicos propuesto por Speck Planche A. *et al* 2011 se plantea el uso de al menos dos mecanismos de acción (dos blancos) con la finalidad de evadir la resistencia que pudiera generar el fitopatógeno (Liu Y. *et al* 2014; Xiao J. J. *et al* 2015)
- Farmacóforo. Es el núcleo activo del agroquímico (átomos, grupo funcional, núcleo químico) que interactuará directamente con el blanco. Es recomendable que se conozca o se haga un diseño adecuado o predicción para elegir la mejor molécula que pueda interactuar en el blanco viral (Smith C. y Gilberson L. 2018; Li X. y Song B. 2017).
- Mecanismo de acción antiviral. Es necesario conocer el mecanismo bioquímico o molecular por el cual la molécula presenta dicha actividad, ya sea induciendo mecanismos de defensa moleculares en la planta o bien directamente afectando replicación del material genético, síntesis de una proteína o desestabilización de la cápside. Este mecanismo deberá de corresponder a lo predicho o esperado en el diseño del blanco viral y el mecanismo del farmacóforo (Li X. y Song B. 2017).
- Mecanismo de translocación al tejido y células. Además de que la molécula presente actividad viricida, es necesario que a su vez esta tenga propiedades fisicoquímicas como la polaridad que permitan moverse a través de las diferentes estructuras tisulares del tejido vegetal, por ejemplo, cruzar la cutícula, la pared celular, la membrana y/o mantenerse estable en el citoplasma (Smith C. y Gilberson L. 2018; Lamberth C. *et al* 2013; Speck Planche A. *et al* 2011).



- Capacidad de alcance celular. Si el virus se aloja en el núcleo, es necesario diseñar o seleccionar alguna molécula que una vez penetrando en la célula pueda dirigirse libremente hasta encontrar su blanco. Por ejemplo, translocarse hasta el núcleo si se trata de un inhibidor de la replicación (Zhang Y. *et al* 2018; Arand K. *et al* 2018).

Las biomoléculas como proteínas y péptidos constituyen una alternativa para el control de enfermedades en plantas, debido a que pueden ser extraídas fácilmente de otras fuentes de origen vegetal, como semillas y follaje en cantidades relativamente grandes, abaratando los costos de producción comparado con los compuestos agroquímicos de origen sintético (Zhao L. *et al* 2016; Islam W. *et al* 2018; Zabielski R. *et al* 2008; Barbosa Pelegrini P. *et al* 2011).

Utilizando los principios descritos en los párrafos anteriores para el diseño y/o selección de agroquímicos con actividad antiviral, en esta tesis presento el estudio bioquímico para la obtención racional de péptidos derivados de la globulina de amaranto (*Amaranthus hypochondriacus*) con actividad antiviral contra el *Virus del enrollamiento de la hoja amarilla del tomate*, TYLCV (del inglés: *Tomato yellow leaf curl virus*) el cual es uno de los virus de mayor relevancia fitosanitaria en cultivos de importancia económica a nivel mundial (Rybicki E. P. 2015). Uno de los objetivos principales de esta tesis es mostrar si la aplicación exógena de los péptidos obtenidos con afinidad química hacia el origen de replicación de TYLCV tienen actividad correctiva contra dicho virus, sin la necesidad de desarrollar líneas transgénicas, proponiendo así un modelo para el control agroquímico directo de la enfermedad causada por TYLCV en cultivos comerciales de alta importancia como el tomate. Además, presento el estudio del efecto biológico que el extracto de péptidos de las globulinas de amaranto puede tener en crecimiento y activación de respuesta de defensa en tomate contra TYLCV, así como la activación de respuesta de defensa en gramíneas para contrarrestar el desarrollo de tizón de halo en maíz.

## 2. ANTECEDENTES

### 2.1 Cereales y pseudocereales como fuente de moléculas bioactivas.

Los cereales y pseudocereales han sido utilizados como fuente de alimento de alto valor nutricional y energético, proporcionando aminoácidos esenciales para la dieta humana y ganadera, debido a la calidad y cantidad proteica que poseen, además, tienen un alto contenido energético debido a la calidad de almidón que contienen sus semillas. Al igual que los cereales, algunas plantas leguminosas como el frijol, el haba, la soja y otras asociadas a la familia *Amaranthaceae* como la quinoa y el amaranto han sido utilizados para la producción de harinas, consumo de follaje, etc (Zhu F. 2017; Nieto Barrera J. O. *et al* 2016). A diferencia de los primeros, estas plantas forman parte del grupo de las dicotiledóneas, por lo que son considerados pseudocereales. Se ha reportado que el contenido proteico en del amaranto es en algunos casos mayor que el de los cereales tradicionales como el trigo, el maíz y el arroz, asimismo tienen un mayor contenido de aminoácidos esenciales como el triptófano y algunas moléculas antioxidantes (Gorinstein S. y Arruda P. 1991; López D. N. 2018). En la agricultura, el amaranto debido al elevado rendimiento de la cosecha por hectárea de esta planta, representa una valiosa alternativa agroindustrial para la búsqueda de compuestos de interés farmacéutico, nutracéutico y agrícola (Venskutonis P. R. y Kraujalis P. 2013; Subia García C. 2012).

### 2.2 El amaranto.

El amaranto (*Amaranthus*) es un género de planta perteneciente a la familia *Amaranthaceae*; este género comprende más de 60 especies. La planta es una dicotiledónea del orden *Caryophyllales*, que comprende plantas anuales o perennes. Entre las especies principales en México se encuentra *A. hypochondriacus*, *A. cruentus*, *A. caudatus*, *A. hybridus* y *A. spinosus* (Fuente: Asociación Mexicana del Amaranto, 2018). La distribución geográfica de siembra en el país es en orden creciente: Puebla, Tlaxcala, Morelos, Estado de México y Ciudad de México. Siendo la especie más explotada *Amaranthus hypochondriacus* en sus diferentes razas (Azteca, Mercado, Mixteco) y sus variedades mejoradas en México (Nutrisol y Rojita),

de las cuales la raza azteca y variedad Nutrisol (derivada de raza Azteca) son consideradas la de mayor potencial productivo, ya que cada planta puede generar en promedio de 100 a 150 gramos de semilla por planta, teniendo una rentabilidad por hectarea de 1.4-1.5 toneladas (Subía García C. 2012; Ayala Garay A. V. *et al* 2014).

### 2.2.1 Perfil bioquímico de la semilla y la planta

La semilla de amaranto al igual que otras semillas contienen proteínas de reserva como globulinas, albúminas, prolaminas y glutelinas. El contenido proteico del amaranto es mayor comparado a los cereales, pseudocereales y leguminosas utilizadas en México; este oscila en peso seco de semillas en un 18-20%, mientras que para maíz: 9-10%, arroz: 8-10%, frijol: 17-19% y avena: 9-10%. La composición de la semilla de *A. hypochondriacus* en base seca es: proteínas crudas 18%, extracto etéreo 6.1%, fibra cruda 5.0%, cenizas 3.3%, hidratos de carbono 62% y energía 370 Kcal (Ayala Garay A. V. *et al* 2014). Aunque otras especies de amaranto como *A. caudatus* y *A. cruentus* tienen un aporte nutricional mayor que los cereales comparados anteriormente, su contenido proteico es menor que el descrito para *A. hypochondriacus*, siendo el contenido proteico del 13% para *A. caudatus* y de 14.1% para *A. cruentus* (Ayala Garay A. V. *et al* 2014). Dentro de los aminoácidos esenciales más importantes que contiene el amaranto destacan: metionina, cisteína, treonina, isoleucina, valina, lisina, fenilalanina, leucina y triptófano, este último encontrado de 1.8 g por cada 100 g de proteína (Alvaro Montoya Rodríguez *et al*, 2015). Las proteínas más abundantes en la semilla de amaranto son las globulinas representando un 48-50 % del total, en segundo lugar, se encuentran la fracción albúmina ocupando un 20%, seguida por glutelinas y prolaminas con un 30 y 2 %, respectivamente (Romero Zepeda H. y Paredes López O. 1995; Vasco Méndez N.L. *et al* 1999; Venskutonis P. R. y Kraujalis, P, 2013).

La fracción globulina se compone por la globulina 11S y 7 S. La globulina 11S es un polipéptido de 504 aminoácidos, formada por dos subunidades: una ácida, que tiene un peso molecular de 35-37 KDa y una básica que tiene un peso molecular de 25-28 KDa. Esta última unidad monomérica se asocia con otras 5 unidades formando un complejo hexamérico de peso molecular de 350 KDa. La fracción 7S es un polipéptido de 430 aminoácidos con un

peso molecular de 150 KDa, formado por 3 subunidades de 66, 52 y 38 KDa, respectivamente (Romero Zepeda H. y Paredes López O. 1995; Vasco Méndez N.L. *et al* 1999; Tandang Silvas M.R. *et al* 2012; Venskutonis P. R. y Kraujalis P. 2013). Ambas globulinas tienen estructura tridimensional tipo globular. Su extracción de la semilla se logra mediante la mezcla con soluciones amortiguadores con bajas concentraciones de sales, o usando soluciones ligeramente alcalinas.

### 2.2.2 Aplicaciones nutraceuticas.

Debido al alto valor nutricional de las proteínas contenidas en la semilla de amaranto, así como a su fácil digestión en condiciones fisiológicas (digestibilidad >90%), se ha reportado su uso potencial como agentes terapéuticos, como es el caso de la lunasina, la cual se encuentra principalmente dentro de la fracción glutelina; este péptido de 43 amino ácidos tiene actividad citotóxica en células cancerígenas de la línea HeLa teniendo como mecanismo de acción la inducción de apoptosis, cabe señalar que dichas moléculas no indujeron actividad citotóxica significativa en fibroblastos, mostrando así especificidad hacia células neoplásicas (Silva Sánchez C. *et al* 2008). Además, las proteínas de amaranto pueden derivarse a subproductos como son péptidos obtenidos a partir de digestión enzimática. El estudio de secuencias de péptidos bioactivos en proteínas como la globulina 11 y 7S ha permitido obtener modelos de péptidos con capacidad de inhibición *in vitro* de la enzima convertidora de la angiotensina, ACE (del inglés: angiotensin-converting enzyme), además de se ha podido predecir mediante ensayos bio informáticos posibles péptidos con actividad antioxidante e inhibidores de la enzima dipeptidil-peptidasa 4, DDP4 (del inglés: Dipeptidyl peptidase-4) (Silva Sánchez C. *et al* 2008; Quiroga A.V. *et al* 2012; Malaguti M. *et al* 2014; Montoya Rodríguez A. *et al* 2015).

### 2.2.3 Aplicaciones agrícolas del amaranto

Las aplicaciones del amaranto en el área agrícola aún son poco estudiadas. Por ejemplo, trabajos descritos por Rivillas-Acevedo 2007a y 2007b reportan la purificación del péptido Ay-AMP a partir de la semilla de *A. hypochondriacus*. Este péptido tiene actividad antifúngica *in vitro* sobre los hongos fitopatógenos *Fusarium oxysporum* y *Alternaria alternata*. Por otro lado, Valdés Rodríguez S. *et al* 2010, reportan la sobreexpresión de una cistatina de *A. hypochondriacus* (AhCPI), lo cual resultó en una actividad antifúngica contra *F. oxysporum*, *Rhizoctonia solani* y *Sclerotium seviporum*. De manera natural, la cistatina está involucrada en mecanismos de defensa que presentan las plantas contra insectos y algunos fitopatógenos, su principal función es ser un inhibidor de las cistein-proteinasas. Además, se ha descrito que cuando el amaranto se encuentra cultivado en climas áridos o muy húmedos, dicha proteína tiende a acumularse en el follaje, incrementando la resistencia de la planta a estrés biótico (Díaz I. 2018; Valdés Rodríguez S. *et al* 2010). Otros péptidos con actividad antimicrobiana descritas en especies de amaranto son péptidos antimicrobianos tipo Heveina (AcAMP1) descrito principalmente en *Amaranthus caudatus*, los cuales han mostrado actividad antifúngica contra el hongo fitopatógeno *Cercospora beticola* (Stotz H.U. *et al* 2013).

De acuerdo con los antecedentes mencionados en esta sección, el amaranto se presenta como un cultivo con potencial aplicación agroindustrial, debido a la alta cantidad de moléculas bioactivas tipo proteico (Cuadro 1), pudiendo ser utilizadas como moléculas que participen en la protección vegetal de otros cultivos de alto interés agroeconómico en México como es el maíz y el tomate.

**Cuadro 1. Potenciales aplicaciones de las proteínas de amaranto en el área agrícola.**

PROTEÍNA/PÉPTIDO	FAMILIA	FUENTE	ACTIVIDAD AGRO-BIOLÓGICA	REFERENCIA
AY-AMP	Proteína de unión a quitina	<i>A. hypochondriacus</i> (semilla)	Antifúngica contra <i>F. oxysporum</i> y <i>A. alternata</i>	Rivillas Acevedo et al 2007 a y b
CISTATINA	Cistein-proteinasas	<i>A. hypochondriacus</i> (hoja)	Antifúngica contra <i>F. oxysporum</i> , <i>Rhizoctonia solani</i> y <i>Sclerotium seviporum</i>	Valdés Rodríguez et al 2010
ACAMP1	péptidos antimicrobianos tipo Heveina	<i>A. caudatus</i> (hoja)	Antifúngica contra <i>Cercospora beticola</i>	Stotz H.U. et al 2013
KNOTTINAS	Knottinas	<i>A. hypochondriacus</i> (hoja)	Inhibidores de alfa-amilasa	Stotz H.U. et al 2013

## 2.3 El tomate, biología y cultivo

### 2.3.1 Generalidades agrobiológicas del tomate.

Taxonómicamente el tomate (*Lycopersicon esculentum*) es una planta dicotiledónea, perteneciente a la clase *Angiospermae*, del orden *Solanales* y familia *Solanaceae*. Se describe como una planta perenne de porte arbustivo, puede tener un desarrollo rastrero o de forma erecta. Esta última forma de desarrollo es preferible en los invernaderos de alta producción, mientras que la forma arbustiva se presenta generalmente en campo abierto. El cultivo es ligeramente tolerante a la salinidad (no en etapas iniciales de desarrollo), ambientes templados a cálidos y alta incidencia de iluminación. Una de las características notables que presentan sus hojas es que en el envés de estas se encuentra un alto número de estomas lo que potencializa la entrada de agroquímicos foliares a la planta (Cepeda-Siller M. 2009).

El desarrollo del cultivo desde la germinación hasta la etapa de senescencia abarca en promedio 150 días, teniendo a las etapas de maduración y de vida adulta con la duración más larga del ciclo de vida con un promedio de 80 días. Esta especie se considera como cultivo de crecimiento rápido, aunque se puede considerar un cultivo robusto de acuerdo con sus requerimientos agronómicos ya que es importante considerar su temperatura óptima que

oscila de los 18-28°C, sobre suelos francos bien drenados con un pH de 5.0 a 7.0, incidencia luminosa de al menos 10 horas por día, y una cantidad (kg) de fertilizante recomendado por hectárea sembrada en promedio de 100-150 N, 65-110 P y 160-240 de K (Cepeda-Siller M. 2009; Al-Amri, S. M. 2013 )

### 2.3.2 Enfermedades del cultivo del tomate

El estudio de plagas y enfermedades del tomate, así como las estrategias de control integrado de estas, es de vital importancia para evitar pérdidas en producción con consecuencias económicas y garantizar frutos con alta calidad nutricional. Además, de las plagas causadas por insectos y ácaros, las enfermedades microbianas son unas de las principales responsables de las pérdidas productivas del cultivo. Dentro de las enfermedades más comunes se encuentran las de origen fúngico como el tizón tardío y la cenilla, seguidas de estas se encuentran las enfermedades causadas por virus, siendo estas de las más devastadoras debido a que hay pocas estrategias de control químico o biológico, comparado con el control de enfermedades de origen fúngico. Dentro de las virosis más importantes en México se encuentran aquellas causadas por begomovirus como el *Virus Huasteco de la vena amarilla del chile*, PHYVV (del inglés: *Pepper Huasteco yellow vein virus*) así como el *Virus del mosaico dorado del chile*, PepGMV (del inglés: *Pepper golden mosaic virus*) los cuáles se han descrito como un fitopatógenos endémicos en México afectando no solo a tomate si no a otros hospedantes como chile y tomatillo (Melendrez Bojorquez N. *et al* 2016; Rentería Canett I. *et al* 2011) el *Virus del enrollamiento de la hoja amarilla del tomate*, TYLCV tiene una incidencia importante a nivel nacional, por ejemplo, tan solo en el valle agrícola de Culiacán en el año 2011 es el de mayor incidencia junto con otros virus asociados a su mismo género (Lugo Melchor O.Y. *et al* 2011); a nivel mundial representa el primer lugar en importancia fitosanitaria de la familia *Geminiviridae* (Rybicki E. P. 2015). En el grupo de enfermedades bacterianas dentro de las más reportadas se encuentra principalmente la enfermedad de la peca bacteriana causada por *Pseudomonas syringae* pv *tomato*, mientras que en el caso de enfermedades asociadas a nemátodos el género *Meloidogyne* y la mayoría de sus especies tiene la capacidad de infectar al tomate induciendo formación de agallas. En el (Cuadro 2), se resumen las principales especies microbianas y virales que afectan el cultivo de tomate a nivel nacional y mundial.

**Cuadro 2. Principales agentes fitopatógenos (microorganismos y virus) que afectan el cultivo de tomate.**

<b>Grupo Patógeno</b>	<b>Agente etiológico</b>	<b>Enfermedad</b>	<b>Referencia</b>
<b>Bacterias</b>	<i>Pseudomonas syringae</i> pv. <i>tomato</i>	Peca bacteriana	Tsitsigiannis D.I. et al 2008; Rodríguez Alvarado G. et al 2011; DGSV-Nayarit
	<i>Xanthomonas campestris</i> pv. <i>Vesicatoria</i>	Manchado/tizón bacteriano	
	<i>Ralstonia solanacearum</i>	Marchitez bacteriana	
	<i>Clavibacter michiganensis</i> subsp. <i>michiganensis</i>	Cáncer bacteriano	
<b>Hongos y oomicetos</b>	<i>Phytophthora infestans</i>	Tizón tardío	Sanoubar R. y Barbanti L. 2017; Tsitsigiannis et al 2008; Rodríguez Alvarado et al 2011; DGSV-Nayarit
	<i>Alternaria solani</i>	Tizón temprano	
	<i>Phytophthora parasitica</i>	Pudrición radicular	
	<i>Fusarium oxysporum</i>	Fusariosis del tallo y pudrición radicular, marchitamiento	
	<i>Rhizoctonia</i> spp.	<i>Damping-off</i> , pudrición radicular	
	<i>Oidium neolycopersici</i>	Cenicilla	
	<i>Sclerotium rolfsii</i>	Podredumbre negra	
	<i>Septoria lycopersici</i>	Manchado de la hoja	
<b>Nemátodos</b>	<i>Meloidogyne</i> spp.	Agallas	Quiroga Madrigal R. et al 2007.
<b>Virus</b>	<i>Tomato yellow leaf curl virus</i> , TYLCV	Enrollamiento amarillo de la hoja del tomate	Hanssen I.M. et al 2010; Camacho Beltrán E. et al 2015 Gámez-Jiménez et al 20 Melendrez Bojorquez N. et al 2016; Rentería Canett I. et al 2011
	<i>Pepper Huasteco yellow vein virus</i> , PHYVV		
	<i>Pepper golden mosaic virus</i> , PepGM	Mosaico dorado	
	<i>Tomato mosaic virus</i> , ToMV	mosaico	
	<i>Tomato torrado virus</i> , ToTV	Marchitez	
	<i>Cucumber mosaic virus</i> . CMV	mosaico	
	<i>Tomato spott wilt virus</i> , TSWV	Manchado necrótico	
	<i>Pepino Mosaic virus</i> , PepMV	Necrosis de fruto	
<i>Tomato marchitez virus</i> , ToMarV	Marchitamiento		



## **2.4 Virus del enrollamiento amarillo de la hoja del tomate, TYLCV**

### 2.4.1 Clasificación y diversidad

El virus del enrollamiento de la hoja amarilla del tomate (del inglés, *Tomato yellow leaf curl virus*, TYLCV) es un virus de DNA de cadena sencilla circular, con una longitud aproximada de 2780 nucleótidos (Glick E. et al 2007). El material genético se encapsula en una cápside icosaédrica geminada, la cual está formada por 110 unidades de proteína de cápside organizadas como 22 capsómeros pentaméricos. El virus se encuentra clasificado dentro del género *Begomovirus* perteneciente a la familia *Geminiviridae* (Zerbini F. et al 2017). A diferencia de otros miembros del género *Begomovirus*, TYLCV presenta un genoma único (monopartita) que codifica para todas sus proteínas (estructurales y no estructurales), mientras que otros virus de este género como PHYVVV, presentan dos genomas (bipartita): el componente DNA-A y el componente DNA-B (Moreno Félix M.L. et al 2018). Además, se ha descrito que el genoma de los begomovirus monopartitas es muy parecido en organización y función al componente DNA-A de los bipartitas (Melgarejo T.A. et al 2013).

La distribución de este virus es mundial, fue reportado por primera vez en Israel en los años sesenta (Cohen S. y Nitzany F.E 1960, 1966). El virus ha sido movilizadado desde su centro de origen (medio oriente) por casi toda la región mediterránea europea hasta alcanzar el hemisferio occidental, afectando principalmente países del Caribe, Centro y Norte América, siendo el Caribe la puerta de entrada de TYLCV al continente alrededor de los años 80s (Wan H.J. et al 2014; Mabvakure B. et al 2016). En México el primer reporte de esta enfermedad data de 1999 en la Península de Yucatán (Ascencio Ibáñez J.T. et al 1999) y posteriormente se detectó en Sinaloa. Se reconocen siete cepas de este virus, sin embargo, las cepas Mild (Mld) e Israel (IL) son las que se han distribuido mundialmente (Brow J.K. et al, 2015). Se ha descrito que la variabilidad genómica entre especies de TYLCV aisladas en la región geográfica de Shangai es menor al 3%, sin embargo, dentro del genoma las zonas más variables en secuencia son la región intergénica “IR” (sin tomar en cuenta el origen de replicación, estructura de tallo y asa, el cual es muy conservado entre los geminivirus) y la región terminal 5’ de V2, mientras que las regiones más conservadas son las que se

sobreponen entre los genes V1 y V2 (Yang X. *et al* 2014; Silva S. J. C *et al* 2012; Campos-Olivas R. *et al* 2002).

#### 2.4.2 Genoma y replicación

El genoma de TYLCV está formado por genes codificados por la cadena viral o VS, los cuales son aquellos que se codifican directamente por el DNA viral monocatenario contenido en la cápside, y genes complementarios codificados por la cadena complementaria a la cadena viral, CS. En la (Figura 1) se representa el genoma de TYLCV clona LV2015SATom. (Acs: KU836749.1), el cual al igual que todos los genomas reportados de este virus tiene seis marcos de lectura abiertos, 2 para VS y 4 para CS, los cuales se encuentran superpuestos entre sí. Dentro de los genes codificados por VS se encuentra *v1* y *v2*, mientras que los genes *c1*, *c2*, *c3* y *c4* se encuentran en la CS (Glick E. *et al* 2007); en el (Cuadro 3), se detalla la función biológica de cada una de estos genes y sus proteínas codificadas. Entre la región *c1* y *v2* se encuentra la región intergénica, la cual a pesar de tener flancos con una alta variación como se mencionó anteriormente, presenta una secuencia altamente conservada que da origen a una estructura secundaria de tallo y asa u horquilla. La secuencia del asa TAATATT↓AC, es donde se inicia el proceso replicativo cuando ésta es reconocida por el producto de *c1* en la zona (↓). Dentro de las funciones de los genes codificados en VS, se encuentra la formación de la proteína de cápside viral (CP), que participa en encapsidación y en procesos de regulación de la replicación junto con V2, mientras que los productos de los genes CS, se encuentra la proteína iniciadora de la replicación (Rep) codificada en el gen *c1*, así como proteínas participantes en el desarrollo de la enfermedad como son C2, Ren, y C4; su función es principalmente silenciamiento de respuesta inmune de la planta, potencializador de la replicación del virus y reguladores transcripcionales de proteínas relacionadas a patogénesis en la planta, respectivamente (Wang L. *et al* 2017).

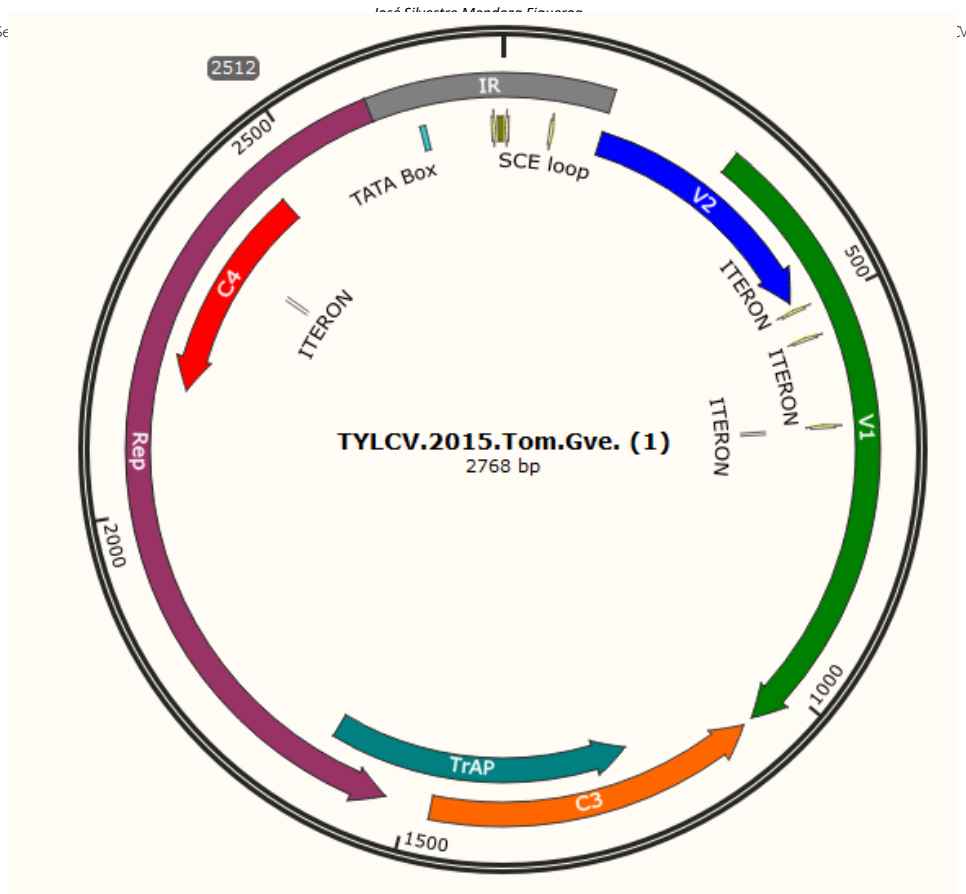


Figura 1. Mapa genómico de TYLCV clona LV2015SATom. Acs: KU836749.1 aislado Sinaloa

Cuadro 3. Función de Genes y proteínas de TYLCV.

Gen	Proteína	Función	Peso Molecular (KDa)	Referencia
<i>I</i>	CP	Proteína de cápside, envoltura y formación del virión, interacción con vector, movimiento celular, podría actuar como gen temprano regulador de replicación	29.9	Basak J, 2016; Gover O. <i>et al</i> 2014.
<i>v2</i>	V2	Suprime silenciamiento génico de la planta al virus, interacciona con cistein-proteasas	13.4	Bar-Ziva A. <i>et al</i> 2016; Hak H. <i>et al</i> 2015
<i>c1</i>	C1/Rep	Iniciador de la replicación por corte enzimático de la región TAATATT↓AC en la estructura de asa de la región IR y actividad circularización de la nueva cadena viral	41	Campos-Olivas <i>et al</i> 2002; Basak J. 2016
<i>c2</i>	C2/TrAP	Determinante patológico, induce decaimiento en respuesta inmune por supresión de la producción de ácido jasmónico. Puede actuar como gen tardío para regular la sobreexpresión de CP	15	Rosas-Díaz T. <i>et al</i> 2016; Gover O. <i>et al</i> , 2014.
<i>c3</i>	C3/Ren	“Potenciador de la replicación”, aunque se describe por interactuar con Rep en fases tardías, no por interacción directa con el DNA	15.9	Gover O. <i>et al</i> 2014.
<i>c4</i>	C4	Desregulador del sistema inmune de la planta o regulador post transcripcional, involucrada en ciclo del metilo	10.9	Kim N. <i>et al</i> 2016
<i>IR</i>	No codificante	Zona de inicio de la replicación, es altamente conservada entre la familia viral.	300-314 pares de bases	Gover O. <i>et al</i> 2014; Mori T. <i>et al</i> 2013

El proceso replicativo del virus se lleva a cabo dentro del núcleo de las células del floema. Este inicia cuando el virión es translocado dentro de la célula y el DNA viral monocatenario (ssDNA, VS) se mueve al interior del núcleo. Una vez dentro, se llevará a cabo una replicación inicial del ssDNA, para formar la cadena complementaria (cDNA, CS) utilizando las polimerasas de la planta, las cuales pudieran ser las polimerasas tipo TLS (Ritcher K.S. *et al* 2016). Una vez formado el intermediario replicativo de doble cadena (formado por el ssDNA y el cDNA) se lleva a cabo la transcripción del gen *c1* para dar origen a la proteína Rep, la cual reconocerá parte de la región intergénica y específicamente en la estructura de tallo y asa en la zona TAATATT↓AC realizará un corte en la cadena de DNA de la cadena VS, dejando un extremo 3' -OH el cual servirá como iniciador de la replicación por el modelo del círculo rodante (Laufs J. *et al* 1995; Campos-Olivas R. *et al* 2002). Los nucleótidos se irán incorporando, usando como molde la cadena CS, desplazando al resto de la cadena VS conforme la replicación avance. Una vez sintetizada una nueva cadena viral, la Rep actuará como ligasa para circularizar a la cadena VS desplazada permitiendo que esta quede libre en el interior del núcleo para formar nuevas cadenas CS o bien empaquetarse en la cápside (Pooggin M.M. 2013). Algunas de las proteínas como Ren participarán en el incremento del material genético por interacción directa con la proteína CP a nivel tardío, para incrementar el número de virus encapsidados (Gover O. *et al* 2014).

#### 2.4.3 Biología de la infección.

Naturalmente TYLCV es un virus transmitido por la mosca blanca (*Bemisia tabaco*, Gennadius 1889) principalmente por los biotipos B y Q, siendo en algunas ocasiones las hembras quienes presentan mejor eficiencia de adquisición y transmisión (Ning W. *et al* 2015). TYLCV es un virus persistente, circulativo y tiene capacidad de invadir órganos reproductivos de la mosca, sin embargo, no se ha observado que el virus tenga la capacidad replicativa en el vector (Sánchez-Campos S. *et al* 2016). Las moscas blancas adquieren al virus durante su periodo de alimentación, estas se alimentan directamente del floema acarreado a los virus presentes en su estilete. Una vez instalado el virus en las glándulas salivales del vector, este comenzará a circular por su cuerpo, produciendo alteraciones conductuales en la mosca (Czosnek H. *et al* 2017). Cuando una *B. tabaci* infectada con

TYLCV se mueva a una planta sana, ésta diseminará la infección al alimentarse, los viriones serán depositados en el floema y estos interaccionaran directamente con proteínas asociadas a choque térmico de la planta como la HSP70 (del inglés: Host shock protein 70) las cuáles facilitarán la translocación del virión hasta el núcleo de las células acompañantes en dicho tejido para iniciar los procesos replicativos descritos anteriormente (Gorovit R. y Czosnek H. 2017). Debido a la tasa de reproducción del vector y fácil adaptación a climas de zonas de producción hortícola, además de la persistencia del virus en el vector, las virosis causadas por TYLCV se consideran una de las más dañinas a nivel fitosanitario.

Una vez instalada la infección dentro de la planta se producirán los síntomas característicos de la enfermedad como se muestra en la (Figura 2), hojas con enrollamientos hacia el haz, ampollamientos, clorosis marginal y generalizada, enanismo, acortamientos de nudos y abortos florales si la infección es avanzada. Aunque la sintomatología dependerá del grado de infección, clima, variedad de la planta, infecciones mixtas con otros virus u otros patógenos y persistencia del vector; se puede considerar la presencia de los síntomas arriba descritos un indicativo de una enfermedad viral por begomovirus. Dentro de las afecciones más importantes es el aborto floral el cual no permitirá desarrollo de frutos, y si estos logran desarrollarse serán de tamaño pequeño y con propiedades bromatológicas de baja calidad. El acortamiento de los nudos (Figura 2 B) inducirá falta de crecimiento de la planta lo que conllevará a que estas presenten “enanismos” comparadas a plantas sanas.



**Figura 2. Síntomas de la enfermedad causada por TYLCV (aislado Sinaloa) en plantas de tomate Rio Grande bajo condiciones de invernadero de producción.**

A) Síntomas generales asociados a la enfermedad del enrollamiento de la hoja amarilla del tomate como enrollamiento hacia el haz, ampollamiento, clorosis generalizada y marginal, deformación total de la planta, reducción de láminas foliares. B) Acercamiento mostrando el enrollamiento hacia el haz de la hoja, conocido también como acucharamiento. C) Acercamiento mostrando el acortamiento de nudos y hojas con clorosis marginal. Las plantas mostradas fueron infectadas con el virus TYLCV LV2015SATom Acs: KU836749.1 clonado en *Agrobacterium tumefaciens* GVR3101 mediante el método de agroinfección. Las plantas se mantuvieron libres de vector. Foto tomada en San Andrés Nicolás Bravo, Malinalco, Estado de México, septiembre 2017.

Además del tomate, se ha reportado un amplio rango de hospedantes para dicho virus como tomatillo (*Physallis ixocarpa*) (Gámez-Jiménez et al, 2009), chile (*Capsicum annum*), soja (*Glycine max*) (Kil E.J et al 2017) y malezas (Smith H.A. et al 2015), sin considerar el amplio rango de hospederos del vector. El virus se transmite verticalmente, este puede moverse a través de la planta y localizarse en flores y en el fruto prevaleciendo desde su desarrollo hasta su maduración, convirtiendo a este en un foco de diseminación de la enfermedad debido a movimientos comerciales. El virus, además, prevalece en el embrión generando semillas que contienen virus, las cuales darán origen a nuevas plantas de tomate que congénitamente estarán infectadas con TYLCV, siendo focos de diseminación de la enfermedad en campo (Just K. et al 2014 y 2017; Kil E.J. et al 2016).

#### 2.4.4 Respuesta inmunológica de la planta ante la infección por TYLCV.

Se ha descrito que en plantas de tomate susceptibles a infección por TYLCV la producción de especies reactivas de oxígeno, ROS (del inglés: reactive oxygen species) es más elevada que en variedades resistentes (Moshe A. et al 2012). Al respecto se ha reportado que la actividad de la enzima polifenol oxidasa (POD) es mayor en plantas resistentes que en plantas susceptibles a TYLCV (Huang Y. et al 2016a), lo que sugiere la existencia de un balance en la activación de la respuesta inmune, planteando al estrés oxidativo como una de las primeras barreras químicas que la planta de tomate puede desencadenar contra TYLCV. Se han descrito que factores transcripcionales como WRKY asociados al grupo III, principalmente el 41 y 53 se sobre expresan en infecciones por TYLCV en tomate, el silenciamiento de estos factores hace más susceptible a la planta para el desarrollo de la infección (Huang Y. et al 2016b). La activación de estos factores transcripcionales activa a las proteínas-quinasas activadas por mitógeno, MAPK (del inglés: mitogen-activated protein kinase) como la MAPK 1, 2 y 3, siendo la MAPK3 la mayormente asociada a respuesta de defensa durante infecciones de TYLCV. La activación de estas proteínas-quinasas da origen a la expresión de proteínas relacionadas a patogénesis, PRs (de las ingles: pathogenesis related proteins) como PR1, PR1b/SILapA, SIP1-I y SIP1-II (Li Y. et al 2017). Además, se ha visto que su activación conlleva a un incremento en la producción de ácido salicílico (SA) el cual es un transductor de activación inmunológica (Li Y. et al 2017). La sobreproducción de SA ha sido también

descrita en variedades resistentes a TYLCV (Moshe A. *et al* 2012). Asimismo, otros metabolitos encontrados en tomate infectado son poliaminas, fenoles, indoles, ferulatos (Dagan S. *et al* 2015), siendo estos últimos reportados como agentes antivirales de fitovirus (Guang G.Y. *et al* 2013). Otro gen necesario en la respuesta inmune de TYLCV es el *gen tipo-lipocalina*, el cual se encuentra altamente expresado en variedades resistente. Los productos de este gen son proteínas con función de enlace a pequeñas moléculas hidrofóbicas y a receptores encontrados en la superficie celular para formación de complejos, donde pudiera tener función activadora de proteínas asociadas a las llamadas “guardianas”; el silenciamiento de este gen rompe la resistencia contra TYLCV (Dagan S. *et al* 2012).

## **2.5 Estrategias para el manejo de la enfermedad del enchinamiento de la hoja amarilla del tomate.**

Para un buen manejo de virosis en cultivos hortícolas se deben de considerar medidas profilácticas y medidas correctivas de emergencia. Dentro de las primeras resalta el uso de semillas de variedades resistentes, limpieza y desinfección de herramientas de poda, eliminación de hospederos alternativos para el vector, eliminación del vector previo al inicio del cultivo e inducción de resistencia mediante estimulación inmunológica. En las medidas correctivas de emergencia resalta el uso de insecticidas para eliminar vectores y el uso de soluciones nutritivas (mezcla de aminoácidos y hormonas) que ayuden a amortiguar el estrés en la planta causado por la infección viral. Hasta el momento la ningnanmicina se conoce como antiviral correctivo utilizado en campo en China; este compuesto es utilizado principalmente en infecciones causadas por el *Virus del mosaico del tabaco*, TMV (del inglés: *Tobacco mosaic virus*) (Han Y. *et al* 2014; Li X. *et al* 2017).

### **2.5.1 Estrategias biológicas para el manejo de la enfermedad.**

El manejo biológico de la enfermedad generada por TYLCV está dado por el uso de variedades resistentes de tomate las cuales poseen genes de resistencia contra el virus, el uso de microorganismos inductores de resistencia sistémica y el control del vector mediante parasitismo por hongos entomopatógenos. Las variedades resistentes de tomate a TYLCV se caracterizan por poseer los genes *Ty*, en los cuales se encuentra la resistencia específica a



este virus. Aunque los genes *Ty*, formen parte de genes de resistencia transgeneracional (genes R), no se han asociado a la producción de hipersensibilidad (HR) o muerte celular (Verlaan M.G. *et al* 2013), como lo hacen sus homólogos participantes en la defensa antibacteriana y antifúngica. Se conocen los genes *Ty-1*, *Ty-2*, *Ty-3*, *Ty-4* y *ty-5*, estos genes dan lugar a diferentes productos proteicos. Si bien no se conoce completamente su mecanismo de acción, se ha descrito que para los genes *Ty-1/3* el producto de este es una RNA Polimerasa RNA-dependiente, RDR (del inglés: RNA-dependent RNA polymerase); se propone que la función de estas RDR es potencializadora en la formación de iRNA, favoreciendo el silenciamiento de los transcritos virales de TYLCV (Verlaan M.G. *et al* 2013). El gen de mayor resistencia conocido es el *ty-5*, recientemente se describe que su función es sintetizar un factor “vigilante” de RNA denominado “Pelota o pelo”. Este factor está involucrado en la fase de reciclamiento ribosomal en la síntesis de proteínas; cuando este factor es silenciado, las variedades de tomate susceptibles a TYLCV pueden adquirir fenotipo de resistencia, mientras que cuando es sobre expresado, las variedades resistentes se vuelven susceptibles (Lapidot M. *et al* 2015).

Otra estrategia biológica para el control de la enfermedad radica en la inducción de resistencia sistémica mediante microorganismos, por ejemplo, bacterias y hongos promotores de crecimiento. Recientemente se describe el uso de *Enterobacter asburiae* BQ9 como una rizobacteria que tiene efectos de promoción de crecimiento en la planta, y además induce la expresión de PRs (PR1a y b) en plantas de tomate sanas e infectadas con TYLCV. La expresión de estos genes se observa en tan solo 6 horas post inoculación, con una consecuente reducción de la carga viral, además, la presencia de esta rizobacteria incrementa la producción de ROS y enzimas relacionadas a defensa como la fenilalanin-amonio-liasa (PAL) (Li H. *et al* 2016). Otro ejemplo de inducción de resistencia contra TYLCV es mediado por la micorriza *Piriformospora indica*, que tiene efectos de promoción de crecimiento; en variedades susceptibles de tomate se ha visto una reducción de la enfermedad significativa comparada con sus grupos control. Hasta ahora, no se conoce el mecanismo de acción de este microorganismo (Wang H. *et al* 2015). Se ha descrito que la micorriza *Rhizophagus intraradices* induce la expresión del gen relacionado a patogénesis *Pl* ante una

infección por TYLCV en tomate, activando parcialmente el sistema de defensa (Valle Castillo L.B. 2016).

El control del insecto vector es una de las estrategias más utilizadas para evitar virosis. Se emplea el uso de hongos entomopatógenos que tienen actividad parasitaria contra *B. tabaci*, por ejemplo, *Lecanicillium muscarium*, *Isaria fumosorosea* y *Metarhizium anisopliae* son los ejemplos más comunes; el mecanismo de acción es parasitar al insecto hasta la muerte de este (Dong T. *et al* 2016; Ali S. *et al* 2017).

Otras estrategias utilizadas son el silenciamiento mediante siRNA. Se ha reportado que la inducción de silenciamiento de proteínas supresoras como la CP de TYLCV mediante RNA de doble cadena disminuye la expresión de la proteína con una consecuente disminución del fenotipo de la enfermedad en *N. benthamiana* (Zrachya A. *et al* 2007). Además, el silenciamiento de otros genes como C2 y C4 inducen la tolerancia a la infección por TYLCV (Peretz Y. *et al* 2011). Una nueva alternativa para el control molecular del virus es mediante la tecnología de repeticiones palindrómicas cortas agrupadas y regularmente interespaciada mejor conocida como CRISPR/Cas9 (del inglés: clustered regularly interspaced short palindromic repeats); se ha reportado recientemente su uso para generar inmunidad o tolerancia contra TYLCV y otros geminivirus principalmente por generar interferencia con secuencias en CP y Rep y regiones IR no codificantes (Ali Z. *et al* 2016; Tashkandi et al, 2017).

### 2.5.2 Control de geminivirus basado en proteínas y péptidos

Una alternativa que ha sido explorada para el control de virosis causadas por begomovirus es el uso de proteínas y péptidos, ya sea por el uso de ingeniería genética generando líneas transgénicas que sobre expresen proteínas virales para inducir una respuesta inmunológica o que desempeñen alguna función de enlace hacia una proteína viral o región genómica del virus, o bien, mediante la aplicación exógena de este tipo de moléculas desempeñando una función antiviral. Se ha reportado la generación de líneas transgénicas de tomate sobre expresando fragmentos de la proteína Rep, mostrando que sus siguientes generaciones

muestran resistencia a desarrollar la enfermedad con severidad (Cilio F. y Palukaitis P. 2014, Yang Y *et al* 2004; Tamarziz *et al* 2009). La sobre expresión de la proteína Rep puede servir para inducir su reconocimiento como un patrón molecular asociado a patógeno, PAMP (del inglés: pathogen associate molecular pattern), de esta manera se induce a la planta a sintetizar moléculas de inmunidad como MAPK3, WRKY53 y SA descritas previamente como moléculas de defensa ante una infección por TYLCV.

En el bloqueo de mecanismos de replicación directos se han descrito el diseño de plantas transgénicas sobre expresando fragmentos de anticuerpos que reconocen Rep, demostrando la reducción de título viral en plantas de *N. benthamiana* infectadas con TYLCV (Safarnejad M.R. *et al* 2009). El uso de péptidos como control de infecciones por geminivirus es otra estrategia que se propone para el control de replicación viral. Por ejemplo, se han reportado el uso de péptidos aptámeros (Reverdatto S. *et al* 2015) que reconocen la región N terminal de Rep de algunos geminivirus; estos aptámeros fueron seleccionados mediante la técnica de doble híbrido de levadura. Los péptidos aptámeros que mostraron mayor interacción con la zona blanco redujeron el título viral en células infectadas con *Tomato golden mosaic virus* (TGMV) y *Cabbage leaf curl virus* (CaLCV) (López-Ochoa L. *et al* 2006). Posteriormente los péptidos aptámeros seleccionados fueron evaluados para estudiar su capacidad de reconocer la región N terminal de otros géneros asociados a la familia *Geminiviridae* como *Beet curly top virus*, (BCTV, *Curtovirus*) y *Maize strike virus* (MSV, *Mastrevirus*); en los ensayos de interacción bioquímica se observó que estas moléculas tuvieron alta afinidad a las proteínas de replicación entre los tres géneros analizados de la familia *Geminiviridae*. Con estos péptidos aptámeros se crearon líneas transgénicas de tomate, las cuáles sobre expresaron a estas moléculas y se evaluó si la sobre expresión de estos péptidos en las plantas podrían modular la infección por TYLCV y *Tomato mottle virus* (ToMoV). Los resultados mostraron el abatimiento títulos virales para ambos virus y una consecuente reducción de síntomas de la enfermedad, debido a la interferencia de estos péptidos aptámeros con la proteína de inicio de replicación, alterando el ciclo replicativo de los virus (Reyes M.I. *et al* 2013).

La proteína Rep y el origen de replicación en la IR del genoma de geminivirus pueden ser un blanco terapéutico relevante para el desarrollo de agroquímicos antivirales, debido a la alta conservación de las secuencias de Rep entre la familia *Geminiviridae*, así como la secuencia del origen de replicación en la IR. Además de péptidos aptámeros que reconozcan Rep, se ha descrito proteínas tipo dedos de Zinc, que pueden competir con Rep a nivel de sitio de unión. Estas proteínas reconocen la zona de enlace de Rep en la región IR de TYLCV (zona de iterones), así como la secuencia de corte catalítico TAATATT↓AC, realizando entonces una mimetización de la actividad bioquímica de la molécula de inicio de la replicación viral, no se han reportado ensayos *in vivo* que muestren su actividad antiviral (Mori T. *et al* 2012; Chen W. *et al* 2014).

Además del uso de la tecnología del DNA recombinante para la generación de líneas transgénicas que sobre expresen proteínas o péptidos antivirales, se ha planteado el uso de estas biomoléculas de manera exógena. Se ha observado que proteínas esterificadas derivadas de suero como lactoglobulina, lactoalbúmina y lactoferrina presentan actividad antiviral contra TYLCV, se reportó que plantas de tomate infectadas con TYLCV al ser tratadas con estas moléculas el contenido de DNA viral disminuyó (efecto curativo) (Abdelbacki A.M. *et al* 2010). Aunque no se ha descrito el mecanismo de acción de estas biomoléculas en este modelo de infección, se ha observado que estas proteínas inducen una respuesta altamente relacionada a una activación inmunológica en un modelo infectivo de tratamiento con TMV (Wang J. *et al* 2013).

### 2.5.3 Propuesta para el control químico directo de TYLCV

Comúnmente se utiliza el término control químico para referirse al uso de moléculas sintéticas o pequeñas moléculas naturales purificadas y aplicadas exógenamente a la planta. Se ha reportado el uso de eugenol, una molécula del grupo guaicol, la cual se considera como un inductor de resistencia contra TYLCV. Se ha observado que el tratamiento con esta molécula de manera profiláctica incrementa la acumulación de ROS y SA, así como la expresión de PR1 en plantas de tomate (Wang Chunmei y Fan 2013). El eugenol también activa la sobre expresión de la proteína SiPer1, el cual se ha sugerido ser un gen R, este es

inducible por ácido salicílico y ácido jasmónico, y se ha observado que el eugenol puede inducirlo y ofrecer una protección eficiente contra el desarrollo de la enfermedad causada por TYLCV (Sun W. *et al* 2016). Otros compuestos como derivados químicos de aminoácidos de la arginina e histidina han mostrado inducción inmunológica al activar enzimas relacionadas a defensa como peroxidasa (POD) y fenilalanina amonio liasa, PAL (de las ingles: phenylalanine ammonia lyase) manteniendo su actividad de activador de defensa en 3 líneas de tomate distintas infectadas con TYLCV (Deng Y. *et al* 2015). Hasta el momento no se ha reportado alguna molécula sintética pequeña que directamente interfiera con los eventos replicativos de TYLCV u otros geminivirus.

## **JUSTIFICACIÓN, HIPÓTESIS Y OBJETIVOS.**

### **Justificación**

La agricultura es una de las principales actividades humanas para el sustento nutricional y comercial. Los virus fitopatógenos son uno de los agentes etiológicos de mayor importancia fitosanitaria en los sistemas agrícolas debido a las pérdidas agroeconómicas que generan, además de la falta de estrategias para su control. Una de las virosis más importantes debido a su tipo de transmisión, dispersión geográfica y rango de hospedantes es la causada por el *Virus del enrollamiento de la hoja amarilla del tomate*, TYLCV. A pesar de que existen estrategias basadas en el uso de biomoléculas para el control directo del virus, estas requieren el uso de plantas transgénicas las cuáles su uso aún es controversial entre organizaciones internacionales de agricultura, haciendo difícil su aplicación en campo. Debido a lo anterior en este trabajo se plantea el uso de biomoléculas de origen vegetal como una alternativa para el control de esta virosis utilizando péptidos derivados proteínas de reserva de amaranto (*Amaranthus hypochondriacus*), eligiendo a aquellos que tras un proceso de selección molecular puedan unirse al origen de replicación del DNA de TYLCV y así bloquear o disminuir su proceso de replicación, actuando como un control correctivo del virus cuando este sea aplicado de manera exógena sobre plantas infectadas con el virus.

La hipótesis planteada en este trabajo es:

La semilla de amaranto contiene un alto porcentaje de proteínas de reserva, las cuales tienen un elevado porcentaje de aminoácidos básicos y aromáticos que pueden dar origen a péptidos con actividad biológica de unión a DNA. Si la interacción de algunos péptidos de amaranto es de alta afinidad hacia la secuencia de DNA del origen de replicación del TYLCV, entonces se espera que estos presenten actividad antiviral por alteración en la tasa de replicación del virus.

Para abordar esta hipótesis, se planteó el siguiente objetivo general:

Obtener y seleccionar péptidos derivados de la digestión enzimática de las globulinas de amaranto los cuales presenten actividad antiviral contra TYLCV.

Objetivos específicos:

- Determinar si los péptidos derivados de globulinas de amaranto presentan actividad biológica en plantas de promoción de crecimiento y activación de defensa contra TYLCV.
- Realizar la purificación de péptidos derivados de la fracción hidrolizada de globulina/albumina de semillas de *A. hypochondriacus*.
- Selección de péptidos con mayor interacción química hacia el origen de replicación de TYLCV mediante métodos espectrofotométricos y su posterior evaluación de su actividad antiviral en hospedantes experimentales y naturales.
- Demostrar el mecanismo de acción de los péptidos con mayor actividad antiviral mediante evaluación de su tasa replicativa y ensayos estructurales de interacción entre péptido y horquilla de replicación.

## 3.0 MATERIALES Y MÉTODOS

### 3.1 Obtención, purificación y aislamiento de péptidos bioactivos de globulinas y albúminas de amaranto.

A partir de semillas de amaranto, se procedió a la extracción de globulinas y albúminas como describen Romero-Zepeda y Paredes-López, 1995 con ligeras modificaciones. La harina producida tras la molienda de la semilla de amaranto se susendió en agua y se ajustó a pH 8.5, luego se extrajo por maceración con agitación a 4 °C durante 8 h y se reajustó nuevamente el pH a 7.0, para su posterior hidrólisis con papaína por 18 h. Una vez transcurrido el tiempo de hidrólisis se monitoreó por RP-HPLC en una columna de fase reversa C18 y en electroforesis SDS-PAGE. El proceso de hidrólisis y su monitoreo se repitió al menos 6 veces para asegurar repetibilidad. Los péptidos menores a 10 KDa se separaron mediante ultrafiltración. La solución obtenida se fraccionó en una columna de RP-HPLC C18, colectando las fracciones con señal de absorbancia a 280 nm. Este se tomó como criterio para incluir péptidos que posiblemente tuvieran aminoácidos aromáticos en su secuencia promoviendo interacción con bases nitrogenadas de esta biomolécula (Rajeswari M.R *et al* 1992; Rajeswari M.R *et al* 1987; Lee S. *et al* 2016; Kim Y. y Jo K. 2011). Además, en algunos casos la presencia de ese residuo de aminoácidos promueve la translocación hacia el interior celular (Chan D. I. *et al* 2006), favoreciendo su posible aplicación exógena en la planta. Los péptidos con señal mayor a 280 nm se purificaron completamente utilizando cromatografía de fase reversa (RP-HPLC). Una vez purificados, cada péptido se analizó por espectrometría de masas (MALDI-TOF) para analizar su relación carga/masa y así mismo se analizó la presencia de aminoácidos aromáticos mediante espectroscopia de fluorescencia.



### 3.2 Selección de péptidos con capacidad de interacción química hacia el OriRep de TYLCV.

Los péptidos puros se mezclaron separadamente de manera equimolar con una solución del oligonucleótido OriRep (5'-CGTATAATATTACCGGATGGCCGCGC-3), el cual incluye la secuencia que forma parte de la estructura de tallo y asa ubicada en la horquilla del origen de replicación de TYLCV y que es necesaria para el inicio de la replicación de todos los geminivirus a través del modelo del círculo rodante; la mezcla se incubó durante 10, 30, y 60 minutos y se procedió a medir la fluorescencia intrínseca del péptido con la fluorescencia de una solución del péptido sin oligonucleótido, utilizando la misma concentración y volumen final, durante el tiempo mencionado. En aquellos péptidos que se presentó un mayor abatimiento de la fluorescencia intrínseca se tomaron como candidatos para medir su constante de disociación ( $K_d$ ) mediante resonancia de plasmón localizada en superficie (LSRP) con nanopartículas de oro, se utilizó como control de interacción el péptido NIQGAKSSSDVKSYIDK (llamado RepApep, dicho péptido no mostró fluorescencia intrínseca, por lo cual se utilizó la técnica de LSRP) el cual contiene la secuencia de reconocimiento y corte catalítico de la proteína Rep hacia el asa del origen de replicación. El valor de  $K_d$  se calculó utilizando el método y modelo propuesto por Tan L. *et al* 2012. Sólo tres péptidos mostraron afinidad hacia OriRep en diferentes grados. El péptido con mayor índice de abatimiento fluorescente y con una menor  $K_d$  fue llamado AmPep1, seguido por AmPep2 y con muy baja afinidad el péptido AmPep3. AmPep1 se utilizó para los ensayos posteriores debido a su alta afinidad hacia OriRep.

### 3.3 Secuenciación e identificación de secuencias de los péptidos purificados

Una vez seleccionados los péptidos con mayor afinidad (AmPep1 y AmPep2) se analizaron por MALDI-TOF-TOF con la finalidad de obtener la secuencia del péptido. Las secuencias resultantes se analizaron bio-informáticamente en el servidor BLAST (Stephen F. *et al* 1997) restringiendo el alineamiento de secuencias a proteínas de plantas de la familia *Amaranthaceae*.

### 3.4 Inhibición de síntesis *in vitro* de DNA.

Utilizando la técnica de amplificación por el círculo rodante (RCA, del inglés *Rolling circle replication*), la cual utiliza como molde DNA circular, se procedió a verificar si el péptido AmPep1 y el péptido control RepApep tienen un efecto de bloquear o disminuir la síntesis *in vitro* de DNA viral. Se utilizó como molde un extracto de DNA proveniente de una planta infectada con TYLCV-[LV2015SATom] (Acceso no. KU836749.1), se cuantificó el DNA mediante qPCR absoluta y se ajustó la concentración de DNA viral. Se probaron concentraciones crecientes de ambos péptidos de manera separada (0, 1, 2, 5, 10, 20 y 30  $\mu\text{M}$ ) manteniendo constante la concentración de DNA viral a  $5 \times 10^6$  moléculas ( $N=3$  réplicas por concentración). Los oligonucleótidos utilizados en RCA para TYLCV se diseñaron para cubrir todo su genoma (ver Cuadro1, artículo 1) con una modificación de tipo PTO en la región 5'. Como control se utilizó el plásmido pUC18, el cual contiene horquillas de replicación de secuencia diferente a la de los geminivirus, utilizando el mismo número de copias de DNA que las utilizadas con TYLCV y las mismas concentraciones de péptidos. Para esta reacción se utilizaron iniciadores hexámeros aleatorios (Random primers) con la misma modificación tipo PTO. Los productos de RCA del virus y plásmido se analizaron por electroforesis en gel de agarosa para observar el efecto sobre la síntesis; dichos productos se ajustaron a una concentración constante y se digirieron con enzimas de restricción para observar el DNA viral monomérico y comparar el efecto de las distintas concentraciones de los péptidos en la síntesis. Los productos de la digestión enzimática se analizaron en gel de agarosa y la intensidad de la banda se cuantificó (número de píxeles por banda). El promedio de la intensidad de bandas entre las distintas concentraciones se comparó con la intensidad promedio de las bandas en la concentración 0  $\mu\text{M}$  de péptido, la cual representó un 100% de eficiencia media en la síntesis viral. Se realizó un análisis estadístico utilizando el modelo ANOVA de 1 vía, para encontrar si existía una diferencia significativa entre las diferentes concentraciones de péptidos en la reacción comparado con el control de 0  $\mu\text{M}$  de péptidos.

### 3.5 Pruebas biológicas

#### 3.5.1 Actividad biológica del extracto de péptidos en plantas de tomate y maíz.

##### *3.5.1.1 Efecto del extracto de péptidos sobre el crecimiento de tomate e inducción de defensa primaria.*

Se sembraron semillas de tomate (*S. lycopersicum*) en una mezcla de sustrato vermiculita: perlita (1:1). Durante todo el desarrollo del experimento las plantas se mantuvieron en una cámara climática con un fotoperiodo de 16 horas luz/8 horas oscuridad y se fertilizaron con una solución nutritiva comercial Hydrosol ® la cual contiene una proporción de macroelementos N:P: K (10:10:10). Una vez que las plántulas alcanzaron tres semanas de edad, fueron tratadas mediante aspersión foliar con una solución del extracto de péptidos a concentraciones de 100, 10, 1 y 0.1 mg/mL. Se utilizó una N=8 para cada grupo experimental. Un grupo experimental se asperjó con agua y funcionó como control basal. El tratamiento consistió en las aspersión de las soluciones de péptidos tres veces por semana durante 2 semanas consecutivas, una vez finalizado el esquema de tratamiento, se monitoreó el efecto en crecimiento en las semanas posteriores al tratamiento. 1 día concluido el esquema de tratamiento se colectaron muestras de hojas apicales y se evaluó la formación de especies reactivas de oxígeno (ROS) en los diferentes tratamientos, se realizó la tinción con diaminobenzidina (DAB) y paralelamente con azul de nitrotetrazolio (NBT) sumergiendo las hojas en una solución de de DAB 1 mg/mL o en NBT 0.1 mg/mL exponiéndolas a vacío por 15 minutos y posteriormente se incubaron durante 12 horas, posteriormente las hojas se traspasaron a una solución de destinción (etanol:ácido acético:glicero, 3:1:1) hasta la decoloración de clorofila. La formación de ROS se observó con el microscopio estereoscópico dando como resultado positivo a formación de peróxido la presencia de precipitados marrón en las hojas en la tinción con DAB y como positivo a la formación de superóxido la presencia de precipitados azules en la tinción con NBT.

### 3.5.1.2 Efecto del extracto de péptidos en la inducción de defensa en plantas de tomate contra TYLCV.

Se sembraron semillas de tomate del híbrido comercial Maya de la variedad bola bajo las condiciones descritas anteriormente. Una vez alcanzadas las tres semanas las plántulas fueron transplantadas en sustrato nuevo y fueron cultivadas en invernadero, fertilizando como se mencionó arriba. Una semana posterior al trasplante se realizaron los tratamientos experimentales. Se crearon grupos experimentales de plantas en ambas variedades de prueba teniendo una N=6 por grupo experimental. El primer grupo fue el control basal, el cual solo fue asperjado con agua sin infección viral. El grupo control de infección fueron plantas asperjadas con agua y posteriormente al esquema de tratamiento se infectaron con TYLCV aislado Sinaloa clona LV2015SATom Acs: KU836749.1. Un tercer grupo experimental fue asperjado con una solución de extracto de péptidos a concentración de 1mg/mL (concentración que ejerció mejor crecimiento e inducción de respuesta inmunológica primaria), asperjando hasta escurrimiento durante tres días consecutivos por dos semanas consecutivas y sin infección viral con la finalidad de observar el efecto del péptido en la fisiología de la planta (*Mock*). El cuarto grupo fue tratado con el extracto de péptidos como se describe anteriormente, pero fue agroinfectado con TYLCV para observar si el extracto de péptidos ejerce defensa contra la enfermedad. Una vez agroinfectadas las plantas se mantuvieron en invernadero; cuando el control de infección comenzó a desarrollar síntomas se extrajo DNA mediante el método CTAB (Doyle J.J. y J.L. 1987) y se realizó una PCR estándar utilizando los iniciadores degenerados universales para begomovirus AC1048 y AV548 (Wyatt y Brown 1996) para verificar la infección sistémica y se monitoreó el desarrollo de síntomas por 15 días más. Una vez transcurrido este tiempo se colectaron muestras de hojas apicales de todos los grupos y variedades experimentales y se procedió a extraer DNA y se cuantificó el título viral mediante qPCR utilizando los oligonucleótidos OVS/OCS reportados por Rodríguez Negrete E.A. *et al* 2014. Se realizó un análisis estadístico utilizando el modelo ANOVA de 1 vía, para encontrar si existía una diferencia significativa del título viral entre los diferentes tratamientos. Paralelamente se colectaron muestras de los grupos experimentales para extraer RNA utilizando el kit Spectrum™ Plant Total RNA Kit, se cuantificó el RNA y se ajustó a una concentración de 50 ng y se realizó

una reacción de retrotranscripción (RT) y posteriormente una PCR estándar para amplificar una región del gen *LePAL* el cual codifica para la enzima Fenilalanina amonio liasa, PAL utilizando los oligonucleótidos *forward* 5'-CTGGGGAAGCTTTTCAGAATC-3' y *reverse* 5'-TGCTGCAAGTTACAAATCCAGAG-3' (Song Y. *et al* 2015). Como gen de referencia se utilizó a el gen que codifica para la ubiquitina 3 (*UBI*) con los oligonucleótidos *forward* 5'-TCCATCTCGTGCTCCGTCT-3' y *reverse* 5'-GAACCTTTCCAGTGTCATCAACC-3' (Mascia T. *et al* 2010). Los productos de la RT-PCR se analizaron en electroforesis en gel de agarosa.

El experimento se monitoreó hasta que los frutos en las plantas se maduraran y con un desarrollo óptimo para cosecha. Se cosecharon los frutos y se comparó la producción entre grupos experimentales y entre variedades.

### 3.5.1.3 Efecto del extracto de péptidos en el desarrollo de tizón foliar en maíz.

Con la finalidad de estudiar si el extracto de péptidos tiene actividad biológica en otras especies vegetales y si induce defensa contra otros fitopatógenos se procedió a realizar un ensayo *in vitro* para verificar dicha premisa. Se cortaron fragmentos de hojas de maíz de 4 semanas de edad. Se realizaron grupos experimentales con una N=3 como sigue: Un grupo denominado control sano, se trató únicamente con agua destilada estéril; un segundo grupo denominado control de infección se trató con agua destilada estéril y una suspensión 100000 conidios/mL de *Helminthosporium* sp; un tercer grupo tratado con una solución de Actigard® a 300mg/L e infectado posteriormente con *Helminthosporium* sp, y un cuarto y quinto grupo tratados con una concentración de 1 y 0.1 mg/mL del extracto de péptidos y posteriormente infectados con el hongo. Las hojas se asperjaron con agua, BTH o extracto de péptidos según el grupo experimental y 24 horas después se infectaron agregando 50 µL de la suspensión de *Helminthosporium* sp. en 4 puntos equidistantes sobre la hoja. Se monitoreó el desarrollo de lesiones durante una semana. Las hojas fueron mantenidas en cámaras húmedas durante el experimento y en fotoperíodo de 16 horas luz/8 horas oscuridad.

### 3.5.2 Actividad antiviral en *Nicotiana benthamiana* y *Solanum lycopersicum*

Plantas de *N. benthamiana* y *S. lycopersicum* de tres semanas de edad se agroinocularon con el virus TYLCV-[EE-Imp-05-08] (Acceso no. HF548826). Cuando las plantas manifestaron indicios de síntomas de la enfermedad, aproximadamente a las 2 semanas de inoculación, se extrajo DNA de las hojas apicales utilizando el método de CTAB (Doyle J.J. y J. 1987). Se realizó una PCR estándar para verificar la infección sistémica utilizando los iniciadores degenerados universales para begomovirus AC1048 y AV548 (Wyatt y Brown 1996). Una vez que se confirmó la infección, se agruparon plantas infectadas con un N=6, un grupo asignado como “Tratamiento” se infiltró con una solución de péptido 100 mg/L (concentración aproximada a 30  $\mu$ M que muestra efecto de abatimiento de síntesis *in vitro* de DNA viral en la reacción de RCA, ver artículo 1, figura 3) en todas las hojas apicales con síntomas. Un segundo grupo se utilizó como control de infección (sin tratamiento) y un tercer grupo se infiltró con buffer. Un grupo de plantas sanas (N=6), se utilizó como control sano, y otro grupo fue tratado con el péptido. El progreso de la enfermedad se monitoreó a los 0, 7, 15 y 21 días post tratamiento (dpt). En cada día de monitoreo se tomaron muestras de las hojas apicales nuevas para extracción de DNA y se cuantificó el virus mediante qPCR utilizando los oligonucleótidos OVS/OCS reportados por Rodríguez Negrete E.A. *et al* 2014.

### 3.5.3 Evaluación *in vivo* de la tasa replicativa del virus.

Plantas de *N. benthamiana* de tres semanas de se agroinocularon con TYLCV -[EE-Imp-05-08] (Acceso: HF548826) y se verificó la infección sistémica como se describió en la sección anterior tanto en hojas apicales como en hojas completamente extendidas. En las hojas más extendidas y sistémicamente infectadas (superiores a donde se inoculó) se infiltró en la mitad derecha de dicha hoja una solución de 5, 15 y 30  $\mu$ M de AmPep1 de manera separada (2 hojas por planta y 3 plantas por cada concentración, teniendo en consideración que fueran de homólogas en su desarrollo), mientras que en la parte izquierda se infiltró solución de infiltración (ver figura 3, manuscrito 2). Siguiendo el mismo diseño experimental, otro grupo de plantas fue tratado bajo las mismas condiciones, pero con el péptido control RepApep. Se

tomó una muestra de cada hoja y planta de las diferentes concentraciones a las 0, 12, 48 y 72 horas post tratamiento, paralelamente un grupo de plantas sistémicamente infectadas fueron tratadas en hojas homólogas a los tratamientos mencionados, pero utilizando solo solución de infiltración tanto del lado izquierdo como derecho; estas fueron usadas como control de infección.

De cada muestra se extrajo DNA mediante el método de CTAB y se procedió a cuantificar las cadenas virales (VS) y complementaria (CS) de TYLCV, así como el DNA viral total en la planta, de acuerdo con el protocolo descrito por Rodríguez Negrete *et al* 2014 y manuscrito 2. Los resultados obtenidos fueron analizados para observar si existía una alteración en la producción de VS o CS dependiente de la concentración del péptido en el tejido tratado como en el no tratado con péptido, asimismo una dependencia entre concentración-respuesta-tiempo. Se realizó un análisis tipo ANOVA de dos vías, comparando todos los tratamientos con el control de infección.

#### 3.5.4 Translocación del péptido en las células.

El péptido AmPep1 fue marcado con isotiocianato de fluoresceína isómero I (FITC, Sigma-Aldrich) de acuerdo con las indicaciones de manufactura. Se utilizaron hojas apicales pequeñas (aprox. 1 cm<sup>2</sup>) de *N. benthamiana* con tres semanas de edad. Las hojas se incubaron en una solución acuosa de AmPep1-FITC 5 µM por 10, 30 y 60 minutos a temperatura ambiente y otro lote a 4 °C (3 hojas por tiempo). Inmediatamente cumplido el tiempo de incubación las hojas se lavaron con una solución de SDS 0.5% y se fijaron en una solución de glutaraldehído 1% (Pasternak T. *et al* 2015). Posteriormente, las muestras se tiñeron con 2-(4-amidinofenil)-1*H*-indol-6-carboxamida (DAPI) a una concentración de 1 µg/mL. Como control se utilizaron plántulas no tratadas con péptido marcado. Las plántulas se analizaron en el microscopio confocal Nikon A1R+ STORM utilizando un láser de argón con longitud línea de excitación de 492 nm para el FITC y un filtro de excitación de 405 nm para el DAPI. La auto fluorescencia de la clorofila se detectó empleando un filtro de paso entre

650–800 nm, las observaciones se realizaron en un objetivo de inmersión de agua de 60X. Las imágenes se analizaron en NIS-Elements-Viewer 4.20 (Nikon).

### **3.6 Interacción de AmPep1- OriRep mediante espectroscopia Raman.**

El espectro Raman de cada una de las biomoléculas y de la mezcla de interacción se grabó usando la técnica de drop-coating deposition Raman (DCDR) (Filik, J. y Stone, N. 2007), debido a las bajas concentraciones de biomoléculas que se estaban manejando en este experimento. Para preparar las soluciones de análisis Raman, a partir de las soluciones concentradas tanto de AmPep1 y del oligonucleótido 5'-GGCCATCCGTATAATATTACCGGATGGCC-3' correspondiente a la horquilla de replicación de TYLCV, se tomó una alícuota necesaria para obtener 1  $\mu\text{mol}$  de cada biomolécula, esta alícuota se concentró hasta sequedad y se solubilizó en 10  $\mu\text{L}$  de buffer (10mM Tris-HCL, 50mM NaCl, pH 7.4). Para realizar la interacción, se preparó por separado cada una de las biomoléculas como se mencionó con anterioridad a una concentración final de 1  $\mu\text{mol}$ , cada una fue solubilizada en 5  $\mu\text{L}$  de buffer y estas soluciones se mezclaron en un solo tubo (relación molar final 1:1), se homogenizaron por 1 minuto con pipeta y se incubaron 10 minutos a temperatura ambiente para permitir la interacción entre las moléculas. Posteriormente 10  $\mu\text{L}$  de cada solución analítica (Péptido, DNA o mezcla) se depositaron sobre un sustrato de vidrio forrado con aluminio y se dejaron secar a temperatura ambiente hasta la formación de un anillo sobre la zona de depósito de la gota. El espectro Raman de cada condición se adquirió usando el equipo Confocal-Microscopy Witek Raman Alpha 300 con un objetivo de agua 100X, N.A. 0.9 y con un láser de excitación de 532 nm. Los datos espectrales se capturaron por un lector CCD, con un tiempo de integración de 3s y una potencia del láser de 26.4 mW para la muestra de DNA y de 20 mW para el péptido y la mezcla de interacción. La zona de enfoque se realizó en la región del anillo de la gota seca formada. Previamente se obtuvo un espectro Raman del buffer para descartar señales en el análisis. Se obtuvieron espectros de 10 diferentes áreas, se obtuvo el promedio de los espectros utilizando OriginPro software versión 2017, se realizó el suavizado de los espectros usando el método Adjacent-Averaging y se normalizaron con la señal del pico máximo del espectro en la región de 600 a 1800  $\text{cm}^{-1}$ . Se realizó un análisis de deconvolución de la región



de 1620 a 1720  $\text{cm}^{-1}$  utilizando el programa PeakFit v4.12 considerando un buen análisis de deconvolución cuando la  $R^2$  alcanzó un valor mayor a 0.99.

## 4.0 RESULTADOS Y DISCUSIÓN

### 4.1 Péptidos bioactivos derivados de globulinas de amaranto.

La hidrólisis enzimática de las globulinas y albúminas de amaranto se realizó con papaína, a pesar de que la enzima no genera un patrón de corte hacia aminoácidos específicos como lo hace la tripsina, por ejemplo, se lograron obtener condiciones reproducibles para todas las repeticiones de hidrólisis de acuerdo con su monitoreo en RP-HPLC y patrón de masas. La papaína es una enzima tipo serina-proteasa que ha mostrado tener preferencia hacia residuos de glutamina en sitios de corte P1 y P1' seguido por residuos de valina, alanina y serina en la posición P2 y P2' de la zona de hidrólisis (St. P.M. *et al* 1999; Choe Y. *et al* 2006). El uso de enzimas con una baja especificidad, así como el uso de cocteles enzimáticos es preferible para la obtención de péptidos bioactivos, debido a que se puede incrementar la población de residuos terminales en el péptido, lo que conlleva a generar una población peptídica con diferentes propiedades fisicoquímicas como punto isoeléctrico, solubilidad, transporte al interior de tejidos, propiedades ópticas como fluorescencia intrínseca, etc (Panchaud A. *et al* 2012).

Como primera parte de esta tesis se analizó la actividad biológica del extracto de péptidos obtenidos sobre plantas de tomate y maíz analizando si estos pueden tener actividades como promotores de crecimiento o inductores de defensa contra TYLCV y otros fitopatógenos. De esta manera se puede especular acerca de la diversidad en la población de estas biomoléculas al generar más de una bioactividad en plantas. Se demostró que este extracto puede generar inducción de crecimiento y desarrollo en plantas de tomate, ver artículo 3. Como se observa en la (Figura 3A) a concentraciones de 1 y 0.1 mg/mL comparado con el control basal únicamente tratado con agua, hay un incremento visible en el desarrollo de la planta; una explicación para el efecto observado puede ser asociada a que algunos de los péptidos pueden generar cascadas de señalización las cuáles enciendan la expresión de genes codificantes para la proteína expansina en tejidos aéreos tal y como demostró Ertani A. *et al* 2017 al verificar que un hidrolizado proteico de alfalfa induce la sobreexpresión del gen mencionado en tomate, así como la sobre expresión del gen codificante para la glutatión-S-trasferasa y otros

genes relacionados al catabolismo de amino ácidos. A concentraciones de 10 mg/mL el desarrollo apical de la planta es visulamente similiar al control basal, lo que podría sugerir que un incremento en la concentración del extracto peptídico no favorece la entrada o penetración de estas moléculas al interior del tejido y esto puede ser debido al tamaño de la gota atomizada que se forma, la cual visulamente es mas grande a concentraciones de 10mg/L comparado con las gotas generadas por el espray de las concentraciones de 1 y 0.1 mg/mL. Se ha reportado que la prescencia de moléculas poliméricas incrementa el tamaño de las gotas de un espray en formulaciones agroquímicas a manera concentración dependiente (Williams P. A. *et al* 2008), esto puede traer beneficios en una formulación completa, sin embargo también se corre el riesgo que el aumento en el tamaño de la gota favorezca que esta caiga de la superficie foliar no deando tiempo a que las moléculas activas ingresen al tejido (*Pesticide Environmental Stewardship*, Consultado Noviembre de 2018), reduciendo significativamente su actividad biológica como se observa en este estudio en concentraciones de 10 mg/mL.

En la (Figura 3B) se observó además que el extracto peptídico puede activar la respuesta inmune innata por la producción de ROS y puede deberse a que una parte de la población de péptidos en el extracto presenten secuencias similares a patrones moleculares asociados a patógeno o a daño. Se ha descrito que algunos péptidos en *Arabidopsis thaliana* pueden inducir defensa al actuar como factores de transcripción para proteínas de membrana necesarias para activar defensa primara (Krol E. *et al* 2010; Yamada K. *et al* 2016. Se evaluó si la defensa inducida por el extracto peptídico en tomate es capaz de prevenir el desarrollo de la infección por TYLCV.

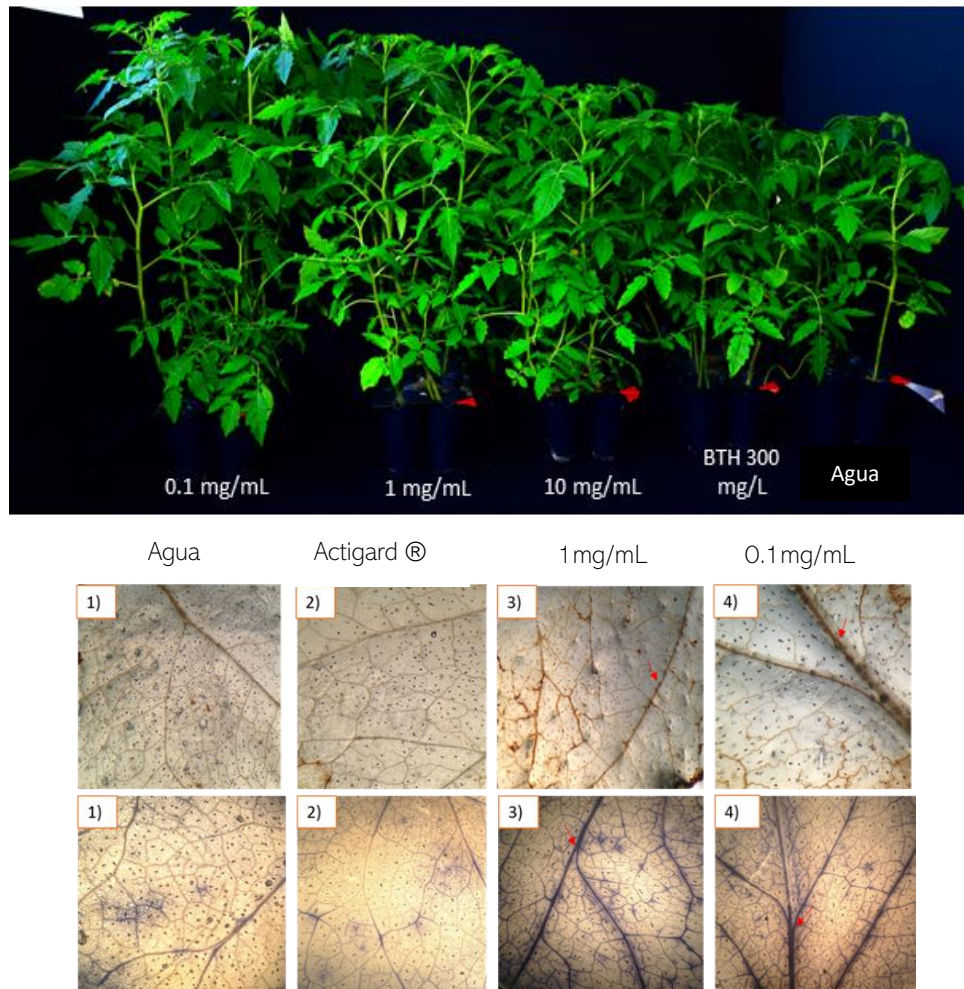


**Figura 3. Efecto de los péptidos derivados del hidrolizado de globulina de amaranto en la promoción de crecimiento e inducción de especies reactivas de oxígeno en tomate.** A)

Las plantas de tomate (N=8 por tratamiento) fueron asperjadas con tres concentraciones distintas del extracto peptídico, se observa que las concentraciones de 1 y 0.1 mg/mL inducen la mejor promoción en desarrollo foliar y desarrollo apical. B) El extracto de péptidos induce formación de ROS en hojas de tomate (flechas rojas), se observa la formación de peróxido (precipitados marrones) en las zonas intervenales del tejido así como la formación de superóxido (precipitado azul) en ambas dosis experimentales. Para ambos experimentos se utilizó el compuesto comercial inductor de resistencia sistémica Actigard® que contiene como principio activo benzotiadiazol-S-mentil (BTH), nuestros resultados indican que el extracto peptídico además de inducir respuestas de defensa primaria tiene la función de inducir crecimiento, mientras que el BTH no presenta la función de promoción de desarrollo comparado con el control basal tratado con agua.

Para corroborar dicho efecto se evaluó un híbrido comercial (tomate Maya) y una variedad comercial (bola), los resultados mostrados en la (Figura 4 A y B) muestran que el tratamiento

con el extracto de péptidos previene el desarrollo severo de la virosis, es notorio como los síntomas se ven reducidos en la planta tratada e infectada comparado con las plantas del control de infección la cual presenta enanimos comparado con las demás, enchinamientos, disminución de lámina foliar, ampollamientos y clorosis, el efecto protector del extracto de péptidos es además reflejado en el título viral el cual disminuye significativamente en las plantas tratadas comparado con las no tratadas, (Figura 4B). Para explicar el posible mecanismo de acción que generan el extracto se monitoreó la activación de un gen relacionado a la vía del ácido shikímico, la cual es una de las principales vías metabólicas relacionada a defensa en las plantas (Alvarez A. *et al* 2016), en la (Figura 4C) se observa que la enzima fenilalanina amonio liasa, PAL, se sobre expresa en plantas tratadas (*Mock*) con el extracto de péptidos respecto al control basal. Dicha enzima se encargará de la síntesis de precursores de coumarinas, ácido salicílico y precursores de lignina, los cuales participarán en el desarrollo de defensa molecular y estructural, respectivamente (Al-Amri S. M. 2013). Se puede pensar que otra vía por la cuál la planta activa señales de defensa al ser tratada con un extracto peptídico derive del catabolismo de los aminoácidos, es bien sabido que el catabolismo de lisina en plantas es dado por la ruta de la sacaropina, dicha ruta metabólica genera productos relacionados a defensa como el pipercolato el cual es un metabolito indispensable para mantener la homeostasis en estrés biótico y abiótico (Braun H. *et al* 2015). El catabolismo de los aminoácidos además generará moléculas intermediarias de vías anfibólicas como acetil coenzima A, succinato, acetoacetato, etc. El incremento en la producción de estos intermediarios de vías centrales traería como consecuencia un mejor desarrollo de la planta y de los frutos, en la (Figura 4D) se observa un incremento significativo en el tamaño de los frutos de las plantas tratadas con el extracto peptídico comparado al control basar y al control de infección.

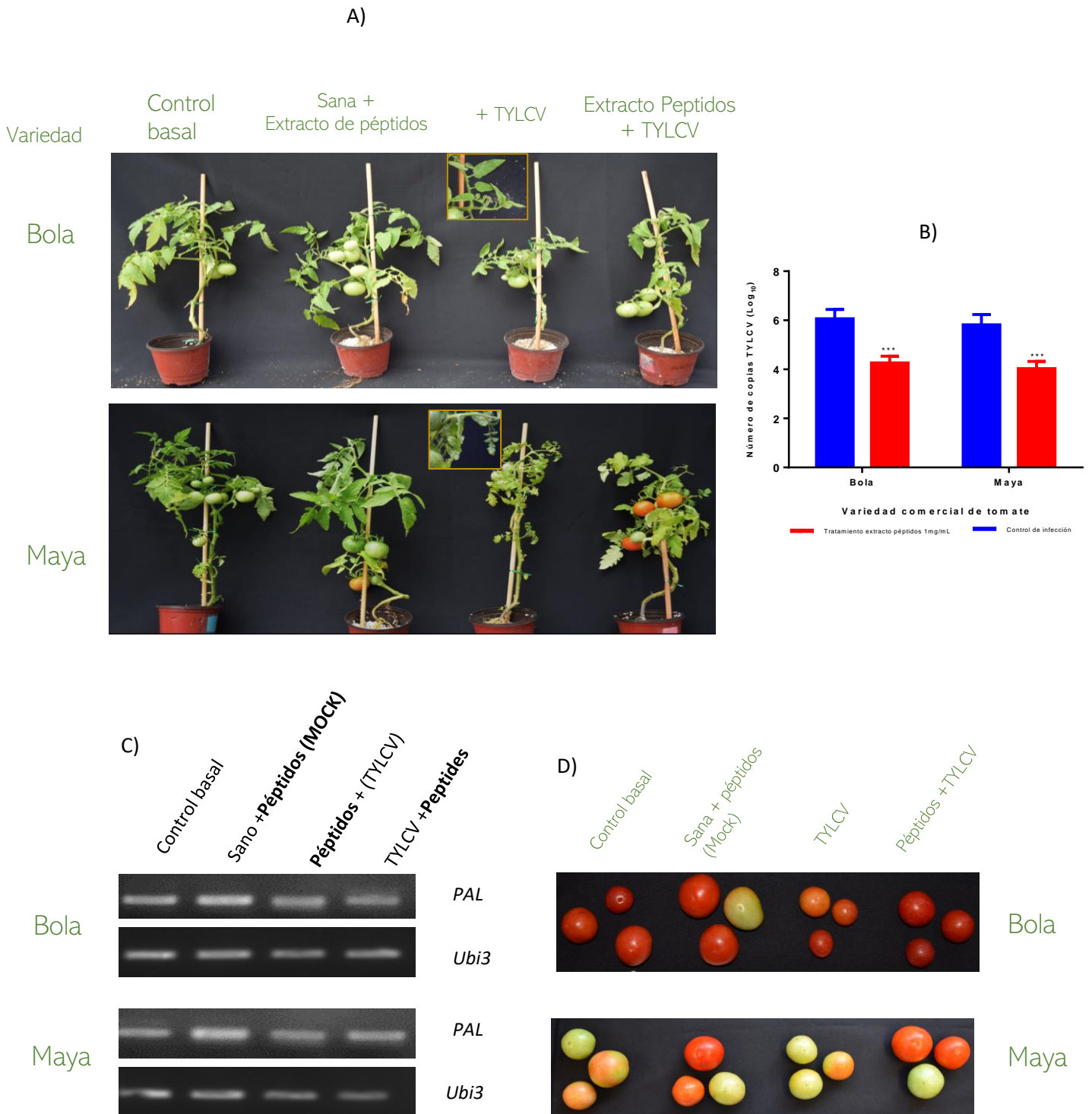


**Figura 4. Efecto de inducción de defensa del extracto de péptidos en tomate sobre el desarrollo de la enfermedad por TYLCV.** A) Se evaluó el efecto de inducción de defensa sobre plantas de tomate (N= 6 por grupo experimental) generado por el hidrolizado de globulinas de amaranto en dos

variedades comerciales de tomate (Bola y Maya) susceptibles a TYLCV. Las plantas fueron tratadas a la concentración de 1 mg/mL durante dos semanas, una semana post tratamiento las plantas fueron infectadas con el aislado Sinaloa de TYLCV clona LV2015SATom. Acs: KU836749.1 mediante agroinoculación. Las plantas se mantuvieron en condiciones de invernadero. El desarrollo de síntomas se monitoreó por aproximadamente un mes post inoculación. En la imagen se muestra el efecto sobre el desarrollo sintomático que induce el tratamiento con el hidrolizado. En ambas variedades, las plantas tratadas con dicha solución no muestran desarrollo severo de síntomas comparado con el control de infección, el cual muestra en variedad Bola enanismo, ampollamientos en hojas, encucharamientos, disminución de lámina foliar, acortamiento entre nudos y clorosis generalizada en el caso de la variedad Maya (ver fotos de acercamientos). Es notorio como además se aprecia visiblemente un incremento en el desarrollo foliar en los tratamientos *Mock*, los cuales son plantas sanas asperjadas únicamente con la solución de péptidos. B) Cuantificación de DNA viral. Se observa que las plantas tratadas con el extracto muestran un título viral significativamente menor a un mes post infección comparado al control de infección, los asteriscos indican diferencia significativa con respecto al grupo control de infección con una ( $P < 0.05$ ), el resultado es un promedio del análisis de 6 muestras biológicas independientes para cada grupo. C) El tratamiento con el extracto de péptidos induce la expresión de la enzima Fenilalanina-amonio-liasa (PAL). Se observa que en ambas variedades estudiadas la enzima PAL, se encuentra ligeramente inducida cuando estas son tratadas con la solución de péptidos a 1mg/mL, el efecto es mejor observado en el grupo *Mock*. La enzima PAL es una de las principales participantes en la vía del ácido skikimico la cual es una ruta central para la biosíntesis de metabolitos relacionados a defensa; *Ubi3*, gen de referencia codificante para la Ubiquitina de tomate utilizado para realizar la RT-PCR, la imagen es una representación de tres muestras biológicas distintas para cada grupo experimental. D) Imagen representativa sobre los efectos de producción de tomate entre los diferentes grupos experimentales en las dos variedades de prueba respecto a los tratamientos con hidrolizado de globulina de amaranto. Las plantas del grupo *mock* presentan los tomates con mayor desarrollo, se observa que las plantas del control de infección tienen la fruta más pequeña respecto a los demás grupos experimentales, mientras que las plantas infectadas y tratadas desarrollan frutos similares al control basal, indicando el potencial efecto biológico de protección y desarrollo generado por el extracto de péptidos.

Para corroborar si el efecto inductor de defensa puede extrapolarse en otras especies vegetales, se realizó una prueba de inducción de defensa en maíz. En la (Figura 5) se puede observar que el tratamiento con el extracto peptídico previene la formación de lesiones asociadas a tizón foliar causado por *Helminthosporium* sp. teniendo un efecto similar al generado por un inductor de defensa comercial (Actigard®, el cual contiene como principio activo benzotiadizol-S-metil). Una característica notable es que el tratamiento con el extracto induce lesiones de hipersensibilidad cuando se encuentra el patógeno lo que puede dar indicio de que este ha activado la respuesta inerte para detener el avance del patógeno por el tejido (ver artículo 3).

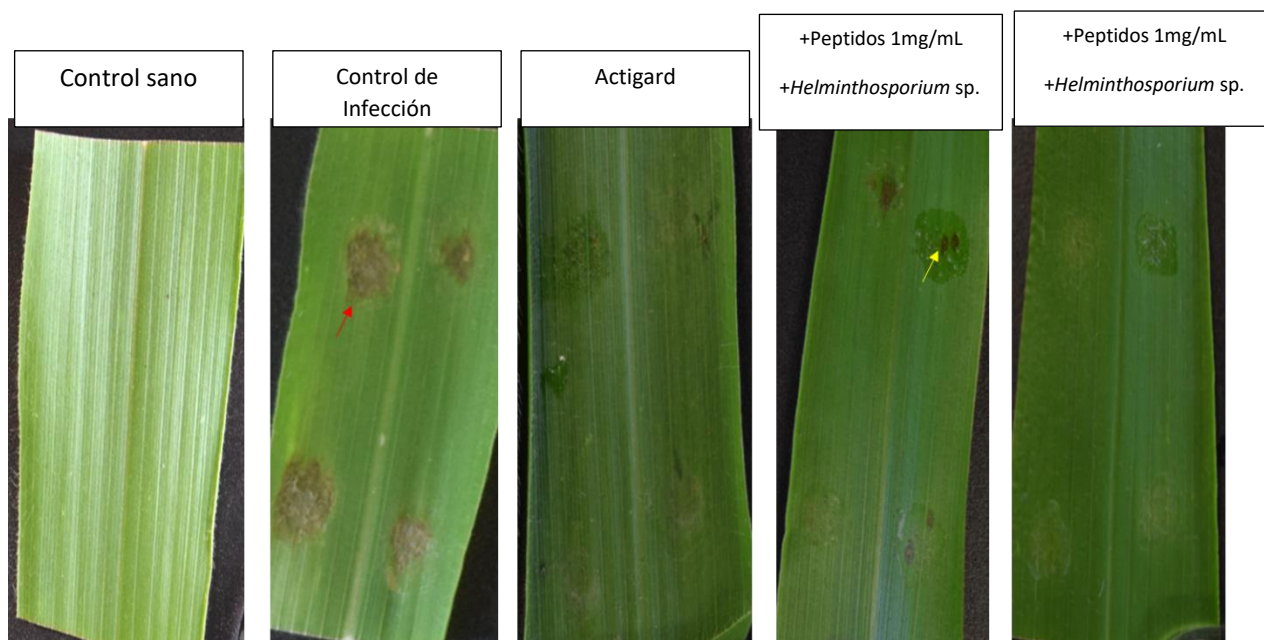


**Figura 5. El hidrolizado de glubulinas de amaranto induce respuesta preventiva contra manchado foliar por *Helminthosporium* sp. en maíz.** Con la finalidad de evaluar si el efecto biológico de inducción de defensa producido por el extracto de péptidos podría ser repetible en otra especie vegetal y en otro modelo fitopatológico, se realizó un ensayo de protección en hojas de maíz contra la enfermedad de tizón foliar causado por *Helminthosporium* sp. Las plantas fueron asperjadas con la solución de péptidos y 24 horas después infectadas con una suspensión de esporas del hongo, se observa que el extracto de péptidos a las concentraciones de 1 y 0.1 mg/mL protegen del desarrollo de lesiones características de tizón comparadas con el control de infección, en donde se observa claramente la zona de desarrollo fúngico (flecha roja). El extracto de péptidos tiene una actividad similar al inductor comercial de resistencia Actigard®, retardando el desarrollo del tizón. Flecha amarilla señala zonas de hipersensibilidad generadas por exaservación de respuesta de defensa. Imagen representativa de tres experimentos independientes a 5 días por infección.

Los resultados de esta sección indican que la digestión de proteínas de amaranto genera una población de péptidos con uso potencial en agricultura para promoción de crecimiento y protección vegetal contra TYLCV en tomate y previene el desarrollo de manchado foliar fúngico en maíz.



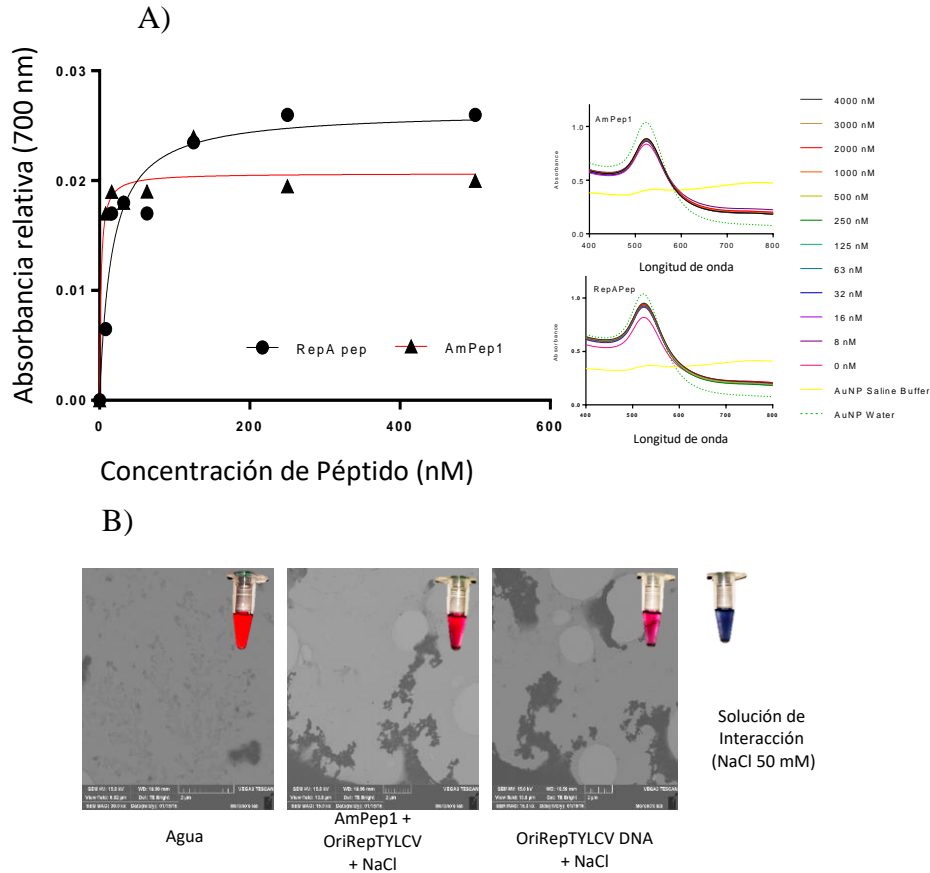
## 4.2 Selección y purificación de péptidos con afinidad hacia el OriRep de TYLCV.

El extracto peptídico se separó cromatográficamente mediante RP-HPLC usando una columna C18, de este análisis se obtuvieron dos fracciones principales las cuales se recircularon en la columna cromatográfica para separar sub-fracciones que presentaron señal de absorción a 280 nm, como se mencionó en la sección de metodología, este fue un criterio de inclusión de péptidos para ensayos posteriores debido a que la presencia de aminoácidos aromáticos como triptófano, además de tener una ventaja para su análisis de interacción con otra biomolécula. Teniendo en cuenta estas consideraciones se seleccionaron 10 péptidos de los cuales, solo tres mostraron interacción con el OriRep (utilizando la técnica de titulación de fluorescencia y por LSRP). El de mayor afinidad fue llamado AmPep1 ( $K_d = 1.4$  nM), seguido por AmPep2 ( $K_d = 1.8$   $\mu$ M) y finalmente AmPep3 mostró muy poca afinidad (valor de  $K_d$  arriba de 10 mM, lo que significa que no tiene afinidad suficiente al receptor). AmPep1 se seleccionó para los posteriores ensayos de actividad biológica debido a que su constante de disociación con OriRep es muy similar al péptido sintético RepApep, el cual contiene la secuencia de Rep que tiene capacidad de unión a la estructura de asa en la secuencia TAATATTAC en el origen de replicación así como el sitio catalítico para apertura de esta estructura secundaria, por lo que este péptido se utilizó como control de interacción (Figuras 6 y Figura 2 del artículo1).

La fuerte interacción de AmPep1 con OriRep puede deberse a una interacción directa entre la lisina (K), arginina (R) y el triptófano (W) del péptido AmPep1 (SVGRKWRMKWAQMRQQ) con el esqueleto de fosfatos y las bases nitrogenadas de OriRep. La presencia de aminoácidos básicos como K y R pueden favorecer la interacción electrostática entre los grupos con carga positiva de los residuos de la cadena lateral de K y R con la carga negativa presente en el esqueleto de fosfato, los grupos amino de K y guanidino de R se encuentran protonados al pH de trabajo (pH 7.4). Se ha observado que dichos aminoácidos básicos pueden alterar la estructura secundarias de DNA, pudiendo alterar la conformación de dicha molécula (Rajeswari M.R *et al* 1992 ; Roy K.B. *et al* 1992). Además, puede ser favorable la formación de puentes de hidrógeno por estos aminoácidos. La presencia de W es químicamente importante en proteínas o péptidos de unión a DNA ya que

estos pueden interactuar directamente mediante electrones  $\pi$ . Esta interacción fue observada al analizar el decaimiento en la fluorescencia intrínseca del péptido cuando este se hace interactuar con OriRep (ver Figura 2 del artículo 1). Se ha reportado que la presencia de las secuencias continuas de KW favorece la unión de estas biomoléculas a DNA, y favorablemente en regiones ricas en adenina (A) y timina (T), como es el caso de la secuencia del oligonucleótido en estudio (Rajeswari M.R *et al* 1987; Lee S. *et al* 2016; Kim Y. y Jo K. 2011). En la secuencia de AmPep 1 los residuos de triptófano (W) se encuentran próximos (SVGRKWRMKWAQMRQQ) a diferencia del péptido AmPep2 (MSVGRKWRSTMKWAQ), la cercanía de estos residuos en AmPep1 podría potencializar un enlace más fuerte al blanco viral mediante interacciones  $\pi$  (Roy K.B. *et al* 1992).

Para corroborar la afinidad química de AmPep1 sobre OriRep se realizó la técnica de RCA, demostrándose que el péptido AmPep1 afecta de manera dependiente de la concentración a la síntesis *in vitro* de DNA viral, utilizando como control el plásmido pUC18 (el cual contiene también estructuras de inicio de replicación tipo tallo y asa). Se observó que la síntesis *in vitro* de este, no es afectada por AmPep1, sugiriendo que el tamaño y disposición tridimensional del asa en TYLCV lo hace más afín a AmPep1 que las localizadas en el plásmido (Ver Figura 3 del artículo 1). De manera interesante, se observó que la síntesis de DNA de PHYVV, es también inhibida por el péptido AmPep1, debido a que en ambos virus la secuencia de la horquilla de replicación es conservada, lo que sugirió explorar la actividad biológica antiviral *in vivo* de este péptido en modelos infectivos con ambos virus.



encuentran asociadas a una biomolécula o a un complejo de interacción (tubo azul), así mismo la agregación física es menor a cuando estas únicamente tienen capeado el oligonucleótido de prueba. Dichos cambios se presentan en forma de concentración dependiente. Detalles ver artículo 1).

### **4.3 Actividad antiviral de AmPep1**

Se infectaron plantas de *N. benthamiana* y tomate mediante agroinoculación con TYLCV y se trataron mediante infiltración de AmPep1 en las hojas apicales sintomáticas, después de 7 y 15 días de monitoreo. Las plantas de ambas especies comenzaron a disminuir el desarrollo sintomático (enchinamiento, clorosis, enanismo) comparado con el fenotipo medio del grupo control de infección (plantas infectadas sin tratamiento). Se midió además la concentración de DNA viral en todos los tratamientos, mostrando que las plantas tratadas de manera correctiva con AmPep1 disminuyen la concentración de DNA viral. Dicho resultado concuerda con los datos arrojados por los estudios químicos de interacción entre AmPep1 y OriRep, los cuales demuestran una alta afinidad entre estas dos moléculas y que *in vivo*, presentan repercusiones en la tasa de DNA viral, sugiriendo que AmPep1 interfiere directamente con los eventos de replicación del virus, teniendo como consecuencia una desaceleración en el progreso de la enfermedad (desarrollo sintomático y disminución del título viral) (Figura 7 y ver figura 4 del artículo 1). Cabe señalar que AmPep1 también mostró efecto antiviral sobre el progreso de la enfermedad causada por PHYVVV en *N. benthamiana*, que como se ha explicado anteriormente conserva la misma secuencia de la horquilla de replicación de TYLCV la cual es conservada entre toda la familia *Geminiviridae* (ver figura 5 del artículo 1).

Con el objetivo de verificar si el mecanismo de acción antiviral de AmPep1 fue debido a alteración de efectos replicativos de TYLCV, se procedió a cuantificar la cantidad de cadena VS y CS formada post tratamiento con el péptido utilizando la técnica de “2-steps-qPCR” propuesta por Rodríguez Negrete et al, 2014. En una mitad de una hoja de *N. benthamiana* agroinfectada con TYLCV, se realizó tratamiento con el péptido AmPep1 y RepApep de manera separada, mientras que la otra mitad fue tratada con solución amortiguadora. De las concentraciones ensayadas para ambos péptidos, 15 y 30  $\mu\text{M}$  mostraron una tendencia de abatir la concentración de VS y CS comparado con la concentración de estos intermediarios

genómicos virales en las zona de tejido foliar no tratada (ver Figura 3 del manuscrito 2), sin embargo a las 72 horas post tratamiento de la concentración de 30  $\mu\text{M}$  de AmPep1, se observó una diferencia significativa en la síntesis de dichos intermediarios comparado con la concentración inicial de VS y CS, además ambas concentraciones mostraron diferencia significativa con la zona del tejido foliar sin tratar. El péptido RepApep se utilizó como control mostrando de igual manera una reducción de la síntesis de cadenas viral y complementaria desde las 12 horas post tratamiento. La síntesis de VS es un producto directo de la síntesis por el modelo de círculo rodante, si VS tendió a disminuir en plantas tratadas con ambos péptidos (Rodríguez Negrete E.A. *et al* 2014). En nuestros resultados pudimos observar que AmPep1 tiene una acción directa bloqueando el inicio de la replicación viral al medir el abatimiento de la tasa de VS y CS, posiblemente interfiriendo la con la acción de la proteína iniciadora de la replicación en TYLCV (Rep) (ver Figura 8 y Figura 3 del manuscrito 2).

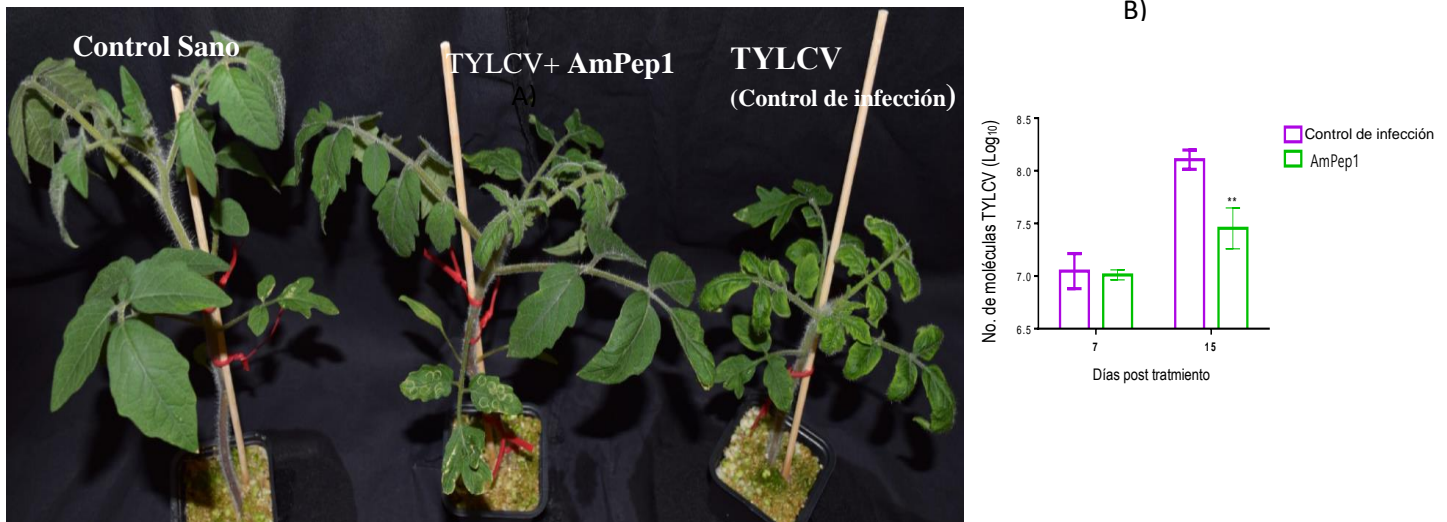


**Figura 7. Actividad antiviral de AmPep1 sobre TYLCV en plantas de tomate.** A)

Imagen comparativa entre las plántulas sanas, infectadas e infectadas con tratamiento de AmPep1 a los 15 días post tratamiento. El progreso de la enfermedad de las plántulas tratadas con AmPep1 fue comparado con aquel desarrollado por plántulas no infectadas y no tratadas (control de infección) a 15 días post tratamiento, el grupo de plántulas tratadas con AmPep1 presentan un retraso en el desarrollo sintomático comparado con el grupo control de infección el cual muestra una clara clorosis marginal, enanismo y enrollamiento notable, el grupo de plántulas tratadas con AmPep1 muestran solo ligeros enrollamientos en las hojas apicales sin clorosis evidente (todos los grupos analizados tiene una N=6). B) Cuantificación del

DNA total de TYLCV en hojas apicales de plántulas tratadas y no tratadas (control de infección) a los 7 y 15 dpTx. SD es indicada en líneas verticales, asteriscos: diferencia significativa de la media comparada con el control de infección ( $P < 0.05$ ), cada barra representa un contenido promedio de DNA viral de 6 plántulas.

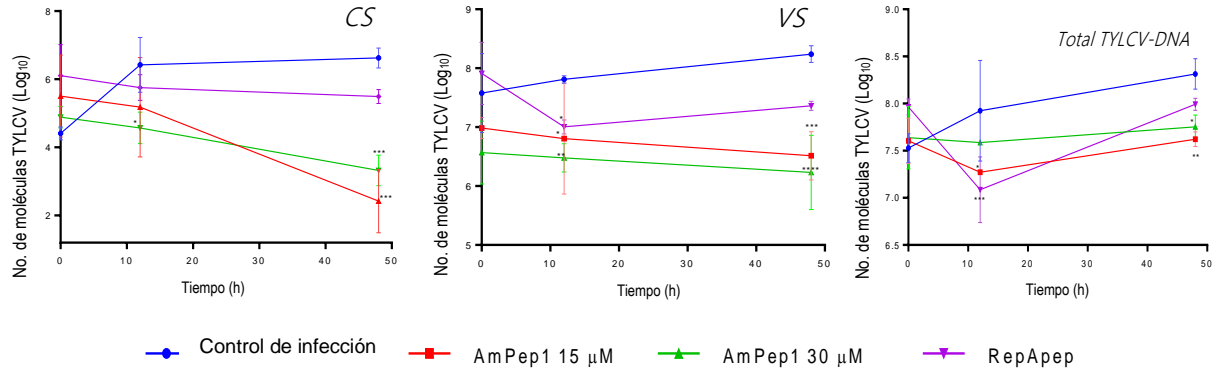


**Figura 8. El péptido AmPep1 disminuye la síntesis de intermediarios replicativos virales de TYLCV en *N. benthamiana*.**

A) Evaluación del efecto de AmPep1 sobre la síntesis de DNA de sentido complementario (CS) de TYLCV. C) Efecto de AmPep1 sobre la síntesis de DNA de sentido viral (VS) de TYLCV. D) Cuantificación del DNA total de TYLCV en post tratamiento con AmPep1. Los efectos sobre la tasa de replicación de CS, VS Y DNA total fueron monitoreados a las 0, 12 y 48 horas post tratamiento. Línea azul: control de infección (hojas sin tratamiento en ambos lados), roja: AmPep1 (15 uM), verde: AmPep1 (30 uM), morado: RepApep (control, 15uM), cada punto en el tiempo es una representación promedio del título de DNA de 6 hojas, barras verticales: desviación estándar (SD), asteriscos: Diferencia significativa de la media respecto al control de infección con una ( $P < 0.05$ ). (detalles ver manuscrito 2 Figura 3).

#### 4.4 Estudio de la interacción molecular entre AmPep1 y OriRep mediante espectroscopia Raman y modelado teórico.

La interacción entre la secuencia correspondiente al origen de replicación de TYLCV (OriRepTYLCV) y el péptido AmPep1, derivado de la globulina de amaranto, se estudió mediante espectroscopia confocal Raman. Se utilizaron el péptido AmPep1, purificado de un hidrolizado de globulina de amaranto y el oligonucleótido sintético 5'-GGCCATCCGTATAATATTACCGGATGGCC-3', correspondiente a la región tipo horquilla del OriRepTYLCV. Los espectros Raman correspondientes a cada una de estas dos biomoléculas se adquirieron de manera individual (ver figura 7, tabla 1 y figura 1 manuscrito 2). Para el caso del péptido AmPep1 (SVGRKWRMKWAQMRQQ), las señales observadas son generadas principalmente por el Trp, Ser y la Amida I. En el caso del Trp, los modos vibracionales observados se encuentran en las bandas de la región 760, 1010, 1074, 1550 y 1618  $\text{cm}^{-1}$  correspondiente a la respiración del anillo aromático, respiración del anillo fuera de fase del benceno y del pirrol, vibración de doblado en el plano de los C-C del Trp, estiramiento C2-C3 del anillo pirrólico, y el estiramiento C=C del anillo aromático, respectivamente (Wei F. *et al* 2008; Takeuchi H. 2003). Las señales del residuo de serina se representan principalmente por la banda de 853  $\text{cm}^{-1}$  que corresponde al estiramiento C-C adjunto al grupo OH (Jarmelo S. *et al* 2007). La señal de la amida I indica la estructura secundaria que el péptido adopta bajo las condiciones de estudio y corresponde principalmente a una estructura tipo alfa hélice y desordenada indicado por las bandas en posición 1658, 1670 y 1686  $\text{cm}^{-1}$  (Overman S. A. *et al* 1998; Rivas Arancibia S. *et al* 2017). Este hecho se pudo corroborar en la deconvolución de la banda de amida I dentro de la región de 1640 a 1700  $\text{cm}^{-1}$ , donde las señales deconvolucionadas en el espectro Raman a 1658, 1671 y 1689  $\text{cm}^{-1}$ ) corresponden a las señales de la estructura mencionadas, ver Tabla 2, manuscrito 2, contribuyendo mayoritariamente a la estructura del péptido.

El espectro del oligonucleótido OriRepTYLCV muestra señales Raman características de DNA (ver Figura 9 y Figura 1 del manuscrito 2), como modos vibracionales del enlace fosfodiéster (O-P-O) a 786 y 840  $\text{cm}^{-1}$  los cuales corresponden al alargamiento simétrico de este enlace, y la banda característica a 1092  $\text{cm}^{-1}$  representa la vibración del enlace dióxido del grupo fosfato (PO<sub>2</sub>) (Jangir D. K. *et al* 2014; Pagba C. V. *et al* 2010, Hernández B. *et*

al 2012). Otras señales que contribuyen a la formación del espectro Raman del DNA son las generadas por las bases púricas y pirimídicas, las bandas observadas en la región de 1332 y 1574  $\text{cm}^{-1}$  corresponden al alargamiento del anillo aromático de las bases púricas (A,G) (Gorelik V. S. *et al* 2014; Jangir D. K. *et al* 2014) , las contribuciones de sus grupos funcionales adjuntos a estas bases como el  $\text{NH}_2$  puede ser observado en la región de 1253  $\text{cm}^{-1}$  y a 1480  $\text{cm}^{-1}$  la señal correspondiente a la deformación del enlace C8=N7 de la Guanina (Ruiz Chica A. J. *et al* 2004; Lord R. C. *et al* 1967; Dina N. E. 2016). Las señales generadas por las bases pirimídicas se encuentran principalmente generadas por la timina, en las regiones de 1369  $\text{cm}^{-1}$  correspondiente al alargamiento C-N del anillo pirimidínico (Gorelik V. S. *et al* 2014; Dina N. E. 2016) , además esta base nitrogenada genera una banda de respuesta amplia en la región de 1660 a 1711  $\text{cm}^{-1}$  (ver manuscrito 2, Figura 1D), constituida principalmente por la contribución del alargamiento de los enlaces C=O, principalmente por el C2=O a 1660-1662  $\text{cm}^{-1}$ , y con una menor contribución del enlace C4=O en la región de 1690-1  $\text{cm}^{-1}$ (Movileanu L. *et al* 2002; Wojtuszewski K. *et al* 2004).



**Cuadro 4. Asignación de bandas del espectro Raman del oligonucleótido OriRepTYLCV, del péptido AmPep1 y de la matriz de interacción de ambas biomoléculas.**

Desplazamiento Raman (cm <sup>-1</sup> )			Desplazamiento Raman desde el origen	Asignación
Moléculas puras		Mezcla		
DNA (OriRepTYLCV)	Péptido AmPep1	OriRepTYLCV + AmPep1		
675		675	0	dG (respiración)
729		729	0	dA(est. C1-N9)
	760	751	-9	Trp (respiración en fase)
786		786	0	fosfodiéster (est. sim O-P-O)
840		840	0	fosfodiéster (est. asim O-P-O)
	853	857	+4	Ser (est. fuera del plano CH <sub>2</sub> -O)
	870	879	+9	Trp (curv. NH)
	884	879	-5	Trp (curv. indol más curv. del NH)
	945	958	+13	Ser (est. C-O)
	1010	1014	+4	Trp (resp.. fuera del plano de benceno y pirrol)
1019		1019	0	dG(def N-H)
1062		1070	+8	Desoxirribosa (est. C-O)
	1074		nd	Trp (curv. en el plano C-C)
1092		1096	+4	PO <sub>2</sub> <sup>-1</sup> (est)
	1131		nd	Péptido (balanceo C-NH <sub>3</sub> <sup>+</sup> )
1181		1181	nd	dA,G (est C5-C6)/ dT( est. en plano del anillo CH <sub>3</sub> )
	1202		nd	Trp (est. C-C)
		1249		dT (est. en plano del anillo)
1253		1257	+4	C ( est. anillo y est. C-NH <sub>2</sub> )
	1263		nd	Amida III (desordenada)
1332	1336	1328	+/-4	dA,dG (est. anillo Purinas)/ Péptido (est CH <sub>3</sub> -CH <sub>2</sub> )
1369		1374	+5	dT, dA, dG (est C-N)
1427	1437/35	1427	+/-8	Desoxirribosil (def 5'-H <sub>2</sub> )/ péptido (def CH <sub>2</sub> / CH)
1480		1485	+5	G (def N7, C8=N7-H <sub>2</sub> )
	1550		nd	Trp est. pirrol C2-C3)
1574		1578	+4	Purinas (estiramiento)
	1618		nd	Trp C=C
	1658	1654	-4	Amida I (α-helix)
1662		1662	0	Timina (est. C=O)
1682			nd	dA (tjereteo NH <sub>2</sub> )
	1686	1690	+4	Amida I (desordenada sin puentes de H, giros β)

Notas; resp: respiración, est: estiramiento, sim: simétrico, asim: asimétrico, curv: curvatura, def: deformación, tij: tjereteo, A: adenina, G: Guanina, C: citocina, T: Timina, d: desoxy (A,G,C,T)

Una vez que el péptido AmPep1 y el oligonucleótido OriRepTYLCV se hicieron interactuar, el espectro Raman de la matriz formada de esta interacción se obtuvo, mostrando contribución de los espectros de las biomoléculas analizadas (ver Figura 9, Cuadro 4 y Figura de 1 manuscrito 2). La interacción de estas biomoléculas genera un espectro el cual tiene contribuciones de señales de ambas biomoléculas, pero mostrando alteraciones en su número de onda y/o su intensidad. Con respecto a los desplazamiento en las señales del péptido se observa que las señales debidas a las vibraciones de la respiración anillo aromático del Trp muestran un desplazamiento comparado con el espectro original que va de 760 a 751  $\text{cm}^{-1}$  y de 1010 a 1014  $\text{cm}^{-1}$ , indicando que existe una posibilidad de que el grupo benceno del Trp interactúe con algunas bases nitrogenadas del oligonucleótido (Takeuchi H. 2003), principalmente por interacciones débiles tipo Pi o por la posible formación de puentes de Hidrógeno (Tsuboi M. *et al* 2003). Dicha interacción de este residuo sobre el OriRepTYLCV fue observada en el análisis por apagamiento en la señal de fluorescencia intrínseca del péptido cuando este interactúa de manera dosis dependiente con OriRepTYLCV (ver Figura 2 del artículo 1) correlacionando este último fenómeno con el corrimiento y disminución de la intensidad de banda correspondiente a la respiración del anillo aromático del Trp de 760  $\text{cm}^{-1}$  a 751  $\text{cm}^{-1}$ , la afectación de este modo vibracional en el Trp representa un marcador estructural refiriéndose a residuos de Trp involucrados en una fuerte interacción hidrofóbica (Takeuchi H. 2003), la disminución de la intensidad en el marcador conformacional de Trp a 1550  $\text{cm}^{-1}$  es afectado, mostrando un posible reordenamiento estructural de la cadena lateral Trp cuando interactúa con el DNA. Otras bandas que se ven afectadas son el estiramiento C-C acoplado al -OH de la serina, que va de 853 a 857  $\text{cm}^{-1}$  y el modo vibratorio de C-O (de 945 a 958  $\text{cm}^{-1}$ ) posiblemente debido a la formación de enlaces de hidrógeno con DNA (Murli C. *et al* 2006). También se observó un desplazamiento en la señal de la cadena alifática del péptido de 1336  $\text{cm}^{-1}$  que disminuyó hasta 1328  $\text{cm}^{-1}$  posiblemente debido a un re-arreglo estructural en la interacción con DNA (Wei F. *et al* 2008). El efecto sobre el re-arreglo en la estructura secundaria del péptido concuerda con el análisis de deconvolución de la banda de amida I en la mezcla de reacción (ver manuscrito 2 Figura 1C-tabla 2) mostrando un aumento del porcentaje de la señal debida a la conformación alfa hélice por más del 3% a 1653  $\text{cm}^{-1}$  con una disminución en el porcentaje de estructura

desordenada ( $1681\text{ cm}^{-1}$ ) en comparación con el espectro del péptido puro (Camerlingo C. *et al* 2014).

Con respecto a los cambios en las señales Raman del oligonucleótido tras una interacción con el péptido se observa que sólo la señal del alargamiento del grupo fosfato correspondiente a dioxi fosfato es afectada, mostrando un desplazamiento de la señal original que va de  $1092$  a  $1096\text{ cm}^{-1}$ , no se observe una afección en el alargamiento del enlace fosfodiester O-P-O, se puede atribuir que los oxígenos libres del grupo  $\text{PO}_2$  pueden interaccionar de manera electrostática o por puentes de H con grupos funcionales catiónicos del péptido como los grupos amino de la arginina o lisina (Filho P. *et al* 2007; Faria J. 2009; Sereda V. *et al* 2017). Algunos otros modos vibraciones del DNA fueron afectados principalmente como la vibración de los grupos  $\text{NH}_2$  de G y C desplazando la señal de  $1253$  a  $1257\text{ cm}^{-1}$ , así como las vibraciones correspondientes al enlace C-N de timina (T), adenina (A) y guanina (G), mostrando un desplazamiento que va de  $1369$  a  $1374\text{ cm}^{-1}$ , así como los grupos C8-N7 de G (Jangir D. *et al* 2014; Hernández B. *et al* 2012), desplazando la señal Raman de  $1480$  a  $1485\text{ cm}^{-1}$ . El desplazamiento hacia números de onda mayores indica la formación de una interacción estable que involucre distancias cortas de enlace, de acuerdo con la naturaleza de estos grupos funcionales afectados (aminos); en las bases nitrogenadas se puede presumir de una posible formación de puentes de hidrógeno (Jangir D. *et al* 2014) con algunos elementos del péptido AmPep1. Este fenómeno de desplazamiento hacia frecuencias menores se observa en la región correspondiente al enlace C=O de la T ( $1600$  a  $1711\text{ cm}^{-1}$ ), esta región contiene además la contribución de la amida I del péptido, en la (figura 1C, manuscrito 2) se observa que las bandas características de la timina del oligonucleótido (letra b) tienen desplazamientos marcados de  $1691$  a  $1995\text{ cm}^{-1}$  en la señal del C2=O, presentando la premisa de la potencial formación de puentes de H. Otros modos vibracionales afectados son aquellos generados por los anillos de las bases puricas la cual muestra un cambio en la frecuencia de alargamiento que va de  $1574$  a  $1578\text{ cm}^{-1}$ , indicando una posible interacción entre los sistemas aromáticos de la A y G con el grupo indol del Trp mediante interacciones tipo Pi (Takeuchi H. 2003; Duraisamy P. y Iyandurai N. 2011)

Con base a estos resultados se propone que el péptido AmPep1 interacciona principalmente con adeninas, timinas y citosinas del OriRepTYLCV las cuales se encuentran de manera

abundante en la zona blanco de la proteína iniciadora de la replicación (Rep) de TYLCV que involucra a la región del asa (marcado en negritas y flecha) de la secuencia 5'-GGCCATCCGTATAATATTA↓CCGGATGGCC-3'.

Para buscar una explicación molecular los datos experimentales de interacción entre ambas biomoléculas, se procedió a realizar un análisis teórico de dichos sistema, para lo cual se realizó el modelado de la estructura de la horquilla formada por la secuencia de OriRepTYLCV, siguiendo la predicción de estructura secundaria reportada previamente para este tipo de secuencias y calculada en el servidor RNA structure web server (Orozco B. M. y Hanley Bowdoin L. 1996). El péptido se modeló en el servidor Pep-Fold, y optimizado de acuerdo a lo observado en el análisis por Raman. Una vez optimizada la geometría de ambas biomoléculas, estas se hicieron interaccionar. Los resultados muestran el acomodo más estable del péptido en la horquilla de replicación de TYLCV, se observa que este se distribuye principalmente en la región central y extremo 3' del asa, con poca perturbación en la región del tallo de la horquilla de replicación. Las interacciones que mayoritariamente son observadas son de tipo puente de hidrogeno, electrostáticas e interacciones entre sistemas aromáticos.

En el caso de enlaces de hidrógeno, se predice la formación de tres puentes entre los residuos de adenosina 14 y 11, así como con la citosina (C) 20, la adenina(A) 14 interacciona con el residuo glutamina 16, mientras que la adenina 11 y citosina 20 interaccionan principalmente con el esqueleto del enlace peptídico (ver Figura 9 y manuscrito 2 en la Figura 2b.1), dichas interacciones se presentan entre los grupos NH<sub>2</sub> la C y A y del N7 de la A con el grupo carboxilo de la glutamina y el C=O del enlace peptídico (Nagy P. I. 2014). Estas predicciones teóricas correlacionan con los resultados experimentales de interacción arrojados por el análisis Raman donde se observa un desplazamiento de banda de 1253 a 1257 cm<sup>-1</sup> (alargamiento NH<sub>2</sub>), y el desplazamiento de la banda de 1369 a 1374 cm<sup>-1</sup> correspondiente al estiramiento del C-N de la A, el cual se puede ver afectado por la formación de un enlace de H con el N7 de la purina. El efecto de este enlace en la estructura del péptido puede verse reflejado en el cambio en la señal Raman del esqueleto del péptido de 1336 a 1328 cm<sup>-1</sup> y un cambio en la señal de la amida I, principalmente un corrimiento de la banda de la alfa hélice de 1658 a 1653 cm<sup>-1</sup> (Camerlingo C. *et al* 2014).

Otro tipo de interacciones moleculares observada en el modelo teórico son de tipo electrostáticas, formado entre los grupos fosfatos del oligonucleótido cargado negativamente y con cargas positivas del péptido, principalmente derivadas de aminoácidos básicos como lisina y arginina. El modelo predice la interacción del grupo  $\text{-NH}_2^+$  de la cadena lateral de los residuos asina 5, arginina 4 y arginina 14 del péptido directamente con el grupo  $\text{PO}_2^{-1}$  y con el oxígeno del enlace O-P-O de la cadena principal del DNA a la altura de los residuos de bases A5, T6 Y T10, respectivamente. Dicha interacción electrostática afecta el tallo de la horquilla de replicación y una parte del asa en la región 3' la cual es la zona de reconocimiento para la proteína Rep. Se ha mostrado que la alteración en secuencia en esta zona abate la tasa replicativa de los geminivirus, lo que podría ayudar a entender la actividad antiviral mostrada en este trabajo (Orozco B. M. Hanley-Bowdoin, L. 1996). Además, el utilizar una secuencia altamente conservada como blanco antiviral, no solo en estructura si no en función, podría mitigar la generación de resistencia por parte del virus contra este péptido si este fuese aplicado en campo. Siguiendo los principios del diseño racional de agroquímicos propuesto por (Liu Y. *et al* 2014; Xiao J. J. *et al* 2015), ese modelo de estudio presenta dos mecanismos de acción antiviral: correctivo (péptido AmPep1) y preventivo en el modelo de extracto total, lo que ayudaría a mitigar la potencial generación de resistencia. Cabe señalar que es importante realizar pruebas con otros géneros de la familia *Geminiviridae* para asegurar la especificidad de este modelo de tratamiento y evaluar su eficacia en otros modelos vegetales. La interacción entre estos grupos concuerda con lo observado experimentalmente en el estudio por Raman, correlacionando el desplazamiento de la señal del grupo  $\text{PO}_2$  de  $1092\text{ cm}^{-1}$  en el oligonucleótido hacia valores de  $1096\text{ cm}^{-1}$ , dicha interacción podría tener repercusiones locales en la estructura secundaria en el origen de replicación haciendo que el reconocimiento atómico por la proteína Rep se vea afectado negativamente.

Además, se predicen otro tipo de interacciones débiles entre el DNA y el péptido, como son las interacciones entre los sistemas aromáticos principalmente por electrones tipo Pi y átomos cargados negativamente, así como una tendencia a formación de un apilado. Este tipo de interacciones se observa principalmente en los anillos aromáticos de los triptófanos 6 y 10, el benceno del residuo W 6 interacciona potencialmente en la modalidad Pi-anión con el grupo  $\text{C4=O}$  de la T18, y posiblemente forma un apilado con la A19 en forma de T. El

residuo W10 presenta una potencial interacción con el residuo T10 del DNA (Lucas X. *et al* 2016; Wilson K. *et al* 2014).

Los resultados experimentales y teóricos indican que el péptido AmPep1 interacciona con el OriRep de TYLCV, dichos enlaces podrían alterar localmente la conformación de la horquilla de replicación y dificultar el reconocimiento molecular por Rep o bien realizar un impedimento estérico que no permita la adecuada síntesis de DNA viral en la planta.

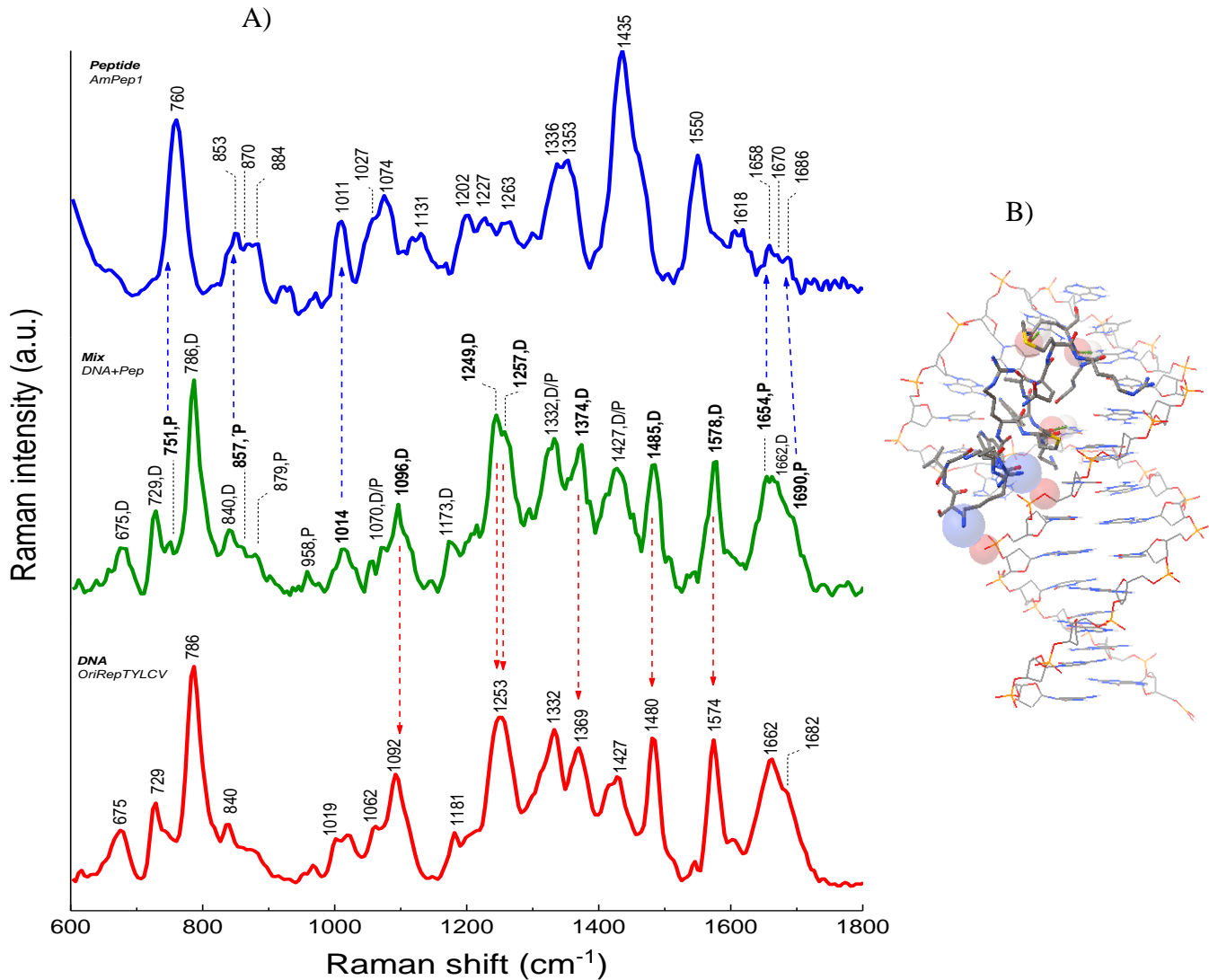


**Figura 9. Modelo experimental y teórico de la interacción entre AmPep1 y OriRepTYLCV utilizando espectroscopía Raman y modelado molecular.** A) Análisis Raman, en azul el espectro Raman del péptido AmPep1, el espectro rojo corresponde a la señal Raman del DNA de la secuencia

OriRepTYLCV, mientras que en verde se muestra el espectro correspondiente a la interacción entre AmPep1 y OriRepTYLCV. En el espectro de interacción se señalan con negritas las bandas que fueron consideradas para realizar el estudio de interacción molecular debido a su desplazamiento en número de onda o en intensidad (para consultar los valores de números de onda ver cuadro 4). B) Modelo teórico de interacción mostrando la zona de mejor interacción del péptido con el DNA es la zona del extremo 3' de la horquilla de replicación de TYLCV (detalles ver Figura 2 del manuscrito 2).

#### 4.5 Transporte del péptido en el tejido vegetal.

Con base en los resultados anteriores se reportó la habilidad del péptido AmPep1 para controlar la replicación de TYLCV *in vivo*, lo que hace sospechar que esta molécula tiene la capacidad de translocarse al interior de las células, ya que el virus se replica en el núcleo. Para corroborar este hecho, se procedió a analizar si el péptido tiene la capacidad de cruzar eficientemente las barreras celulares y llegar eficientemente hasta el núcleo, para dicho efecto el péptido AmPep1 fue marcado con isotiocianato de fluoresceína, FITC obteniéndose AmPep1-FITC y se monitoreó la capacidad de penetración celular en *N. benthamiana*. En la (Figura 10) se observa que en los primeros 10 minutos el transporte del péptido (señal fluorescente) no es muy elevada comparada con los posteriores tiempos de monitoreo y que además puede ser posiblemente ligado a procesos de difusión o a un proceso de endocitosis, principalmente debido a la observación de formación de vesículas o puntos de transporte en la membrana o pared celular (Kauffman W. *et al* 2016; Rafiqi M. *et al* 2010), sin embargo, a los 30 y 60 minutos la señal fluorescente del péptido aumenta significativamente y de manera homogénea concentrándose principalmente en citoplasma y el núcleo de células epiteliales y estomas, así como en células del mesófilo. Para corroborar si este proceso es únicamente dependiente de energía (endocitosis) se procedió a incubar tejido de *N. benthamiana* en la solución del AmPep1 a baja temperatura (4°C) encontrándose que el transporte del péptido no se ve afectado, y que la señal de la sonda es similar a aquella reportada en la incubación de 1 hora a temperatura ambiente, este hecho se puede explicar debido a que el péptido no presenta requerimientos energéticos para su transporte y que debido a su secuencia puede entonces clasificarse como un péptido penetrador de células, la baja temperatura reorganiza la fluidez y estructura de la membrana permitiendo que el

péptido entre de manera pasiva por translocación espontanea tal vez por un mecanismo de *flip-flop* no dependiente de energía (Yamashita H. *et al* 2016; Gräslun A. *et al* 2011; Jiao C. *et al* 2009; Castanho M. *et al* 2008). La fácil permeabilidad del péptido hacia el interior de la célula permite que éste pueda llegar hasta el núcleo de las células para poder interferir con la replicación de TYLCV.

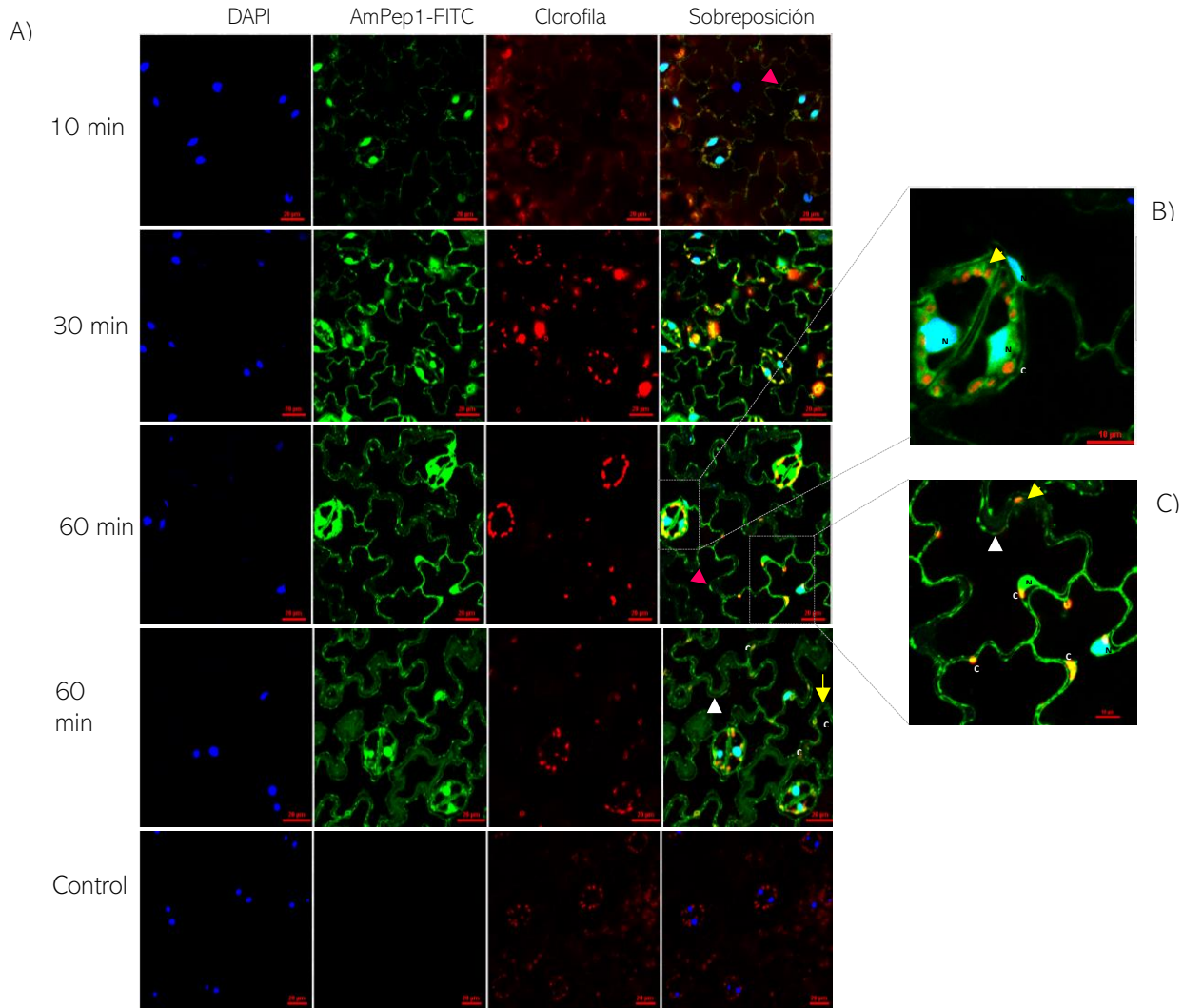


**Figura 10. Translocación del péptido AmPep1 en células de *N. benthamiana*.** A) Imágenes representativas de una cinética de internalización de AmPep1. Señal fluorescente de izquierda a derecha, DAPI (azul): núcleos, FITC (verde): Péptido AmPep1, Autofluorescencia-Clorofila (rojo): cloroplastos. De arriba a abajo incubación a los 10, 30 y 60 minutos a rt o 4 °C por 60 minutos, imagen en inferior: control no incubado con AmPep1. Después de 10 minutos de incubación se aprecia la formación puntos de transporte a través de la membrana (cabeza de flecha rosa) y traslocación ligera hacia el núcleo. A 30 y 60 minutos a temperatura



ambiente, se observa un incremento en la translocación del péptido y acumulación alrededor del tonoplasto (cabeza de flecha blanca) y en el citoplasma (flecha amarilla), en una incubación a baja temperatura no se observa afección en el transporte, presentándose acumulación de AmPep1 alrededor del tonoplasto, núcleo y citoplasma, en control, no se observa señal de la marca FITC. Imágenes tomadas con un objetivo 60x-agua, barras inferiores= 20 $\mu$ m, B) Ampliación digital de un estoma y C) ampliación digital de células epidérmicas a 60 min de incubación con AmPep1 a temperatura ambiente. N= núcleo, C: cloroplasto. Barras en B) y C) = 10  $\mu$ m.

## 5.0 CONCLUSIONES

- ✓ El extracto de péptidos derivado de la hidrólisis enzimática de las globulinas de amaranto induce promoción de crecimiento y activación de vías de defensa sistémica en tomate, generando protección contra la infección por TYLCV.
- ✓ El extracto de péptidos induce respuesta de defensa en maíz previniendo el desarrollo de tizón foliar por *Helminthosporium* sp.
- ✓ Se aisló un péptido (denominado AmPep1) derivado de la hidrólisis enzimática de las globulinas de amaranto el cual presentó afinidad hacia la secuencia que forma la horquilla del origen de replicación de *Tomato yellow leaf curl virus*.
- ✓ El péptido AmPep1 mostró un efecto antiviral correctivo en plantas de *N. benthamiana* y tomate infectadas con TYLCV, retardando el progreso de la enfermedad y disminución del título viral en ambas especies.
- ✓ El péptido AmPep1 mitiga la formación de intermediarios replicativos de TYLCV como VS y CS.
- ✓ El péptido AmPep1 interacciona principalmente con la secuencia de la horquilla de replicación mediante formación de puentes de hidrógeno, interacciones electrostáticas e interacciones Pi, principalmente en la región 3' del asa de dicha secuencia.
- ✓ El péptido AmPep1 tiene la capacidad de translocación hacia el interior de las células llegando hasta el núcleo.

## 6.0 REFERENCIAS

1. Abdelbacki A.M. *et al.* Inhibition of tomato yellow leaf curl virus (TYLCV) using whey proteins. *Viol. J.* **26**, 7 (2010).
2. Al-Amri, S. M. Improved growth, productivity and quality of tomato (*Solanum lycopersicum* L.) plants through application of shikimic acid. *Saudi J. Biol. Sci.* **20**, 339–345 (2013).
3. Al-Amri, S. M. Improved growth, productivity and quality of tomato (*Solanum lycopersicum* L.) plants through application of shikimic acid. *Saudi J. Biol. Sci.* **20**, 339–345 (2013).
4. Ali, S. *et al.* Toxicological and biochemical basis of synergism between the entomopathogenic fungus *Lecanicillium muscarium* and the insecticide matrine against *Bemisia tabaci* ( Gennadius ). *Nat. Publ. Gr.* 1–14 (2017).
5. Ali Z. *et al.* CRISPR/Cas9-Mediated Immunity to Geminiviruses: Differential Interference and Evasion. *Sci. Rep.* **6**, (2016).
6. Alvarez A, Montesano M, Schmelz E and Ponce de León. Activation Shikimate, Phenylpropanoid, Oxylipins, and Auxin Pathways in *Pectobacterium carotovorum* Elicitors-Treated Moss. *Front. PlantSci.* **7**:328 (2016). doi: 10.3389/fpls.2016.00328
7. Arand K. *et al.* The Mode of Action of Adjuvants - Relevance of Physicochemical Properties for Effects on the Foliar Application, Cuticular Permeability, and Greenhouse Performance of Pinoxaden. *J. Agric. Food Chem.* **66**, 5770–5777 (2018).
8. Ascencio-Ibáñez J. T. *et al.* First Report of Tomato Yellow Leaf Curl Geminivirus in Yucatán, México. *APS* **83**, 1,178.1 - 1,178.1 (1999)
9. Ayala Garay, A. V. *et al.* La rentabilidad del cultivo de amaranto (*Amaranthus* spp.) en la región centro de México. *Cienc. Ergo Sum* **21**, 47–54 (2014).
10. Ayala Garay, A. V. *et al.* La rentabilidad del cultivo de amaranto (*Amaranthus* spp.) en la región centro de México. *Cienc. Ergo Sum* **21**, 47–54 (2014).
11. Barbosa Pelegrin P., Del Sarto, R. P., Silva, O. N., Franco, O. L. & Grossi-De-Sa, M. F. Antibacterial peptides from plants: What they are and how they probably work. *Biochem. Res. Int.* **2011**, (2011).
12. Bar-ziv, A., Levy, Y., Citovsky, V. & Gafni, Y. Biochemical and Biophysical Research Communications The Tomato yellow leaf curl virus ( TYLCV ) V2 protein inhibits enzymatic activity of the host papain-like cysteine protease CYP1. *Biochem. Biophys. Res. Commun.* **460**, 525–529 (2015).
13. Basak, J. Tomato Yellow Leaf Curl Virus: A Serious Threat to Tomato Plants World Wide. *J. Plant Pathol. Microbiol.* **07**, (2016).
14. Braun, H., Hildebrandt, T. M., Nesi, A. N. & Arau, W. L. Amino Acid Catabolism in Plants. *Mol. Plant.* 1563–1579 (2015). doi:10.1016/j.molp.2015.09.005
15. Brown, J. K. *et al.* Revision of Begomovirus taxonomy based on pairwise sequence comparisons. *Arch. Virol.* **160**, 1593–1619 (2015).

16. c. Enhanced tomato disease resistance primed by arbuscular mycorrhizal fungus. *Frontiers in Plant S.* **6**, 1–13 (2015).
17. Camacho-Beltrán, E. *et al.* First report of pepper as a natural new host for Tomato marchitez virus in Sinaloa, Mexico. *Can. J. Plant Pathol.* **37**, 384–389 (2015).
18. Camerlingo C., d'Apuzzo, F., Grassia, V., Perillo, L. & Lepore, M. Micro-Raman Spectroscopy for Monitoring Changes in Periodontal Ligaments and Gingival Crevicular Fluid. *Sensors* **14**, 22552–22563 (2014).
19. Campos-Olivas R., Louis, J. M., Cle, D., Gronenborn, B. & Gronenborn, A. M. The structure of a replication initiator unites diverse aspects of nucleic acid metabolism. **99**, 5–10 (2002).
20. Castanho M. a & Santos, N. C. What can light scattering spectroscopy do for membrane-ctive peptide studies. *J. Pept. Sci.* **14**, 1084–1095 (2008).
21. Cepeda-Siller M. El tomate rojo. Cultivo y control parasitológico. Trillas, 2009.
22. Chan, D. I., Prenner, E. J. & Vogel, H. J. Tryptophan- and arginine-rich antimicrobial peptides: Structures and mechanisms of action. *Biochim. Biophys. Acta - Biomembr.* **1758**, 1184–1202 (2006).
23. Chen W., Qian, Y. & Wu, X. Inhibiting replication of begomoviruses using artificial zinc finger nucleases that target viral-conserved nucleotide motif. *Virus genes.* 494–501 (2014).
24. Choe Y. *et al.* Substrate profiling of cysteine proteases using a combinatorial peptide library identifies functionally unique specificities, *J. Biol. Chem.* **281**, 12824–12832, (2006).
25. Cillo F., Palukaitis P. *Transgenic resistance. Advances in Virus Research* **90**, (Elsevier Inc., 2014).
26. Cohen S., Nitzany, F.E. Curly Top Virus of Tomatoes: Its Identification and Mode of Transmission, Israeli Plant Protection and Inspection Services. (1960)
27. Cohen S., Nitzany, F.E. Transmission and host range of tomato yellow leaf curl virus. *Phytopathology* **56**, 1127–1131. (1966)
28. Czosnek, H., Hariton-shalev, A., Sobol, I., Gorovits, R. & Ghanim, M. The Incredible Journey of Begomoviruses in Their Whitefly Vector. *Viruses* **9**, 273 (2017).
29. Dagan S. *et al.* A developmentally regulated lipocalin-like gene is overexpressed in Tomato yellow leaf curl virus -resistant tomato plants upon virus inoculation , and its silencing abolishes resistance. *Plant Mol. Biol.* 273–287 (2012).
30. Dagan S. *et al.* Comparative metabolomics and transcriptomics of plant response to Tomato yellow leaf curl virus infection in resistant and susceptible tomato cultivars. *Metabolomics.* 81–97 (2015).
31. Deng Y. *et al.* Synthesis and biological activity evaluation of novel amino acid derivatives as potential elicitors against Tomato yellow leaf curl virus. *Amino Acids* **47**, 2495–2503 (2015).
32. Diaz, I. Plant Defense Genes against Biotic Stresses. *Int. J. of Mol. Sc.* 1–5 (2018). doi:10.3390/ijms19082446

33. Dina N. E. *et al.* Structural changes induced in grapevine (*Vitis vinifera* L.) DNA by femtosecond IR laser pulses: A surface-enhanced Raman spectroscopic study. *Nanomaterials* **6**, 1–18 (2016).
34. Dong, T., Zhang, B., Jiang, Y. & Hu, Q. Isolation and Classification of Fungal Whitefly Entomopathogens from Soils of Qinghai-Tibet Plateau and Gansu Corridor. *Plos One* 1–12 (2016).
35. Doyle J.J., Doyle J.L., A rapid DNA isolation procedure for small quantities of fresh leaf tissue, *Phytochem Bull.* 19,11–15 (1987).
36. Duraisamy, P. & Iyandurai, N. Structural Analysis of DNA Interactions with Magnesium Ion Studied by Raman Spectroscopy. *Am. J. Biochem. Biotechnol.* **7**, 135–140 (2011).
37. Ertani A., Schiavon, M., Nardi, S. Transcriptome-Wide Identification of Differentially Expressed Genes in *Solanum lycopersicon* L. in Response to an Alfalfa -Protein Hydrolysate Using Microarrays. *Front. Plant Sci.* **8**, 1–19 (2017).
38. Faria, J. L. B. Polarized Raman spectra of L -arginine hydrochloride monohydrated single crystal. *Brazilian J. Phys.* **1**, 288–294 (2009).
39. Filho, P. F. F. *et al.* High Temperature Raman Spectra of L-Leucine Crystals. *Brazilian J. Phys.* **38**, 12 (2007).
40. Filik, J., Stone, N. Drop coating deposition Raman spectroscopy of protein mixtures. *Analyst* **132**, 544–550 (2007).
41. Glick, E., Levy, Y. & Gafni, Y. The viral etiology of tomato yellow leaf curl disease-a review. *Plant Prot. Sci.* **45**, 81–97 (2009).
42. Gorelik V. S., Krylov, A. S. & Sverbil, V. P. Local Raman spectroscopy of DNA. *Bull. Lebedev Phys. Inst.* **41**, 310–315 (2014).
43. Gorinstein, S. & Arruda, P. Alcohol-Soluble and Total Proteins from Amaranth Seeds and Their Comparison with Other Cereals. *J. Agric. Food Chem* 848–850 (1991). doi:10.1021/jf00005a005
44. Gorovits, R. & Czosnek, H. The Involvement of Heat Shock Proteins in the Establishment of Tomato Yellow Leaf Curl Virus Infection. *Front. Plant Sci.* **8**, 1–12 (2017).
45. Gover, O., Peretz, Y. & Sela, I. Only minimal regions of tomato yellow leaf curl virus ( TYLCV ) are required for replication , expression and movement. *Arch Virol* 2263–2274 (2014)
46. Gräslun, A., Madani, F., Lindberg, S., Langel, Ü. & Futaki, S. Mechanisms of cellular uptake of cell-penetrating peptides. *J. Biophys.* **2011**, (2011).
47. Hak, H. *et al.* TYLCV-Is movement in planta does not require V2 protein. *Virology* **477**, 56–60 (2015).
48. Han Y. *et al.* Induction of systemic resistance against tobacco mosaic virus by Ningnanmycin in tobacco. *Pestic. Biochem. Physiol.* **111**, 14–18 (2014).
49. Hanssen I. M., Lapidot, M. & Thomma, B. P. H. J. Emerging Viral Diseases of Tomato Crops. *Mol. Plant-Microbe Interact.* **23**, 539–548 (2010).

50. Hernández B., Coïc, Y. M., Gouyette, C. & Ghomi, M. Probing the interactions of oligodeoxynucleotides with a cationic peptide by Raman scattering. *Adv. Biomed. Spectrosc.* **5**, 58–71 (2012).
51. Huang, G.Y. *et al.* Synthesis and characteristics of (Hydrogenated) ferulic acid derivatives as potential antiviral agents with insecticidal activity. *Chem. Cent. J.* **7**, 33 (2013).
52. Huang, Y. *et al.* Comparative proteomic analysis provides novel insight into the interaction between resistant vs susceptible tomato cultivars and TYLCV infection. *BMC Plant Biol.* 1–21 (2016) (1).
53. Huang, Y. *et al.* Members of WRKY Group III transcription factors are important in TYLCV defense signaling pathway in tomato ( *Solanum lycopersicum* ). *BMC Genomics* 1–18 (2016) (2).
54. Islam, W. *et al.* Management of Tobacco Mosaic Virus through Natural Metabolites. ... *Nat. Prod.* **5**, 403–415 (2018).
55. Jangir D. K. & Mehrotra, R. Raman spectroscopic evaluation of DNA adducts of a platinum containing anticancer drug. *Spectrochim. Acta - Part A Mol. Biomol. Spectrosc.* **130**, 386–389 (2014).
56. Jarmelo, S., Carey, P. R. & Fausto, R. The Raman spectra of serine and 3,3-dideutero-serine in aqueous solution. *Vib. Spectrosc.* **43**, 104–110 (2007).
57. Jeschke, P. Progress of modern agricultural chemistry and future prospects. *Pest Manag. Sci.* **72**, 433–455 (2016).
58. Jiao C. Y. *et al.* Translocation and endocytosis for cell-penetrating peptide internalization. *J. Biol. Chem.* **284**, 33957–33965 (2009).
59. Jones, R. A. C. Using epidemiological information to develop effective integrated virus disease management strategies. *Virus Res.* **100**, 5–30 (2004).
60. Just K., Arif U., Luik U., Kvarnheden A. Monitoring infection of tomato fruit by
61. Kauffman W. B., Fuselier, T., He, J. & Wimley, W. C. *Trends Biochem Sci.* **40**, 749–764 (2016).
62. Kil E.J., Park J., Choi H.S., Kim C.S., Lee S. Seed Transmission of *Tomato yellow leaf curl virus* in White Soybean (*Glycine max*). *The Plant Pathol J.* **33**,4, 424-428. (2017).
63. Kil, E.J. *et al.* Tomato yellow leaf curl virus (TYLCV-IL): a seed-transmissible geminivirus in tomatoes. *Sci. Rep.* **6**, 19013 (2016).
64. Kim, N. *et al.* Comparative Analyses of Tomato yellow leaf curl virus C4 Protein-Interacting Host Proteins in Healthy and Infected Tomato Tissues. *Plant Pathol. J.* **32**, 377–387 (2016).
65. Kim, Y. & Jo, K. Neutravidin coated surfaces for single DNA molecule analysis. *Chem. Commun.* **47**, 6248–6250 (2011).
66. Krol E. *et al.* Perception of the Arabidopsis danger signal peptide 1 involves the pattern recognition receptor AtPEPR1 and its close homologue AtPEPR2. *J of Biol. Chem.* **285**(18),13471–13479 (2010)

67. Lamberth, C., Jeanmart, S., Luksch, T. & Plant, A. Current challenges and trends in the discovery of agrochemicals. *Science* (80). 341, 742–746 (2013).
68. Lapidot, M. *et al.* A Novel Route Controlling Begomovirus Resistance by the Messenger RNA Surveillance Factor Pelota. *PLoS Genet.* 1–19 (2015).
69. Laufs, J. *et al.* In vitro cleavage and joining at the viral origin of replication by the replication initiator protein of tomato yellow leaf curl virus. *PNAS* **92**, 3879–3883 (1995).
70. Lee, S. *et al.* DNA binding fluorescent proteins for the direct visualization of large DNA molecules. *Nucleic Acids Res.* 44, e6 (2016).
71. Li X. & Song B. Progress in the development and application of plant-based antiviral agents. *J. Integr. Agric.* 16, 2772–2783 (2017).
72. Li Y. *et al.* SIMAPK3 enhances tolerance to tomato yellow leaf curl virus (TYLCV) by regulating salicylic acid and jasmonic acid signaling in tomato (*Solanum lycopersicum*). 1–21 (2017)
73. Li, H. *et al.* Control of tomato yellow leaf curl virus disease by *Enterobacter asburiae* BQ9 as a result of priming plant resistance in tomatoes. *Turkish J. Biol.* **40**, 150–159 (2016).
74. Li, X. *et al.* Ningnanmycin inhibits tobacco mosaic virus virulence by binding directly to its coat protein discs. *Oncotarget.* **8**, 82446–82458 (2017).
75. Liu, Y. *et al.* Design, synthesis, and antiviral, fungicidal, and insecticidal activities of tetrahydro-??-carboline-3-carbohydrazide derivatives. *J. Agric. Food Chem.* 62, 9987–9999 (2014).
76. López, D. N., Galante, M., Robson, M., Boeris, V. & Spelzini, D. International Journal of Biological Macromolecules Amaranth, quinoa and chia protein isolates: Physicochemical and structural properties. *Int. J. Biol. Macromol.* 109, 152–159 (2018).
77. Lopez-Ochoa L., Ramirez-Prado, J. & Hanley-Bowdoin, L. Peptide aptamers that bind to a geminivirus replication protein interfere with viral replication in plant cells. *J. Virol.* **80**, 5841–53 (2006).
78. Lord R. C. & Thomas, G. J. Raman studies of nucleic acids - II aqueous purine and pyrimidine mixtures. *Biochim. Biophys. Acta - Nucleic Acids Protein Synth.* **142**, 1–11 (1967).
79. Lucas X., Bauzá, A., Frontera, A. & Quiñonero, D. A thorough anion- $\pi$  interaction study in biomolecules: On the importance of cooperativity effects. *Chem. Sci.* **7**, 1038–1050 (2016).
80. Lugo-Melchor O. Y. *et al.* Geminivirus Transmitidos por Mosca Blanca (*Bemisia tabaci*) en Tomate, en el Valle Agrícola de Culiacán, Sinaloa. *Rev. Mex. Fitopatol.* **29**, 109–118 (2011).
81. Mabvakure, B. *et al.* Ongoing geographical spread of Tomato yellow leaf curl virus. *Virology* **498**, 257–264 (2016).
82. Malaguti, M. *et al.* Bioactive peptides in cereals and legumes: Agronomical, biochemical and clinical aspects. *Int. J. Mol. Sci.* **15**, 21120–21135 (2014).

83. Mascia, T., Santovito, E., Gallitelli, D. & Cillo, F. Technical advance Evaluation of reference genes for quantitative reverse-transcription polymerase chain reaction normalization in infected tomato plants. *Mol. Plant. Pathol.* **11**, 805–816 (2010).
84. Melgarejo T. A. *et al.* Characterization of a New World Monopartite Begomovirus Causing Leaf Curl Disease of Tomato in Ecuador and Peru Reveals a New Direction in Geminivirus Evolution. *J. Virol.* **87**, 5397–5413 (2013).
85. Mendoza-Figueroa J.S. *et al.* Peptide Extract of Hydrolyzed Amaranth Globulin Induces Growth and Immunological Response in Tomato and Maize Plants. *Int. J. Plant Soil Sci.* **19**, 1–10 (2017).
86. Mendoza-Figueroa, J. S. *et al.* A peptide derived from enzymatic digestion of globulins from amaranth shows strong affinity binding to the replication origin of Tomato yellow leaf curl virus reducing viral replication in *Nicotiana benthamiana*. *Pestic. Biochem. Physiol.* **145**, 56–65 (2018).
87. Montoya-Rodríguez, A., Milán-Carrillo, J., Reyes-Moreno, C. & de Mejía, E. G. Characterization of peptides found in unprocessed and extruded amaranth (*Amaranthus hypochondriacus*) pepsin/pancreatin hydrolysates. *Int. J. Mol. Sci.* **16**, 8536–8554 (2015).
88. Montoya-Rodríguez, A., Milán-Carrillo, J., Reyes-Moreno, C. & de Mejía, E. G. Characterization of peptides found in unprocessed and extruded amaranth (*Amaranthus hypochondriacus*) pepsin/pancreatin hydrolysates. *Int. J. Mol. Sci.* **16**, 8536–8554 (2015).
89. Moreno-Félix M.L., Rodríguez-Negrete E.A., Meléndrez-Bojórquez N., Camacho-Beltrá, E., Leyva-López N.E. and Méndez-Lozano J. A new isolate of *Pepper huasteco yellow vein virus* (PHYVV) breaks geminivirus tolerance in tomato (*Solanum lycopersicum*) commercial lines. *Acta Hort.* **1207**, 35-44 (2018).
90. Mori, T., Takenaka, K., Domoto, F., Aoyama, Y. & Sera, T. Inhibition of Binding of Tomato Yellow Leaf Curl Virus Rep to its Replication Origin by Artificial Zinc-Finger Protein. *Mol. Biotechnol.* **54**, 198–203 (2013).
91. Moshe A. *et al.* Metabolomics : Open Access Stress Responses to Tomato Yellow Leaf Curl Virus ( TYLCV ) Infection of Resistant and Susceptible Tomato Plants are Different. *Metabolomics.* 1–13 (2012).
92. Movileanu L., Benevides, J. M. & Thomas, G. J. Temperature dependence of the Raman spectrum of DNA. II. Raman signatures of premelting and melting transitions of poly(dA)·poly(dT) and comparison with poly(dA-dT)·poly(dA-dT). *Biopolymers* **63**, 181–194 (2002).
93. Murli C., Vasanthi, R. & Sharma, S. M. Raman spectroscopic investigations of dl-serine and dl-valine under pressure. *Chem. Phys.* **331**, 77–84 (2006).
94. NagyP. I. Competing intramolecular vs. Intermolecular hydrogen bonds in solution. *International Journal of Molecular Sciences* **15**, (2014).
95. Nicaise, V. Crop immunity against viruses: outcomes and future challenges. *Front. Plant Sci.* **5**, 1–18 (2014).



96. Nieto-barrera, J. O., Mendoza, S. & Casta, E. Improved functional properties of pasta : Enrichment with amaranth seed fl our and dried amaranth leaves. *J. of Cereal Sc.* **72**, 84–90 (2016).
97. Ning, W. *et al.* Transmission of Tomato Yellow Leaf Curl Virus by Bemisia tabaci as Affected by Whitefly Sex and Biotype. *Nat. Publ. Gr.* 1–8 (2015)
98. Orozco B. M. Hanley-Bowdoin, L. A DNA structure is required for geminivirus replication origin function. *J. Virol.* **70**, 148–158 (1996).
99. Overman S. A. & Thomas, G. J. Amide modes of the  $\alpha$ -helix: Raman spectroscopy of filamentous virus fd containing peptide 13C and 2H labels in coat protein subunits. *Biochemistry* **37**, 5654–5665 (1998).
100. Pagba, C. V., Lane, S. M. & Wachsmann-Hogiu, S. Raman and surface-enhanced Raman spectroscopic studies of the 15-mer DNA thrombin-binding aptamer. *J. Raman Spectrosc.* **41**, 241–247 (2010).
101. Panchaud A. *et al.* Mass spectrometry for nutritional peptidomics: how to analyze food bioactives and their health effects, *J. Proteome* **75**, 3546–3559, (2012).
102. Pasternak, T. *et al.* Protocol: An improved and universal procedure for whole-mount immunolocalization in plants. *Plant Methods* **11**, 1–10 (2015).
103. Peretz, Y., Eybishtz, A. & Sela, I. Silencing of ORFs C2 and C4 of Tomato Yellow Leaf Curl Virus Engenders Resistant or Tolerant Plants. *The Open Virol J.* 141–147 (2011).
104. Pinstrup Andersen P. The Future World Food Situation and the Role of Plant Diseases. The Plant Health Instructor. 2001. DOI: 10.1094/PHI-I-2001-0425-01.
105. Pooggin, M. M. How can plant DNA viruses evade siRNA-directed DNA methylation and silencing? *Int. J. Mol. Sci.* **14**, 15233–15259 (2013).
106. Quiroga, A. V., Aphalo, P., Ventureira, J. L., Martínez, E. N. & Añón, M. C. Physicochemical, functional and angiotensin converting enzyme inhibitory properties of Amaranth (*Amaranthus hypochondriacus*) 7S globulin. *J. Sci. Food Agric.* **92**, 397–403 (2012).
107. Quiroga-Madrigal R, Rosales-Esquinca, María, Rincón-Espinosa, Patricia, Hernández-Gómez, Elizabeth, & Garrido-Ramírez. Enfermedades Causadas por Hongos y Nematodos en el Cultivo de Tomate (*Lycopersicon esculentum* Mill.) en el Municipio de Villaflores, Chiapas, México. *Revista Mexicana de Fitopatología* **25**, 114–119 (2007).
108. Rafiqi M. *et al.* Internalization of Flax Rust Avirulence Proteins into Flax and Tobacco Cells Can Occur in the Absence of the Pathogen. *Plant Cell* **22**, 2017–2032 (2010).
109. Rajeswari M.R. *et al.* Binding of oligopeptides to d-AGATCTAGATCT and d-AAGCTTAAGCTT: can tryptophan intercalate in DNA hairpins? *Biochemist* **31**, 6237–6241 (1992).
110. Rajeswari, M. R. *et al.* Does Tryptophan Intercalate in DNA ? A Comparative Study of Peptide Binding to Alternating and Nonalternating, *Biochemistry* **68**, 6825–6831 (1987). doi:10.1021/bi00395a036

111. Rentería-canett, I., Xoconostle-cázares, B., Ruiz-medrano, R. & Rivera-bustamante, R. F. Geminivirus mixed infection on pepper plants : Synergistic interaction between PHYVV and PepGMV Geminivirus mixed infection on pepper plants : Synergistic interaction between PHYVV and PepGMV. *Viol. J.* **104**, (2011).
112. Reverdatto, S. et al. Peptide aptamers: development and applications Current topics in medicinal chemistry vol. 15,(12) 1082-101. (2015)
113. Reyes M. I., Nash, T. E., Dallas, M. M., Ascencio-Ibanez, J. T. & Hanley-Bowdoin, L. Peptide Aptamers That Bind to Geminivirus Replication Proteins Confer a Resistance Phenotype to Tomato Yellow Leaf Curl Virus and Tomato Mottle Virus Infection in Tomato. *J. Virol.* **87**, 9691–9706 (2013).
114. Richter, K. S., Götz, M., Winter, S. & Jeske, H. The contribution of translesion synthesis polymerases on geminiviral replication. *Virology* **488**, 137–148 (2016).
115. Rivas-Arancibia S., Rodríguez-Martínez, E., Badillo-Ramírez, I., López-González, U. & Saniger, J. M. Structural Changes of Amyloid Beta in Hippocampus of Rats Exposed to Ozone: A Raman Spectroscopy Study. *Front. Mol. Neurosci.* **10**, 1–11 (2017).
116. Rivillas Acevedo (1), L. & Soriano García, M. Antifungal activity of a protean extract from *Amaranthus hypochondriacus* seeds. *J. Mex. Chem. Soc.* **51**, 136–140 (2007).
117. Rivillas-Acevedo (2), L. A. & Soriano-García, M. Isolation and biochemical characterization of an antifungal peptide from *Amaranthus hypochondriacus* seeds. *J. Agric. Food Chem.* **55**, 10156–10161 (2007).
118. Rodríguez-Alvarado, G., García-López, J. & Fernández-Pavia, S. Enfermedades en Invernadero en la Zona Centro de Michoacán. *Rev. Mex. Fitopa* **29**, 50–60 (2011).
119. Rodríguez-Negrete, E. A. et al. A sensitive method for the quantification of virion-sense and complementary-sense DNA strands of circular single-stranded DNA viruses. *Sci. Rep.* **4**, 6438 (2014).
120. Romero-Zepeda, H. & Paredes-López, O. Isolation and Characterization of Amaranthin, the 11S Amaranth Seed Globulin. *J. Food Biochem.* **19**, 329–339 (1995).
121. Rosas-Díaz, T.; Macho, A.P.; Beuzón, C.R.; Lozano-Durán, R.; Bejarano, E.R. The C2 Protein from the Geminivirus *Tomato Yellow Leaf Curl Sardinia Virus* Decreases Sensitivity to Jasmonates and Suppresses Jasmonate-Mediated Defences. *Plants* **5**, 8 (2016)-
122. Roy K.B. et al. Hairpin and duplex forms of a self-complementary dodecamer, d AGATCTAGATCT, and interaction of the duplex form with the peptide KGWGK: can a pentapeptide destabilize DNA? *Biochemist* **31**, 6241–6245 (1992).
123. Ruiz-Chica A. J., Medina, M. A., Sánchez-Jiménez, F. & Ramírez, F. J. On the interpretation of Raman spectra of 1-aminooxy-spermine/DNA complexes. *Nucleic Acids Res.* **32**, 579–589 (2004).

124. Rybicki, E. P. A Top Ten list for economically important plant viruses. *Arch. Virol.* **160**, 17–20 (2015).
125. Sacristan, S., Diaz, M., Fraile, A. & Garcia-Arenal, F. Contact Transmission of Tobacco Mosaic Virus: a Quantitative Analysis of Parameters Relevant for Virus Evolution. *J. Virol.* **85**, 4974–4981 (2011).
126. Safarnejad M. R., Fischer R., & Commandeur, U. Recombinant-antibody-mediated resistance against Tomato yellow leaf curl virus in *Nicotiana benthamiana*. *Arch of Virol.* **154**, 457–467. (2009).
127. Sánchez-campos, S. *et al.* Tomato yellow leaf curl virus: No evidence for replication in the insect vector *Bemisia tabaci*. *Nat. Publ. Gr.* 1–6 (2016).
128. Sanfaçon, H. Grand challenge in plant virology: Understanding the impact of plant viruses in model plants, in agricultural crops, and in complex ecosystems. *Front. Microbiol.* **8**, 2013–2016 (2017).
129. Sanoubar, R. & Barbanti, L. Fungal diseases on tomato plant under greenhouse condition. *Eur. J. Biol. Res.* **7**, 299–308 (2017).
130. Sereda, V. *et al.* Polarized Raman Spectroscopy for Determining the Orientation of di-D-phenylalanine Molecules in a Nanotube. *J Raman Spectrosc.* **47**, 1056–1062 (2017).
131. Silva S. J. C. *et al.* Species diversity, phylogeny and genetic variability of begomovirus populations infecting leguminous weeds in northeastern Brazil. *Plant Pathol.* **61**, 457–467 (2012).
132. Silva-Sánchez, C. *et al.* Bioactive Peptides in Amaranth Seed. *J. Agric. Food Chem.* **56**, 1233–1240 (2008).
133. Smith H.A. *et al.* Evaluating Weeds as Hosts of *Tomato yellow leaf curl virus*, *Environ Entomol.* **44**, 4, 1101–1107 (2015).
134. Smith, C. & Gilbertson, L. Rational Ligand Design to Improve Agrochemical Delivery Efficiency and Advance Agriculture Sustainability. *ACS Sustain. Chem. Eng.* (2018). doi:10.1021/acssuschemeng.8b03457
135. Speck-Planche, A. *et al.* Rational design of new agrochemical fungicides using substructural descriptors. *Pest Manag. Sci.* **67**, 438–445 (2011).
136. St P.M. *et al.* Fluorescence quenched solid phase combinatorial libraries in the characterization of cysteine protease substrate specificity, *J. Comb. Chem.* **1**, 509–523, (1999).
137. Stephen F. *et al.* Gapped BLAST and PSI-BLAST: a new generation of protein database search programs, *Nucleic Acids Res.* **25**, 3389–3402. (1997).
138. Stotz, H. U., Waller, F. & Wang, K. Antimicrobial Peptides and Innate Immunity. **29–52** (2013). doi:10.1007/978-3-0348-0541-4
139. Subia García C. Caracterización agronómica, bromatológica, isoenzimática y radiosensibilidad de poblaciones de amaranto (*Amaranthu* spp.) colectadas en las principales áreas de producción de México. TESIS. Colegio de Postgraduados, México. (2012).
140. Sudo, M., Takahashi, D., Andow, D. A., Suzuki, Y. & Yamanaka, T. Optimal management strategy of insecticide resistance under various insect life histories:

- Heterogeneous timing of selection and interpatch dispersal. *Evol. Appl.* **11**, 271–283 (2018).
141. Sun W. *et al.* Eugenol confers resistance to Tomato yellow leaf curl virus (TYLCV) by regulating the expression of SlPer1 in tomato plants. *New Biotech* **33**, (2016).
  142. Takeuchi H. Raman structural markers of tryptophan and histidine side chains in proteins. *Biopolym. - Biospectroscopy Sect.* **72**, 305–317 (2003).
  143. Tamarzizt B. *et al.* Use of Tomato leaf curl virus (TYLCV) truncated Rep gene sequence to engineer TYLCV resistance in tomato plants. *Acta Virologia* **53**, 99–104. (2009).
  144. Tan L. *et al.* Affinity analysis of DNA aptamer peptide interactions using gold nanoparticles, *Anal. Biochem.* **421**, 725–731 (2012)
  145. Tandang-Silvas, M. R. *et al.* Crystal structure of a major seed storage protein, 11S proglobulin, from *Amaranthus hypochondriacus*: Insight into its physico-chemical properties. *Food Chem.* **135**, 819–826 (2012).  
Tomato yellow leaf curl virus. *Plant Pathol.* **66**, 522–528 (2017).
  146. Tsitsigiannis, D. I., Antoniou, P. P., Tjamos, S. E. & Paplomatas, E. J. Major Diseases of Tomato, Pepper and Eggplant in Greenhouses. *Eur. J. Plant Sci. Biotechnol.* **2**, 106–124 (2008).
  147. Tsuboi M., Overman, S. A., Nakamura, K., Rodriguez-Casado, A. & Thomas, G. J. Orientation and interactions of an essential tryptophan (Trp-38) in the capsid subunit of Pf3 filamentous virus. *Biophys. J.* **84**, 1969–1976 (2003).
  148. Turner R. After the famine: Plant pathology, *Phytophthora infestans*, and the late blight of potatoes, 1845–1960. *Historical Studies in the Physical and Biological Sciences*, 35(2) 341-370. (2005).
  149. Urech, P. A. The agrochemical industry: Its contribution to crop protection and environmental policy. *Plant Pathol.* **48**, 689–692 (1999).
  150. Valdes-Rodriguez, S. *et al.* Recombinant amaranth cystatin (AhCPI) inhibits the growth of phytopathogenic fungi. *Plant Physiol. Biochem.* **48**, 469–475 (2010).
  151. Valle Castillo L.B. Evaluación de micorrizas arbusculares como inductores de mecanismos de defensa contra Begomovirus en plantas de tomate. Tesis, Instituto Politécnico Nacional, 2016.
  152. Vasco-Méndez, N. L., Soriano-García, M., Moreno, A., Castellanos-Molina, R. & Paredes-López, O. Purification, crystallization, and preliminary X-ray characterization of a 36 kDa amaranth globulin. *J. Agric. Food Chem.* **47**, 862–866 (1999).
  153. Venskutonis, P. R. & Kraujalis, P. Nutritional Components of Amaranth Seeds and Vegetables: A Review on Composition, Properties, and Uses. *Compr. Rev. Food Sci. Food Saf.* **12**, 381–412 (2013).
  154. Verlaan, M. G. *et al.* The Tomato Yellow Leaf Curl Virus Resistance Genes Ty-1 and Ty-3 Are Allelic and Code for DFDGD-Class RNA-Dependent RNA Polymerases. *PLoS Genet.* **9**, (2013).

155. Vurro, M., Bonciani, B. & Vannacci, G. Emerging infectious diseases of crop plants in developing countries: Impact on agriculture and socio-economic consequences. *Food Secur.* **2**, 113–132 (2010).
156. Wan, H. J. *et al.* Assessment of the genetic diversity of tomato yellow leaf curl virus. *Genet. Mol. Res. GMR* **14**, 529–537 (2014).
157. Wang, H., Zheng, J. & Ren, X. Effects of *Piriformospora indica* on the growth, fruit quality and interaction with Tomato yellow leaf curl virus in tomato cultivars susceptible and resistant to TYCLV. *Plant Growth Regul.* 303–313 (2015).
158. Wang, J., Zhu, Y. K., Wang, H. Y., Zhang, H. & Wang, K. Y. Inhibitory effects of esterified whey protein fractions by inducing chemical defense against tobacco mosaic virus (TMV) in tobacco seedlings. *Ind. Crops Prod.* **37**, 207–212 (2012).
159. Wang, L. *et al.* Inference of a geminivirus–host protein–protein interaction network through affinity purification and mass spectrometry analysis. *Viruses* **9**, (2017).
160. Wei F., Zhang, D., Halas, N. J. & Hartgerink, J. D. Aromatic amino acids providing characteristic motifs in the raman and SERS spectroscopy of peptides. *J. Phys. Chem. B* **112**, 9158–9164 (2008).
161. Whitfield, A. E., Falk, B. W. & Rotenberg, D. Insect vector-mediated transmission of plant viruses. *Virology* 479–480, 278–289 (2015).
162. Williams, P. A. *et al.* The influence of the extensional viscosity of very low concentrations of high molecular mass water-soluble polymers on atomisation and droplet impact. *Pest. Man. Sc.* 504, 497–504 (2008).
163. Wilson K. A., Kellie, J. L. & Wetmore, S. D. DNA-protein  $\pi$ -interactions in nature: Abundance, structure, composition and strength of contacts between aromatic amino acids and DNA nucleobases or deoxyribose sugar. *Nucleic Acids Res.* **42**, 6726–6741 (2014).
164. Wojtuszewski K. Mukerji, I. The HU – DNA binding interaction probed with UV resonance Raman spectroscopy: Structural elements of specificity. 2416–2428 (2004).
165. Wyatt, S. Detection of Subgroup III Geminivirus Isolates in Leaf Extracts by Degenerate Primers and Polymerase Chain Reaction. *Phytopathology* 86, 1288 (1996).
166. Xiao, J. J. *et al.* Design, synthesis and anti-tobacco mosaic virus (TMV) activity of 5-chloro-n-(4-cyano-1-aryl-1H-pyrazol-5-yl)-1-aryl-3-methyl-1H-pyrazole-4-carboxamide derivatives. *Molecules* 20, 807–821 (2015).
167. Yamada K, *et al.* Danger peptide receptor signaling in plants ensures basal immunity upon pathogen-induced depletion of BAK1. *Eur. Mol. Biol. Organ. J.* **35**:46–61(2016).
168. Yamashita H. *et al.* Development of a Cell-penetrating Peptide that Exhibits Responsive Changes in its Secondary Structure in the Cellular Environment. *Sci. Rep.* **6**, 2–9 (2016).
169. Yang Y. *et al.* Use of Tomato yellow leaf curl virus (TYLCV) Rep gene sequences to engineer TYLCV resistance in tomato. *Phytopathol.* **94**, 490–496. (2004).

170. Yang, X., Zhou, M., Qian, Y., Xie, Y. & Zhou, X. Molecular variability and evolution of a natural population of tomato yellow leaf curl virus in Shanghai, China. *J. Zhejiang Univ. Sci. B* **15**, 133–142 (2014).
171. Zabielski, R., Godlewski, M. M. & Guilloteau, P. Control of development of gastrointestinal system in neonates. *J. Physiol. Pharmacol.* **59**, 35–54 (2008).
172. Zadoks, J. C. & Waibel, H. From pesticides to genetically modified plants: History, economics and politics. *NJAS - Wageningen J. Life Sci.* **48**, 125–149 (2000).
173. Zadoks, J. Fifty years of crop protection, 1950–2000. *NJAS - Wageningen J. Life Sci.* **50**, 181–193 (2003).
174. Zerbini, F. M. *et al.* ICTV Virus Taxonomy Profile: Geminiviridae. *J. Gen. Virol.* **98**, 131–133 (2017).
175. Zhang, Y. *et al.* Physicochemical property guidelines for modern agrochemicals. *Pest Manag. Sci.* **74**, 1979–1991 (2018).
176. Zhao, L. *et al.* Advances and prospects in biogenic substances against plant virus: A review. *Pestic. Biochem. Physiol.* **135**, 15–26 (2016).
177. Zhu, F. Structures , physicochemical properties , and applications of amaranth starch Structures , physicochemical properties , and applications of amaranth starch. *Crit. Rev. Food Sci. Nutr.* **57**, 313–325 (2017).
178. Zrachya A. *et al.* Production of siRNA targeted against TYLCV coat protein transcripts leads to silencing of its expression and resistance to the virus. *Transgenic crops.* 385–398 (2007).



## A peptide derived from enzymatic digestion of globulins from amaranth shows strong affinity binding to the replication origin of Tomato yellow leaf curl virus reducing viral replication in *Nicotiana benthamiana*



J.S. Mendoza-Figueroa<sup>a</sup>, A. Kvarnheden<sup>b</sup>, J. Méndez-Lozano<sup>c</sup>, E.-A. Rodríguez-Negrete<sup>d</sup>, R. Arreguín-Espinosa de los Monteros<sup>a</sup>, M. Soriano-García<sup>a,\*</sup>

<sup>a</sup> Department of Biomacromolecular Chemistry, Instituto de Química, Universidad Nacional Autónoma de México. Mexico City, Mexico

<sup>b</sup> Department of Plant Biology, Swedish University of Agricultural Sciences, Uppsala, Sweden

<sup>c</sup> Department of Agrobiotechnology, Centro Interdisciplinario de Investigación para el Desarrollo Integral Regional-Sinaloa, Instituto Politécnico Nacional, Guasave, Sinaloa, Mexico

<sup>d</sup> CONACYT, Instituto Politécnico Nacional, Department of Agrobiotechnology, Centro Interdisciplinario de Investigación para el Desarrollo Integral Regional-Sinaloa, Instituto Politécnico Nacional, Guasave, Sinaloa, Mexico

### A B S T R A C T

Tomato yellow leaf curl virus (TYLCV; genus *Begomovirus*; family *Geminiviridae*) infects mainly plants of the family Solanaceae, and the infection induces curling and chlorosis of leaves, dwarfing of the whole plant, and reduced fruit production. Alternatives for direct control of TYLCV and other geminiviruses have been reported, for example, the use of esterified whey proteins, peptide aptamer libraries or artificial zinc finger proteins. The two latter alternatives affect directly the replication of TYLCV as well as of other geminiviruses because the replication structures and sequences are highly conserved within this virus family. Because peptides and proteins offer a potential solution for virus replication control, in this study we show the isolation, biochemical characterization and antiviral activity of a peptide derived from globulins of amaranth seeds (*Amaranthus hypochondriacus*) that binds to the replication origin sequence (OriRep) of TYLCV and affects viral replication with a consequent reduction of disease symptoms in *Nicotiana benthamiana*. Aromatic peptides obtained from papain digests of extracted globulins and albumins of amaranth were tested by intrinsic fluorescent titration and localized surface resonance plasmon to analyze their binding affinity to OriRep of TYLCV. The peptide AmPep1 (molecular weight 2.076 kDa) showed the highest affinity value (K<sub>d</sub> = 1.8 nM) for OriRep. This peptide shares a high amino acid similarity with a part of an amaranth 11S globulin, and the strong affinity of AmPep1 could be explained by the presence of tryptophan and lysine facilitating interaction with the secondary structure of OriRep. In order to evaluate the effect of the peptide on *in vitro* DNA synthesis, rolling circle amplification (RCA) was performed using as template DNA from plants infected with TYLCV or another begomovirus, pepper huasteco yellow vein virus (PHYVV), and adding AmPep1 peptide at different concentrations. The results showed a decrease in DNA synthesis of both viruses at increasing concentrations of AmPep1. To further confirm the antiviral activity of the peptide *in vivo*, AmPep1 was infiltrated into leaves of *N. benthamiana* plants previously infected with TYLCV. Plants treated with AmPep1 showed a significant decrease in virus titer compared with untreated *N. benthamiana* plants as well as reduced symptom progression due to the effect of AmPep1 curtailing TYLCV replication in the plant. The peptide also showed antiviral activity in plants infected with PHYVV. This is the first report, in which a peptide is directly used for DNA virus control in plants, supplied as exogenous application and without generation of transgenic lines.

### 1. Introduction

Plant diseases caused by viruses affect crops worldwide resulting in large economic losses [1]. For production of tomato (*Solanum*

*lycopersicum*), tomato yellow leaf curl virus (TYLCV; family *Geminiviridae*; genus *Begomovirus*) is one of the most important viruses [2]. The symptoms that TYLCV induces are curling of leaves, chlorosis, dwarfing and floral abortion. TYLCV is naturally transmitted by whiteflies of the

\* Corresponding author.

E-mail address: [soriano@unam.mx](mailto:soriano@unam.mx) (M. Soriano-García).

*Bemisia tabaci* species complex producing a systemic infection, in which the virus is translocated to the sieve elements and is spread throughout the plant [3]. The virus can accumulate in the fruit, including the seed embryo [4a,b,5], allowing this virus to be transmitted by seeds [6], which in turn increases the risk of spread of the virus.

TYLCV has a genome of a circular and single stranded (ss) DNA (viral sense, VS) with an approximately length of 2.8 Kb. The genome has six overlapping open reading frames (ORFs), with two ORFs on the viral sense strand (V1 and V2) and the other four ORFs on the complementary DNA strand (C1, C2, C3 and C4) [7]. The replication of this virus is mediated by a rolling circle replication (RCR) mechanism or recombination dependent replication (RDR). The intergenic region (IR) of the TYLCV genome contains the replication origin, which is a sequence of 25 nucleotides forming a secondary structure of “loop” shape [8], and this loop has the function to regulate replication through RCR, mainly by being target for the Rep protein (encoded by the C1 gene), which is the initiator of this replication process [8,9]. Once the viral DNA (VS) enters the nucleus of the host cell, synthesis of the complementary strand (CS) occurs. Subsequently, when the Rep protein is expressed, it binds specifically to the loop type structure in the IR and nicks it leaving a free hydroxyl group for start of DNA synthesis through RCR [9]. As the new chain grows, it displaces the original VS strand, resulting in the production of a new VS strand, which will be used as a template for synthesis of the CS strand as well as for the packaging of new viral particles [10,11].

Proteins and peptides have been offering an alternative method for control of pathogens in crops, showing biological activity as inducers of systemic acquired resistance against fungal [12] and viral pathogens [13] in the experimental models of maize and tobacco, respectively. It has also been found that peptides with hydrophobic characteristics have direct antifungal activity on *Fusarium oxysporum* [14], as well as direct antibacterial activity against *Xylophilus ampelinus* and *Agrobacterium vitis* in grape plants [15]. Furthermore, it has been found that peptide extracts derived from enzymatic digestion of vegetable proteins induce growth in tomato and promote root development in maize [16].

Peptides have shown the ability to control infections by plant viruses because of their ability to bind specifically to molecular targets. Screening of aptamer peptide libraries identified peptides that showed affinity for the Rep protein of the begomovirus tomato golden mosaic virus (TGMV) and interfered with viral replication in cell cultures [17]. When two of these peptides were expressed in tomato plants infected by TYLCV or another begomovirus, tomato mottle virus (ToMoV), a decrease in symptoms development was observed in the transgenic lines [17]. Another effort for virus control with peptides has been reported using an artificial zinger protein, which has a strong affinity to the IR of the TYLCV genome [18]. However, no plant experiments were done in this study.

Cereals and pseudocereals offer a big source of bio-macromolecules, as they contain high amounts per gram-tissue of proteins, polysaccharides and lipids in comparison to other plants [19,20,21]. These molecules can be purified or partially purified and be a source of derivative molecules such as peptides and oligosaccharides, hence increasing the library of possible compounds with biological activity from natural sources. Seeds of amaranth (*Amaranthus hypochondriacus*) contain large amounts of proteins in comparison to other cereals and pseudocereal plants, making this plant a good candidate for extraction of bioactive molecules such as peptides. The albumin and globulin fraction in amaranth represents approximately 19–20% of the total protein content, and can be used directly or as peptides for the design of molecules with bio-functional activity [22,23,24].

Previous research on amaranth proteins has focused mainly on the antihypertensive, cytotoxic, antioxidant and antifungal activities, while the antiviral activity properties of these proteins in animal or plant systems are still unknown. Peptide derivatives obtained through enzymatic digestion of water-soluble proteins from amaranth keep the bioactivities mentioned above. *In vitro* experiments have shown that the

bioactivity of peptides may be higher because the size of the biomolecule is smaller allowing improved uptake into the cell and interaction with cell receptors [25].

In the present work, we describe the anti-viral activity of a peptide obtained through enzymatic digestion of the globulin fraction of amaranth seeds. When the peptide solution was infiltrated into *Nicotiana benthamiana* plants infected by TYLCV, it showed antiviral activity by reducing symptoms and viral titer. The possible mechanism of action of this molecule is that AmPep1 binds with highly affinity to the virus origin of replication preventing further interaction with viral replicase and subsequent viral replication. To our knowledge, this is the first report, which uses a peptide derived directly from a plant source for direct treatment against TYLCV and applies it in an exogenous way without the generation of transgenic plants.

## 2. Material and methods

### 2.1. Cultivation of plants and bacteria

Seeds of *N. benthamiana* and *S. lycopersicum* cv. “Moneymaker” were disinfected with ethanol (70%) for one minute and then rinsed several times with sterile water. Plants were cultivated separately in pots with a mixture of perlite-vermiculite (1:1) and incubated in a growth chamber with a photoperiod of 18/6, light and darkness, respectively, at 28 °C and a relative humidity of 72%.

Cells of *Agrobacterium tumefaciens* C58C1 containing an 1.8-mer construct (1.8 genome units) of the genome for TYLCV-[EE-Imp-05-08] (Accession no. HF548826) [4b,4] cloned in pLH7000\*, were grown in LB with antibiotics (rifampicin 50 µg/mL, streptomycin 300 µg/mL) for 24 h with shaking (28 °C, 200 rpm). The preparation of inoculum for agroinoculation was essentially as described previously [5].

### 2.2. Synthetic peptide and oligonucleotides

The oligonucleotide OriRep (5'-CGTATAATATTACCGGATGGCCG CGC-3') [26] was used as viral target. This is a conserved DNA sequence of TYLCV and other geminiviruses, located in the origin of replication loop structure, which is recognized by the Rep protein to initiate replication. The short peptide RepApep (NIQGAKSSSDVKSIDK; MW 1.84 kDa, pI 8.43), contains the domain of Rep binding to the TYLCV replication origin (sequence mentioned above) and was used as a positive control for interaction assays [8,26]. Oligonucleotide primers for rolling circle amplification (RCA) were designed to cover the complete genome of TYLCV (Table 1). For detection of systemic infection by TYLCV using standard PCR, the universal degenerate begomovirus primers AC1048 and AV548 were used [27]. For TYLCV DNA

**Table 1**

Primers used for Rolling Circle Amplification to TYLCV. Primers cover forward and reverse sense of whole viral genome, \* PTO modification for stabilization during reaction.

Primer name	Primer 5'—> 3'	%GC	Tm	Size
V2 173	TTCCTGAAT*C	40	28	10
V2 488	CAGGGCTTC*G	70	34	10
CP 519	GCCCATGTA*A	50	30	10
CP 593	CACGAGTAA*C	50	30	10
CP 694	GCAGAATCA*C	50	30	10
CP 796	ACTGGGCTC*A	60	32	10
CP 882	CCTCTGGAA*T	50	30	10
CP 1050	TAGATGCGT*A	40	28	10
C3 1105	TGAGTTTCT*G	36.36	30	10
C3 1473	GATTCACGC*A	50	30	10
C2 1247	CCAGTCTGA*G	60	32	10
C2 1608	CCTCTACGA*G	60	32	10
C1 1670	CTTCGTCTA*G	50	30	10
C1 2024	GAAGAGTGG*G	60	32	10
C1/C4 2150	AGTCCTTG*G	50	30	10
C1/C4 2606	ATGCCTCGT*T	50	30	10



quantification by qPCR, the TYLCV primers OVS and OCS were used [28]. Normalization of qPCR was performed using the primers 25SUNIV (+) and 25SUNIV (–) (TAG Copenhagen A/S), which target the 25S nuclear ribosomal RNA gene (accession no. ×13557). This gene is conserved among plants within the family Solanaceae and these primers have been used for normalization of geminivirus quantification in plants of *N. benthamiana* and tomato [28,29,30].

### 2.3. Extraction of aqueous protein fraction of amaranth seeds

Amaranth globulins and albumins were extracted according to the protocol of Romero-Zepeda & Paredes-Lopez, 1995 [31] with slight modifications. In brief, amaranth flour was obtained from ground heated seeds, and the flour was defatted and conserved at room temperature until use. A flour suspension was prepared in water and the pH was adjusted to 8.5 with 0.1 M NaOH. The suspension was incubated at +4 °C overnight and centrifuged. The supernatant containing globulins and albumins was collected and the pH adjusted to 7.0. The globulin/albumin suspension was digested with 0.05% of papain (Sigma-Aldrich) for 18 h at 37 °C with shaking. After the incubation, the digested suspension was collected quickly in cryo-concentrator devices [32]. The eluted peptide extract was passed through an ultrafiltration system (Amicon) with a cut range membrane of 10 KDa. Liquid that passed through the membrane (< 10 KDa) was collected and the upper remnant was discarded.

### 2.4. Purification and partial characterization of peptide fraction

The UV spectrum (Shimadzu, U160) of the peptide total extract (PTE) was measured to identify the maximum absorption peaks for downstream application. Then, the PTE was pre-fractionated in a Kromasil C18 250 mm HPLC column using a linear gradient of water: 0–30% acetonitrile for 20 min with a flow rate of 1 mL/min and detection channels at 210 and 280 nm. Two main fractions were collected, and each fraction was recirculated in the same HPLC C18 column as mentioned above under the following conditions: Fraction 1 linear water gradient with 0–4% acetonitrile, flow 1 mL/min for 15 min; Fraction 2 linear water gradient with 5–15% acetonitrile, flow 1 mL/min for 15 min. The peaks with high absorbance at 280 nm were collected; this was an exclusion criterion in order to get peptides with aromatic residues, which have higher probability for crossing through cell walls and membranes in plants than non-aromatic peptides [33,34]. Each collected peak was recirculated in the HPLC C18 column. The molecular weights of the purified fractions were analyzed by MALDI-TOF (Bruker Microflex). To confirm the content of aromatic amino acids, purified peptides were analyzed using intrinsic fluorescence with an excitation wavelength of 280–295 nm (Trp excitation wavelength) and an emission wavelength of 310–410 nm.

### 2.5. Interaction affinity assay of amaranth peptides and TYLCV DNA by nanogold localized surface resonance plasmon (LSRP)

#### 2.5.1. Interaction assay

The interaction between the DNA oligonucleotide OriRep and amaranth peptide was studied using LSRP with gold nanoparticles (AuNP) [35]. Nine peptide concentrations (1000, 500, 250, 125, 63, 32, 16, 8 and 0 nM) were used to test the affinity between peptides and OriRep. In brief, to each well of a microplate, 70 µL of AuNP, 10 µL of the oligonucleotide OriRep at different concentrations and 10 µL of milliQ water were added, followed by the addition of 10 µL of amaranth peptide dilutions in interaction buffer (0.2 M NaHCO<sub>3</sub>, 0.5 M NaCl, pH 7.4) and incubation for 10 min at room temperature with gentle shaking. The absorbance spectra were then recorded at 400–800 nm. The dissociation constant ( $K_d$ ) was calculated with non-linear regression [35]. Data was collected from three repetitions with three

technical replicates for each condition, and was analyzed using non-linear regression in GraphPad version 6 (GraphPad Software, Inc).

#### 2.5.2. Electronic microscopy and dynamic light scattering (DLS)

The AuNP-DNA-peptide system was prepared as described in Section 2.5.1 in a total volume of 100 µL. After the incubation time, one aliquot was analyzed in an electronic microscope (VEGA3 TESCAN in mode TE Bright, HV 15.0 KV) to evaluate the grade of particle aggregation. Another aliquot of the AuNP-DNA-peptide system was analyzed using DLS, recording the hydrodynamic ratio at 25 °C. Three technical replicates were used. One-way ANOVA was used for comparing the hydrodynamic ratio of AuNP with different treatments against the ratio of gold particles in water.

### 2.6. Effect of AmPep1 peptide on *in vitro* TYLCV DNA synthesis

The isolated amaranth peptide with the strongest interaction with OriRep of TYLCV was called AmPep1, and was selected for studying its effect on *in vitro* TYLCV DNA synthesis by rolling circle amplification (RCA, phi29 system, Thermo Scientific). The DNA of TYLCV clone LV2015SATom (Accession no: KU836749.1) was used for this purpose. Specific primers were designed for amplification of the TYLCV genome by RCA and they were synthesized with a PTO modification at the 3' end for increased stability (Table 1). The RCA premix consisted of the 16 TYLCV-specific primers at a final concentration of 0.4 µM each, 1 × phi29 DNA polymerase buffer, 5 × 10<sup>6</sup> copies of TYLCV in total tomato DNA extract (viral copy number quantified by qPCR as described below) and water in a final volume of 10 µL. The premix solution was denatured for 3 min at 95 °C and cooled. After that, the denatured premix solution was used for RCA in a volume of 20 µL and with a final concentration of 0.4 µM of each TYLCV RCA oligonucleotide, 1 × phi29 DNA polymerase buffer, 15 mM of dNTPs, 2 U/µL of phi29 DNA polymerase, water and the amaranth peptide (AmPep1) or positive control (RepApep) in final concentrations of 0, 0.5, 1, 2, 5, 10, 20, 30 µM. The reaction was incubated at 30 °C for 18 h followed by a final enzyme inactivation step at 65 °C for 10 min. Negative controls for the assay were DNA of a healthy plant as well as pUC18 plasmid. Oligonucleotides used for the negative controls were nonspecific PTO modified Random Primers (Thermo Scientific). The RCA products were analyzed by agarose gel electrophoresis and 1 µg of RCA product of all treatments was digested with *Bam*HI (Thermo Scientific) to generate monomeric virus genome units. Digestion products were analyzed by agarose gel electrophoresis. The intensity of bands in the gel was used for relative quantification of the effect of peptide on *in vitro* viral DNA synthesis. Band intensity was estimated using the pixel number in the band area with the software Quantity-one (Bio-Rad) from three independent reactions for each condition, and the results are presented as the average of intensity between the three replicates (Fig. 3). A statistical analysis using One-Way ANOVA was performed, in which the band intensity of the reaction with peptide was compared to the treatment control (RCA reaction without peptide). Calculations were done in GraphPad version 6.

#### 2.6.1. Effect of AmPep1 on the *in vitro* DNA synthesis of another begomovirus

Because the TYLCV IR sequence chosen as the molecular target for the AmPep1 peptide has a sequence highly conserved among viruses within the genus *Begomovirus*, it was decided to explore if AmPep1 had the same effect reducing *in vitro* viral DNA synthesis of another begomovirus: *Pepper huasteco yellow vein virus* (PHYVV). Amplification with RCA and electrophoretic analysis were performed as described in section 2.6, but using as template the DNA-A component of PHYVV LV2014GveCap9 (Accession no. KP890827). The *Eco*RI enzyme (Thermo Scientific) was used for digestion of PHYVV RCA products.

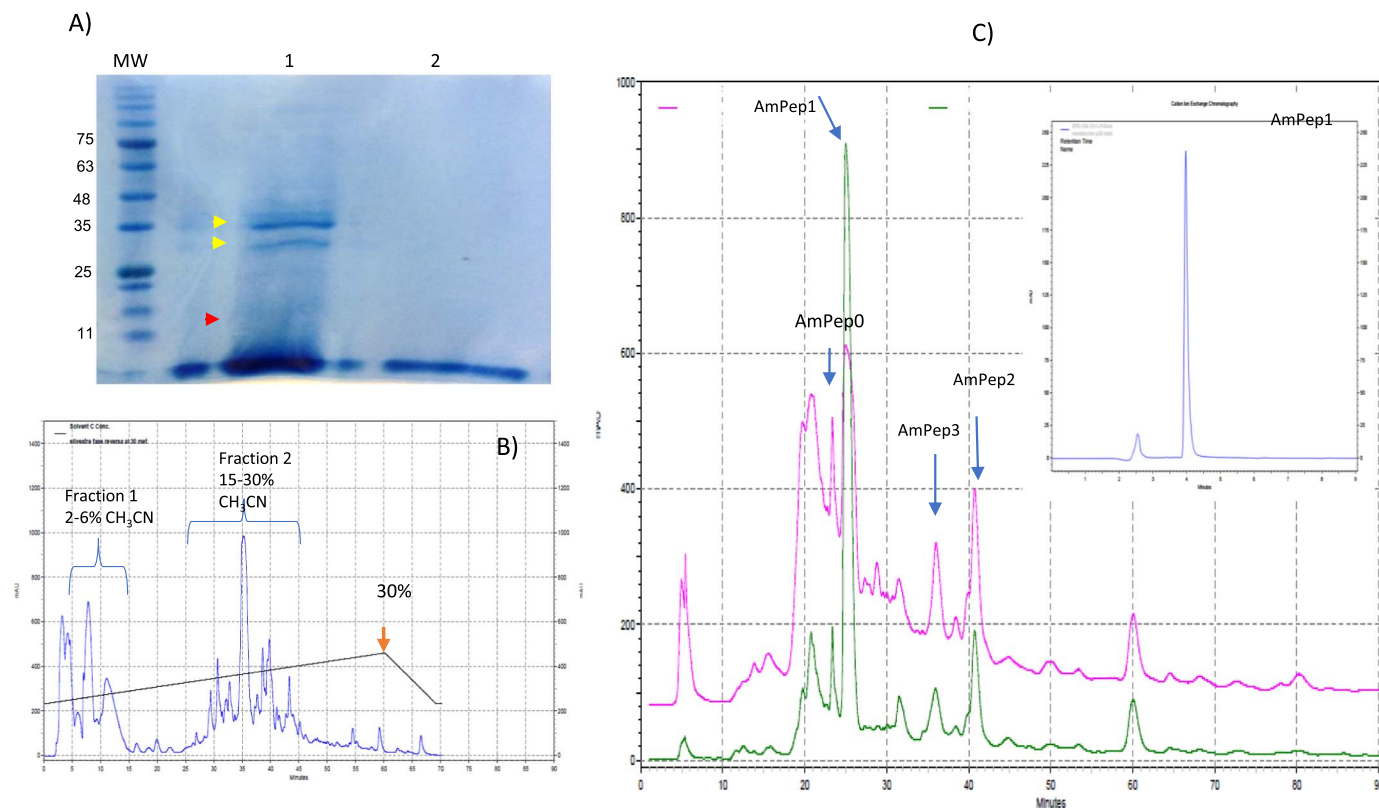


**Fig. 1.** Protein extraction and peptide purification. (A) As SDS-PAGE shows, the soluble proteins in alkaline conditions (pH 8.5) were globulins and albumins: globulin subunits (36 and 27 kDa) marked with yellow arrow heads, albumin precursor marked with red arrow head (weak band around 12 kDa), lane 1. After extraction, the protein suspension was hydrolyzed with papain, and after 18 h of enzymatic digestion, no remaining proteins were observed, just peptides with a molecular weight of < 11 kDa, lane 2. MW: molecular weight ruler, BlueEye Prestained Protein Marker, Jena Bioscience. (B) The peptide extract was concentrated and analyzed by RP-HPLC using a C18 column. Almost all peptides in the extract were eluted with < 30% of acetonitrile, and two main fractions were separated for further purification steps. Peaks with strong abundance and absorbance at 280 nm were collected in both fractions (C), purified with RP-HPLC and analyzed for intrinsic fluorescence. Only peptides from fraction 2 showed this last property. The purified peptide AmPep1 was used for subsequent biological experiments (inner chart C) due to its ability to bind with TYLCV DNA. (For interpretation of the references to colour in this figure legend, the reader is referred to the web version of this article.)

## 2.7. Antiviral activity in *Nicotiana Benthamiana* plants

At the age of 3 weeks, *N. benthamiana* plants were agroinoculated with an infectious clone of TYLCV as described in Section 2.1. At 15 days post-inoculation (dpi), plants started to display symptoms of disease, and samples of each plant were collected to extract DNA using a CTAB method [36]. A standard PCR was performed to verify systemic infection using universal begomovirus primers as described in section 2.2 [27]. Once infection was confirmed, groups of 6 plants ( $n = 6$ ) were used to evaluate the effects of peptide treatment on disease development. Infected plants in the first group were infiltrated in the upper symptomatic leaves with a solution of AmPep1 (100 mg/L), plants in the second group with RepApep (100 mg/L), and plants in the third group only with infiltration buffer (untreated control). As another control, a group of healthy plants were infiltrated with infiltration buffer. Disease progress was evaluated during 15 days after treatment. Samples of new apical leaves were collected for DNA extraction at 0, 7 and 15 days after treatment. Symptom evaluation was performed through 15 days after treatment. Plant height and inter-node distance were considered as symptom indicators.

To evaluate the effect of AmPep1 on infection by another begomovirus, *N. benthamiana* plants were infected with PHYVV (component A and B) as described in Section 2.1. After symptoms had developed in new apical leaves, AmPep1 (100 mg/L) was infiltrated in all apical symptomatic leaves of six infected plants, and the progress of disease symptoms was evaluated. A group of six PHYVV-infected plants

infiltrated with infiltration buffer was used as untreated control and another group of healthy plants infiltrated with infiltration buffer was also used as a control.

## 2.8. Quantification of viral DNA amount in treatments

To evaluate the amount of TYLCV DNA in *N. benthamiana* plants after treatment with AmPep1, qPCR was performed using primers OVS/OCS [27] and SensyFAST SYBR Lo-Rox (Bioline) mix according to manufacturer's instructions. The reactions were performed in a CFX-Connect Real-Time PCR detection Machine (Bio-Rad). For normalization of the qPCR results, amplification of the host reference gene 25S rRNA with the primer set 25UNIV(+)/25 UNIV(-) was used [27,28]. The relative amount of viral DNA was determined in individual plants for each treatment according to the  $2^{-\Delta\Delta Ct}$  formula [37], comparing the relative DNA titer of treated against untreated infected plants. One-Way ANOVA was used for analyzing the differences statistically.

## 2.9. Peptide sequence and BLAST analysis

Purified peptides samples were analyzed using MALDI-TOF-TOF method at The Mass Spectrometry Center of Boston College. The BLAST server [38] was used for identifying the origin of the peptide, restricting the analyses to only proteins of plants belonging to the family Amaranthaceae.

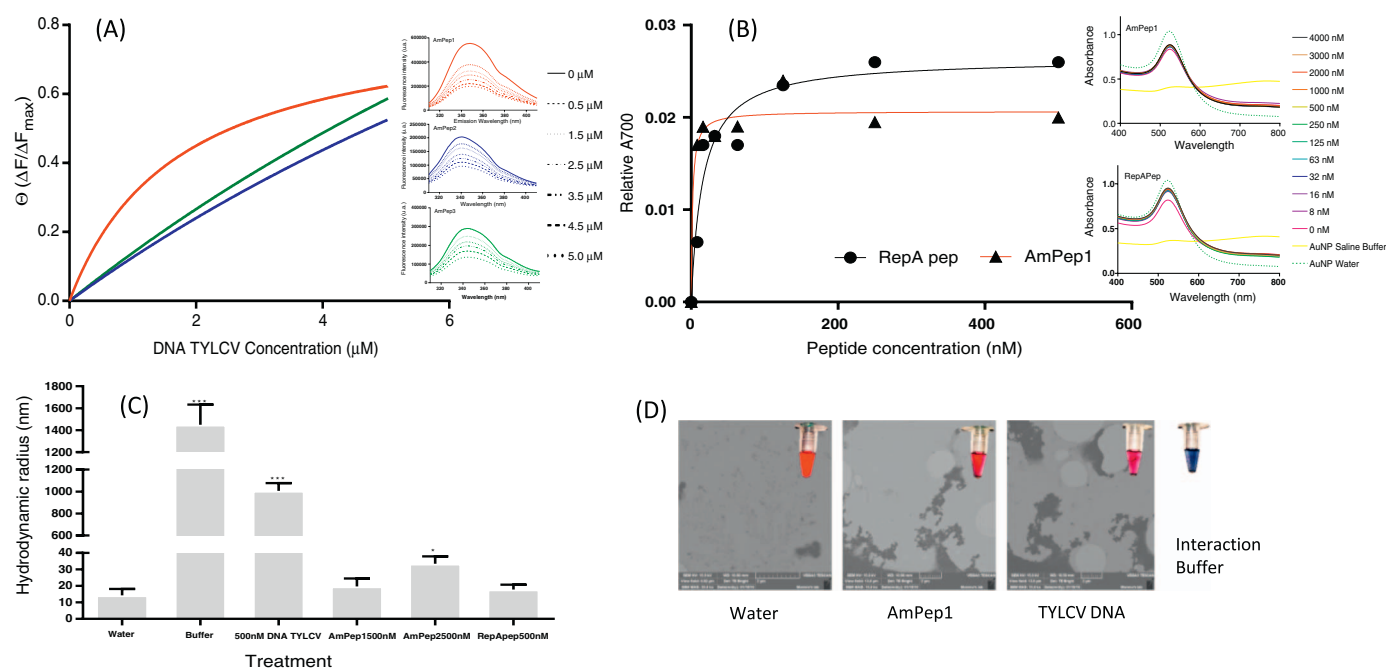


**Fig. 2.** Screening and interaction of amaranth peptides (AmPep) with TYLCV origin of replication. (A) Saturation curves of three purified amaranth peptides (AmPep1, 2 and 3, red, blue and green chart, respectively) with OriRep TYLCV oligonucleotide (target). The inner plots show the quenching of intrinsic fluorescence by peptides at increasing concentrations of OriRep. AmPep1 (red) showed faster saturation (inflection in the curve) than the other two peptides. (B) The dissociation constant ( $K_d$ ) of AmPep1 and RepApep with OriRep was calculated using LSRP. Gold nanoparticles were coated with 500 nM of OriRep, and then peptides (AmPep1 or RepApep) dissolved in interaction buffer (IB) were added separately in increasing concentration. Langmuir charts were plotted using the relative absorbance at 700 nm as interaction indicator, and non-linear regression was performed to calculate  $K_d$  values. The inner plots show the effect of peptides protecting aggregation of AuNP (increase of plasmon signal at 520 nm) under saline conditions, compared with AuNP coated just with the oligonucleotide OriRep (bottom pink line). (C) The hydrodynamic radius of AuNP was estimated to confirm interaction between OriRep and peptides. Strong binding between target and ligand (DNA and peptide) protects the AuNP from aggregation in IB (the aggregated particles should be increasing the radius), keeping the size and distribution of AuNP similar to water conditions. (D) TEM micrographics of AuNP (left to right) in water conditions, AuNP coated with OriRep after adding AmPep1 in IB and AuNP coated with OriRep in IB. The last blue tube contains non-coated AuNP after adding only IB, showing the displacement of plasmon to 700 nm (blue colour) due to complete aggregation of AuNP. Error bars represent SD, asterisk indicates a significant difference ( $P < 0.05$ ). (For interpretation of the references to colour in this figure legend, the reader is referred to the web version of this article.)

### 3. Results

#### 3.1. Purification and biochemistry study of peptides from aqueous amaranth extract

Soluble proteins in alkaline aqueous conditions (globulins and albumins) of *Amaranthus hypochondriacus* seeds were extracted and then digested with papain. The main protein fraction observed under the extraction conditions (water pH 8.5) was polypeptides of 11S globulin and polypeptides of albumins (Fig. 1A). After digestion, reverse phase HPLC was performed to purify the main peptide fraction for further applications, and a fraction with high absorbance in 280 nm was collected (Fig. 1B). The aromaticity in peptides have been shown to increase the ability of peptides to cross through cell membranes, which means that they can be used easily for exogenous application in plant treatments. Four main aromatic sub-fractions from fraction 2 were collected (Fig. 1C), purified and analyzed for intrinsic property of fluorescence confirming the presence of tryptophan residues in the purified peptides (peptide fractions from fraction 1 did not show intrinsic fluorescence for Trp, Tyr or Phe). This last chemistry property was used also to study the interaction of amaranth peptides with the viral DNA target. Three out of four peptides showed strong intrinsic fluorescence (AmPep1, AmPep2, AmPep3) at different intensities. When a solution of viral DNA target (OriRep) was added at an equimolar ratio, AmPep1 showed the highest quenching effect on fluorescence in comparison with the other two peptides (Fig. 2A, inner plots). The interaction effect was best visualized when OriRep with increased concentration was added to the peptide solution, showing faster saturation of binding sites for AmPep1 compared with the other two ligands (see

inflection of the curve in the red chart, Fig. 2A). For this reason, we chose AmPep1 as the model for downstream studies on antiviral activity.

To identify the physicochemical binding parameters of AmPep1 with viral DNA (OriRep), LSRP was performed. This method was selected to compare the interaction of AmPep1 versus the control peptide RepApep, which represents the binding domain of the TYLCV RepA protein to the OriRep DNA sequence, used as the target in this study. Because RepApep has not shown any intrinsic fluorescence feature, we decided to use the LSRP method. AmPep1 and RepApep showed similar dissociation constant values (Table 2) when increasing concentrations of both peptides were added (Fig. 2B), confirming the interaction identified for AmPep1 by quenching fluorescence (Fig. 2A). LSRP uses nanogold particles (AuNP) as the matrix, and plasmons in AuNP are used to detect any change in the surface after being coated with a target in saline buffer media. High ionic strength of the interaction buffer causes physical aggregation of AuNP, and this increase in particle size changes the plasmon absorbance to 700 nm. When the viral target oligonucleotide OriRep was attached to AuNP, this protected AuNP against aggregation in the interaction buffer due to electrostatic and steric effects. When a ligand (peptide) in the same saline buffer is added to DNA-coated AuNP, the ligand binds to target (if the ligands have affinity), increasing the electrostatic repulsion effect and the distance between particles. Hence, the aggregation reaction is avoided, and the plasmon absorbance is kept at 520 nm (see inner charts in Fig. 2B). Also, the size of the AuNP in the saline conditions is a direct measure of the ligand-binding interaction. We observed that particles coated with only DNA significantly increased the radius compared to the smaller radius of particles in water. When particles were coated with DNA and

**Table 2**

Biochemistry properties of peptides derived from enzymatic digestion of proteins of *Amaranthus hypochondriacus*. MW: Molecular weight,  $K_d$ : dissociation constant with OriRep DNA, pI: Isoelectric point.

Peptide	MW (KDa)	Sequence	pI	$K_d(\mu\text{M})$	Origin
RepApep	1.84	NIQGAKSSSDVKSYIDK	8.43	$1.4 \times 10^{-2} \pm 4.25$	RepA TYLCV
AmPep1	2.076	SVGRKWRMKWAQMRQQ	12.3	$1.8 \times 10^{-3} \pm 0.22$	Partial Complementary with 11S Globulin
AmPep2	1.852	MSVGRKWRSTMKWAQ	12.0	$12.84 \pm 1.97$	Partial Complementary with AmA1 protein

peptides were added (AmPep1 and RepApep), the radius was smaller than in the case of particles coated just with DNA. Also, AmPep2 was tested in order to confirm the weak interaction observed in fluorometric analyses, showing a significant increase of the particle radius compared with AuNP in water or with AmPep1 (Fig. 2C,D). These results indicate a strong interaction of the amaranth peptide AmPep1 with DNA of TYLCV.

**3.2. AmPep1 could affect *in vitro* viral DNA synthesis**

The oligonucleotide OriRep is a short sequence located in the replication origin of TYLCV and other geminiviruses. It is part of a structured DNA loop that has the function to bind the RepA protein and initiate the replication of viral DNA according to the rolling circle replication model. The idea of using this viral target was to use a

candidate molecule with antiviral activity to affect directly virus replication in the plant. An assay of *in vitro* viral DNA synthesis was carried out for evaluating the effect of AmPep1 on DNA synthesis. If the peptide had a strong affinity to TYLCV DNA, it was expected that *in vitro* DNA synthesis would be blocked because the peptide could interfere with DNA synthesis by clogging sterically the activity of the phi29 DNA-polymerase and decrease the amount of synthesized DNA product. The assay showed that AmPep1 and the control peptide RepApep were both able to decrease *in vitro* synthesis of the TYLCV genome at concentrations above 5  $\mu\text{M}$  (Fig. 3A, B). At a peptide concentration above 10  $\mu\text{M}$ , there was a significant reduction in the amount of RCA product. Interestingly, the peptide AmPep1 could also decrease the *in vitro* DNA synthesis of another begomovirus: PHYVV. In order to verify specific binding of AmPep1 to the viral target and rule out an unspecific effect of the peptide on the DNA-polymerase, an RCA reaction with pUC18

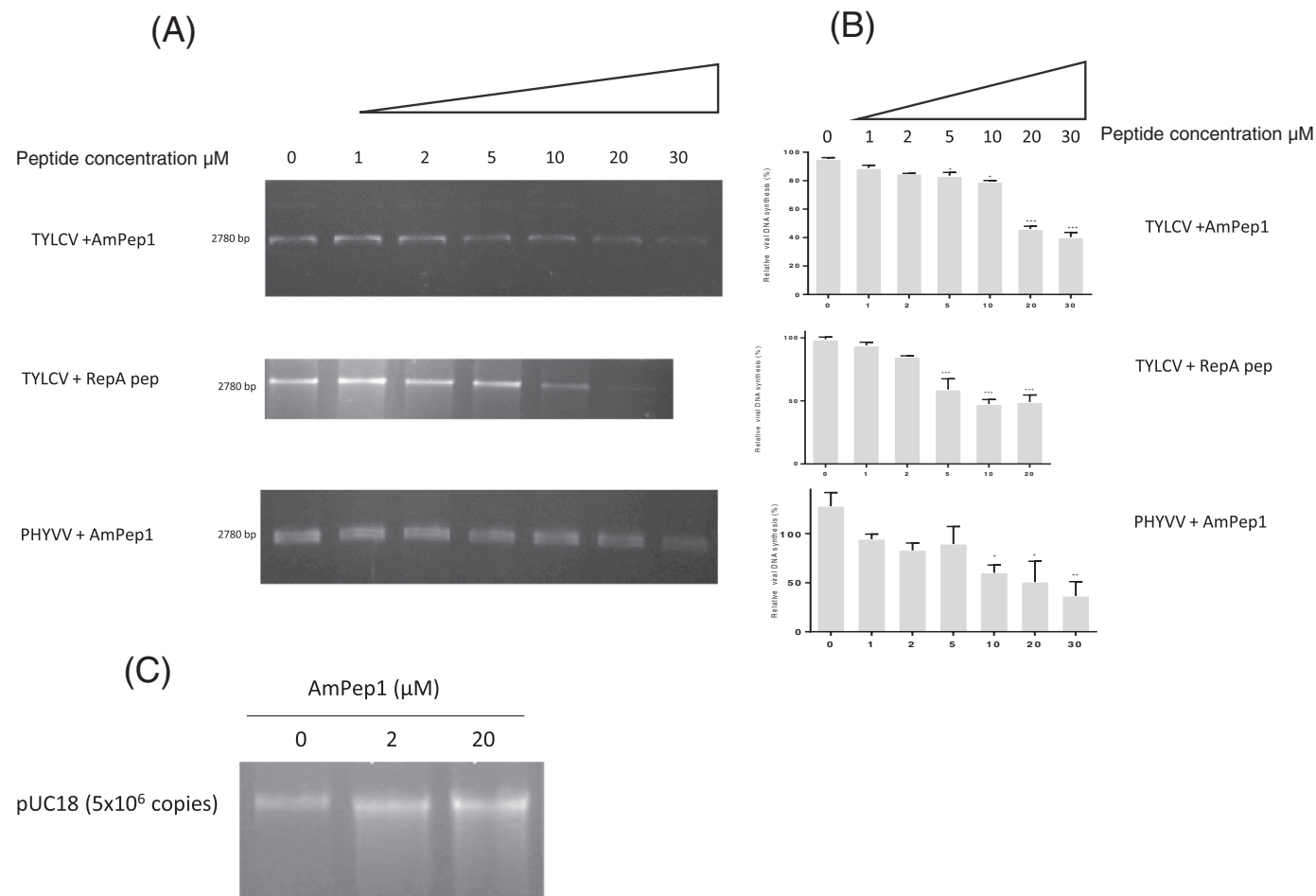


**Fig. 3.** AmPep1 decreases the *in vitro* synthesis of TYLCV and PHYVV DNA. (A) RCA reaction with increasing concentration of AmPep1 or RepApep (0, 1, 2, 5, 10, 20 and 30  $\mu\text{M}$ ) and in all treatments, equal DNA concentration. Top to bottom: DNA of TYLCV and AmPep1, DNA of TYLCV and RepApep, DNA of PHYVV and AmPep1. (B) Relative quantification of percentage of viral DNA synthesis by RCA in the presence of peptides. The results were obtained using densitometric analyses of bands in gels shown in (A). Top to bottom: DNA of TYLCV and AmPep1, DNA of TYLCV and RepApep, DNA of PHYVV and AmPep1. (C) Control RCA reaction. The plasmid pUC18 was used as control with the same copy number as used for TYLCV. Two concentrations of AmPep1 were used (2 and 20  $\mu\text{M}$ ). No decrease in plasmid DNA synthesis by RCA was observed as a result of peptide treatment. Error bars represent SD, asterisk indicates a significant difference ( $P < 0.05$ ).

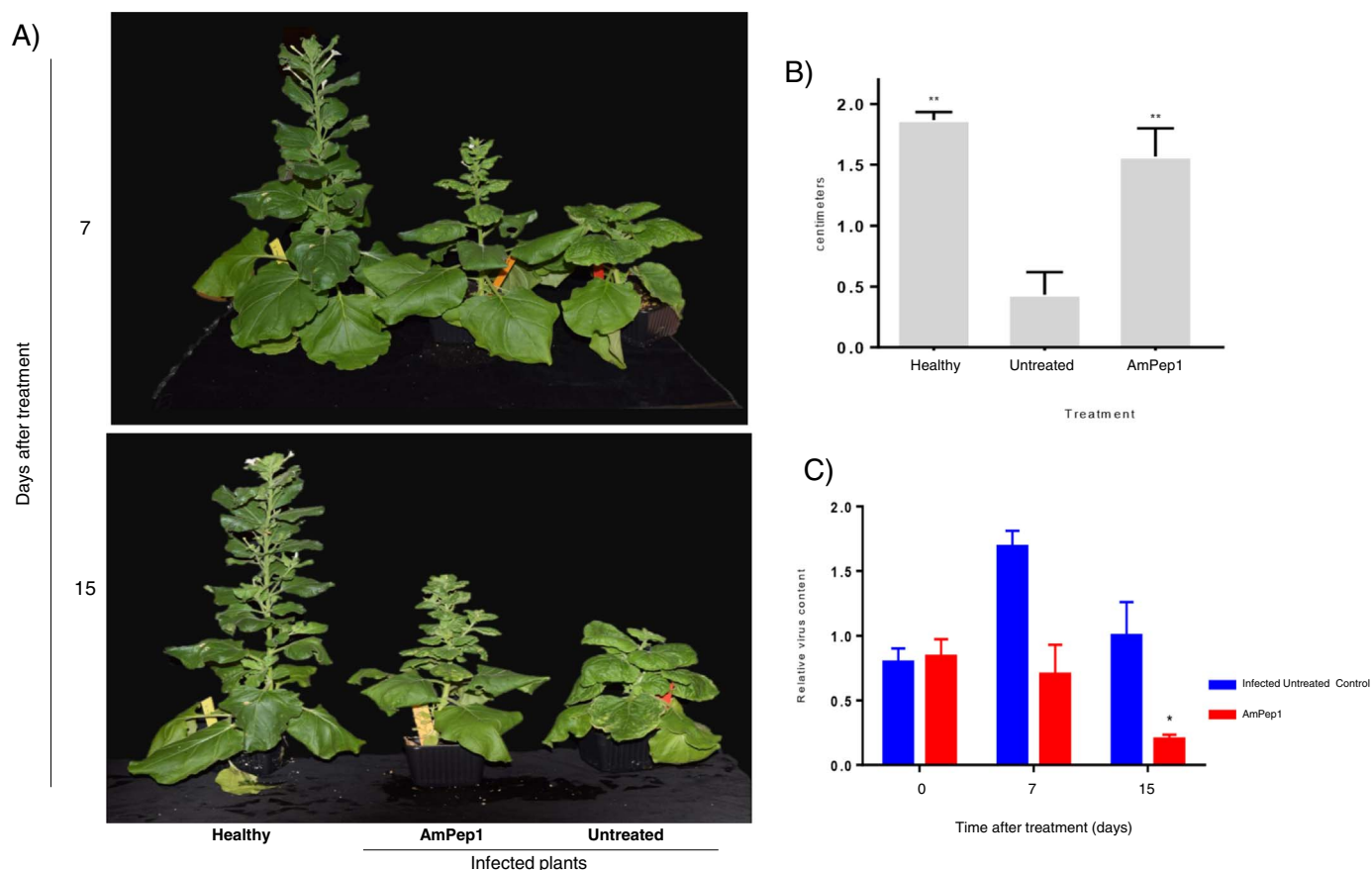


**Fig. 4.** Antiviral activity of AmPep1 in *N. benthamiana* plants infected with TYLCV. (A) Disease progress after treatment. Four-week-old plants were agroinfected with TYLCV, and when plants started to present symptoms of viral infection, one group of infected plants were infiltrated with AmPep1 in all apical leaves, while the other infected plants were used as a control group without peptide treatment. A group of healthy plants infiltrated with AmPep1 were used in order to compare the progress of disease. At 7 days post-treatment (dtr), infected plants treated with AmPep1 showed increased flowering and growth of stem internodes compared to infected plants not treated with AmPep1. (B) Internode distances between new leaves emerging after the peptide-infiltrated leaves were measured as symptom indicator showing a protection from dwarfing in treated plants. (C) Relative quantification of TYLCV DNA was performed using qPCR, and the virus DNA level had decreased significantly at 15 dtr. Error bars represent SD, asterisk indicates a significant difference ( $P < 0.05$ ).

plasmid as template was performed. No significant changes in band intensity of pUC18 RCA product were observed when AmPep1 was added at a low or high concentration (2 or 20  $\mu\text{M}$ , respectively), indicating that AmPep1 specifically binds to TYLCV DNA (Fig. 3C).

### 3.3. Antiviral activity of AmPep1 in *Nicotiana Benthamiana*

*Nicotiana benthamiana* plants were infected with TYLCV. After ensuring systemic infection, the plants were treated once by infiltration with AmPep1 in apical symptomatic leaves (infiltrating the whole leaf), and the progress of disease was quantified at 7 and 15 dpt. The internode distance was measured between new leaves after treatment. Dwarfing of the plant is an important symptom indicator of the TYLC complex disease. The length of the internodes was increasing in infected plants treated with AmPep1, and also flowering was increasing in these plants (Fig. 4A, B). The data of qPCR revealed a significant reduction in relative virus accumulation in new apical leaves at 15 dpt compared with the infected control, which show *in vivo* the expected antiviral effect of the amaranth peptide (Fig. 4C). In order to study the effect of AmPep1 on another begomovirus, *N. benthamiana* plants were infected with PHYVV. After ensuring systemic infection, the plants were treated with a solution of AmPep1, and at 15 dpt, the treated batch showed a decrease in symptom severity compared with untreated plants (Fig. 5). The effect of AmPep1 treatment on PHYVV titer was not determined, but the visual effects on the development of disease symptoms were evident. The effects on PHYVV infection were expected because the replication origin (target of AmPep1), as mentioned above, is highly

conserved in the geminivirus family, making AmPep1 a robust candidate agrochemical against geminivirus infections in crops.

### 3.4. Peptide sequence analysis

The amaranth peptide sequences (AmPep1 SVGRKWRMKWAQMRQQ and AmPep2 MSVGRKWRSTMKWAQ) were analyzed by comparing them with available protein sequences of plants belonging to the family Amaranthaceae. AmPep1 showed four conserved residues, which matched with the basic subunit of 11S amaranth globulin (Fig. 6A), while AmPep2 contained residues, which matched with the reported sequence of albumin subunit AmA1 (Fig. 6B), both from *Amaranthus hypochondriacus*. Lack of a 100% identity between the amaranth peptides and these proteins can be because of the variety of amaranth used in these experiments, which was a native *A. hypochondriacus* variety. Also, there are not enough reported sequences of amaranth globulins and albumins to develop a consensus sequence analysis, nor to verify if the amino acids that matched residues in AmPep1 and AmPep2 are part of a conserved sequence in these kinds of proteins.

## 4. Discussion

The amaranth plant is a crop with potential industrial application. It has a high content of essential amino acids, among which aromatic residues represent around 19%. The protein content in the amaranth grain is around 20% higher than for other cereal plants. Globulin and albumin are the main protein fractions, representing around 48% and

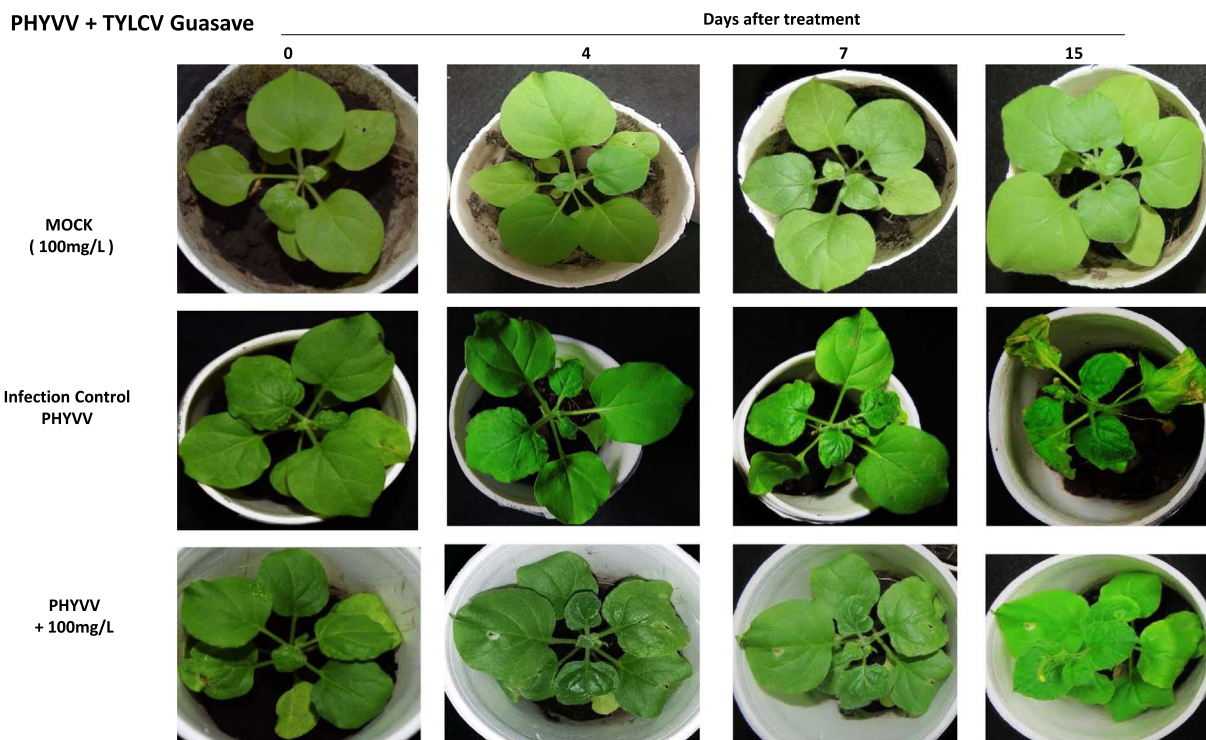


Fig. 5. Effect of AmPep1 in *Nicotiana benthamiana* plants infected with PHYVV. Three-week-old seedlings were agroinfected with PHYVV, and when plants started to present symptoms of viral infection, one group of infected plants were infiltrated with AmPep1 in all apical leaves, while the other infected plants were used as a control group without peptide treatment. A group of healthy plants infiltrated with AmPep1 were used in order to compare the progress of disease. The progress of disease symptoms was evaluated for 15 days. Plants treated with AmPep1 showed a decrease in symptom development. The image is a representation of 10 replicates of each condition.

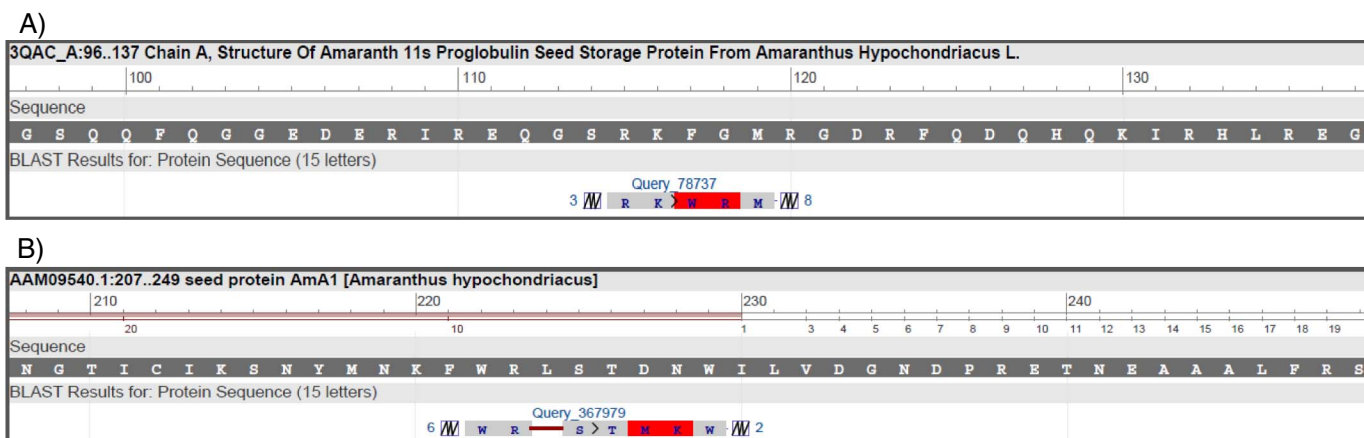


Fig. 6. Alignment analysis of AmPep1 and AmPep2 with amaranth proteins 11S globulin (3QAC\_A) and albumin (AAM09540). A) AmPep1 showed partial identity with Chain A of amaranth 11S globulin and B) AmPep2 showed partial identity with amaranth albumin (AmA1) protein. Both proteins were extracted under our experimental conditions from amaranth seeds. There are not enough of reported sequences of either protein to perform a consensus sequence analysis. The protein sequences are shown in dark gray, amino acid residues conserved between peptide and protein in light gray, and different amino acids in red. The numbers above the protein sequences indicate amino acid position. (For interpretation of the references to colour in this figure legend, the reader is referred to the web version of this article.)

20%, respectively [23]. Albumin is soluble in water, while globulin mainly is soluble in low concentration salt buffer. However, in alkaline conditions, around pH 8.5, extraction of both proteins is enhanced [39,40]. A few studies have reported the use of proteins against plant virus infections. In experiments with tobacco mosaic virus (TMV), esterified lactoferrin and lactoferrin were shown to have an inhibitory effect on TMV multiplication in tobacco when added together with the virus inoculum [41]. The mechanism of action was explained mainly by the induction of defense gene expression [41]. Another study has reported the use of lactoferrin and lactoalbumin from milk whey against TYLCV infection [42], showing a decrease of viral DNA after treatment, however without clarification of the possible mechanism of action.

Only one example of direct control of TYLCV replication has been reported [18], where an artificial zinc finger (AZF) protein was designed that binds to the replication origin of TYLCV, the same DNA sequence used in the present study. The AZF protein was shown to have one thousand times higher affinity than the Rep protein to viral DNA, with the affinity measured using electrophoretic mobility shift assay (EMSA). Compared with the affinity methods described here, for example, LSRP, which can quickly and in an inexpensive way analyze several candidate compounds simultaneously, the EMSA requires more experimental time, and is a more limiting method for exploring a big library of bio-molecules. Moreover, these authors did not report the antiviral activity in plants. A previous study by these authors [43] has shown the

interaction and binding effect between the AZF mentioned above with the replication origin of another geminivirus: beet severe curly top virus. They also reported that the concentration for avoiding binding between the RepA protein and the replication origin, determined using EMSA, is 10 nM of AZF. The AZF was also expressed in a transgenic *Arabidopsis* line. These transgenic plants did not show symptoms of viral disease, and the replicative forms of the virus decreased, indicating inhibition of replication. Transgenic crops are under higher regulation worldwide, making the benefits of the technology less accessible. Here, we are presenting the use of a peptide extracted from a plant source with antiviral function when it is applied exogenously, showing to be a cheaper alternative for control of viruses in plants.

The OriRep sequence is conserved within the whole geminivirus family, making it a molecular target for the control of viral replication. As observed in this study, the AmPep1 peptide decreases the DNA synthesis of TYLCV and PHYVV and also decreases symptom expression caused by both viruses in *N. benthamiana* plants, giving us an indication that the peptide has strong affinity for a highly conserved viral region and consequently reduces the rate of virus replication. The results indicate that this approach may be explored for controlling viruses of the genus *Begomovirus* and other viruses classified within the family *Geminiviridae*.

Until now, the use of bioactive peptides from storage seed proteins with antiviral activity in plants has not been reported. In order to explore the potential antiviral activity of peptides derived from hydrolyzed protein fractions from amaranth, we performed a non-specific enzymatic hydrolysis using papain. The peptides from these proteins can keep the same biological activity, enhance or have a new one, but they change in physicochemical properties, for example isoelectric point, solubility, permeability, etc. Non-specific enzymes such as papain or a cocktail of enzymes should be used for increasing the range of physicochemical and biological properties of peptides derived from proteins [44]. Papain has a non-specific cleavage site, which is not highly conserved as for trypsin for example, but has preference for cleavage between glutamine residues, followed by valine, alanine, and serine at the P2 and P2' positions, respectively. The peptides AmPep1 and AmPep2 analyzed here showed this cleavage pattern [45,46].

The aim of antiviral agrochemical development is discovering molecules that, besides control of the viral target, can efficiently cross cell barriers such as cell walls and membranes [47]. In this study, we infiltrated the peptide solution to ensure entrance to the parenchyma tissue. It seems that the peptide can move with certain freedom into all plant tissues, because it is able to control a virus located in the phloem. This translocation mechanism is supported also by the peptide sequence. AmPep1 is a basic peptide with two aromatic residues in its structure. The amino acid composition of this peptide is similar to peptides grouped as cell-penetrating peptides, which have the particularity of containing basic and aromatic residues. These peptides easily cross the cell membrane through a putative mechanism of action similar to a “flip-flop” mode allowing a direct passage through the membrane [48]. In this transport model, basic residues could interact with phosphates in the membrane, while aromatics (mainly tryptophan and phenylalanine) interact with the inner aliphatic chains, thereby disordering the phospholipids and facilitating translocation into the cytoplasm. This transport is mainly free from energy consumption. Cell-penetrating peptides can also be distributed into the nucleus with the same mechanism described for crossing cell membranes [49]. These kinds of peptides are located in several cellular proteins, viral capsids, etc. [33]. In plant proteins, the globulins contain basic sub-units; amaranth seeds have a basic subunit that contains aromatic residues such as tryptophan and phenylalanine as well as basic residues.

The antiviral mechanism of action of AmPep1 can be explained by the presence of tryptophan in its sequence. Besides giving the peptide the ability to cross cell structures, this amino acid has showed high affinity for DNA loop structures [50]. Tryptophan contains an indole ring that can be intercalated into a nucleotide base and interacts by

stacking forces between rings (indole and bases). In the affinity binding experiments between AmPep1 and TYLCV DNA a prominent quenching of intrinsic fluorescence emission was observed, supporting the idea of direct interaction between tryptophan residues and DNA. Peptides containing tryptophan and basic residues as well as being larger than four residues have been shown to discriminate loop DNA sequences as opposed to shorter peptides that are more non-specific [50,51]. This is explained by the flexibility of the molecule, which allows it to move through the DNA loop for binding in the best physicochemical condition (steric effect, proper partial charges, enough space for staking between indole rings and base rings). In our experiments, we showed that the peptide from amaranth does not affect synthesis of non-viral DNA, which might be because the size of the peptide (16 residues) enhances the specificity for the secondary structure of the replication origin of TYLCV.

From the present results, it can be concluded that proteins of amaranth seeds are a source of potential antivirals for application in crop protection. These peptides are rich in aromatic and basic amino acid residues, improving the uptake into plant cells, and increasing the affinity for replication structures. Further studies are being developed in our research group for revealing the complete molecular mechanism of action from a structural point of view.

## 5. Conclusions

The AmPep1 peptide derived from globulin hydrolysis of plant seeds of *Amaranthus hypochondriacus* has high affinity binding to the TYLCV replication origin loop structure. The exogenous application of this peptide reduced viral replication resulting in the suppression of symptoms caused by this virus in *N. benthamiana*.

Supplementary data to this article can be found online at <https://doi.org/10.1016/j.pestbp.2018.01.005>.

## Acknowledgments

José Silvestre Mendoza Figueroa is a doctoral student from Programa de Doctorado en Ciencias Biomédicas, Universidad Nacional Autónoma de México (UNAM) and received fellowship 363126 from CONACYT. We also want to thank Programa de Apoyo a los Estudios de Posgrado (PAEP-UNAM) for economical support in 2014 and 2016 enabling José Silvestre Mendoza Figueroa to develop two academic stays at Swedish University of Agricultural Sciences. This project was supported by SAGARPA-COFUPRO “Programa de Innovación, Investigación, Desarrollo Tecnológico y Educación (PIDETEC) Componente de Recursos Genéticos Agrícolas 2014” Project number: A/GTO/RGAG-2014-003.

We express our gratitude to the Department of Plant Biology of Swedish University of Agricultural Sciences, Uppsala, Sweden, for all facilities to develop part of this work.

## References

- [1] K.B.G. Scholthof, S. Adkins, H. Czosnek, P. Palukaitis, E. Jacquot, T. Hohn, G.D. Foster, Top 10 plant viruses in molecular plant pathology, *Mol. Plant Pathol.* 12 (2011) 938–954, <http://dx.doi.org/10.1111/j.1364-3703.2011.00752.x>.
- [2] E.P. Rybicki, A top ten list for economically important plant viruses, *Arch. Virol.* 160 (2015) 17–20, <http://dx.doi.org/10.1007/s00705-014-2295-9>.
- [3] C. Wege, Movement and localization of Tomato Yellow Leaf Curl Viruses in the Infected Plant, in: H. Czosnek (Ed.), *Tomato Yellow Leaf Curl Virus Disease*, Springer, 2007, [http://dx.doi.org/10.1007/978-1-4020-4769-5\\_11](http://dx.doi.org/10.1007/978-1-4020-4769-5_11).
- [4] (a) K. Just, U. Arif, A. Luik, A. Kvarnheden, Monitoring infection of tomato fruit by *Tomato yellow leaf curl virus*, *Plant Pathol.* 66 (2017) 522–528, <http://dx.doi.org/10.1111/ppa.12596>;  
(b) K. Just, W.N. Leke, M.N. Sattar, A. Luik, A. Kvarnheden, Detection of *Tomato yellow leaf curl virus* in imported tomato fruit in northern Europe, *Plant Pathol.* 63 (2014) 1454–1460, <http://dx.doi.org/10.1111/ppa.12205>.
- [5] K. Just, M.N. Sattar, U. Arif, A. Luik, A. Kvarnheden, Infectivity of *Tomato yellow leaf curl virus* isolated from imported tomato fruit in Estonia, *Zemdirbyste-Agriculture* 104 (2017) 47–52, <http://dx.doi.org/10.13080/z-a.2017.104.007>.
- [6] S. Kil, Y. Kim, H.S. Lee, J. Byun, H. Park, C.S. Seo, J.K. Kim, J.H. Shim, J.K. Lee,

- K.Y. Kim, H.S. Lee, S. Choi, *Tomato yellow leaf curl virus* (TYLCV-IL): a seed-transmissible geminivirus in tomatoes, *Sci. Rep.* 6 (2016) 19013, <http://dx.doi.org/10.1038/srep19013>.
- [7] E. Glick, Y. Levy, Y. Gafni, The viral etiology of tomato yellow leaf curl disease – a review, *Plant Prot. Sci.* 45 (2009) 81–97.
- [8] R. Campos-Olivas, J.M. Louis, D. Clerot, B. Gronenborn, A.M. Gronenborn, The structure of a replication initiator unites diverse aspects of nucleic acid metabolism, *Proc. Natl. Acad. Sci. U. S. A.* 99 (2002) 10310–10315. doi.org/<https://doi.org/10.1073/pnas.152342699>.
- [9] W. Traut Laufs, F. Heyraud, V. Matzeit, S.G. Rogers, J. Schell, B. Gronenborn, In vitro cleavage and joining at the viral origin of replication by the replication initiator protein of tomato yellow Leaf Curl virus, *Proc. Natl. Acad. Sci. U. S. A.* 92 (1995) 3879–3883.
- [10] H. Jeske, Replication of geminiviruses and the use of Rolling Circle Amplification for their diagnosis in tomato yellow leaf curl disease, Springer, Dordrecht, 2007.
- [11] K.S. Richter, M. Götz, S. Winter, H. Jeske, The contribution of translesion synthesis polymerases on geminiviral replication, *Virology* 488 (2016) 137–148, <http://dx.doi.org/10.1016/j.virol.2015.10.027>.
- [12] J.S. Mendoza-Figueroa, F.J. Rivera-Lopez, I.J. Luna-Romero, M. Soriano-García, A peptide extract of hydrolyzed amaranth globulin induces growth and immunological response in tomato and maize plants, *Int. J. Plant Soil Sci.* 19 (2017) 1–10, <http://dx.doi.org/10.9734/IJPS/2017/37089>.
- [13] J.Y. Park, S.Y. Yang, Y.C. Kim, Antiviral peptide from *Pseudomonas chlororaphis* O6 against tobacco mosaic virus (TMV), *J. Korean Soc. Appl. Biol. Chem.* 55 (2012) 89, <http://dx.doi.org/10.1007/s13765-012-0015-2>.
- [14] R. Gopal, H. Na, C.H. Seo, Y. Park, Antifungal activity of (KW)<sub>n</sub> or (RW)<sub>n</sub> peptide against *Fusarium solani* and *Fusarium oxysporum*, *Int. J. Mol. Sci.* 13 (2012) 15042–15053, <http://dx.doi.org/10.3390/ijms131115042>.
- [15] M. Visser, D. Stephan, J.M. Jaynes, J.T. Burger, A transient expression assay for the *in planta* efficacy screening of an antimicrobial peptide against grapevine bacterial pathogens, *Lett. Appl. Microbiol.* 54 (2012) 543–551, <http://dx.doi.org/10.1111/j.1472-765X.2012.03244.x>.
- [16] G. Colla, Y. Roupheal, R. Canaguier, E. Svecova, M. Cardarelli, Biostimulant action of a plant-derived protein hydrolysate produced through enzymatic hydrolysis, *Front. Plant Sci.* 5 (2014) 448–453, <http://dx.doi.org/10.3389/fpls.2014.00448>.
- [17] M.I. Reyes, T.E. Nash, M.M. Dallas, J.T. Ascencio-Ibanez, L. Hanley-Bowdoin, Peptide aptamers that bind to geminivirus replication proteins confer a resistance phenotype to tomato yellow leaf curl virus and tomato mottle virus infection in tomato, *J. Virol.* 87 (2013) 9691–9706, <http://dx.doi.org/10.1128/JVI.01095-13>.
- [18] T. Mori, K. Takenaka, F. Domoto, Y. Aoyama, T. Sera, Inhibition of binding of tomato yellow leaf curl virus Rep to its replication origin by artificial zinc-finger protein, *Mol. Biotechnol.* 54 (2013) 198–203, <http://dx.doi.org/10.1007/s12033-012-9552-5>.
- [19] P.R. Venskutonis, P. Kraujalis, Nutritional components of amaranth seeds and vegetables: a review on composition, properties, and uses, *Compr. Rev. Food Sci. Food Saf.* 12 (2013) 381–412, <http://dx.doi.org/10.1111/1541-4337.12021>.
- [20] V.M. Caselato-Sousa, J. Amaya-Farfán, State of knowledge on amaranth grain: a comprehensive review, *J. Food Sci.* 77 (2012) 93–104, <http://dx.doi.org/10.1111/j.1750-3841.2012.02645.x>.
- [21] M. Duranti, C. Gius, Legume seeds: Protein content and nutritional value, *Field Crop Res.* 53 (1997) 31–45, [http://dx.doi.org/10.1016/S0378-4290\(97\)00021-X](http://dx.doi.org/10.1016/S0378-4290(97)00021-X).
- [22] O.F. Castellani, E.N. Martínez, M.C. Añón, Amaranth globulin structure modifications induced by enzymatic proteolysis, *J. Agric. Food Chem.* 48 (2000) 5624–5629, <http://dx.doi.org/10.1021/jf000624o>.
- [23] N.L. Vasco Méndez, M. Soriano-García, A. Moreno, R. Castellanos-Molina, O. Paredes-López, Purification, crystallization, and preliminary X-ray characterization of a 36 kDa amaranth globulin, *J. Agric. Food Chem.* 47 (1999) 862–866, <http://dx.doi.org/10.1021/jf9809131>.
- [24] A. Quiroga, E.N. Martínez, H. Rognaux, A. Geairon, M.C. Añón, Globulin-p and 11S-globulin from *Amaranthus hypochondriacus*: are two isoforms of the 11S-globulin, *Protein J.* 28 (2009) 457–467, <http://dx.doi.org/10.1007/s10930-009-9214-z>.
- [25] M.A. Gómez-Favela Montoya-Rodríguez, C. Reyes-Moreno, J. Milán-Carrillo, E. González de Mejía, Identification of bioactive peptide sequences from amaranth (*Amaranthus hypochondriacus*) seed proteins and their potential role in the prevention of chronic diseases, *Compr. Rev. Food Sci. Food Saf.* 14 (2015) 139–158, <http://dx.doi.org/10.1111/1541-4337.12125>.
- [26] F. Heyraud-Nitschke, S. Schumacher, J. Laufs, S. Schaefer, J. Schell, B. Gronenborn, Determination of the origin cleavage and joining domain of geminivirus Rep proteins, *Nucleic Acids Res.* 23 (1995) 910–916 <http://doi.org/5c0003>.
- [27] S. Wyatt, J.K. Brown, Detection of subgroup III geminivirus isolates in leaf extracts by degenerate primers and polymerase chain reaction, *Phytopathology* 86 (1996) 1288–1293, <http://dx.doi.org/10.1094/Phyto-86-1288>.
- [28] E. Rodríguez-Negrete, S. Sánchez-Campos, M.C. Cañizares, J. Navas-Castillo, E. Moriones, E.R. Bejarano, A. Grande-Pérez, A sensitive method for the quantification of virion-sense and complementary-sense DNA strands of circular single-stranded DNA viruses, *Sci. Rep.* 4 (2014) 6438, <http://dx.doi.org/10.1038/srep06438>.
- [29] F. Li, N. Zhao, Z. Li, X. Xu, Y. Wang, A calmodulin-like protein suppresses RNA silencing and promotes geminivirus infection by degrading SGS3 via the autophagy pathway in *Nicotiana benthamiana*, *PLoS Pathog.* 13 (2017) e1006213, <http://dx.doi.org/10.1371/journal.ppat.1006213>.
- [30] G. Mason, P. Caciagli, G.P. Accotto, E. Noris, Real-time PCR for the quantitation of *Tomato yellow leaf curl Sardinia virus* in tomato plants and in *Bemisia tabaci*, *J. Virol. Methods* 147 (2008) 282–289, <http://dx.doi.org/10.1016/j.jviromet.2007.09.015>.
- [31] H. Romero-Zepeda, O. Paredes-Lopez, Isolation and characterization of amaranin, the 11s amaranth seed globulin, *J. Food Biochem.* 19 (1995) 329–339, <http://dx.doi.org/10.1111/j.1745-4514.1995.tb00538.x>.
- [32] J.J. Virgen-Ortiz, V. Ibarra-Junquera, J. Osuna-Castro, P. Escalante-Minakata, N. Mancilla-Margalli, J.D.J. Ornelas-Paz, Method to concentrate protein solutions based on dialysis-freezing-centrifugation: enzyme applications, *Anal. Biochem.* 426 (2012) 4–12, <http://dx.doi.org/10.1016/j.ab.2012.03.019>.
- [33] X. Qi, T. Droste, C.C. Kao, Cell-penetrating peptides derived from viral capsid proteins, *Mol. Plant-Microbe Interact.* 24 (2011) 25–36, <http://dx.doi.org/10.1094/MPMI-07-10-0147>.
- [34] D.M. Copolovici, K. Langel, E. Eriste, Ü. Langel, Cell-penetrating peptides: design, synthesis, and applications, *ACS Nano* 8 (2014) 1972–1994, <http://dx.doi.org/10.1021/nn4057269>.
- [35] L. Tan, K.G. Neoh, E.T. Kang, W.S. Choe, X. Su, Affinity analysis of DNA aptamer-peptide interactions using gold nanoparticles, *Anal. Biochem.* 421 (2012) 725–731, <http://dx.doi.org/10.1016/j.ab.2011.12.007>.
- [36] J.J. Doyle, J.L. Doyle, A rapid DNA isolation procedure for small quantities of fresh leaf tissue, *Phytochem. Bull.* 19 (1987) 11–15.
- [37] K.J. Livak, T.D. Schmittgen, Analysis of relative gene expression data using real-time quantitative PCR and the 2<sup>-ΔΔC<sub>T</sub></sup> method, *Methods* 25 (2001) 402–408, <http://dx.doi.org/10.1006/meth.2001.1262>.
- [38] F. Stephen, T.L. Altschul, A.A. Madden, A. Schäffer, J. Zhang, Z. Zhang, W. Miller, D.J. Lipman, Gapped BLAST and PSI-BLAST: a new generation of protein database search programs, *Nucleic Acids Res.* 25 (1997) 3389–3402.
- [39] M.F. Marcone, F.K. Niekamp, L. Maguer, R.Y. Yada, Purification and characterization of the physicochemical properties of the albumin fraction from the seeds of *Amaranthus Hypochondriacus*, *Food Chem.* 51 (1994) 287–294, [http://dx.doi.org/10.1016/0308-8146\(94\)90029-9](http://dx.doi.org/10.1016/0308-8146(94)90029-9).
- [40] S. Chen, O. Paredes, López, Isolation and characterization of the 11S globin from amaranth seeds, *J. Food Biochem.* 21 (1997) 53–65, <http://dx.doi.org/10.1111/j.1745-4514.1997.tb00224.x>.
- [41] J. Wang, H.Y. Wang, X.M. Xia, P. Li, K.Y. Wang, Inhibitory effect of esterified lactoferrin and lactoferrin against tobacco mosaic virus (TMV) in tobacco seedlings, *Pestic. Biochem. Physiol.* 105 (2013) 62–68, <http://dx.doi.org/10.1016/j.pestbp.2012.11.009>.
- [42] A.M. Abdelbacki, S.H. Taha, M.Z. Sitohy, A.I. Abou Dawood, M.M. Abd-El Hamid, A. Rezk, Inhibition of tomato yellow leaf curl virus (TYLCV) using whey proteins, *Virol. J.* 7 (2010) 26, <http://dx.doi.org/10.1186/1743-422X-7-26>.
- [43] T. Sera, Inhibition of virus DNA replication by artificial zinc finger proteins, *J. Virol.* 79 (2005) 2614–2619, <http://dx.doi.org/10.1128/JVI.79.4.2614-2619.2005>.
- [44] A. Panchaud, M. Affolter, M. Kussmann, Mass spectrometry for nutritional peptidomics: how to analyze food bioactives and their health effects, *J. Proteome* 75 (2012) 3546–3559 <http://dx.doi.org/https://doi.org/10.1016/j.jprot.2011.12.022>.
- [45] P.M. St, M. Willert Hilaire, M.A. Juliano, L. Juliano, M. Meldal, Fluorescence-quenched solid phase combinatorial libraries in the characterization of cysteine protease substrate specificity, *J. Comb. Chem.* 1 (1999) 509–523, <http://dx.doi.org/10.1021/cc990031u>.
- [46] Y. Choe, F. Leonetti, D.C. Greenbaum, F. Lecaille, M. Bogyo, D. Brömme, J.A. Ellman, C.S. Craik, Substrate profiling of cysteine proteases using a combinatorial peptide library identifies functionally unique specificities, *J. Biol. Chem.* 281 (2006) 12824–12832, <http://dx.doi.org/10.1074/jbc.M513331200>.
- [47] R. Hou, Z. Zhang, S. Pang, T. Yang, J.M. Clark, L. He, Alteration of the nonsystemic behavior of the pesticide ferbam on tea leaves by engineered gold nanoparticles, *Environ. Sci. Technol.* 50 (2016) 6216–6223, <http://dx.doi.org/10.1021/acs.est.6b01336>.
- [48] A. Chugh, F. Eudes, Y.S. Shim, Cell-penetrating peptides: Nanocarrier for macro-molecule delivery in living cells, *IUBMB Life* 62 (2010) 183–193, <http://dx.doi.org/10.1002/iub.297>.
- [49] D. Zhang, J. Wang, D. Xu, Cell-penetrating peptides as noninvasive transmembrane vectors for the development of novel multifunctional drug-delivery systems, *J. Control. Release* 229 (2016) 130–139, <http://dx.doi.org/10.1016/j.jconrel.2016.03.020>.
- [50] M.R. Rajeswari, H.S. Bose, S. Kukreti, A. Gupta, V.S. Chauhan, K.B. Roy, Binding of oligopeptides to d-AGATCTAGATCT and d-AAGCTTAAGCTT: can tryptophan intercalate in DNA hairpins? *Biochemist* 31 (1992) 6237–6241, <http://dx.doi.org/10.1021/bi00142a010>.
- [51] K.B. Roy, S. Kukreti, H.S. Bose, V.S. Chauhan, M.R. Rajeswari, Hairpin and duplex forms of a self-complementary dodecamer, d-AGATCTAGATCT, and interaction of the duplex form with the peptide KGWKG: can a pentapeptide destabilize DNA? *Biochemist* 31 (1992) 6241–6245, <http://dx.doi.org/10.1021/bi00142a011>.



**TITLE1. The peptide AmPep1 as potential model of direct treatment against Tomato Yellow Leaf Curl Virus.**

**TITLE 1: Structural changes in the replication origin hairpin of TYLCV with the peptide SVGRKWRMKWAQMRQQ derived from amaranth: Disturbing the viral replication process in Nicotiana and Tomato plants.**

**TITLE 2: The peptide AmPep1 derived from amaranth induces structural changes in the replication origin hairpin of TYLCV, disturbing its replication process in host plants**

Mendoza-Figueroa J.S.<sup>af</sup>, Badillo-Ramírez I.<sup>bf</sup>, Kvarnheden A.<sup>c</sup>, Rosas-Ramírez D.G.<sup>a</sup>, Rodríguez-Negrete E.A.<sup>d</sup>, Méndez-Lozano J.<sup>e</sup>, Saniger-Blesa J.M.<sup>b</sup> and Soriano-García M.<sup>a\*</sup>.

<sup>a</sup>Department of Biomacromolecular Chemistry, Chemistry Institute, Universidad Nacional Autónoma de México. Mexico City, Mexico.

<sup>b</sup>University Lab of Spectroscopy Characterization, Applied Sciences and Technology Institute, Universidad Nacional Autónoma de México. Mexico City, Mexico.

<sup>c</sup>Department of Plant Biology, Swedish University of Agricultural Sciences, Uppsala, Sweden.

<sup>d</sup>CONACYT, Instituto Politécnico Nacional, Department of Agrobiotechnology, Centro Interdisciplinario de Investigación para el Desarrollo Integral Regional-Sinaloa, Instituto Politécnico Nacional, Guasave, Sinaloa, Mexico

<sup>e</sup>Department of Agrobiotechnology, Centro Interdisciplinario de Investigación para el Desarrollo Integral Regional-Sinaloa, Instituto Politécnico Nacional, Guasave, Sinaloa, Mexico.

<sup>f</sup>Equal contributions

\*Corresponding author

## **ABSTRACT**

The development of anti-viral compounds that target the viral replicative processes has been studied as an alternative for the control of begomoviruses. Previously was reported that the peptide AmPep1 isolated from an amaranth globulin hydrolysate showed strong affinity binding to the replicative hairpin sequence of this virus with consequent anti-viral activity. In this work we describe the mechanism of action of this peptide as a novel alternative for plant DNA virus control. When AmPep1 is applied exogenously in tomato and *Nicotiana benthamiana* plants infected with TYLCV was observed a decrease in the synthesis of viral replicative intermediates such as VS and CS with a consequent delay in the development of the disease progress in the treated plants. The anti-viral effect can be explained due to the ability of the peptide to translocate to the cell nucleus and interacts chemically with the hairpin structure of the virus, forming H bonds, electrostatic interactions between the Arg and Lys of the peptide with the phosphate groups of the DNA and the formation of Pi interactions between the Trp of AmPep1 and hairpin purines.

## INTRODUCTION

The *Geminiviridae* family is one of the most devastating plant pathogenic virus group for the cultivation of Solanacea crops worldwide. This family includes the genera *Begomovirus*, *Mastrevirus*, *Turncurtovirus*, *Curtovirus*, *Becurtovirus*, *Eragrovirus*, *Topocuvirus*, *Grablovirus* and *Capulavirus*. Within the genus *Begomovirus* is classified *Tomato yellow leaf curl virus* (TYLCV) which is the main etiological agent of the yellow leaf curling disease in tomatoes crops<sup>1</sup>, inducing symptoms in the leaves as curling, marginal and complete chlorosis, dwarfing, floral abortus and loss in fruit productivity and quality.

The TYLCV genome monopartite<sup>2,3</sup>, is formed by genes encoded directly in the single-stranded viral DNA (VS) contained in the capsid and by complementary genes encoded by the complementary chain of the viral chain, CS. The genome has six open read frames, two for VS and four for CS, which are superimposed on each other. The encoded genes by VS are *v1* and *v2*, while the genes *c1*, *c2*, *c3* and *c4* are located in the CS, between the *c1* and *v2* regions is the intergenic region (IR)<sup>4</sup>, which despite having flank sequences with a high sequence variation it presents in the origin of replication a highly conserved sequence (5'-GGCCATCCGTATAATATTACCGGATGGCC-3') that forms a secondary structure with shape of stem-loop type (hairpin)<sup>5,6</sup>, the sequence found in the loop region 5'-TAATATT ↓ AC-3' is where the replicative process starts when it is recognized by the *c1* protein product in the area marked with (↓)<sup>7,8</sup>.

The replicative process of the virus starts when the virion is translocated into the cell and the single-stranded viral DNA (ssDNA, VS) translocate into the nucleus, once inside, a first replication of the ssDNA will be performed to form the complementary chain (cDNA, CS) using some plant polymerases, which could be the TLS type polymerases<sup>9</sup>, once the double chain replicative intermediary has been formed (by the ssDNA and cDNA) the transcription of *c1* gene is performed to give origin to the Rep protein, which will recognize part of the intergenic region, specifically the stem and loop structure in the TAATATT↓AC area and this enzyme will make a nick to the DNA VS strand, leaving a 3'-OH end which serves as an initiator of the rolling circle replication model<sup>10</sup>. The nucleotides will be incorporated using the CS chain as a template, displacing the rest of the VS chain as the replication progresses, once a new viral chain is synthesized, the Rep will act as a ligase to circularize the displaced VS chain allowing it to be free inside of the nucleus to form new CS chains, pack itself in the capsid or translocated to neighboring cells<sup>10,11,12</sup>.

Some strategies that have been reported for the management of this viral disease, for example, the use of resistant tomato varieties to TYLCV due they possess *Ty* type resistance (R) genes<sup>13</sup>, as well as the use of microorganisms as inducers of systemic resistance, for example *Enterobacter asburiae* BQ9<sup>14</sup>. The generation of transgenic tomato lines has reported the overexpression of Rep protein fragments, showing resistance to the severe development of the disease<sup>15</sup>. About the TYLCV control blocking directly the replication mechanisms is reported the design of transgenic plants overexpressing fragments of antibodies that recognize Rep protein, demonstrating the reduction of viral titer of TYLCV in infected *Nicotiana benthamiana* plants<sup>16</sup>.

The use of peptides as a control for geminivirus infections is another strategy that is proposed due the direct control of viral replication, for example, aptamer peptides libraries have been tested to recognize the N terminal region of Rep, the peptides that showed the highest interaction with the target reduced the viral titer in cells infected with *Tomato golden mosaic virus* (TGMV) and *Cabbage leaf curl virus*<sup>17</sup>, subsequently these peptides were evaluated to study their capacity to recognize the N terminal region of other geminivirus as *Beet curly top virus* (*Curtovirus*) and *Maize strike virus* (*Mastrevirus*). With these peptides transgenic lines of tomato were created overexpressing these molecules, showing a reduction of symptoms caused by the TYLCV and *Tomato mottle virus* (ToMoV) infection due to the peptide interference with the viral replication process<sup>18</sup>.

The Rep protein and the origin of replication in the IR of the geminivirus genome are an important agrochemical target for development antiviral molecules, due to the participation of Rep in the replicative process in the *Geminiviridae* family, as well as the conserved sequence of the replication origin in the IR<sup>19,20</sup>. In a recent work we have reported that the AmPep1 peptide derived from an enzymatic hydrolysis of globulins of *Amaranthus hypochondriacus* has the ability to chemically recognize the sequence that forms the loop at the TYLCV replication origin, showing a consistent high affinity towards that sequence, and also the treatment with this molecule in *N. benthamiana* plants infected with TYLCV decreases the DNA titer of the virus with a consequent symptomatic decrease<sup>21</sup>.

The aim of this work was to show the antiviral mechanism of the AmPep1 peptide on TYLCV from a structural and molecular point of view, showing the entry mechanism of the peptide in plant tissue and the anti-viral effect on a natural host (tomato) applied in exogenous way without the need to develop transgenic lines. This paper could help to develop new strategies for improve the control of geminiviruses using peptides, without transgenic models, making cheaper and manageable the production and applications in fields of these class of biomolecules.

## RESULTS

The The peptide AmPep1(SVGRKWRMKWAQMRQQ), purified from hydrolysate amaranth globulin and the synthetic oligonucleotide 5'-GGCCATCCGTATAATATTACCGGATGGCC-3', corresponding to the hairpin region of the OriRepTYLCV, were used as target, respectively. Raman spectra of both pure biomolecules were recorded individually, previously to the interaction. Figure 1A shows the spectrum of the peptide, in blue, while the DNA is in red line. Pure Raman spectrum of AmPep1 peptide depict bands that are mainly generated by characteristic amide I and III, skeletal and residual amino acids vibrational modes. Wavenumber position of the amide I band indicates the secondary structure that the peptide adopts under analysis conditions, which corresponds mainly to an alpha helix conformation with contribution of unordered structure<sup>25,26</sup>, indicated by bands at positions 1658, 1670 and 1686 cm<sup>-1</sup>. On the other hand, amide III position at 1263 cm<sup>-1</sup>, corroborates the unordered structure of the peptide. In addition, a detailed peak fitting of the amide I interval (1640-1700 cm<sup>-1</sup>) in Figure 1B, provides semiquantitative information about abundance percentage of each

sub-band, where  $\alpha$ -helix (28%) is the main abundant, followed by the unordered structure (26%) with minor contributions of random and turn conformations in the secondary structure (table 2)<sup>25,26,34,35,45</sup>. Residual amino acid that depict characteristic bands are coming mainly from tryptophan (Trp) and serine (Ser); where Trp exhibits one of the most intense bands in the spectra at 760  $\text{cm}^{-1}$ , from the breathing mode of the aromatic ring<sup>22,23</sup>; band at 1010  $\text{cm}^{-1}$  indicates the out-of-plane breathing mode of benzene and pyrrole rings<sup>22,23</sup>; band at 1074  $\text{cm}^{-1}$  coming from the C-C in-plane bending mode<sup>22,23</sup>; band at 1550  $\text{cm}^{-1}$  due to the stretching C2-C3 of the pyrrolic ring; and band at 1618  $\text{cm}^{-1}$  describes the C = C stretching mode of the aromatic ring<sup>22,23</sup>. On the other hand, Ser shows two small but characteristic bands at 853 and 945  $\text{cm}^{-1}$  due to C-C and C-O stretching modes, respectively, from the attached OH residual group<sup>24</sup>. Skeletal vibration of the backbone in the aliphatic chain of the peptide, are shown by the CH and CH<sub>2</sub> multiple deformation modes in the 1300-1500  $\text{cm}^{-1}$  range (See table 1 for detailed assignment).

Raman spectrum of oligonucleotide OriRepTYLCV (bottom plot, red line) shows the characteristic DNA Raman bands; where vibrational modes of the phosphodiester bond (O-P-O) at 786 and 840  $\text{cm}^{-1}$ , due to the symmetric and asymmetric stretching modes<sup>27</sup>, respectively, are the most representatives. In addition, characteristic band at 1092  $\text{cm}^{-1}$  is due to the dioxide bond of the phosphate group (PO<sub>2</sub>)<sup>27,28,29</sup>. Other bands contributing to the pure Raman spectrum of DNA are those generated by the purine bases, at 1332 and 1574  $\text{cm}^{-1}$ , coming from the aromatic ring stretching mode of purines A and G<sup>27,30</sup>, while the band at 1480  $\text{cm}^{-1}$  is due to the deformation of C8 = N7 in Guanine<sup>31</sup>. In addition, contributions of the C-N stretching of amine modes in G can be observed<sup>31,32</sup> at 1253  $\text{cm}^{-1}$ . Bands generated by the pyrimidine bases, mainly from the contribution of thymine, which shows bands at 1369  $\text{cm}^{-1}$ , due to the C-N stretching of the pyrimidine ring mode<sup>30,33</sup>; and a broad band from the C = O stretching bonds<sup>34,35</sup>, originated mainly from the C2 = O at 1660-1662  $\text{cm}^{-1}$ , with minor contribution of C4 = O bond at 1690-1711  $\text{cm}^{-1}$ . Band fitting of the 1660-1711  $\text{cm}^{-1}$  interval is presented in Fig 1.D for better assignment of the C = O stretching bonds contributions, (Fig 1d. See table 1 and 2)..

Raman spectrum of the matrix interaction of AmPep1 with the oligonucleotide OriRepTYLCV is described in green color in Figure 1A, showing contributions from both biomolecules with evident altered Raman profiles, due to the chemical interaction. Characteristic Raman bands of peptide show changes both in wavenumber position and band intensities; vibrations of the aromatic ring breathing modes of Trp show notable shifts after the interaction, from 760 to 751  $\text{cm}^{-1}$  and from 1010 to 1014  $\text{cm}^{-1}$ , indicating that the benzene ring of Trp is strongly affected after the interaction. In addition, there is a strong decreased intensity of the Trp pyrrole ring at 1150  $\text{cm}^{-1}$ . Those evidences indicates that there is a strong interaction between the two biomolecules due to preferential aromatic interactions; one possibility is the strong pi-pi type aromatic coupling between the benzene ring of Trp with the ring purine and pyrimidine bases of the oligonucleotide<sup>23</sup>; a second possibility is the preferential hydrogen bonding (H-bonding) with the indole ring in Trp, which is a well-known marker of Trp for hydrophobic interactions<sup>23</sup>. The aforementioned observations were previously intuited by Mendoza-Figueroa et al, 2018<sup>21</sup>, where a quenching of intrinsic fluorescence of peptide was observed when it interacts in a dose-dependent manner with the OriRepTYLCV; these results matched with the decreased intensity and downshifting of the band at 760

cm<sup>-1</sup> to 751 cm<sup>-1</sup>. Moreover, the C-C stretching mode, coupled to the OH in the serine residues, undergoes a shift from 853 to 857 cm<sup>-1</sup>, followed by a shift from 945 to 958 cm<sup>-1</sup>, in the vibrational mode of C-O stretching, corroborating the preferential hydrogen bondings with DNA<sup>24,46</sup>. In addition, characteristic bands from the peptide backbone are strongly affected, such as the aliphatic chain downshifts from 1336 to 1328 cm<sup>-1</sup> as well as the decrease intensity of the multiple aliphatic CH and CH<sub>2</sub> deformation modes at 1435 cm<sup>-1</sup>, indicating a strong structural rearrangement of the peptide with the DNA and interestingly, the strong decreased intensity at 1435 band of the peptide can indicate a hide underneath the large DNA structure. Detailed peak fitting of the amide I band of the mixture in Fig. 1C, shows a broad band after the interaction, where the alpha helix secondary structure shows an increased area percentage of over 3% and now centered at 1653 cm<sup>-1</sup>, while the disordered structure decrease its abundance, without band shifting position (1670 and 1681 cm<sup>-1</sup>)<sup>45</sup>. These observations support the effect under the spatial conformational arrangement of the peptide, indicating that the full structure is more packed when is in close contact with the DNA structure. Moreover, downshifted of the alpha-helix amide I band position from 1658 to 1653, after the interaction, supports the strong influence due to H-bonding from the DNA over the peptide, leading to disturb its conformational arrangement.

Chemical interaction between both biomolecules also modify the PO<sub>2</sub> vibrational mode of the dioxiphosphate group, leading to a shift from 1092 to 1096 cm<sup>-1</sup>, which can be attributed to the electrostatic interaction between negatively charged PO<sub>2</sub><sup>-</sup> group with positively charged amino acid side chains such as Arg or Lys<sup>29,41,42,43</sup>, this interaction is reflected from the decreased band of NH<sub>3</sub><sup>+</sup> vibrational mode of the peptide at 1131 cm<sup>-1</sup>. In addition, other characteristic vibrational modes of DNA are affected, for example; ring stretching of G and C bases are shifted from 1253 to 1257 cm<sup>-1</sup>; C-N stretching vibrations of T, A, and G, are shifted from 1369 to 1374 cm<sup>-1</sup>; C-N stretching vibration in groups C8-N7 of G, redshift from 1480 to 1485 cm<sup>-1</sup>; as well as the vibrational modes coming from the rings moieties of the purine bases leading to a higher shifted from 1574 to 1578 cm<sup>-1</sup>, which are the mayor DNA interaction markers<sup>27,29</sup>. These evidences supports the strong ring interaction between the aromatic systems of A and G with the indole group of Trp, mainly through Pi-Pi type interactions<sup>23</sup>. On the othe hand, slightly shifting in the C = O stretching of T in the displacements of 1660 to 1662 cm<sup>-1</sup> and from 1691 to 1695 cm<sup>-1</sup> from the vibrational modes of C4=O and C2 = O, respectively, supports the notion that hydrogen bonding is preferentially originated with T moety<sup>29</sup>. Interestingly, changes in the DNA backbone after the interaction can only be observed due the Raman shift from 1062 to 1072 cm<sup>-1</sup>, corresponding to the stretching mode of C-O bonds in deoxyribose, indicating a slightly rearrangement of the DNA structure<sup>38</sup>. However, no changes at 786 neither at 811 cm<sup>-1</sup> were observed, which are markers of sugar puckering as well DNA conformation, indicating that the DNA secondary structure is not fully affected after the interaction, thus, peptide interaction is well preserved and localized preserving the DNA structure<sup>27,38</sup>. The aforementioned Raman results indicate that the AmPep1 peptide interacts mainly with Adenines, Thymines and Cytosines from the OriRep, which are found abundantly in the target zone of the replication initiator protein (Rep) of TYLCV that involves the region of the loop (marked in bold and arrow) of sequence 5'- GGCCATCCGTATAATATTA↓CCGGATGGCC-3'.

To corroborate the experimental interaction provides by Raman spectroscopy, a theoretical analysis of the system was carried out. A computational 3D models of the hairpin structure formed by the OriRepTYLCV sequence and for the peptide AmPep1 were modeled. Once the geometry of both biomolecules was optimized, a Docking process was developed, leading to the most stable arrangement of the peptide in the replication hairpin of TYLCV, showed in (Figure 2A). It is observed that the favorable site of peptide binding is located mainly in the cavity region formed in the loop and also forming contacts in the 3' extreme of the loop sequence, with a slight perturbation in the stem region of the whole hairpin.

Interactions that were mostly observed after the docking were electrostatic hydrogen bonding and interactions between aromatic and ring systems. In the case of H bonds, they were predicted to be formed between residues of Adenosine 14 and 11, as well as with Cytosine 20 (see Figure 2B). The residues A14 interacts with Glutamine (Q16) residue, while the A11 and C20 interact mainly with the backbone of the peptide bond, all of them are forming bond distance less than 2.5 Å considering them as strong H bond<sup>47</sup>. These theoretical predictions can be corroborated with the experimental results from the Raman analysis, in the following shifting: a band displacement from 1253 to 1257  $\text{cm}^{-1}$  in the stretching mode of  $\text{NH}_2\text{-C}$  of Cytosine and from 1369 to 1374  $\text{cm}^{-1}$  corresponding to the stretching of the CN of the A and the shift at 1574 to 1578  $\text{cm}^{-1}$  corresponding also to purine stretching. The effect of this H bond in the structure of the peptide can be seen in the change in the Raman signal of the peptide backbone from 1658 to 1653  $\text{cm}^{-1}$  corresponding to signal of the alpha helix secondary structure in the amide I region (figure 1b,c) inducing a re-structuration of the peptide structure this is confirming due the increase of abundance of the signal corresponding to alpha helix<sup>45</sup> when it is interacting with DNA (table 2), the affection in the alteration of peptide structure is also confirmed in the shift showed in the vibration mode of the aliphatic chain of peptide due 1336 to 1328  $\text{cm}^{-1}$ .

Electrostatics interactions between the negatively charged phosphate groups of the oligonucleotide with positive charges basic amino acids, K and R, of the peptide are also depicted in the molecular model. Theoretical model predicts the interaction of the  $\text{NH}_3^+$  group of the side chain of residues K5, R4 and R14 of the peptide directly with the  $\text{PO}_2^-$  group and with the oxygen of the O-P-O bond of the DNA backbone in the DNA residues of bases A5, T6 and T10, respectively (figure b.2). This electrostatic interaction affects both the stem of the hairpin and a short part of the loop. The interaction agrees with Raman experimental observations, due to the shifting from 1092  $\text{cm}^{-1}$  to 1096  $\text{cm}^{-1}$  of the PO2 vibrational mode in the oligonucleotide and the decrease in intensity of the band at 1131  $\text{cm}^{-1}$  corresponding to the vibration of  $\text{NH}_3^+$  groups of the peptide residues. This interaction could have repercussions in the vibrational mode of DNA backbone affecting the original conformational structure or just inducing local changes, the biological consequences of the interaction could produce a poor recognition of the Rep protein towards its target (the hairpin).

In addition, other types of weak interactions between DNA and peptide are predicted, such as the interactions between aromatic systems mainly by Pi -type interactions (anion-pi, pi-pi), (Figure 2C). This type of interaction is observed mainly in the aromatic rings of tryptophan 6 and 10; the benzene of the W6 residue potentially interacts in the Pi-anion

mode with the C4 = O group of the T18, and possibly forms stacking with the A19 in T - shape (figure 2c.1). The W10 residue has a potential interaction with the T10 residue of the DNA due the closely distance between each other<sup>48,49</sup>. The Raman analysis is showing an affection in both the displacement and the intensity of signal corresponding to the main aromatic vibrational modes of Trp (W) (from 760 to 751 cm<sup>-1</sup> and at 1010 to 1014 cm<sup>-1</sup>). The shift of these signals and intensities also correlates with the intrinsic fluorescence quenching that AmPep1 shows when it interacts with OriRepTYLCV, due to the electrostatic and aromatic coupling.

Experimental and theoretical results have shown that the peptide AmPep1 interacts with the OriRep of TYLCV, these formed bonds between these biomolecules could either alter the conformation of the replication hairpin structure and hinder molecular recognition by Rep or perform a steric hindrance that does not allow adequate synthesis of viral DNA in the plant.

To verify if the chemical interaction between the AmPep1 peptide and the replication loop of TYLCV has secondary effects on viral replication, the replicative rate of TYLCV in plants of *N. benthamiana* was evaluated *in vivo*. *N. benthamiana* plants were infected by agroinoculation, systemic infection was ensured in the most extended apical leaves, and the viral titer was measured on the left and right side of the central vein to verify the symmetry of the viral titer in the model plant. The left half of the leaf served as a control treated only with buffer and the right half was treated with AmPep1 or RepApep (Figure 3A). Quantification of viral sense (VS) and complementary sense (CS) of viral DNA was performed in both sides of the leaves of all treatments and controls<sup>11</sup>. The (Figure 3B) shows that on the left side of the leaf (UnTx) comparing with infection control, no significant difference of CS concentration is observed in any treatment except for the leaves where the right side was treated with concentrations of 30 μM of AmPep1. On the right side of the leaf (+Tx) at concentrations of 15 and 30 μM of AmPep1 the amount of CS decreases significantly compared to infection control and compared with the time zero of treatment, indicating a potential effect of tamper the replication process. The leaves sides treated with RepApep peptide also showed a decreasing titer of CS significantly compared to the infection control but not significant difference comparing with the time zero of treatment, keeping the viral titer significantly stable for all replicative molecules, meaning a static effect on the viral replication, compared also with infection control where the viral titer trends to increase significantly through the time. The significant decrease of viral titer on the left side of the leaf in concentrations of 30 μM might be due to a possible translocation of the peptide through the vascular bundles due to a potential ease of crossing the cell membranes due to its sequence similar like cell-penetrating-peptides<sup>50</sup>.

The replication of TYLCV is based in the models of RCR and recombination -dependent replication (RDR), in the first case, it starts with the synthesis of a complementary strand (CS) to VS (which titer is usually lower than VS), to form a double-stranded intermediate (dsDNA), this replicative form will serve as a template for the synthesis of new viral DNA (VS) through the rolling circle replication model, when CS concentration decreases after a treatment with AmPep1, it was observed that the VS formation in the plant is significantly lower (Figure 3C) in the right side of the leaf (+Tx) since 12 hours post treatment with 15 and 30 μM of AmPep1 compared with the infection control. Comparing

the initial titer of this replicative intermediary under these experimental concentrations the VS amount keeps stable during the experimental time, inducing a static effect over the viral replication. In the left side of the leaf at concentrations of 30  $\mu$ M, the VS titer decrease significantly respect to the control. VS concentration is also negatively affected in the treatment with the peptide RepApep. These results indicate that the peptide AmPep1 interacts directly in the replication cycle of the virus, by partially tamper the synthesis of new VS chains, which will be used as new CS templates or for the formation of new virions.

Because the concentration of VS and CS decreased on the treated side of the leaf (right), the total viral DNA titer was negatively affected in the case of treatments with AmPep1 (Figure 3D) mainly on the right side (+Tx), on the left side (UnTx) only in the leaves treated with 30  $\mu$ M of AmPep1 showed a significant decrease in viral DNA compared with infection control, suggesting again that the peptide can be translocated.

In order to test if the AmPep1 has the same anti-viral efficacy in one of the natural hosts of TYLCV, tomato seedling were infected with this virus, once the systemic infection was assured, a treatment with AmPep1 was carried out in all the apical leaves, in (Figure 4A) it is observed that in seedlings infected with TYLCV and treated with AmPep1 there is a significant reduction of the characteristic symptoms of TYLCV disease in this host, comparing with the infection control, the infected plants treated with AmPep1 does not present a high rate of leaves showing curling and marginal chlorosis at 7 and 15 dpTx, nor is there observed dwarfism and shortening of internodes compared with the symptomatic development of the untreated plants. Visually, severe symptomatic development is delayed until 15 days after treatment with the peptide (Figure 4C). In addition, the viral DNA titer in the treated plants is significantly lower compared to the infection control at 15 dpTx (Figure 4B), then, we can propose that the visual decrease in symptoms is directly proportional to the lower viral DNA concentration in the tissue possible due the alteration of replication rate of the virus. Correlating these data with the analysis of viral replication in *Nicotiana*, it can be proposed that the peptide has a similar mechanism in this natural host, binding to the replication hairpin of the virus making a steric hindrance for the correct recognition of Rep and consequently tampering the correct realization of the viral replication by rolling circle model, decreasing CS and VS and consequently the concentration of total viral DNA.

In the previous experiments, was showed the ability of AmPep1 peptide to control the replication of TYLCV *in vivo*, which made us suspect that this molecule could easily translocate to the interior of the cells, since the virus replicates in the nucleus. To corroborate this fact, we proceeded to analyze if the peptide can efficiently cross the cellular barriers and efficiently reach the nucleus, for this effect the AmPep1 peptide was labeled with FITC (AmPep1-FITC) and the internalization capacity was monitored in cells of in *N. benthamiana*. In (Figure 5) it can be observed that AmPep1 could internalize within cells, and that this is dependent on incubation time and no energy-depended. It is observed that in the first 10 minutes the transport of the peptide (fluorescent green signal) is not very high compared to the subsequent monitoring times and that it can also be possibly linked to an endocytosis process, mainly due to the observation of vesicle formation or transportation points in the cell wall or membrane<sup>51,52</sup>, however, at 30 and 60 minutes, the green fluorescent signal of peptide increases significantly and uniformly



around the tonoplast, mainly in cytoplasm and nucleus of epithelial and stomatal cells. To confirm if translocation AmPep1 is an energy-dependent process (endocytosis) was proceeded to incubate leaf tissue of *N. benthamiana* in a solution of AmPep1 at low temperature (4 °C) and was found that peptide transport is not affected, and that the signal of the green probe increases, with a greater accumulation within the cytoplasm and nucleus with respect to the incubation time of 1 hour at room temperature, this fact can be explained because the peptide does not present energetic requirements for its transport and due its sequence it can be related as a cell-penetrating-peptide (CPP), the low temperature rearranges the fluidity and structure of the membrane allowing this peptide to enter passively by spontaneous translocation, perhaps by a non-energy dependent flip-flop mechanism<sup>53,54,55,56</sup>. The easy permeability of the peptide to the interior of the cell allows it to reach the nucleus of the cells interfering with the replication of TYLCV with a subsequent anti-viral activity.

## DISCUSSION

We have been able to show the capability of the peptide AmPep1 as a potential anti-viral against TYLCV, showing that it interacts chemically with the sequence of replication origin of this virus showing the biological effects of decreasing the viral replication rate and reducing the disease progress. In addition, the easy translocation of AmPep1 inward the plant cells make this molecule a potential candidate for explore it in the agrochemical area without the need to develop transgenic lines. Until now, the use of peptides as anti-viral molecules applied in an exogenous way as a direct control of geminivirus has been poorly reported. Previously we have shown that AmPep1 has high affinity binding to the hairpin of the replication origin of TYLCV, decreasing the TYLCV DNA in *N. benthamiana* with a consequent decline of symptoms progress .

The hairpin structure located in the intergenic region of some DNA viruses such as geminiviruses, circoviruses and nanoviruses is a crucial factor in the initiation of viral replication process because it is target for the replication initiator protein or replicase<sup>57</sup>. In the case of geminiviruses, this sequence-structure is preserved throughout the viral family<sup>6,7</sup>. Through the results showed here we described that the AmPep1 interferes with the replication of TYLCV by altering the structure and replicative events of the virus, decreasing the synthesis of DNA replicative intermediaries molecules like VS and CS DNA within the plant tissue, the efficient synthesis of these intermediaries is crucial for the correct viral replication to establish a successfully systemic infectious process in the plant<sup>11</sup>.

The effectiveness of the AmPep1 peptide reducing the replicative intermediaries and the symptoms development in plant can be attributed to its sequence (SVGRKWRMKWAQMRQQ), which contains amino acids with a DNA binding potential such as Lysine (K), Arginine (R) and Tryptophan (W)<sup>49,58,59,60</sup> which increases the possibility of strongly interaction with the sequence OriRepTYLCV, promoting the arrangement of electrostatic interactions, hydrogen bonds and interactions between aromatic rings between purines and tryptophan. AmPep1 also has the ability to translocate inward of cells in a non-mediated and non-energy-dependent manner, this also enhances its internalization to the nucleus, which helps explain why the peptide has anti-viral activity against a virus whose replicative cycle is limited to this organelle. Correlating

these results with those obtained in the biochemical analysis of interaction, it has been reported that the alteration in the begomoviral loop sequence, precisely in the region 5'-TTAC-3' affects directly the replication rate of begomoviral DNA<sup>6,7</sup>, in our results, most of the interactions shown in the theoretical model, show interactions between the AmPep1 peptide with the OriRepTYLCV sequence very close or neighboring in to the 5'-TTAC-3' sequence of the hairpin (Figure 2), mainly by electrostatic interactions between the dioxiphosphate groups with R, and by Pi interactions between the A and T with the W.

The RepApep control peptide has the analogous sequence to the catalytic site of Rep that recognizes the TAC region of the loop, it only shows a significant decrease in VS and CS concentration at 12 hpTx, mostly showing a “static” effect in the viral replication, an explanation might be due it contains just tyrosine as unique aromatic amino acid in its sequences not allowing a good interaction with the DNA template by Pi interaction as the tryptophan, as well the amount in basic amino acid content is lower compared with AmPep1, reducing the electrostatic interaction between molecules

Although a strong alteration to the conformation in the secondary structure of the DNA by AmPep1 was not observed in the Raman analysis, it can be speculated that AmPep1 induce local transitions of this conformation according to the vibrational shift of the dioxide bond of the phosphate from 1092 to 1096  $\text{cm}^{-1}$  inferring that it is due to an electrostatic interaction of negative charges of the phosphodioxy group with positive charge of the amino groups of the peptide, as reported in the case of some cationic peptides<sup>29</sup>, when they interact with oligonucleotides, these shift the vibration signal of the phosphodioxy group band with values close to or above 1100  $\text{cm}^{-1}$ , this upward displacement can be explained due to a conformational transition from DNA B to A, however, no emergence of the marked band of this conformational change at 807  $\text{cm}^{-1}$  was observed, suggesting just local transitions of the DNA backbone towards this conformation<sup>27</sup> in the binding sites. The binding of AmPep1 over the hairpin and induction of local conformation transition could produce a steric hindrance for Rep protein not allowing the properly recognition of its target sequence, blocking an accurate start of replication models for the virus, resulting like in our data, a delay in the disease progress.

There is a possibility that AmPep1 has anti-viral action on other begomoviruses or geminiviruses of phytosanitary importance due its conserved molecular target. The use of plant derived peptides as potential agrochemicals against viral infections is presented as an novel alternative to the use of transgenic plants and also of synthetic products considering their mode and cost of production.

## Conclusion

The peptide AmPep1 derived from amaranth globulins binds in the loop of the replicative hairpin structure of TYLCV by electrostatic, Pi and H bond interactions inducing local-structure changes in the hairpin structure, therefore, the biological effect is tampering the replicative process of the TYLCV in tomato and *Nicotiana benthamiana* with a consequent reduction of viral replication process, total virus titer and reduction of disease development.

## MATERIAL AND METHODS

### Plant and bacteria culture

Seeds of *Nicotiana benthamiana* and Tomato “Moneymarker” were disinfected with ethanol 70% per 1 minute, then rise with sterile water several times and cultivated separately in pots with a mixture perlite-vermiculite (1:1) and incubated in growth chamber with a photoperiod 18/6, light and darkness, respectively, at 28°C, relative humidity 72%.

*Agrobacterium tumefaciens* C58C1 containing 1.8mer of TYLCV (Accession no. HF548826) was prepared for agroinfection as describe Just K. *et al* 2017<sup>61</sup>.

### Reagents

The oligonucleotide 5'-GGCCATCCGTATAATATTACCGGATGGCC-3' corresponding to the replication hairpin of TYLCV<sup>6,7,8</sup> was used to study the molecular interaction between this viral region and the AmPep1 peptide by Raman spectroscopy, the synthetic oligonucleotide was purchased from Sigma Aldrich (oligo-synthesis service), with HPLC purity quality, the stock solution was prepared at 100 µM using sterile milli-Q water. The AmPep1 peptide was purified from an amaranth globulin hydrolysate as described by Mendoza-Figueroa et al, 2018<sup>21</sup>. To prepare Raman analysis solutions, an aliquot was taken from the stocks to obtain 1 µmol of each biomolecule, this aliquot was concentrated to dryness and re suspended in 10 µL of buffer (10mM Tris-HCL, 50mM NaCl, pH 7.4)<sup>27,62</sup>. To perform the interaction assay, each of the biomolecules was prepared separately as mentioned above at a final concentration of 1 µmol, each was re-suspended in 5 µL of buffer and these solutions were mixed (final molar ratio 1: 1), then homogenized 1 minute with pipette and incubated 10 minutes at room temperature to allow interaction between these molecules, after this time the mix solution was dropped on the glass-Al substrate to dry.

The peptide NIQGAKSSSDVKS YIDK called RepApep (TAG Copenhagen A/S) containing the binding and catalytic domain of TYLCV Rep protein was used as positive control for replication assays<sup>8,21,63</sup>.

### Oligonucleotides for single PCR

For detection of TYLCV systemic infection in *N. benthamiana* and tomato by standard or single PCR, the set of universal degenerated begomovirus primers AC1048 5'-GGRTTDGARGCATGHGTACATG-3' and AV548 5'-GCCYATRTAYAGRAAGCCMAG-3' were used<sup>64</sup>. Viral strand-specific oligonucleotides for T4 DNA polymerase synthesis containing the TAG sequence were OCS-TAG 5'-AGTTTAAGAACCCTTCCCGCGGACTTTACATGGGCCTTCAC-3' and OVS-TAG 5'-AGTTTAAGAACCCTTCCCGCGAAGGCTGAACTTCGACAGC-3' for detection of viral sense strand (VS) and complementary sense strand (CS), respectively. For strand-specific qPCR, the primers OVS 5'-GAAGGCTGAACTTCGACAGC-3' and OCS 5'-GGACTTTACATGGGCCTTCAC-3' were used combining with TAG primer 5'-AGTTTAAGAACCCTTCCCGC-3' for

quantify the specific VS or CS after T4 synthesis, or just combining OVS and OCS for total TYLCV DNA quantification<sup>11</sup>.

### **Raman measurements**

The Raman spectrum of each biomolecule and the interaction mixture was recorded using drop-coating deposition Raman (DCDR) method<sup>65,28</sup>. In brief, 10  $\mu$ L of each solution was deposited on a glass aluminum mirror substrate, allowed to dry at room temperature until the formation of a characteristic ring. Raman spectrum acquisition of each drop was recorded using a confocal Witec Alpha 300 series Raman-AFM and a Zeiss, 100x, 0.9 N.A. objective. Excitation laser wavelength at 532 nm with thermoelectrically cooled CCD detector with 672 l/mm grating. Integration time of 3s and a laser power of 26.4 mW for the DNA and 20 mW for the peptide and the mixture were performed. Initially, a Raman spectrum of the buffer and aluminum mirror were obtained to discard background signals in the analysis. Raman spectra were acquired in 10 random areas of the formed ring of the dried drop, a total of 10 punctual Raman spectra were recorded within the same parameters. Raman spectra were averaged, smoothed using the adjacent-averaging method and 0-1 normalized, considering exclusively the --/fingerprint/ region (600 to 1800  $\text{cm}^{-1}$ ) for comparative analysis. Peak fit analysis of the amide I band (1620 to 1720  $\text{cm}^{-1}$ ) was performed using PeakFit v4.12 software (Systat Software, Inc), considering a good deconvolution analysis when  $R^2$  reaches a value greater than 0.99.

### **Molecular modelling and Docking**

Docking was carried out with AutoDock 4.2 software (The Scripps Research Institute, La Jolla, CA, USA) using the default parameters<sup>66,67</sup>. HyperChem 8 was necessary to calculate the energy-minimized form with geometric optimization for the ligand. The molecular docking was performed with a model built by homology with of TYLCV hairpin, following the prediction of secondary structure previously reported for these sequences<sup>7</sup> and calculated on the server RNAstructure web server (David H. Mathews, Rochester Med.Center, NY, <https://rna.urmc.rochester.edu/>) the peptide was modeled on the Pep-Fold server<sup>68,69</sup>, and optimized according to secondary structure observed in the Raman analysis. AutoDock tools were first used to prepare all files by adding polar hydrogen atoms and merged non-polar hydrogens to the hairpin structure and computing Gasteiger charges for the molecular model of analyzed AmPep1 peptide. The entire system was subjected to a surface scanning and refined docking, the grid map was 80  $\times$  80  $\times$  80 grid point, with the center corresponding to the hairpin, which was held rigid during the docking process. The Lamarckian genetic algorithm was applied<sup>66</sup>. During the docking experiment, 100 runs were carried out.

### ***In vivo* analysis of the TYLCV replication in *Nicotiana benthamiana* by Two-step qPCR**

*Nicotiana benthamiana* plants with 3-old weeks were agroinfected with 1.8 mer DNA of TYLCV-IL (Accession no. HF548826) contained in pLH7000\* (modified binary vector pLH000)<sup>61</sup> in *Agrobacterium tumefaciens* C58C1, after 10 days post infection (dpi), samples from new full expanded apical leaves were collected and DNA was extracted with CTAB method<sup>70</sup> to verify the systemic infection by single PCR. Two infected

expanded leaves of three plants from *N. benthamiana* were treated as show in (figure 3A). The left side were infiltrated with infiltration buffer (MES 10Mm pH 5.7, MgCl<sub>2</sub> 10Mm) and the right side were infiltrated with 15 and 30  $\mu$ M of AmPep1 peptide or RepApep peptide at 15  $\mu$ M dissolved in infiltration buffer. As infection control, 2 leaves of 3 plants were infiltrated with only buffer in both sides. Approximately 0.5 mm<sup>2</sup> of tissue of each side were collected at 0, 12 and 48 hours after treatment and DNA was extracted with CTAB method, with this DNA, Two-step qPCR method was performed according the reported by Rodríguez- Negrete et al, 2014<sup>11</sup> for quantify the viral sense (VS) and complementary (CS) DNA of TYLCV.

First, a single amplification with T4 DNA polymerase (Thermo Scientific) was performed using 1 $\mu$ M of specific viral strands primers (OVS-TAG to CS or OCS-TAG to VS), after this linear amplification, products were cleaned from reaction mixture with GeneJET PCR purification kit (Thermo Scientific) according instructions. The second step of method was performed by standard qPCR, using as template the T4 amplification product and specific primers according to the virus strand: The set OVS /TAG primer to detect CS, and the set primer OCS /TAG to detect VS or OCS/OVS to detect total TYLCV DNA. Standard qPCR was performed according kit instructions (SensyFAST SYBR Lo-Rox Bioline Supermix): 1 cycle at 95°C for 1 minute and 40 cycles at 95°C in 5 seconds and 60°C 15 seconds, melting curves were analyzed after last step under ramp of 0.5°C each 10 seconds from 60° to 90°C in a CFX-Connect Real-Time PCR detection Machine (BioRad).

The results of qPCR were analyzed with absolute quantification using a standard curve. The template for standard curves was prepared using a single PCR amplicon product, this product was obtained for amplified a region of CP gene of TYLCV with the primer set OVS/OCS using DNA from infected TYLCV tomato leaves as template. Five dilutions of the TYLCV PCR amplicon from 10<sup>7</sup> to 10<sup>3</sup> copies were prepared, T4 DNA polymerase linear amplification were performed amplifying one set of dilutions with the primer OCS-TAG and other set with the primer OVS-TAG, then the products were cleaned from the rest of reactions components using GeneJET PCR purification kit (Thermo Scientific) and amplified with standard qPCR with appropriated primers as describe above. For standard curve of total TYLCV DNA, the PCR amplicon dilutions were directly amplified with the primer set OVS/OCS. Standard curve was created using linear regression of the mean of three technical replicates of the C<sub>q</sub> value of each dilution over concentration of those standards in Log<sub>10</sub>. The amount of CS or VS in experimental samples were calculated for extrapolated the mean of C<sub>q</sub> values of each treatment and time (6 biological replicates per treatment with 3 technical replicates in the qPCR analysis).

Two-Way ANOVA statistical analysis was performed for examines the difference between treatments, comparing the titer of CS, VS or Total TYLCV DNA between different peptide treatments through the time respecting the infection control. GraphPad Version 6 was used for calculations.

### **Anti-viral activity of AmPep1 in tomato leaves.**

The anti-viral activity of the AmPep1 peptide was evaluated in the natural host tomato, 10-old days tomato seedlings (containing 2 true leaves) were agroinoculated with TYLCV-IL<sup>61</sup> in the true leaves and cotyledons, 10 days after infection, new apical leaves

started to show curling, then, tissue from apical leaves were collected and DNA was extracted to verify systemic infection using a single PCR, then, a group of plants (N=4) were treated by infiltration with AmPep1 in all new apical leaves of tomato seedlings for 3 consecutive days, Other group of infected plants (N=4) was treated just with infiltration buffer (MES 10 mM, MgCl<sub>2</sub> 10 mM). Samples of apical leaves were collected at 0,7 and 15 days after last day of treatment and DNA was extracted by CTAB method. Symptoms (chlorosis, curling and dwarfing) were consider as disease progress indicator through the observation time. Disease progress was evaluated through 15 days after treatments in both conditions. DNA of TYLCV was quantified absolutely in leaf samples using standard qPCR with the primer set OVS/OCS, experimental and analysis of standard curve was performed as describe above. Two-Way ANOVA was performed to analyze significative difference in the mean of viral titer between the plants treated with AmPep1 comparing with infection control trough the time.

### **Confocal microscopy.**

The peptide AmPep1 was labeled with fluorescein isothiocyanate isomer I (FITC, Sigma-Aldrich) according to the manufacturing indications. Small apical leaves (size approximately 1 cm<sup>2</sup>) of *N. benthamiana* with 3 weeks of age, cultured as mentioned above, were used. The leaves were incubated in an aqueous solution of 5 μM AmPep1-FITC for 10, 30 and 60 minutes (3 leaves per time) at room temperature and at 4°C, immediately after the incubation time the leaves were washed with 0.5% SDS and fixed in a glutaraldehyde solution 1% <sup>71</sup>. Subsequently, the samples were stained with DAPI at a concentration of 1 μg / mL. As control, seedlings not treated with labeled peptide were used. The seedlings were analyzed in the Nikon A1R + STORM confocal microscope using an argon laser with excitation line filter of 492 nm for the FITC and a 405 nm excitation filter for the DAPI. The chlorophyll autofluorescence was detected with the 650-800 nm bandpath filter, observations were performed on a 60X water objective. The images were analyzed in NIS-Elements-Viewer 4.20 (Nikon).

### **Acknowledgment**

JSMF and IBR are doctoral students from Programa de Doctorado en Ciencias Biomédicas UNAM. JSMF received fellowship 363126 from CONACYT, he also expresses the gratitude to the Department of Plant Biology of Swedish University of Agricultural Sciences.

The authors thank to Laboratorio Universitario de Caracterización Espectroscópica, LUCE\_ICAT\_UNAM for the facilities with the Raman equipment.

IBR and JMSB thank the support of the IN-111216 UNAM-DGAPA-PAPIIT project.

### **REFERENCES**

1. Zerbini, F. M. *et al.* ICTV Virus Taxonomy Profile: Geminiviridae. *J. Gen. Virol.* **98**, 131–133 (2017).
2. Moriones, E. & Navas-Castillo, J. Tomato yellow leaf curl virus, an emerging virus complex causing epidemics worldwide. *Virus Res.* **71**, 123–134 (2000).

3. Basak, J. Tomato Yellow Leaf Curl Virus: A Serious Threat to Tomato Plants World Wide. *J. Plant Pathol. Microbiol.* **7**, (2016).
4. Glick, E., Levy, Y. & Gafni, Y. The viral etiology of tomato yellow leaf curl disease—a review. *Plant Prot. Sci.* **45**, 81–97 (2009).
5. Brown, J. K. *et al.* Revision of Begomovirus taxonomy based on pairwise sequence comparisons. *Arch. Virol.* **160**, 1593–1619 (2015).
6. Laufs, J. *et al.* In vitro cleavage and joining at the viral origin of replication by the replication initiator protein of tomato yellow leaf curl virus. **92**, 3879–3883 (1995).
7. Orozco, B. M. & Hanley-Bowdoin, L. A DNA structure is required for geminivirus replication origin function. *J. Virol.* **70**, 148–158 (1996).
8. Campos-Olivas R., Louis, J. M., Cle, D., Gronenborn, B. & Gronenborn, A. M. The structure of a replication initiator unites diverse aspects of nucleic acid metabolism. *Proc. Natl. Acad. Sci. U. S. A.* **9999**, 5–10 (2002).
9. Richter, K. S., Götz, M., Winter, S. & Jeske, H. The contribution of translesion synthesis polymerases on geminiviral replication. *Virology* **488**, 137–148 (2016).
10. Pooggin, M. M. How can plant DNA viruses evade siRNA-directed DNA methylation and silencing? *Int. J. Mol. Sci.* **14**, 15233–15259 (2013).
11. Rodríguez-Negrete, E. A. *et al.* A sensitive method for the quantification of virion-sense and complementary-sense DNA strands of circular single-stranded DNA viruses. *Sci. Rep.* **4**, 6438 (2014).
12. Hak, H. *et al.* TYLCV-Is movement in planta does not require V2 protein. *Virology* **477**, 56–60 (2015).
13. Verlaan, M. G. *et al.* The Tomato Yellow Leaf Curl Virus Resistance Genes Ty-1 and Ty-3 Are Allelic and Code for DFDGD-Class RNA-Dependent RNA Polymerases. *PLoS Genet.* **9**, (2013).
14. Li, H. *et al.* Control of tomato yellow leaf curl virus disease by *Enterobacter asburiae* BQ9 as a result of priming plant resistance in tomatoes. *Turkish J. Biol.* **40**, 150–159 (2016).
15. Yang, Y., Sherwood, T. A., Patte, C. P., Hiebert, E. & Polston, J. E. Use of *Tomato yellow leaf curl virus* (TYLCV) *Rep* Gene Sequences to Engineer TYLCV Resistance in Tomato. *Phytopathology* **94**, 490–496 (2004).
16. Cillo, F. & Palukaitis, P. *Transgenic resistance. Advances in Virus Research* **90**, (Elsevier Inc., 2014).
17. Lopez-Ochoa, L., Ramirez-Prado, J. & Hanley-Bowdoin, L. Peptide aptamers that bind to a geminivirus replication protein interfere with viral replication in plant cells. *J. Virol.* **80**, 5841–53 (2006).
18. Reyes, M. I., Nash, T. E., Dallas, M. M., Ascencio-Ibanez, J. T. & Hanley-Bowdoin, L. Peptide Aptamers That Bind to Geminivirus Replication Proteins Confer a Resistance

Phenotype to Tomato Yellow Leaf Curl Virus and Tomato Mottle Virus Infection in Tomato. *J. Virol.* **87**, 9691–9706 (2013).

19. Mori, T., Takenaka, K., Domoto, F., Aoyama, Y. & Sera, T. Inhibition of Binding of Tomato Yellow Leaf Curl Virus Rep to its Replication Origin by Artificial Zinc-Finger Protein. *Mol. Biotechnol.* **54**, 198–203 (2013).

20. Ali, Z., Ali, S., Tashkandi, M., Zaidi, S. S. E. A. & Mahfouz, M. M. CRISPR/Cas9-Mediated Immunity to Geminiviruses: Differential Interference and Evasion. *Sci. Rep.* **6**, (2016).

21. Mendoza-Figueroa, J. S. *et al.* A peptide derived from enzymatic digestion of globulins from amaranth shows strong affinity binding to the replication origin of Tomato yellow leaf curl virus reducing viral replication in *Nicotiana benthamiana*. *Pestic. Biochem. Physiol.* **145**, 56–65 (2018).

22. Wei, F., Zhang, D., Halas, N. J. & Hartgerink, J. D. Aromatic amino acids providing characteristic motifs in the raman and SERS spectroscopy of peptides. *J. Phys. Chem. B* **112**, 9158–9164 (2008).

23. Takeuchi, H. Raman structural markers of tryptophan and histidine side chains in proteins. *Biopolym. - Biospectroscopy Sect.* **72**, 305–317 (2003).

24. Jarmelo, S., Carey, P. R. & Fausto, R. The Raman spectra of serine and 3,3-dideutero-serine in aqueous solution. *Vib. Spectrosc.* **43**, 104–110 (2007).

25. Overman, S. A. & Thomas, G. J. Amide modes of the  $\alpha$ -helix: Raman spectroscopy of filamentous virus fd containing peptide 13C and 2H labels in coat protein subunits. *Biochemistry* **37**, 5654–5665 (1998).

26. Rivas-Arancibia, S., Rodríguez-Martínez, E., Badillo-Ramírez, I., López-González, U. & Saniger, J. M. Structural Changes of Amyloid Beta in Hippocampus of Rats Exposed to Ozone: A Raman Spectroscopy Study. *Front. Mol. Neurosci.* **10**, 1–11 (2017).

27. Jangir, D. K. & Mehrotra, R. Raman spectroscopic evaluation of DNA adducts of a platinum containing anticancer drug. *Spectrochim. Acta - Part A Mol. Biomol. Spectrosc.* **130**, 386–389 (2014).

28. Pagba, C. V., Lane, S. M. & Wachsmann-Hogiu, S. Raman and surface-enhanced Raman spectroscopic studies of the 15-mer DNA thrombin-binding aptamer. *J. Raman Spectrosc.* **41**, 241–247 (2010).

29. Hernández, B., Coïc, Y. M., Gouyette, C. & Ghomi, M. Probing the interactions of oligodeoxynucleotides with a cationic peptide by Raman scattering. *Adv. Biomed. Spectrosc.* **5**, 58–71 (2012).

30. Gorelik, V. S., Krylov, A. S. & Sverbil, V. P. Local Raman spectroscopy of DNA. *Bull. Lebedev Phys. Inst.* **41**, 310–315 (2014).

31. Ruiz-Chica, A. J., Medina, M. A., Sánchez-Jiménez, F. & Ramírez, F. J. On the interpretation of Raman spectra of 1-aminooxy-spermine/DNA complexes. *Nucleic Acids Res.* **32**, 579–589 (2004).



32. Lord, R. C. & Thomas, G. J. Raman studies of nucleic acids - II aqueous purine and pyrimidine mixtures. *Biochim. Biophys. Acta - Nucleic Acids Protein Synth.* **142**, 1–11 (1967).
33. Dina, N. E. *et al.* Structural changes induced in grapevine (*Vitis vinifera* L.) DNA by femtosecond IR laser pulses: A surface-enhanced Raman spectroscopic study. *Nanomaterials* **6**, 1–18 (2016).
34. Movileanu, L., Benevides, J. M. & Thomas, G. J. Temperature dependence of the Raman spectrum of DNA. II. Raman signatures of premelting and melting transitions of poly(dA)·poly(dT) and comparison with poly(dA-dT)·poly(dA-dT). *Biopolymers* **63**, 181–194 (2002).
35. Wojtuszewski, K. & Mukerji, I. The HU – DNA binding interaction probed with UV resonance Raman spectroscopy : Structural elements of specificity. 2416–2428 (2004). doi:10.1110/ps.04730204.1987
36. Tsuboi, M., Overman, S. A., Nakamura, K., Rodriguez-Casado, A. & Thomas, G. J. Orientation and interactions of an essential tryptophan (Trp-38) in the capsid subunit of Pf3 filamentous virus. *Biophys. J.* **84**, 1969–1976 (2003).
37. M., S., Duraisamy, P. & Iyandurai, N. Structural Analysis of DNA Interactions with Magnesium Ion Studied by Raman Spectroscopy. *Am. J. Biochem. Biotechnol.* **7**, 135–140 (2011).
38. Gobinet, C., Van-gulick, L., Jeannesson, P. & Piot, O. Probing in Vitro Ribose Induced DNA-Glycation Using Raman Microspectroscopy. *Anal. Chem.* **87**, 2655–2664 (2015).
39. Pagba, C. V, Lane, S. M. & Wachsmann-hogiu, S. Conformational changes in quadruplex oligonucleotide structures probed by Raman spectroscopy. *Biomedical Optics* **2**, 1899–1904 (2011).
40. Krafft, C., Benevides, J. M. & Jr, G. J. T. Secondary structure polymorphism in *Oxytricha nova* telomeric DNA. *Nucleic Acids Res.* **30**, 3981-3991 (2002).
41. Filho, P. F. F. *et al.* High Temperature Raman Spectra of L-Leucine Crystals. *Brazilian J. Phys.* **38**, 12 (2007).
42. Faria, J. L. B. Polarized Raman spectra of L -arginine hydrochloride monohydrated single crystal. *Brazilian J. Phys.* **1**, 288–294 (2009).
43. Sereda, V. *et al.* Polarized Raman Spectroscopy for Determining the Orientation of di-D-phenylalanine Molecules in a Nanotube. *J Raman Spectrosc.* **47**, 1056–1062 (2017).
44. Tuma, R. Raman spectroscopy of proteins: From peptides to large assemblies. *J. Raman Spectrosc.* **36**, 307–319 (2005).
45. Camerlingo, C., d'Apuzzo, F., Grassia, V., Perillo, L. & Lepore, M. Micro-Raman Spectroscopy for Monitoring Changes in Periodontal Ligaments and Gingival Crevicular Fluid. *Sensors* **14**, 22552–22563 (2014).

46. Murli, C., Vasanthi, R. & Sharma, S. M. Raman spectroscopic investigations of dl-serine and dl-valine under pressure. *Chem. Phys.* **331**, 77–84 (2006).
47. Nagy, P. I. Competing intramolecular vs. Intermolecular hydrogen bonds in solution. *International Journal of Molecular Sciences* **15**, (2014).
48. Lucas, X., Bauzá, A., Frontera, A. & Quiñonero, D. A thorough anion- $\pi$  interaction study in biomolecules: On the importance of cooperativity effects. *Chem. Sci.* **7**, 1038–1050 (2016).
49. Wilson, K. A., Kellie, J. L. & Wetmore, S. D. DNA-protein  $\pi$ -interactions in nature: Abundance, structure, composition and strength of contacts between aromatic amino acids and DNA nucleobases or deoxyribose sugar. *Nucleic Acids Res.* **42**, 6726–6741 (2014).
50. De Figueiredo, I. R., Freire, J. M., Flores, L., Veiga, A. S. & Castanho, M. A. R. B. Cell-penetrating peptides: A tool for effective delivery in gene-targeted therapies. *IUBMB Life* **66**, 182–194 (2014).
51. Kauffman, W. B., Fuselier, T., He, J. & Wimley, W. C. *Trends Biochem Sci.* **40**, 749–764 (2016).
52. Rafiqi, M. *et al.* Internalization of Flax Rust Avirulence Proteins into Flax and Tobacco Cells Can Occur in the Absence of the Pathogen. *Plant Cell* **22**, 2017–2032 (2010).
53. Yamashita, H. *et al.* Development of a Cell-penetrating Peptide that Exhibits Responsive Changes in its Secondary Structure in the Cellular Environment. *Sci. Rep.* **6**, 2–9 (2016).
54. Gräslund, A., Madani, F., Lindberg, S., Langel, Ü. & Futaki, S. Mechanisms of cellular uptake of cell-penetrating peptides. *J. Biophys.* **2011**, (2011).
55. Jiao, C. Y. *et al.* Translocation and endocytosis for cell-penetrating peptide internalization. *J. Biol. Chem.* **284**, 33957–33965 (2009).
56. M, D. M., S, S. P., Castanho, M. a & Santos, N. C. What can light scattering spectroscopy do for membrane-ctive peptide studies. *J. Pept. Sci.* **14**, 1084–1095 (2008).
57. Blinkova, O. *et al.* Novel circular DNA viruses in stool samples of wild-living chimpanzees. *J. Gen. Virol.* **91**, 74–86 (2010).
58. Chan, D. I., Prenner, E. J. & Vogel, H. J. Tryptophan- and arginine-rich antimicrobial peptides: Structures and mechanisms of action. *Biochim. Biophys. Acta - Biomembr.* **1758**, 1184–1202 (2006).
59. Rajeswari M.R. *et al.* Binding of oligopeptides to d-AGATCTAGATCT and d-AAGCTTAAGCTT: can tryptophan intercalate in DNA hairpins? *Biochemist* **31**, 6237–6241 (1992)
60. Roy K.B. *et al.* Hairpin and duplex forms of a self-complementary dodecamer, d AGATCTAGATCT, and interaction of the duplex form with the peptide KGWGK: can a pentapeptide destabilize DNA? *Biochemist* **31**, 6241–6245 (1992)

61. Just, K., Sattar, M. N., Arif, U., Luik, A. & Kvarnheden, A. Infectivity of Tomato yellow leaf curl virus isolated from imported tomato fruit in Estonia. *Zemdirbyste* **104**, 47–52 (2017).
62. Zhang, W. *et al.* Synthesis, characterization, DNA/protein interaction and cytotoxicity studies of Cu(II) and Co(II) complexes derived from dipyriddy triazole ligands. *Spectrochim. Acta - Part A Mol. Biomol. Spectrosc.* **163**, 28–44 (2016).
63. Heyraud-Nitschke F., Schumacher, S., Laufs, J., Schaefer, S., Schell, J. & Gronenborn, B. Determination of the origin cleavage and joining domain of geminivirus Rep proteins. *Nucleic Acids Res* **23**, 910–916 (1995).
64. Wyatt, S. Detection of Subgroup III Geminivirus Isolates in Leaf Extracts by Degenerate Primers and Polymerase Chain Reaction. *Phytopathology* **86**, 1288 (1996).
65. Filik, J. & Stone, N. Drop coating deposition Raman spectroscopy of protein mixtures. *Analyst* **132**, 544–550 (2007).
66. Morris, G. M. *et al.* AutoDock-related material Automated Docking Using a Lamarckian Genetic Algorithm and an Empirical Binding Free Energy Function. *Comput. Chem. J. Comput. Chem* **19**, 1639–1662 (1998).
67. Huey, R., Morris, G.M., Olson, A.J., Goodsell, D.S. A semiempirical free energy force field with charge-based desolvation. *J. Comput. Chem.* **28**, 1145–1652 (2007).
68. Thévenet, P. *et al.* PEP-FOLD: An updated de novo structure prediction server for both linear and disulfide bonded cyclic peptides. *Nucleic Acids Res.* **40**, 288–293 (2012).
69. Shen, Y., Maupetit, J., Derreumaux, P. & Tufféry, P. Improved PEP-FOLD approach for peptide and miniprotein structure prediction. *J. Chem. Theory Comput.* **10**, 4745–4758 (2014).
70. Doyle J.J., Doyle J.L., A rapid DNA isolation procedure for small quantities of fresh leaf tissue, *Phytochem Bull.* **19**, 11–15 (1987)
71. Pasternak, T. *et al.* Protocol: An improved and universal procedure for whole-mount immunolocalization in plants. *Plant Methods* **11**, 1–10 (2015).

**Table 1. Raman assignments for DNA, peptide and mixed DNA-peptide samples.**

Raman shift (cm <sup>-1</sup> )			Raman Shift from the origin	Assignments	Reference
Pure molecules		Mix			
DNA ( <i>OriRepTYLCV</i> )	Peptide <i>AmPep1</i>	<i>OriRepTYLCV</i> + <i>AmPep1</i>			
675		675	0	dG (breathing)	31
729		729	0	dA(str C1-N9)	36
	760	751	-9	Trp (in-phase breathing)	22,23
786		786	0	phosphodiester (sym str O-P-O)	27
840		840	0	phosphodiester (asym str O-P-O)	27
	853	857	+4	Ser (str out-of-plane CH <sub>2</sub> -O)	24
	870	879	+9	Trp (bending NH)	22,23
	884	879	-5	Trp (bending indole ring coupled NH bending)	22,23
	945	958	+13	Ser (str C-O)	24
	1010	1014	+4	Trp (sym out-of-phase breathing Benzene and pyrrole)	22,23
1019		1019	0	dG(def N-H)	39,40
1062		1070	+8	Deoxyribose (str C-O)	38
	1074		nd	Trp (bending in plane C-C)	22,23
1092		1096	+4	PO <sub>2</sub> <sup>-1</sup> (stretching)	27,28,29
	1131		nd	Peptide (rocking C-NH <sub>3</sub> <sup>+</sup> )	41,42,43
1181		1181	nd	dA,G (str C5-C6)/ dT( str in plane ring CH <sub>3</sub> )	33,39
	1202		nd	Trp (str C-C)	22,23
		1249		dT (str in-plane ring)	38,39
1253		1257	+4	C ( ring str and str C-NH <sub>2</sub> )	32
	1263		nd	Amide III (unordered)	29
1332	1336	1328	+/-4	dA,dG (str,ring Purines)/ Peptide (str CH <sub>3</sub> -CH <sub>2</sub> )	27,30,31
1369		1374	+5	dT, dA, dG (str C-N)	33
1427	1437/35	1427	+/-8	Deoxyribosyl (def 5'-H <sub>2</sub> )/ peptide (def CH <sub>2</sub> / CH)	39, 44
1480		1485	+5	G (def N7, C8=N7-H <sub>2</sub> )	31
	1550		nd	Trp pyrrole (str C2-C3)	22,23
1574		1578	+4	Purine (stretching)	27,30,31
	1618		nd	Trp C=C	22,23
	1658	1654	-4	Amide I ( $\alpha$ -helix)	25,26
1662		1662	0	Thymine (str C=O)	30
1682			nd	dA (scissoring NH <sub>2</sub> )	33
	1686	1690	+4	Amide I (Unordered no H bond, $\beta$ -turns)	26

**Table 2. Deconvolution analysis of the Raman spectra in the region of 1600 to 1710  $\text{cm}^{-1}$ .**

Peak number	Center $\text{cm}^{-1}$	Abundance (%)	Assignment	Reference
<i>Peptide (AmPep1)</i>				
1	1644	5.4	Unordered structure	
2	1658	28.2	$\alpha$ -helix	
3	1670	26.8	Unordered helix + random structure	25, 26,45
4	1682	19.2	$\beta$ - turns/Unordered	
5	1689	14.7	Disordered structure	
6	1699	5.0	Turns and bands	
<i>DNA (OriRepTYLCV)</i>				
a	1660	73.51	Thymine (C4=O) str	
b	1691	24.04	Thymine (C2=O) str	34,35
c	1711	2.43	Thymine (C2=O) str	
<i>Mix (OriRepTYLCV + AmPep1)</i>				
1	1638	8.27	Aromatic amino acid ring mode (Trp)	
2	1653	31.50	$\alpha$ - helix	
a	1662	8.09	Thymine (C4=O) str	25, 26,34,35,45
4	1670	16.54	Unordered helix + random structure	
5	1681	15.58	$\beta$ - turns/Unordered	
b	1695	14.21	Thymine (C2=O) str	
c	1710	5.77	Thymine (C2=O) str	

## -Figure captions:

**Figure 1. Chemical interaction between peptide AmPep1 with the hairpin of replication origin of TYLCV by Raman spectroscopy.** A) Raman spectra of the peptide AmPep1 (blue plot), oligonucleotide OriRepTYLCV (red) and interaction mix AmPep1-OriRepTYLCV (green plot). The upper number in all the spectra indicates the wavenumber (Raman shift  $\text{cm}^{-1}$ ) of each band. In the spectrum of the interaction mix (green) the contribution of each band is marked as **D** if it comes from the OriRepTYLCV DNA or as **P** if it comes from the AmPep1. The bands that show displacements due to the chemical interaction between both molecules are highlighted in bold and indicated with a dotted arrow, showing if the origin and the affected functional group is from DNA (red arrows) or from the peptide (blue arrows). The gray boxes in all the spectra highlight the region from 1620/40 to 1720  $\text{cm}^{-1}$ . B) Deconvolution of the Amida I region of the peptide around 1640 to 1710  $\text{cm}^{-1}$ , C) Deconvolution of the interaction spectrum in the region of 1620 to 1720  $\text{cm}^{-1}$  involving the signals of Amida I and vibrations of C = O of Thymine, D) Deconvolution of the area from 1620 to 1720  $\text{cm}^{-1}$  of the oligonucleotide OriRepTYLCV showing the vibration of the C2/4 = O of Thymine.

**Figure 2. Theoretical model of the interaction between AmPep1- OriRepTYLCV.** A) Three-dimensional model of the peptide-DNA interaction (AmPep1-OriRepTYLCV), the arrangement of the peptide in the region of the replication loop is shown. B) Close contacts between AmPep1 and OriRepTYLCV, b.1) H-bonds interactions, b.2) electrostatic interactions. C) Other weak contacts involved in the peptide-DNA interaction, c.1) formation of Pi-Anion interactions (orange box) between Trp (W) and Adenine. A: Adenine, T: Thymine, C: Cytosine, G: Guanine.

**Figure 3. The peptide AmPep1 tampers the replicative process of TYLCV in *N. benthamiana*.** A) Schematic representation of the assay to evaluate the effect of AmPep1 on the replication process of TYLCV in *N. benthamiana* leaves infected systemically with the virus, the left side was not treated with peptide (UnTx) and the right side was treated (Tx) separately by infiltration with a solution 15 and 30  $\mu\text{M}$  of peptide AmPep1 and with a solution 15  $\mu\text{M}$  of peptide RepApep peptide control. B) Effect of AmPep1 on the synthesis of complementary sense DNA (CS) of TYLCV in the treated and untreated side of the leaf. C) Effect of AmPep1 on the synthesis of viral sense DNA (VS) of TYLCV in the treated and untreated side of the leaf. D) Quantification of the total DNA of TYLCV on the treated and untreated side of the leaf of *N. benthamiana* after treatment with AmPep1. The effects on the replication rate of CS, VS and total DNA were monitored at 0, 12 and 48 hours post treatment. Blue line: infection control (leaves without treatment on both sides), red: AmPep1 (15  $\mu\text{M}$ ), green: AmPep1 (30  $\mu\text{M}$ ), purple: RepApep (control, 15 $\mu\text{M}$ ), each point in time is an average representation of the DNA titer of 6 leaves (3 plants, 2 leaves per plant), vertical bars: standard deviation (SD), asterisks (\*): Significant difference of the mean with respect to infection control ( $P < 0.05$ ).

**Figure 4. Anti-viral activity of AmPep1 in tomato plants infected with TYLCV.** A) Representative image of disease progress in infected seedlings and treated with AmPep1 (100mg7L) at 0, 7 and 15 days post treatment (dpTx), the progress of viral symptoms develop after treatment with AmPep1 was compared with that developed by infection control. At 0 dpTx, the infected seedlings showed the same symptomatic level (curl of apical leaves without chlorosis), at 7dpTx the group of seedlings treated with AmPep1 present a delay in the symptomatic development compared with the infection control group which shows beginning of marginal chlorosis, dwarfism and curling, at 15 dpTx the group of treated seedlings show only slight curling in the apical leaves without evident chlorosis, while the infection control shows advanced marginal chlorosis, blistering and severe curling in the whole apical area (all the analyzed groups have a N = 4). B) Quantification of total DNA of TYLCV in apical leaves of treated and untreated seedlings at 7 and 15 dpTx. SD is indicated in vertical lines, asterisks: significant difference of the mean compared to infection control ( $P < 0.05$ ), each bar represents an average of viral DNA titer in 4 biological replicates. C) Comparative picture between healthy, infected and infected seedlings plus AmPep1 treatment at 15 days post treatment.

**Figure 5. Translocation of AmPep1 into *N. benthamiana* cells.** A) Representative images of an internalization kinetics of AmPep1. Fluorescent signal from left to right, DAPI (blue): nuclei, FITC (green): Peptide AmPep1, Autofluorescence-Chlorophyll (red): chloroplasts. From top to bottom incubation at 10, 30 and 60 minutes at rt or 4 ° C for 60 minutes, bottom image: control not incubated with AmPep1. After 10 minutes of incubation, the formation of transport points through the membrane (pink arrow head) and light translocation towards the nucleus is observed. At 30 and 60 minutes of incubation at rt, there is an increase in the translocation of the peptide and accumulation around the tonoplast (white arrow head) and in the cytoplasm (yellow arrow), in a low temperature incubation the internalization of AmPep1 is not affected negatively, and accumulation of AmPep1 is observed around the tonoplast, nucleus and cytoplasm, in control, no FITC mark signal is observed. Images taken with 60x-water objective, lower bars = 20µm, B) Digital zoom of a stoma and C) digital zoom of epidermal cells at 60 min incubation with AmPep1 at rt. N = nucleus, CL: chloroplast. Bars in B) and C) = 10 µm. rt= room temperature

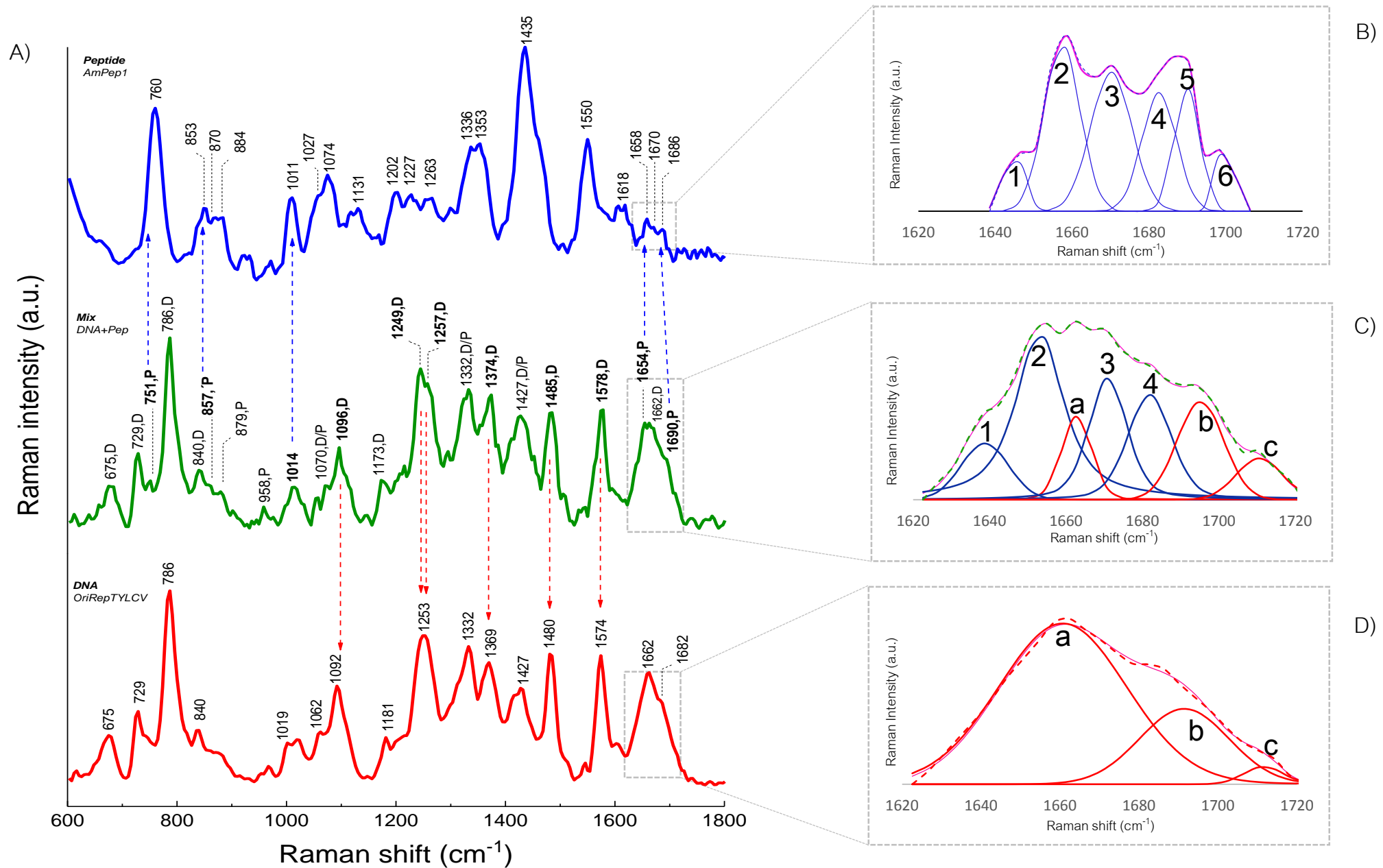


**Figure 1. Chemical interaction between peptide AmPep1 with the hairpin of replication origin of TYLCV by Raman spectroscopy.**



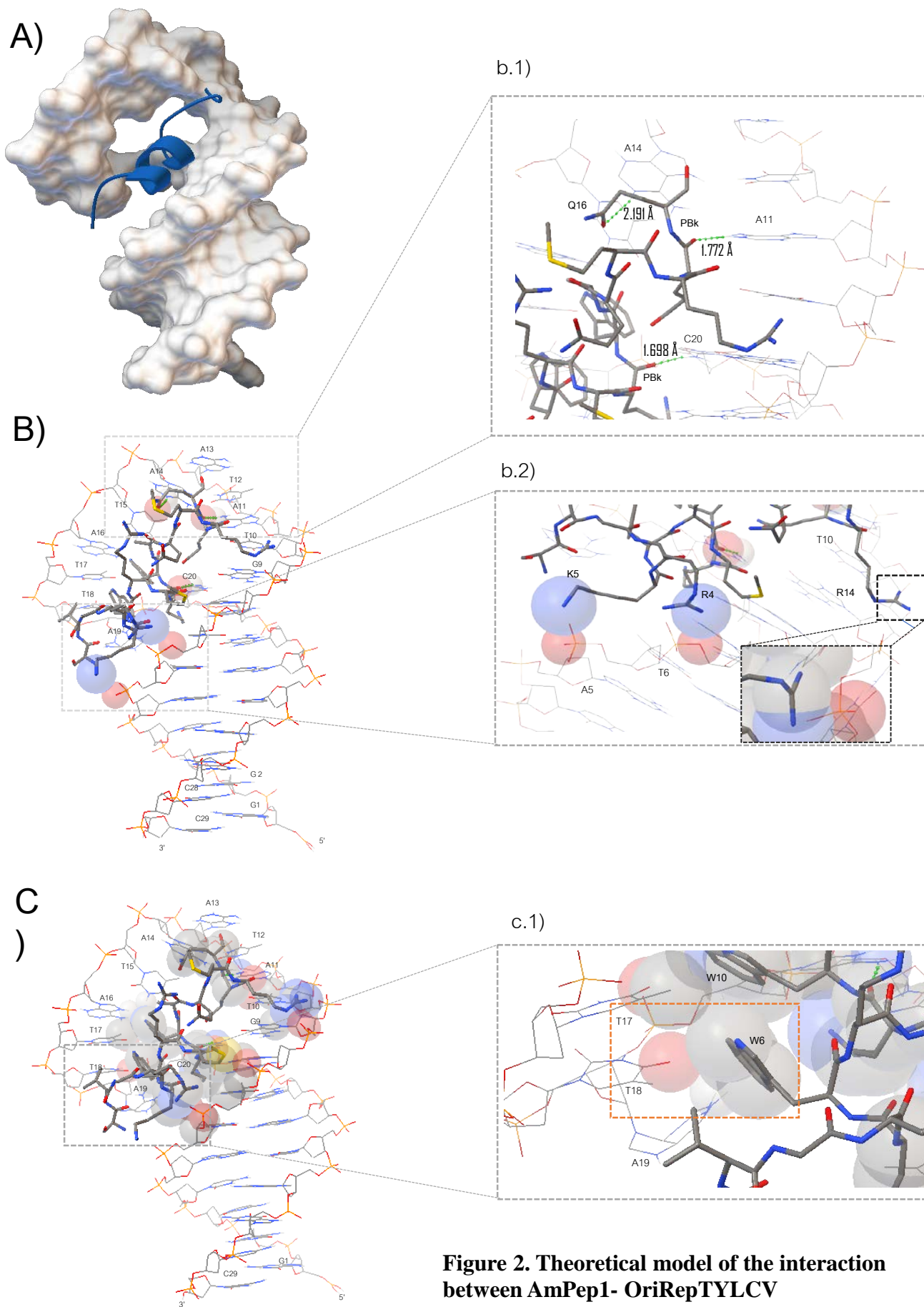


**Figure 2. Theoretical model of the interaction between AmPep1- OriRepTYLCV**

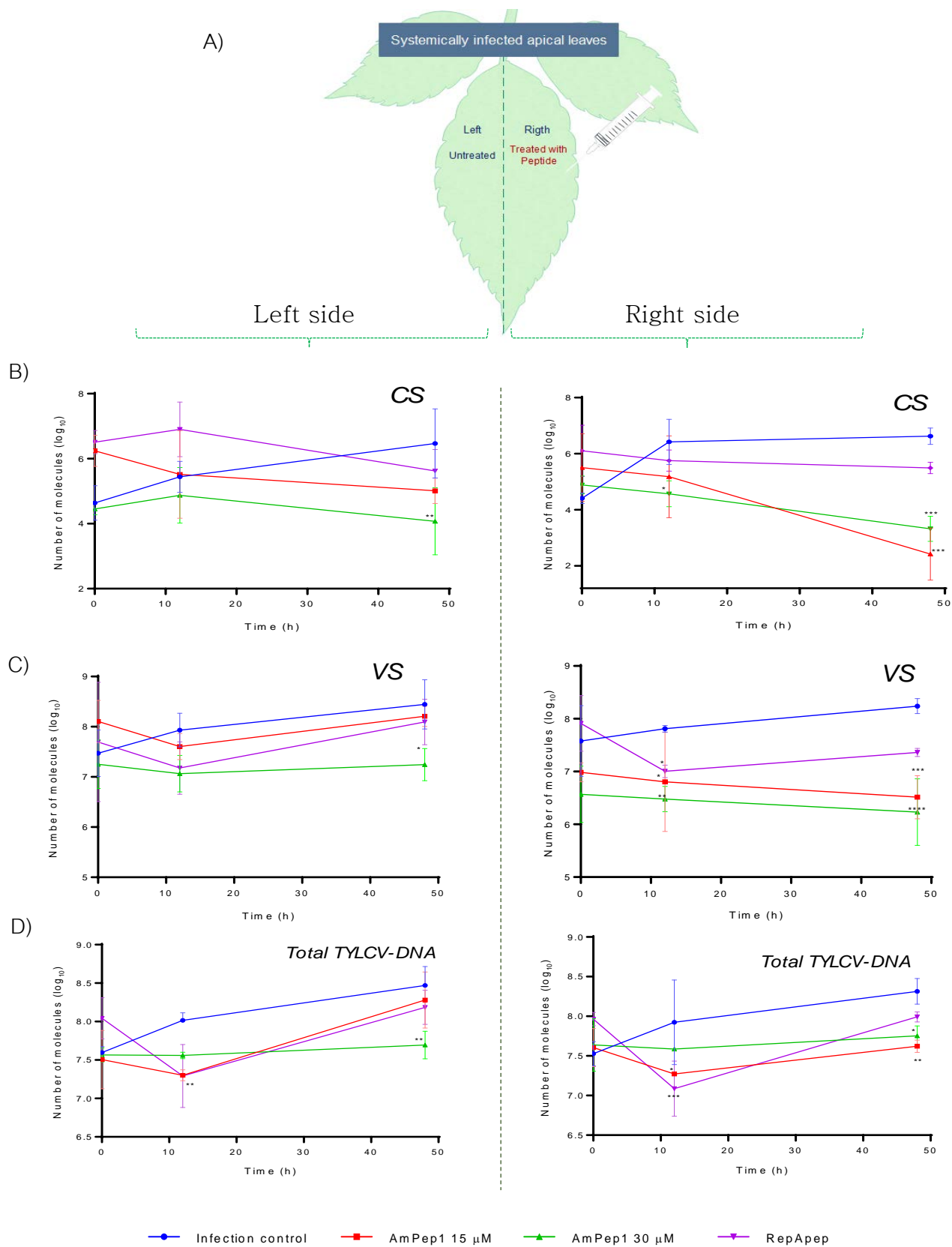


**Figure 3. The peptide AmPep1 tampers the replicative process of TYLCV in *N. benthamiana*.**

+TYLCV

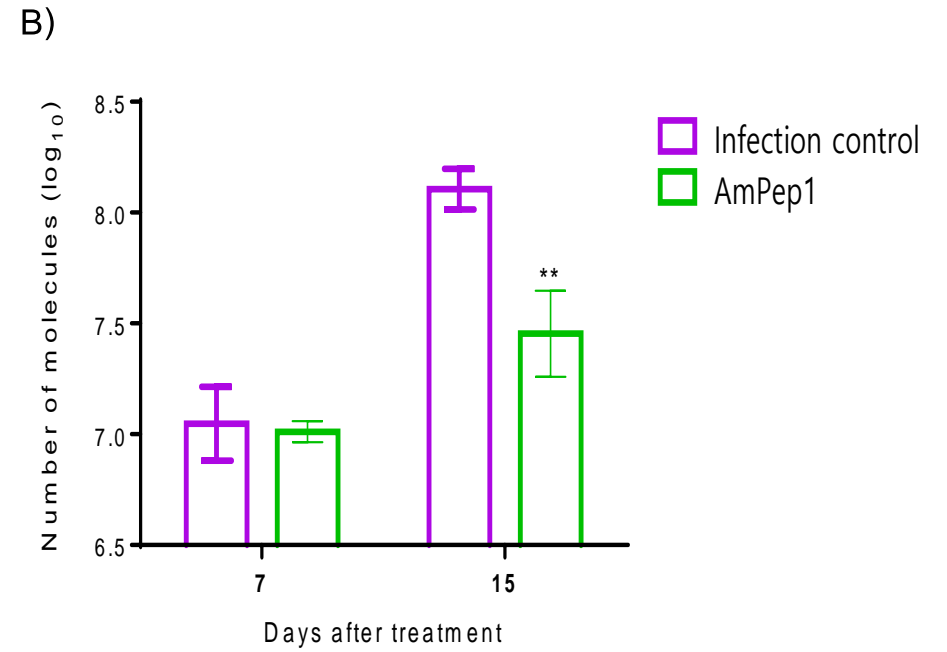
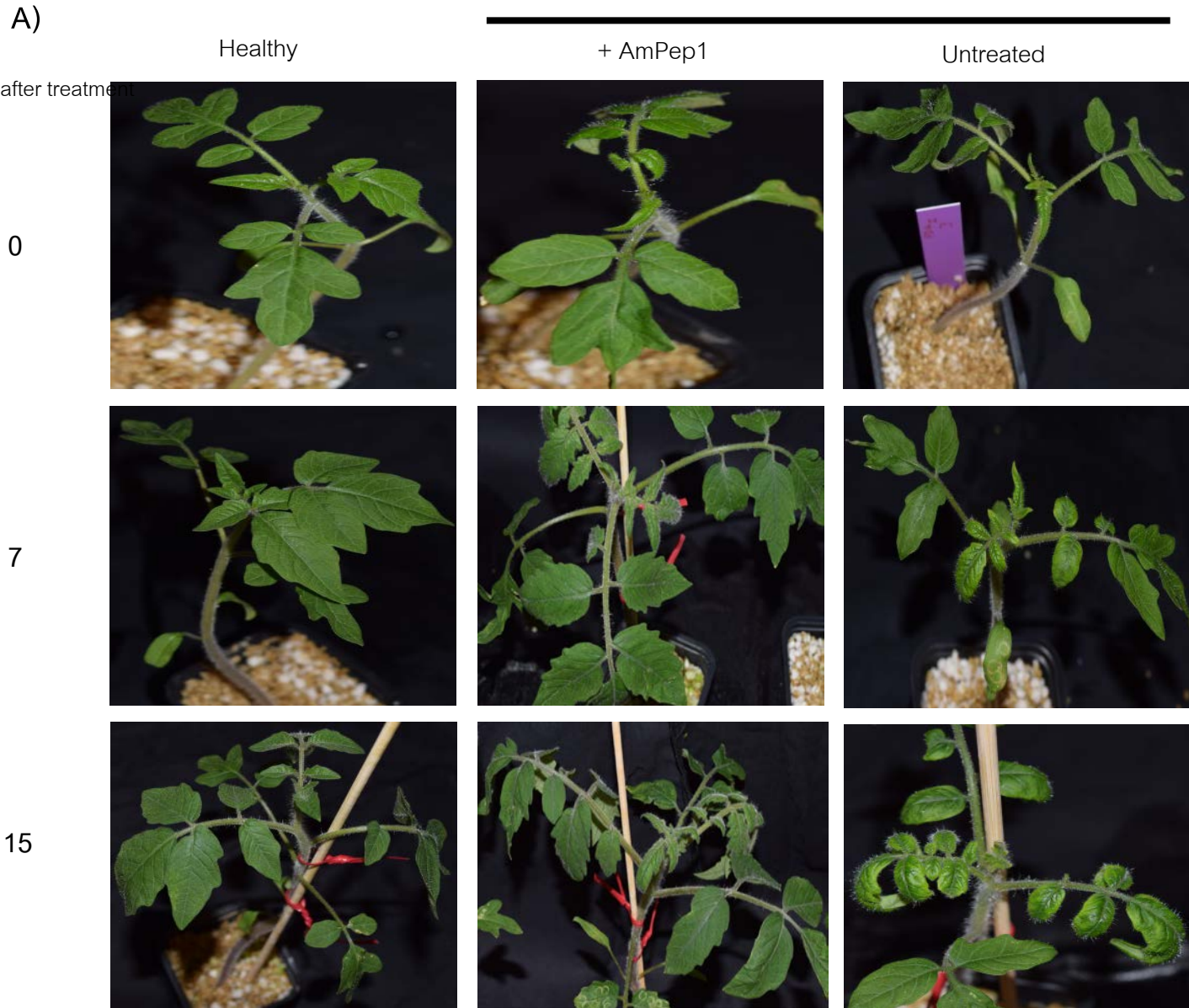


**Figure 4. Anti-viral activity of AmPep1 in tomato plants infected with TYLCV.**

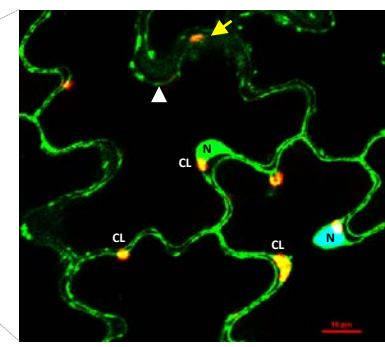
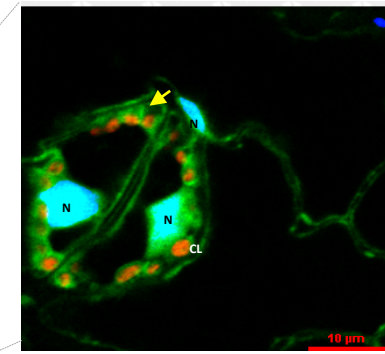
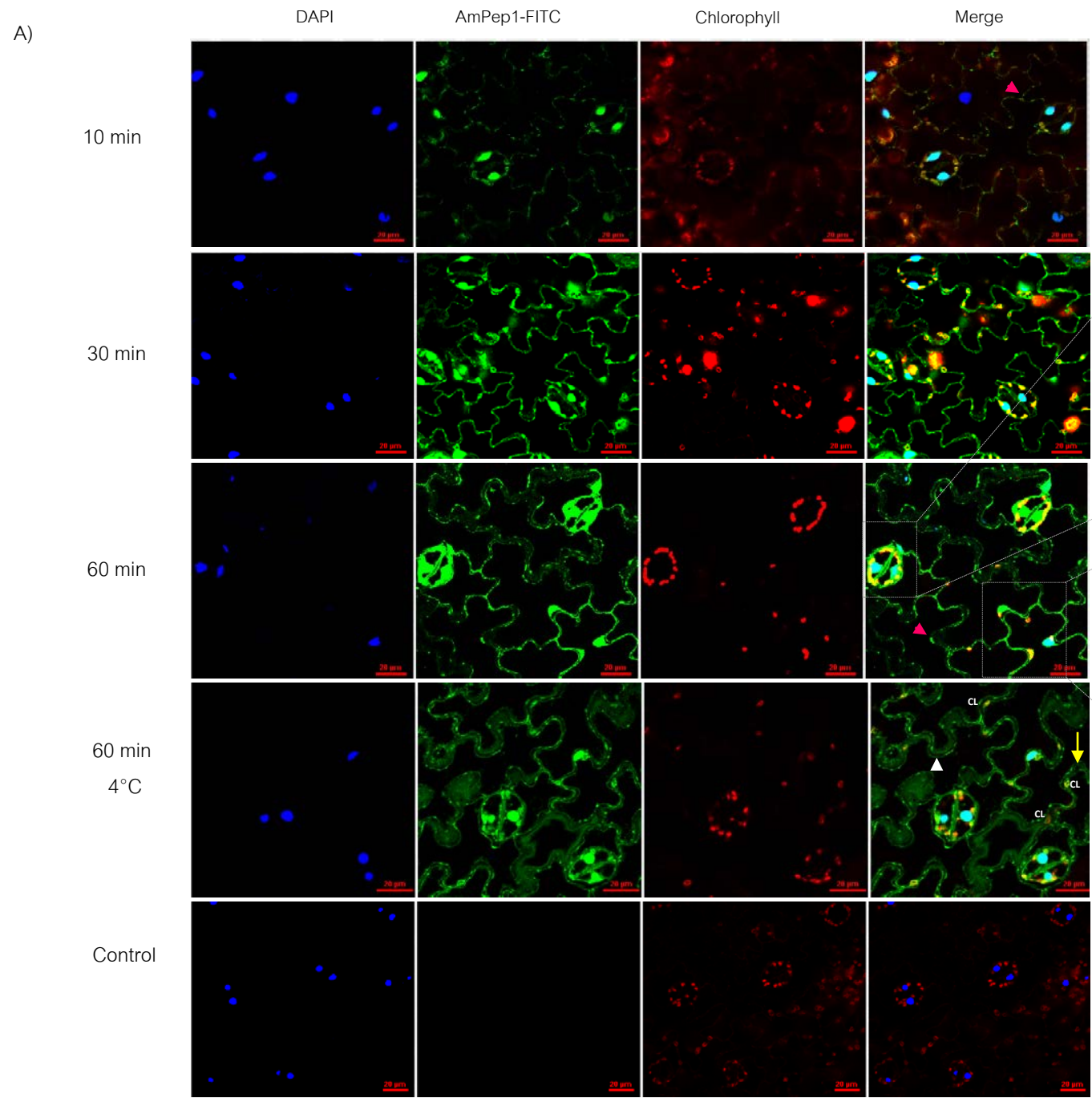


**Figure 5. Translocation of AmPep1 into *N. benthamiana* cells.**



## A Peptide Extract of Hydrolyzed Amaranth Globulin Induces Growth and Immunological Response in Tomato and Maize Plants

Mendoza-Figueroa José Silvestre<sup>1</sup>, Rivera-López Francisco Javier<sup>1</sup>,  
Luna-Romero Isaac Juan<sup>2</sup> and Soriano-García Manuel<sup>1,2</sup>

<sup>1</sup>Molecular Agrochemistry Group, Department of Chemistry of Biomacromolecules Chemistry, Chemistry Institute, Universidad Nacional Autónoma de México, Mexico.

<sup>2</sup>Plant Pathology Laboratory, Department of Microbiology, Escuela Nacional de Ciencias Biológicas, Instituto Politécnico Nacional, Mexico.

### **Authors' contributions**

*This work was carried out in collaboration between all authors. Authors MFJS and SGM designed the study performed, wrote the protocol, managed the literature searches and wrote the first draft and final of the manuscript. Authors MFJS and RLFJ carried out the experimental section. Author SGM managed to get financial funds for this research project. All authors read and approved the final manuscript.*

### **Article Information**

DOI: 10.9734/IJPSS/2017/37089

Editor(s):

(1) Surendra Singh Bargali, Department of Botany, DSB Campus, Kumaun University, Nainital, Uttarakhand, India.

Reviewers:

(1) Okereke Chukwu Nkumah, Ebonyi State University, Nigeria.

(2) Rebecca Yegon, University of Embu, Kenya.

Complete Peer review History: <http://www.sciencedomain.org/review-history/21759>

**Original Research Article**

**Received 30<sup>th</sup> September 2017**  
**Accepted 30<sup>th</sup> October 2017**  
**Published 6<sup>th</sup> November 2017**

### **ABSTRACT**

**Aims:** Evaluate the effect in growth and defense activation of a peptide extract from hydrolyzed globulin of Amaranth in tomato and maize plants.

**Study Design:** Using different concentration of peptides we evaluated the physiological effect of peptide extract from amaranth in two different commercial crops.

**Place and Duration of Study:** Department of Biomacromolecules Chemistry at the Chemistry Institute UNAM, and Plant Pathology Lab, Escuela Nacional de Ciencias Biológicas, UNAM, duration 1 year.

**Methodology:** For evaluating the effect of peptide extract from globulin (GPE), tomato seeds were germinated in different concentration of GPE (10, 1 and 0.1 mg/mL), 5 seed per treatment were

used, the effect of germination was observed for the length of epicotyl and stem development. Activation of plant innate immune response was tested using tomato leaf disc system (5 discs per treatment), tomato disc were exposed to 3 concentration of GPE, boiled bacteria *P. syringae* pv. tomato and plant defense activator BTH for 15 minutes and analyzed with histochemistry detection for ROS. ROS were also quantified in laves of tomato plants treated with GPE, boiled bacteria and BTH, ROS were detected with DMPO using electronic paramagnetic resonance. To evaluate the protective effect in other plants, leaf blight system with *Helminthosporium* sp. was used to know the effect of GPE against fungi infection.

**Results:** GPE showed an improvement of seedling development at the concentration of 1 mg/mL, while innate immune response was induced after 15 minutes with the concentration of 1 and 0.1 mg/mL of GPE. This result also matched with the observed protection assay in a model infection system of leaf blight, showing protection of several blight development at 0.1 mg/mL.

**Conclusions:** The peptides derived from hydrolyzed globulin of *Amaranthus hypochondriacus* induce promotion in growth and develop of tomato, also innate defense in tomato leaves and in maize against fungi infections.

*Keywords:* *Amaranthus hypochondriacus*; peptides; hydrolyzed globulin; induce promotion; growth and develop; tomato; maize; fungi infections.

## 1. INTRODUCTION

*Amaranthus hypochondriacus* is a Mexican plant that have been used since prehispanic times, the amaranth seed contains a large content of proteins compared with other Mexicans grain plants like maize, chia [1,2,3]. The total content of proteins is around 20%, globulins and albumins, represent approximately 48 and 20% respectively, in the total protein fraction [4,5]. Several reports described the nutraceutical activities of the amaranth proteins, and the derived digestion products of these proteins [6]. The main activity of amaranth protein sub-products is the anti-hypertensive function. the amaranth proteins are used mainly for nutraceutical approach, there are no reports about the use of amaranth proteins and sub-products in agricultural applications [6,7]. Peptides have showed to be an attractive crop protection agent in plant systems [8] inducing plant immunity [9], growth promotion [10], anti-viral [11], and anti-bacterial bioactivity [12], however, the synthesis of synthetic peptides entails high production cost. Transgenic plants overexpressing peptides are a good alternative for crop protection; nevertheless, the regulation of genetically modified organism has not a good opinion between populations, yet. Cereal and pseudo-cereal plants have a larger amount of proteins in the seeds comparing with other plant species, these proteins are able to be extracted in easy way with high yield extraction and also represent a good source of obtaining peptides with different bioactivities after digestion with enzymes. The variability in size and physicochemical properties of peptides can

increase the potential bioactivity [13]. In this work, we explored the potential agricultural application of a peptide extract derived from digested globulin of amaranth (*A. hypochondriacus*), evaluating the effect in germination and development in other to market Mexican tomato plant and also evaluating the capability to induce innate immune response for a potential use in crop protection.

## 2. MATERIALS AND METHODS

### 2.1 Geographical Study Area

The geographical localization of this experiment was carried out at University City, National Autonomous University of Mexico, UNAM in México City, longitude: 19.327531, latitude: -99.178831. In Mexico City, the huge capital of Mexico, the climate is subtropical, mild or pleasantly warm during the day, with cool nights in summer and cold nights in winter. In fact, the daily temperature range is remarkable, especially in the dry season with average temperature of 23.5°C.

### 2.2 Protein Extraction and Hydrolysis

*Amarantus hypocondriacus* seeds were ground, the powder was filtered in gauze to remove the fiber. The flour was defatted overnight at 4°C with n-hexane (1:10 w/v) in stirring, then centrifuged at 10000 rpm / 15 min, and the pellets were recovered and dried at room temperature. After that, the flour was suspended in water and the pH was adjusted to 8.5 with

NaOH 0.1 M (modified protocol Romero-Zepeda, H., & Paredes-Lopez) [14], and incubated overnight for extracting the soluble proteins at alkaline pH. The protein extract was then centrifuged at 10000 rpm/ 15 min to delete the starch and non-soluble proteins. The supernatant was recovered, and re adjusted the pH to 7.0 and used for enzymatic digestion. To know the extracted proteins in the supernatant, a SDS-PAGE was performed.

For hydrolysis, one litter of protein extract was mixed with papain (Sigma-Aldrich) in proportion 0.5 g/L and incubated for 15 hours at 37°C to control the hydrolysis activity avoiding the completely proteolysis of proteins. After the incubation time, peptide extract was fractioned in Amicon pressure system with a membrane of 10 KDa, fraction less than 10 KDa were collected and concentrated with cryo-concentration method [15]. C18 RP-HPLC was used to verify the peptide formation after hydrolysis.

### **2.3 Effect of Globulins Peptide Extract (GPE) in Germination of Tomato Seeds**

Tomato seeds commercial variety "Rio Grande" was supplied by the Universidad Autónoma Chapingo, Mexico, were disinfected with common sodium hypochlorite 3% for 5 minutes, and washing with sterile distilled water 3 times to remove the excess of disinfectant. For germination, we used a mix of vermiculite and commercial black soil for vegetables in a proportion 1:1 (w/w), the mix was autoclaved before use. The germination substrate was soaked in different treatments: 1) Water, 2) Commercial Hydroponic nutritive solution Hydro-sol (5:11:26; N:P:K, respectively), 3) GPE 10 mg/mL, 4) GPE 1 mg/mL and 5) GPE 0.1 mg/mL. Once the substrate was prepared, the seeds were seeded in the different treatment lots, 5 independent seeds per treatment. Then the plant germination system was incubated in dark until first signs of germination (emergence of epicotyl and cotyledon), at this time, the measurement of growth of the plant just started and the germination trays were then changed to a light/dark photoperiod (16 hours light/8 hours darkness). The growth and development of the plants were evaluated for next 15 days. The substrate was watered with testing solutions every 2 days during experimental time. The length of the tail or epicotyl in each treatment was used for comparing the effect between each experimental conditions.

### **2.4 Induction of Reactive Oxygen Species (ROS) Production in Tomato Leaves Mediated for GPE**

Tomato plants with 3 weeks-old were used to evaluate the ROS production mediated for GPE. Full expanded new leaves were used for preparing leaf disk around 10 mm of diameter. The leaf's discs were floated in sterile distilled water in dark conditions overnight, then, four treatments were used for study the ROS production: 1) Distillated water, 2) BTH 300 mg/L, 3) 10 mg/mL of GPE and 1 mg/mL of GPE, GPE solution and BTH were diluted in sterile distilled water, 5 leaf discs per treatment were used to evaluate the immune response, 100 µL of each solution were added on leaf discs for 15 minutes, after they were washed 3 times with sterile distilled water and staining for detection of peroxide and superoxide. Peroxide was detected with Diaminobenzidine (Sigma-Aldrich) and superoxide was detected with nitro tetrazolium blue, NTB (Sigma-Aldrich). The presence of brown precipitated or blue complex in the tissue is indicative of peroxide and superoxide production, respectively.

### **2.5 ROS Quantification Using Electron Paramagnetic Resonance**

In order to quantify the ROS production, we performed electron paramagnetic resonance (EPR) to quantify the peroxide and superoxide, in brief, we used leaves of the same plants mentioned in the above section, plants leaves were sprayed with the treatments until saturation: 1) Distillated water, 2) BTH 300 mg/L, 3) 10 mg/mL of GPE and 4) 1 mg/mL of GPE and 5) boiled suspension of bacteria *Pseudomonas syringae* pv. *Tomato*, D.O.600 nm=0.2, GPE solution, BTH and bacteria were diluted in sterile distilled water. 100 mg of leaf sample of each treatment were sampled at different times after spraying the experimental solutions, the samples were taken and immediately added 10 µL of DMPO (Sigma), and then ground fast in tissue lysis machine for 1 minute, after that, the ground material was transferred in a EPR cell. The sample was read in the EPR machine, Jeol JES TE-300 Xband, 100 KHz, and Modulation. The intensity of DMPO adducts coupled with the ROS radical was used for relative quantification of ROS production. The intensity signal of negative control (plants treated with water) was used for comparing the significant difference between treatments; Two-Way ANOVA was used for

comparing treatments between different groups. Data were analyzed in GraphPad Prism 6.0.

## 2.6 Protection Assay against Leaf Blight in Maize

A four week old new leaf of *Zea mays* from 5 different plants were used for experiment, 3 different leaf segments with 4 treated spots per leaf segment were used for each experimental condition. The experimental conditions were: Healthy control (treated with sterile water), infected control (treated with sterile water and infected with suspension of 120000 conidia/mL of *Helminthosporium* sp, BTH 300 mg/L infected with suspension of 120000 conidia/mL, GPE 1 mg/mL infected with suspension of 120000 conidia/mL and PGE 0.1 mg/mL with suspension of 120000 conidia/mL. For treatment, 50  $\mu$ L of sterile water for healthy and infected control, and 50  $\mu$ L of BTH and GPE solution all dissolved in sterile water were dropped in 4 equidistant points in each leaf segments, the testing solutions were allowed to absorb on the leaf for 2 hours. After this time, 10  $\mu$ L of conidia suspension of *Helminthosporium* sp. was inoculated in the treated spot. Leaves were incubated in humidity chamber, under photoperiod 16 hours light/8 hours darkness. The symptoms develop or hypersensitive reaction was monitored for 5 days.

## 3. RESULTS AND DISCUSSION

### 3.1 GPE Stimulates Growth in Tomato Seedlings

Seeds germinated in presence of GPE improves development of tomato seedlings inducing the increase in size, leaf development and size compared to seeds germinated in traditional water system (Fig. 1) It has been demonstrated that the commercial formulation "Trainer" that is composed of a vegetable protein digest, induces the rooting in tomato, as well as its elongation of the stem. Likewise, this commercial formulation induces elongation of coleoptile in maize, similar to the effect of some phytohormones, such as auxins [16]. In this work, it is possible to observe a correlated effect exerted by the GPE extract on tomato seedlings in the initial stages of development and that is also reflected until stages of foliar proliferation. At concentrations of 1 mg/mL of GPE, which is a lower concentration than that used with "Trainer", the size of the plant increases more than plants treated with nutritive

solution, an excess of peptide 10 mg/mL does not show a significant effect in growing compared with nutritive solution, but is notable compared to the treatments that were just treated with water (Fig. 1). The excess of peptide could be inducing intermolecular interaction between peptide that disturbs the function in the cell, the same effect was observed with maize seedlings treated with "Trainer", high concentrations of peptide digest product decreases the bio stimulating effect.

### 3.2 GPE Induces Activation of Innate Plant Response in Tomato Plants

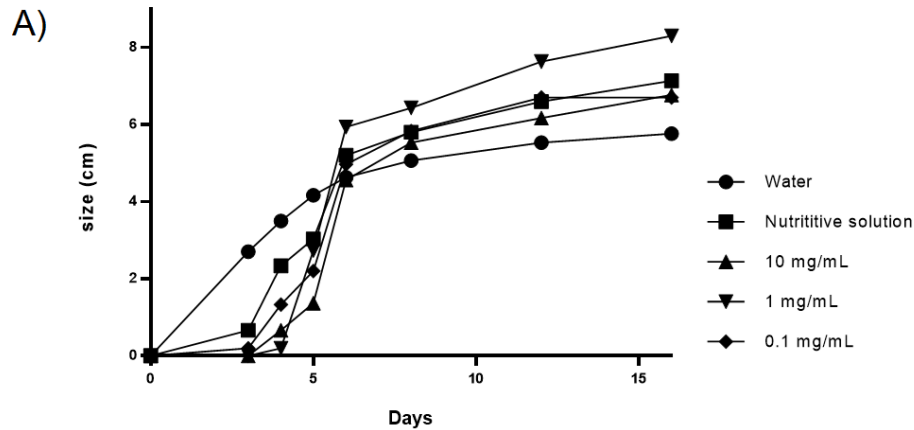
Several peptides derived of pathogen related proteins have been reported for be pathogen associated molecular patterns (PAMPs) to activate the innate defense response in plants. These peptides are short sequence, less than 10 KDa, for example the pathogen associated peptide flg22 and some peptides included in the family PROPEP, the initial response that these peptide produce is the induction of ROS production in apoplastic space [17], to generate an oxidative microenvironment to control the pathogens, with subsequent strong and more specific immunological pathways activation. This work shows that peptides extract from GPE can activate the ROS production in tomato leaves, specifically peroxide and superoxide, in Fig. 2a, tomato leaves produce peroxide (brown precipitate) and superoxide (blue precipitate) in apoplastic regions. That activity was also verified in a different plant, we used the model system plant *Arabidopsis thaliana* Col-0 to extrapolate the results to other species. *A. thaliana* also shows the production of superoxide (blue colored) after GPE exposition for 15 minutes (Fig. 2b). That response in both plants that agree with the time reported for ROS production after peptide like PAMP induction [9,17].

To quantify the oxygen radicals production, EPR was used, the results in Fig. 2c shows a significant increase of ROS response in plants treated with 0.1 mg/mL, the response of ROS production is even greater than that generated in plants treated with a boiled bacteria culture of *P. syringae* pv *tomato*. The response in ROS production shows a decrease after 2 hours, this result is indicating that ROS production is like those with tomato leaf discs in other experiment with tomato. In this experiment is included one commercial immune inductor, that is analogue of salicylic acid, this was acibenzolar-S-methyl, BTH (Actigard, Syngenta), this molecule as same salicylic acid, reduce the oxidative burst in the



first step of plant immune activation but make also after time can induce a lightly ROS production for increase the SA synthesis in the plant to increase the immune response, the results showed no significant difference between

water treated plant and plant treated with BTH in the first 15 minutes, however after 1.5 hour, the feedback response of ROS production increase lightly significant.

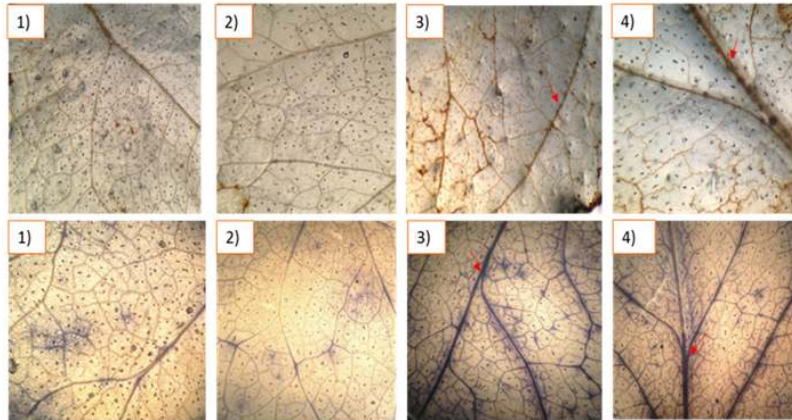


B)

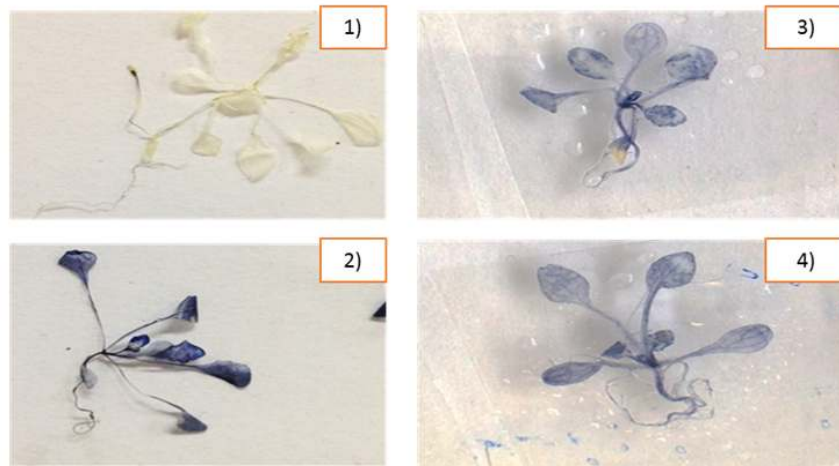


**Fig. 1. Amaranth GPE induces growth promotion in tomato seedlings. A) Effect of GPE on tomato seed germination under different solutions: Water, Nutritive solution Hydrosol®, GPE 10, 1 and 0.1 mg/mL, GPE at 1 mg/mL. B) Phenotypic effect of GPE in tomato “Rio Grande” at 15 days post germination in different conditions in substrate, substrated soaked with 1) water, 2) nutritive solution Hydrosol®, 3) GPE 10 mg/mL, 4) 1 mg/mL and 5) 0.1 mg/mL**

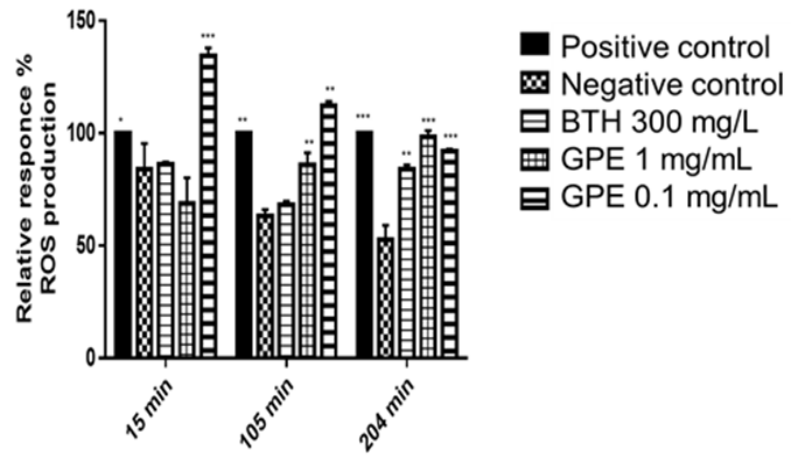
a)



b)



c)



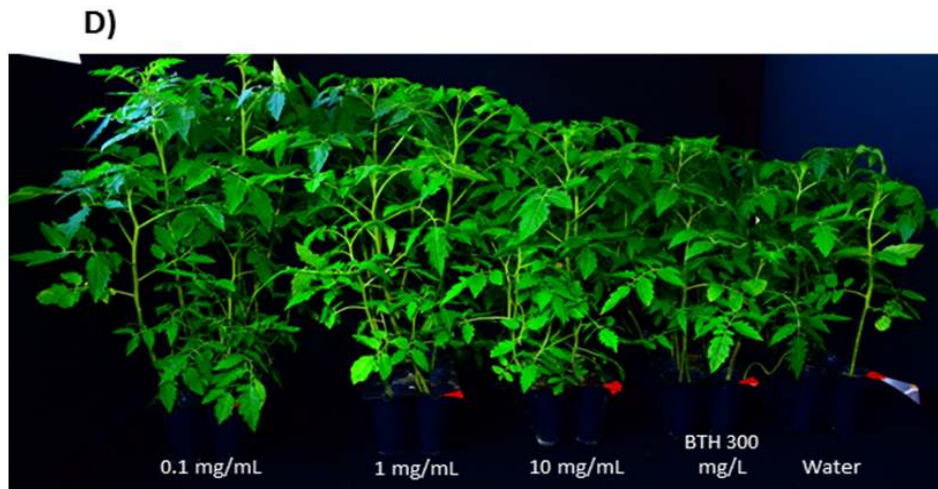


**Fig. 2. Activation of immune pathway in *Arabidopsis thaliana* col-0 and Tomato leaves with GPE. A) The innate immune response activation in tomato plant. ROS like H<sub>2</sub>O<sub>2</sub> (upper B panel) and O<sub>2</sub> (lower B panel) production was evaluated using Diaminobenzidine and NTB, respectively. 1) Distillated water, 2) BTH 300 mg/L, 3) 10 mg/mL of GPE in water and 4) 1 mg/mL of GPE in water. H<sub>2</sub>O<sub>2</sub> and O<sub>2</sub> production show a brown and blue precipitation, respectively. B) ROS production in *A. thaliana* col-0 seedlings with GPE, B.1) Distillated water, B.2) boiled bacteria suspension D.O 0.2, B.3) 1 mg/mL of GPE in water and B.4) 10 mg/mL of GPE in water. C) ROS quantification with Electronic paramagnetic resonance (EPR) in tomato leaves. The relative production response was normalized using the positive control like 100% of ROS signal in EPR. Error bars represent SD, asterisk indicate a significant difference according (P = 0.05). D) Phenotypic effect of GPE in tomato plants od 5 old-weeks, the GPE induce growth promotion comparing with other plant activator like BTH**

Plants treated with peptide and salicylic acid showed difference in phenotype after 15 days post treatment, salicylic acid and analogues are well known that are antagonist as some growth hormones, reducing size of plants, but at the same time inducing protection, this work shows that PGE induce related- innate defense molecules and also promotes plant growth, Fig. 2a, d.

### 3.3 GPE Induces Protection in Maize against Leaf Blight

The activation of immune response showed in tomato was also explored in Maize, with an infection model of leaf blight caused by *Helminthosporium* sp. This fungi strain was isolated from maize cultivation field in Tenango City, Estado de México, México, and characterized in research group of Professor Luna-Romero. GPE extract at concentration of 1 and 0.1 mg/ml induced protection of classic leaf blight development (Fig. 3) compared with the infected control pre-treated with water, these results matched with those observed in tomato

plants for ROS production, supporting our idea of protein extract might contain some peptides with similar sequence of pathogen peptide like-PAMP with capability to induce innate immune response, avoiding pathogen proliferation. However, unlike those MAMP-like peptides such as flg22, AtPep1 and their Pep1 / 2 homologs, the peptides present in GPE not only induce the appearance of molecules associated with immunity downstream of the MAMP recognition, but, in tomato plants, these peptides also showed a favorable effect on growth [18].

In *A. thaliana*, when one of the receptors for flg22 or AtPep1 has been mutated, the antagonistic effect of growth is slightly reversed [19]. In the findings reported in this work, it has shown that the GPE peptide extract induces not only immunological activation but also promotes growth, meaning that the peptides present in the extract may be partially recognized as MAMP or peptides associated with damage (DAMP) but not recognized by LRR-K receptors with high affinity or specificity as flg22 or Pep1 / 2 do [19,20].



**Fig. 3. GPE of amaranth induce protection in maize against leaf blight. Comparing GPE treatments versus infection control they decrease the characteristic leaf blight symptom (red arrow). Concentration on 1 mg/mL of GPE induces small response of hypersensitivity (white arrow) since one day after treatment**

It has been reported that some peptides of Glycine max from its precursor PROPEP, induce defense in these seedlings and growth induction after an exogenous application, activating genes for the synthesis of a nucleotide-binding site leucine-rich repeat protein (NBS-LRR), pectin methylesterase inhibitor (PMEI), Respiratory Burst Oxidase Protein D (RBOHD), indicating a transcriptional reprogramming, which generates not only defense, but also reprogramming in developmental genes [21]. The main possible mechanism of action of peptides presents in GPE could be homologues to this last argument. Analysis of peptide sequences presents in performing to know the similarity of GPE peptides with peptides from PROPEP precursors.

#### 4. CONCLUSION

The extract of peptides derived from the enzymatic digestion of amaranth globulins has a bio-stimulating effect in tomato plants by inducing growth and increase development in leaves at concentrations of 1 and 0.1 mg / mL, also this extract induces the production of immunological molecules such as ROS in tomato leaves. In maize the peptide extract reduces symptoms of blight caused by *Helminthosporium* sp.

#### ACKNOWLEDGEMENTS

We want to thank to M.Sc. Virginia Gómez Vidales for the EPR analysis, Chemistry Institute, UNAM. MFJS is a Ph. D. student from Programa de Doctorado en Ciencias Biomédicas UNAM, with a fellowship 363126 from CONACYT. RLFJ is an undergraduate student of Químico Farmacéutico Biólogo. Facultad de Química, UNAM.

#### COMPETING INTERESTS

Authors have declared that no competing interests exist.

#### REFERENCES

1. Venskutonis PR, Kraujalis P. Nutritional components of amaranth seeds and vegetables: A review on composition, properties, and uses. *Comprehensive Reviews in Food Science and Food Sciences*. 2013;12(4):381–412. Available:<http://doi.org/10.1111/1541-4337.12021>
2. Caselato-Sousa VM, Amaya-Farfán J. State of knowledge on amaranth grain.

- Journal of Food Sciences. 2012;77(4): R93–R104.  
Available:<http://doi.org/10.1111/j.1750-3841.2012.02645.x>
3. Duranti M, Gius C. Legume seeds: Protein content and nutritional value. *Field Crops Research*. 1997;53(1-3):31–45.  
Available:[http://doi.org/10.1016/S0378-4290\(97\)00021-X](http://doi.org/10.1016/S0378-4290(97)00021-X)
  4. Vasco Méndez NL, Soriano-Garcia M, Moreno A, Castellanos-Molina R, Paredes-López O. Purification, crystallization, and preliminary X-ray characterization of a 36 kDa amaranth globulin. *Journal of Agricultural and Food Chemistry*. 1999;47(3):862–66.  
Available:<http://doi.org/10.1021/jf9809131>
  5. Quiroga A, Martínez N, Rogniaux H, Geairon A, Añón MC. Globulin-p and 11S-globulin from *Amaranthus hypochondriacus*: Are two isoforms of the 11S-globulin. *Protein Journal*. 2009;28: 457–67.  
Available:<http://doi.org/10.1007/s10930-009-9214-z>
  6. Montoya-Rodríguez A, Gómez-Favela MA, Reyes-Moreno C, Milán-Carrillo J, González de Mejía E. Identification of bioactive peptide sequences from amaranth (*Amaranthus hypochondriacus*) seed proteins and their potential role in the prevention of chronic diseases. *Comprehensive Reviews in Food Science and Food Sciences*. 2015;14(2):139–158.  
DOI: 10.1111/1541-4337.12125
  7. Castellani OF, Martínez EN, Añón MC. Amaranth globulin structure modifications induced by enzymatic proteolysis. *Journal of Agricultural and Food Chemistry*. 2000;48(11):5624–29.  
Available:<http://doi.org/10.1021/jf000624o>
  8. Albert M. Peptides as triggers of plant defense. *Journal of Experimental Botany*. 2013;64(17):5269–79.  
Available:<https://doi.org/10.1093/jxb/ert275>
  9. Schilling JV, Schillheim B, Mahr S, Reufer Y, Sanjoyo S, Conrath U. Oxygen transfer rate identifies priming compounds in parsley cells. *BMC Plant Biology*. 2015;15(1):282-293.  
DOI: 10.1186/s12870-017-1095-2
  10. Yaginuma H, Hirakawa Y, Kondo Y, Ohashi-Ito K, Fukuda H. A novel function of TDIF-related peptides: Promotion of axillary bud formation. *Plant Cell Physiology*. 2011;52(8):1354–64.  
Available:<https://doi.org/10.1093/pcp/pcr081>
  11. Lopez-Ochoa L, Ramirez-Prado J, Hanley-Bowdoin L. Peptide aptamers that bind to a geminivirus replication protein interfere with viral replication in plant cells. *Journal of Virology*. 2006;80(12):5841–53.  
Available:<http://doi.org/10.1128/JVI.02698-05>
  12. Visser M, Stephan D, Jaynes JM, Burger JT. A transient expression assay for the *in planta* efficacy screening of an antimicrobial peptide against grapevine bacterial pathogens. *Letters of Applied Microbiology*. 2012;54(6):543–51.  
DOI: 10.1111/j.1472-765X.2012.03244.x
  13. Panchaud A, Affolter M, Kussmann M. Mass spectrometry for nutritional peptidomics: How to analyze food bioactives and their health effects. *Journal of Proteomics*. 2012;75(12):3546-59.  
Available:<http://dx.doi.org/10.1016/j.jprot.2011.12.022>
  14. Romero-Zepeda H, Paredes-Lopez O. Isolation and characterization of amarantin, the 11s amaranth seed globulin. *Journal of Food Biochemistry*. 1995;19(5):329–339.  
Available:<http://doi.org/10.1111/j.1745-4514.1995.tb00538.x>
  15. Virgen-Ortiz JJ, Ibarra-Junquera V, Osuna-Castro J, Escalante-Minakata P, Mancilla-Margalli N. Method to concentrate protein solutions based on dialysis-freezing-centrifugation: Enzyme applications. *Analytical Biochemistry*. 2012;426(1):4–12.  
Available:<http://doi.org/10.1016/j.ab.2012.03.019>
  16. Colla G, Roupheal Y, Canaguier R, Svecova E, Cardarelli M. Biostimulant action of a plant-derived protein hydrolysate produced through enzymatic hydrolysis. *Frontiers in Plant Science*. 2014;5:448-453.  
DOI: 10.3389/fpls.2014.00448
  17. Smith JM, Heese A. Rapid bioassay to measure early reactive oxygen species production in Arabidopsis leaf tissue in response to living *Pseudomonas syringae*. *Plant Methods*. 2014;10(6):6-14.  
Available:<https://doi.org/10.1186/1746-4811-10-6>
  18. Zipfel C. Combined roles of ethylene and endogenous peptides in regulating plant

- immunity and growth. Proc. Natl. Acad. Sci. 2013;110(15):5748–59.  
DOI: 10.1073/pnas.1302659110
19. Krol E, Mentzel T, Chinchilla D, Boller T, Felix G, Kemmerling B, Postel S, Arents M, Jeworutzk E, Al-Rasheid KAS, Becker D, Hedrich R. Perception of the Arabidopsis danger signal peptide 1 involves the pattern recognition receptor AtPEPR1 and its close homologue AtPEPR2. Journal of Biological. Chemistry. 2010;285(18):13471–13479.  
DOI: 10.1074/jbc.M109.097394
20. Yamada K, Yamashita-Yamada M, Hirase T, Fujiwara T, Tsuda K, Hiruma K, Saijo Y. Danger peptide receptor signaling in plants ensures basal immunity upon pathogen-induced depletion of BAK1. Eur. Mol. Biol. Organ. J. 2016;35(1):46–61.  
DOI: 10.15252/emboj.20159180
21. Lee MW, Huffaker A, Crippen D, Robbins RT, Goggin F. Plant elicitor peptides promote plant defenses against nematodes in soybean. Molecular Plant Pathology. 2017;1–12.  
DOI: 10.1111/mpp.12570

© 2017 Silvestre et al.; This is an Open Access article distributed under the terms of the Creative Commons Attribution License (<http://creativecommons.org/licenses/by/4.0>), which permits unrestricted use, distribution, and reproduction in any medium, provided the original work is properly cited.

*Peer-review history:*  
*The peer review history for this paper can be accessed here:*  
<http://sciencedomain.org/review-history/21759>

# Peptides and Peptidomics: A Tool with Potential in Control of Plant Viral Diseases

José Silvestre Mendoza-Figueroa<sup>1</sup>, Manuel Soriano-García<sup>1\*</sup>, Laura Beatriz Valle-Castillo<sup>2</sup>, Jesús Méndez-Lozano<sup>2</sup>

<sup>1</sup>Instituto de Química, Universidad Nacional Autónoma de México, Ciudad Universitaria, Coyoacán, Mexico City, Mexico

<sup>2</sup>Instituto Politécnico Nacional, CIIDIR Unidad Sinaloa, Guasave, Mexico

Email: \*[soriano@unam.mx](mailto:soriano@unam.mx)

Received 25 April 2014; revised 28 May 2014; accepted 2 July 2014

Copyright © 2014 by authors and Scientific Research Publishing Inc.

This work is licensed under the Creative Commons Attribution International License (CC BY).

<http://creativecommons.org/licenses/by/4.0/>



Open Access

---

## Abstract

Plant viruses are the most infectious agents in commercially important crops worldwide. Plant viral diseases are important because both decreased yielding and quality of fruits, flowers or vegetables lead to million-dollar losses in production. At present there are no reports which suggest a direct control of plant virus. A new strategy for plant virus control has been raised since 13 years ago—the use of peptides. Peptides could offer a direct interaction by affinity selection against viral proteins involved in infection cycle, like capsid or movement protein (e.g.) and affect viral replication. Peptidomics, as a new tool to study peptides, led us screening and selecting the best peptide with antiviral activity, and re-designing it to enhance the biological effect as well as the potential of bioactivity of those peptides secreted by microbes present in soil. In this paper we review current aspects in the use of peptides and peptidomics as a strategy to study new methods that lead a direct control against plant viral diseases.

## Keywords

Peptidomics, Plant Virus, Peptides, Peptaiboles, Mass Spectrometry, Aptamers

---

## 1. Introduction

Plant diseases are known since men started cropping in ancient times, but concepts about them have been passed through large and continued evolutionary process change in more than 20 centuries. Greeks philosophers as Teofrasto, talked about disease in cultures and they supposed possible origin and some treatments [1]. Commer-

---

\*Corresponding author.

cially important crops such as vegetables, ornamental plants, grasses and cereals are not free to get infections which decrease their yielding and production. One of the main etiologies in plant diseases is caused by viruses; these agents are responsible for high lost in yielding and quality in crops worldwide. These losses are variable year to year, and have been in function of weather, crop management, chemical and cultural control of vectors (insects) and weeds, and in some case reached 100% losses [2].

Pathogens plant viruses are small pathogens and depend on the replication host machinery to replicate and generate progeny [3]. Plant viruses are classified based on features of nomenclature and taxonomy described by International Committee for Taxonomy of Viruses (ICTV) [4]. Currently, there are 2828 species of plant viruses that belong to 455 genera [5].

Last report by MicrobiologyBytes in collaboration with the Molecular Plant Pathology Association described the “Top Ten” of plant virus and highlighted those viruses with more importance in point of view of scientist or economy interest; this ranking is described in **Table 1**.

Frequency of these infections has been increased in most agricultural areas worldwide, pointing the theme of the more important affection in crops. To get control in any disease, it is relevant to know the etiological agent based on identification through miscellaneous laboratory methods, which leads us searching for handling and control of disease. Accurate diagnosis of the viral agent is a determinate factor in developing control alternatives [6].

A strategy to control plant virus is the use of plant resistance genes (R) to viral infection, natural or modified by genetic engineering. If there are R genes over expressed in natural way, these could come into other cultures by techniques like conventional breeding. Although genetic engineering offers unlimited chances to get virus-resistance crops, its application to large scale has generated disgust for researches, government and people [3]. Genetics treatments, based on the use of resistant strains, seem ideal to control these disease, as option to decrease use of pesticides in crops. But, many kinds of reactions can be observed in a short or large time; partial resistance, tolerance and immunity to disease, are some examples. Two alternatives are proposed along this review to get news strategies in plant virus control: 1) the use of arbuscular mycorrhizal fungi, considered as a natural defense in plant besides enhancing yield and resistance [7]; 2) the use of small molecules such as peptides with high specificity to viral target, and block in direct way of the process of replication or viral assembly.

The aim of this review is to collect and disclose current strategies to develop plant viral control using peptides, based on techniques of peptidomics like tool for developing studies of direct molecule-molecule interaction.

**Table 1.** Ranking with principal plant virus in regard to scientist and economy effect (data from MicrobiologyBytes).

Specie	Genus	Host range
<i>Tobacco mosaic virus (TMV)</i>	<i>Tobamovirus</i>	Tobacco, tomato, and other <i>Solanaceae</i>
<i>Tomato spotted wilt virus (TSWV)</i>	<i>Tospovirus</i>	Over 1000 species in 85 families, including many vegetables, peanuts and tobacco
<i>Tomato yellow leaf curl virus (TYLCV)</i>	<i>Begomovirus</i>	Mostly tomato and other <i>Solanaceae</i>
<i>Cucumber mosaic virus (CMV)</i>	<i>Cucumovirus</i>	Cucumbers, squash, melons, peppers, beans, tomatoes, carrots, celery, lettuce, spinach, various weeds and many ornamental plants
<i>Potato virus Y (PVY)</i>	<i>Potyvirus</i>	Important crops such as pepper, potato, tobacco, tomato, some ornamental plants and many weeds.
<i>Cauliflower mosaic virus (CaMV)</i>	<i>Caulimovirus</i>	<i>Arabidopsis thaliana</i> , <i>Brassica</i> spp., <i>Raphanus</i> spp. and other species of <i>Brassicaceae</i> and <i>Resedaceae</i>
<i>African cassava mosaic virus (ACMV)</i>	<i>Begomovirus</i>	<i>Cassava</i> , <i>Nicotiana</i> and <i>Datura</i>
<i>Plum pox virus (PPV)</i>	<i>Potyvirus</i>	Stone fruits including peaches, apricots, plums, nectarines, almonds and sweet and sour cherries
<i>Brome mosaic virus (BMV)</i>	<i>Bromovirus</i>	Mainly monocots such as barley and others in the grass family
<i>Potato virus X (PVX)</i>	<i>Potexvirus</i>	Potato and other <i>Solanaceae</i>



## 2. Peptidomics a Tool for Plant Virus Control

### 2.1. Bioactive Peptide Libraries

Several strategies had been described to get peptides in function microbial agent's control, between them, peptides with target to bacterial membrane [8] or antifungal activity [9]. In some cases those molecules had gotten from specificity selection assays based in directly interaction between molecules as well as modification of bioactive peptides and *de novo* design reported previously in data base like PhytAMP [10]-[13], using combinatory chemistry and computational chemistry like tools to enhance the antimicrobial activity and develop and chose new peptides with a best biological activity [10]. Because, plant virus are particles formed of proteins like capsid (CP), nucleoproteins (N) and movement proteins (MP), we may think in the possibility to produced synthetic peptides or peptides derivate from hydrolysis of big proteins, which target, based via interaction peptide-viral protein or peptide-viral peptide assays, and propose the potential biological effect based on this interaction affinity system [12]. Those studies can use peptide libraries derivate of protein hydrolysis from plants or functional foods like casein (e.g.) [14]. Peptides libraries from plant proteins with antiviral activity is not explorer option yet, but peptides libraries from casein derivate has demonstrated that are able to decrease infection and symptoms in farms of salmons for IHNV (*Infectious hematopoietic necrosis virus*) [15]. Thus, a peptide derivate from FGF (Fibroblast Growth Factor) showed antiviral activity against an influenza virus (H5N1) [16]. Thus, we propose that peptides from protein plant hydrolysis could be a possible way to get peptide libraries with possible anti plant virus activities.

The biopanning assay (selection through interaction) is performed fixing the target molecule (viral protein or viral peptide, viral antigens) on a solid surface; it could be performed in solution (like immunoprecipitation). The peptide libraries, either synthetics, derivate from protein hydrolysis or phagepeptides, after, they will be add onto viral antigen fixed on the surface of reaction system (microplate e.g.), with the aim to let a random molecular interaction, in this way, only peptides with the best affinity to target, will allow interacting. The interaction time and incubation condition for this assay is at least 30 minutes to 1 hour in room temperature [12] [16]-[18]. After incubation time, is necessary to remove the peptides which did not interact or did not bind to the target. Binding peptides are eluted (if we performed the beads to collect the complex peptide-target, likewise immunoprecipitation). Eluted peptides should be analyzed using electrophoresis methods like Two-Dimensional gels (2D gels), or purified using chromatographic methods [12]. 2D gels allow separating in two parameters the complex mix or analyzed pure peptides or proteins, these parameters are 1) mass (Molecular Weight, MW) and 2) charge. Each band in the gel represent a peptide in the mix with itself features such as mass and charge. We could remove each band and confirm the MW by Mass Spectrometry (MS) method. Furthermore, MS can confirm whether peptide contain an S-S bond. In the study of peptides via MS, principal ionization method is MALDI and analyzed with TOF [12] [19]-[21]. MALDI (Matrix Assisted Laser Disruption Ionization) as well as ESI (Electro Spray Ionization) there are soft ionization non-molecule destructive methods, which let know the properties of peptides and proteins such as MW, pure, and S-S association [22] [23]. The MALDI-TOF MS, is a tool to know the MW of peptide selected against target. We could purified the mix of peptides in HPLC (these kind of peptides are not susceptible to degradation in high pressure indeed there are linear, small circular in Phagepeptides (no more 15 amino acids) or derivate from hydrolysis) coupled ESI MS/MS to get purified peptide and know the MW. Furthermore, we could know sequence *de novo* via trypsin digestion of each purified peptide or band in 2D gel, using CID MS/MS or get the fingerprint MALDI TOF/TOF [23]. We could analyze and purified via LC MS, the mix of selected peptides without passing 2D gels like shows in the general process in **Figure 1**.

Once peptides sequences are known, the follow interest is to generate a 3D structure model of the peptide, this approach, will let us theoretical studies of the interaction dynamics of peptide-target and know the docking energy of the system in this interaction. These studies will help us to re-select peptides with the best probability of biological activity [10]. 3D peptide structure is performed by Molecular mechanics or Markov alphabet, first model is a singular mechanics balls-spring system using the real conformation state of the atoms in the peptide [24] [25]. Markov alphabet is a alternative to propose a peptide structure using software which are based in modeling by comparison of the original peptide sequence with a algorithm structural alphabet formed by 27 structural letters [26]. There are software's like PEP-FOLD who modeling peptides with this method (<http://bioserv.rpbs.univ-paris-diderot.fr/PEP-FOLD/>). Spectroscopic techniques like NMR is the way to know the real 3D structure of the peptide, lineal or cyclic [20]. Last method above mentioned, allows get more information about theoretical interactions between two molecules and predicts bioactivity for example in peptides.

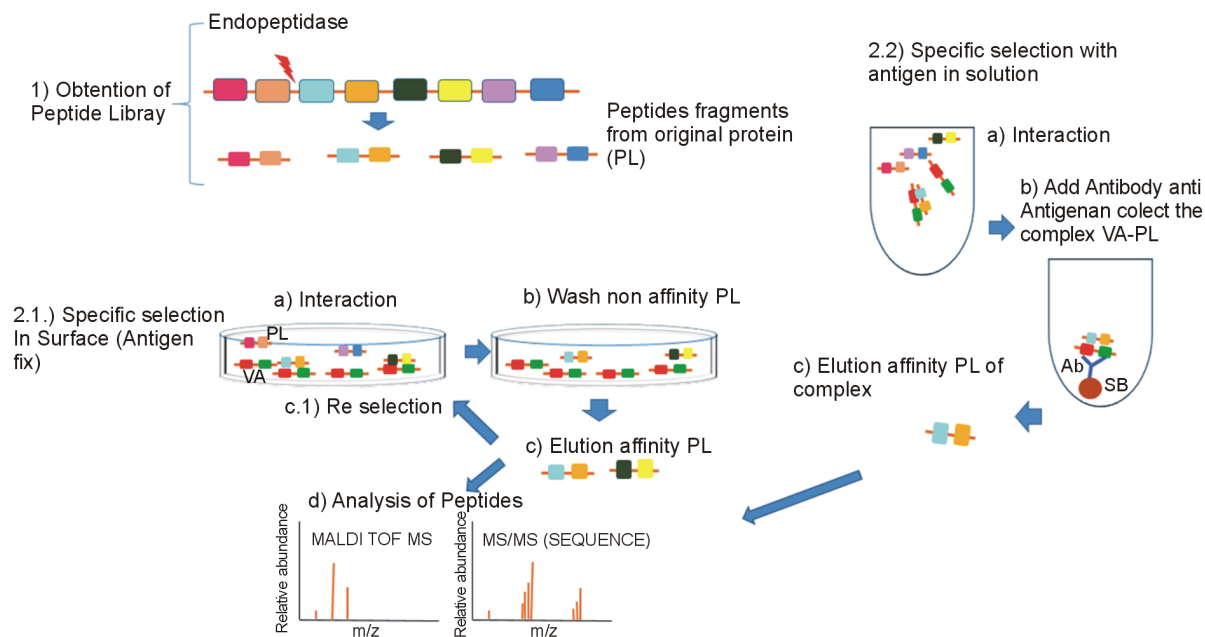


**Figure 1.** Process which described a general method to get peptide library derived from proteins and process to select peptides by biopanning assay, in surface and solution model. 1) Obtaining peptides from purified proteins using endopeptidases. 2.1) Peptides then are selected versus an antigen fixed to solid surface or 2.2) Peptides are selected in solution (the antigen is soluble in buffer), specific peptides (that bind to antigen) are recovered by wash with disruption buffer or by Antibodies (Ab) anti-viral antigen, respectively. Then is necessary elute those peptides from antigens and analyze pure of peptides by MS. PL: Pep-tide Library, VA: Viral Antigen, Ab: Antibody, SB: Sepharose Beads.

## 2.2. Evaluation of Antiviral Bioactivity in Plants

Before evaluation of antiviral bioactivity of peptides is required to know the cytotoxicity activity in the plant, we can perform it experiment in protoplast model [10] with the aim to find the optimum peptide concentration (purified peptide or mix peptides) which are not interfere with plant growth. Starting nontoxic minimum concentration (NTC), add peptides to test viral infection model to find the minimum inhibitory concentration against the viral agent (MIC) [10]. We can choose the best activity and drive and match the biological activity with theoretical biochemical studies of the peptide, like chemistry structure.

Above, we highlight the importance to find bioactive peptides in libraries of plant protein hydrolyzed, therefore, this requires of the selection specificity biopannings techniques in order to get the best peptide against virus. If we think get peptides derivate from this kind of libraries, the more logical is that those peptides are supplied via sprayed [27] or add to substrate in this case maybe those peptides become inducers of resistance genes (R) [27] [28]. To achieve this treatment, we need to know the features of viral pathogenicity, since methods like sprayed could be more efficient in virus with replication and progeny develops in areas as mesophyll in leaves in genera like *Cilevirus*, *Tobravirus*, *Tospovirus* [29]-[31] (see **Table 2**). In first proposal, arise the idea that peptides introduce to mesophyll of leaves through hydathodes and stomata, crossing cell wall and membrane, indeed we may think the chemistry composition of the peptides should contain some hydrophobic residues to cross the membrane and arrive to cytoplasm (the hydrophobicity of a peptide is not 100%, because some peptide molecules could acts in cytoplasm that is aqueous area), another idea is that some peptides can bind to DNA or RNA [11] if previously it were selected versus these targets.

Protection against systemic virus replication can propose in addition of peptides to substrate, in this way the peptides could be absorbed by plant and arrive to infection sites in phloem, e.g. and finally be elicitors of R genes [28]. Those peptides may generate Systemic Induce Resistance (SIR) and turn on some pathways in the plant itself such as the case of salicylic acid [32] [33] or turn on PR synthesis proteins likewise systemic inducers such as BTH (Benzothiadiazole) in geminivirus infections [34], induce turn on of ethylene factor, which induce Programmed Cell Death (PCD) in response TYLCV infections [35] [36]. The treatment proposes could be useful to virus which conducted Long-Distance-Movement (LDM), replication in Sieve Elements (SE) [37] [38], for example *Begomovirus*, *Closterovirus*, *Cucumovirus*, *Tobamovirus* [30] (see **Table 2**, **Figure 3**).

**Table 2.** Summary principal importance virus's which produce local infections (superficial in leaves and roots) and systemic infection (sieve elements).

Replication Site	Genera	Virus
Superficial (Leaves, Roots)	<i>Cilevirus</i> <i>Tobravirus</i> <i>Tospovirus</i>	CiLV-Ci ( <i>Citrus leprosis virus</i> —Citplasmic), TRV ( <i>Tobacco rattle virus</i> ), PepRSV ( <i>Pepper ringspot virus</i> ), INSV ( <i>Impatiens necrotic spot virus</i> )
Phloem (SE)	<i>Begomovirus</i> <i>Cucumovirus</i> <i>Closterovirus</i> <i>Tobamovirus</i>	TYLCV ( <i>Tomato yellow leaf curl virus</i> ), CMV ( <i>Cucurbit mosaic virus</i> ), CTV ( <i>Citrus tristeza virus</i> ), TMV ( <i>Tobacco mosaic virus</i> ), ToMV ( <i>Tomato mosaic virus</i> )

### 3. *In Vivo* Selection of Peptides Libraries against Viral Proteins

In regard to get treatments against systemic viral replication, some strategies had been developed; The form to achieve this aim, is through in plant synthesis of peptides (transgenic plants) derivate from antigenic regions of viral proteins such as CP, MP and Rep [31], in this way, plant will turn on the immune system response against virus, like MAMP's trigger immunity [32] [39]. Another way to achieve this goal is to develop a screening in live system of peptide libraries which interacts and bind with some viral target, commonly using a yeast system (yeast two-hybrid interaction assay [40]-[42]). The basis for this technique is induce the direct interaction through peptide target (viral target) attachment region to DNA (DBD, DNA binding domain) in promoter of reporter selection gen, with, different peptides attachments (each peptide in a plasmid) to AD (Activation Domain in RNA polymerase binding site). In normal conditions this regions interacts and their interaction becomes to up-stream transcription of the gene, see [Figure 2](#). This fact, was used as basis of the method for adding peptides from a libraries to AD region and the targets or viral target in the DBD region, if both sequences are able to interact, these will conduce to closer the DBD and AD regions to drive transcription of the reporter gene. The transcription of reporter gene, leads up to believe that both sequence, target and peptide, are able to bind and is possible to use like bioactive peptide against target, this kind of peptides are called peptides aptamers [43]. The select peptides are after cloning in plants (transgenic plants).

Reports on peptides aptamers with antiviral activity are based in the interaction of peptides derivates of common binding microdomain in N protein of *Tospovirus* (TSWV, TCSV, GRSV, INSV and SYSV) as peptides targets, and a library of peptides derivates from other places in N protein of *Tospovirus*. Results show antiviral activity in *Nicotiana benthamiana* transgenic plants, peptides that closers interaction, decrease symptoms and viral RNA [42].

In case of systemic virus, some more important: geminivirus (TYLCV, TGMV), there are reports with peptide aptamers libraries with target to initiator replication proteins (AL1) [40] and Rep [41], these proteins are significant because are essential to starting replication in several virus [44]. Both reports show that using a *N. benthamiana* transgenic model, containing aptamers peptides with previously screening in YTH, decrease the symptom and DNA level (see [Figure 3](#)).

Once established the peptides aptamers library with best biological activity, we can carry out computational studies to confirm the biological dynamics of peptide and suggest modification to enhance the antiviral activity. These kinds of peptides are able to control localized and systemic virus infection in plants like above mention. Although the system is required in transgenic plants, there are not more studies in which peptides aptamers shows disturb plant metabolism. Results with experimental crop field studies are not reported, yet.

### 4. Antiviral Plant Peptides from Plant-Microbe Interactions

The best nutritional source in plant is the soil. Is also source of pathogen microbe as fungi, bacterial, nematodes and virus. However, there are some microbe groups which are associated with plant roots or live near plant, this sometimes is an advantage in plant because this microbe group yield antimicrobial compounds against plant pathogens. Especially in plant virus, had been described bacteria such as *Pseudomonas chlororaphis* O6 and fungus as *Trichodermapseudokoningii* SMP2, *Spedonium* (*Apiocrea*, sexual phase), *Boletus* sp. [20] [27] [28] [45]. Their populations of these microbes are principally in soil, and can relate with plants [46] [47]. They produce peptides, with difference in generic pathway, and structural, and they plays in Systemic Induced Resistance (SIR), allowing the antiviral response.

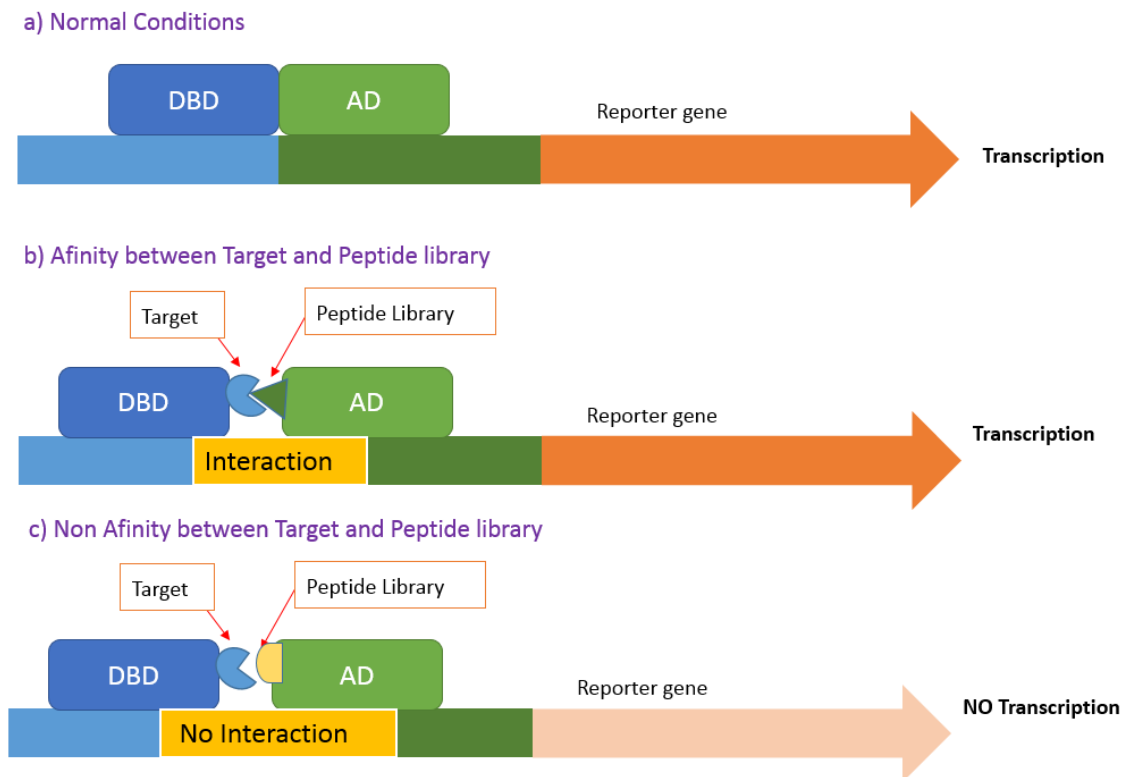


**Figure 2.** Yeast two-hybrid interaction assay. In normal conditions DBD region and AD are closer to let transcription of gen (a); If viral target coupled to DBD region and peptide from libraries coupled to AD region are able to binding, they closer interaction of DBD-AD and let the transcription of reporter gene (b); If not affinity between target and peptide from library the closer of DBD and AD does not occur, and does not transcription of reporter gene (c). DBD: DNA binding domain, AD: Activation domain.

Experiments shows inoculated plants with *P. chlororaphis* O6 enable the plant develop resistance against *Cucumber mosaic virus* (CMV) in *Nicotianatabaccum* [48]. Subsequently Park Y.J. and collaborators, 2012 performed a resistance model with *P. chlororaphis* O6 in tobacco plants infected with TMV, the goal of these experiments were the purification of the active compound which induce SIR against TMV, researchers found in aqueous extract a cyclic peptide, this molecule consist by 7 amino acids and was analyzed by ESI-Q-TOF MS and NMR to structural studies. Pure peptide called "Peptamine" was assayed in tobacco plants TMV infected, peptide was add to plant through spray on the leaves, results showed antiviral activity likewise model only *P. chlororaphis* in substrate [20].

There are other peptide group comprise by non-proteinogenic amino acids called Peptaibols, they are formed with N terminal with acetylation and C terminal amino alcohol, the principal amino acids are  $\alpha$ -aminoisobutyric (Aib) and Isovaline (Iva). Biological activity has broad spectrum against gram positive bacteria, and fungal [49]. However there are 3 kind of peptaibols with antiviral activity in plants such as 1) Chryospermins B and D, its produced *Apiocrea Chrysoperma* [45]. 2) Peptavirins A and B, them produced by *Spedonium* (*Apiocreasp* 14T). Both groups of pure peptaibols have showed resistance against TMV in tobacco plants [27]. 3) Trichokonins, produced in *Trichoderma pseudokoningii* SMP2, were purified and tested in tobacco plants infected with TMV, this peptaibol induced the SIR and decrease severe virus infection in concentration of 100 nM, it was showing decrease of 60% in viral RNA, as well as decline in symptoms severity. Other important date in the experiment is the test of Reactive Oxygen Species (ROS) production such as  $H_2O_2$  and  $O_2^-$  and phenolic compounds showed enhanced the production as well as the ROS enzymes in tobacco leaves; these dates suggest that peptaibols are peptides which acts like SIR elicitors [28], see **Figure 3**.

## 5. Conclusion

In our vision of peptidomics, all these peptides mentioned could be a new frontier to search and design new



- Symbiosis Attenuates Symptom Severity and Reduces Virus Concentration in Tomato Infected by Tomato Yellow Leaf Curl Sardinia Virus (TYLCSV). *Mycorrhiza*, **24**, 179-186. <http://dx.doi.org/10.1007/s00572-013-0527-6>
- [8] Mandal, S.M., Migliolo, L. and Franco, O.L. (2012) The Use of MALDI-TOF-MS and *in Silico* Studies for Determination of Antimicrobial Peptides' Affinity to Bacterial Cells. *Journal of the American Society for Mass Spectrometry*, **23**, 1939-1948. <http://dx.doi.org/10.1007/s13361-012-0453-4>
- [9] Rivillas-Acevedo, L.A. and Soriano-García, M. (2007) Isolation and Biochemical Characterization of an Antifungal Peptide from *Amaranthus hypochondriacus* Seeds. *Journal of Agricultural and Food Chemistry*, **55**, 10156-10161. <http://dx.doi.org/10.1021/jf072069x>
- [10] Zeitler, B., Herrera Diaz, A., Dangel, A., Thellmann, M., Meyer, H., *et al.* (2013) De-Novo Design of Antimicrobial Peptides for Plant Protection. *PLoS ONE*, **8**, e71687. <http://dx.doi.org/10.1371/journal.pone.0071687>
- [11] López-García, B., San Segundo, B. and Coca, M. (2012) Antimicrobial Peptides as a Promising Alternative for Plant Disease Protection. *Small Wonders: Peptides for Disease Control*, 263-294.
- [12] Kool, J., Jonker, N., Irth, H. and Niessen, W.M. (2011) Studying Protein-Protein Affinity and Immobilized Ligand-Protein Affinity Interactions Using MS-Based Methods. *Analytical and Bioanalytical Chemistry*, **401**, 1109-1125. <http://dx.doi.org/10.1007/s00216-011-5207-9>
- [13] Mooney, C., Haslam, N.J., Pollastri, G. and Shields, D.C. (2012) Towards the Improved Discovery and Design of Functional Peptides: Common Features of Diverse Classes Permit Generalized Prediction of Bioactivity. *PLoS ONE*, **7**, e45012. <http://dx.doi.org/10.1371/journal.pone.0045012>
- [14] Phelan, M., Aherne, A., Richard, J., FitzGerald, R.J. and O'Brien, N.M. (2009) Casein-Derived Bioactive Peptides: Biological Effects, Industrial Uses, Safety Aspects and Regulatory Status. *International Dairy Journal*, **193**, 643-654. <http://dx.doi.org/10.1016/j.idairyj.2009.06.001>
- [15] Rodríguez Saint-Jean, S., De las Heras, A., Carrillo, W., Recio, I., Ortiz-Delgado, J.B., Ramos, M., Gomez-Ruiz, J.A., Sarasquete, C. and Pérez-Prieto, S.I. (2013) Antiviral Activity of Casein and  $\alpha_2$  Casein Hydrolysates against the Infectious Haematopoietic Necrosis Virus, a Rhabdovirus from Salmonid Fish. *Journal of Fish Diseases*, **36**, 467-481. <http://dx.doi.org/10.1111/j.1365-2761.2012.01448.x>
- [16] Jones, J.C., Elizabeth, A., Turpin, E.A., Bultmann, H., Curtis, R., Brandt, C.R. and Schultz-Cherry, S. (2006) Inhibition of Influenza Virus Infection by a Novel Antiviral Peptide That Targets Viral Attachment to Cells. *Journal of Virology*, **80**, 11960-11967. <http://dx.doi.org/10.1128/JVI.01678-06>
- [17] Arap, M.A. (2005) Phage Display Technology—Applications and Innovations. *Genetics and Molecular Biology*, **28**, 1-9. <http://dx.doi.org/10.1590/S1415-47572005000100001>
- [18] Foster, G., Johansen, E., Hong, Y. and Nagy, P. (2008) Plant Viral Protocols. 2nd Edition, Human Press, New York. <http://dx.doi.org/10.1007/978-1-59745-102-4>
- [19] Panchaud, A., Affolter, M. and Kussmann, M. (2012) Mass Spectrometry for Nutritional Peptidomics: How to Analyze Food Bioactives and Their Health Effects. *Journal of Proteomics*, **75**, 3546-3559. <http://dx.doi.org/10.1016/j.jprot.2011.12.022>
- [20] Park, J.Y., Yang, S.Y., Kim, Y.C., Dang, Q.L., Kim, J.J. and Kim, I.S. (2012) Antiviral Peptide from *Pseudomonas chlororaphis* O6 against Tobacco Mosaic Virus (TMV). *Journal of the Korean Society for Applied Biological Chemistry*, **55**, 89-94. <http://dx.doi.org/10.1007/s13765-012-0015-2>
- [21] Liao, Y., Alvarado, R., Phinney, B. and Lönnnerdal, B. (2011) Proteomic Characterization of Specific Minor Proteins in the Human Milk Casein Fraction. *Journal of Proteome Research*, **10**, 5409-5415.
- [22] Kathleen, L., Wei, J. and Siuzdak, G. (2006) Matrix-Assisted Laser Desorption/Ionization Mass Spectrometry in Peptide and Protein Analysis. In: Meyers, R.A., Ed., *Peptides and Proteins, Encyclopedia of Analytical Chemistry*, 5880-5894.
- [23] Seidler, J., Zinn, N., Boehm, M.E. and Lehmann, W.D. (2010) *De Novo* Sequencing of Peptides by MS/MS. *Proteomics*, **10**, 634-649. <http://dx.doi.org/10.1002/pmic.200900459>
- [24] Schlick, T. (2010) Molecular Modeling and Simulation. An Interdisciplinary Guide. 2nd Edition, Springer, Berlin. <http://dx.doi.org/10.1007/978-1-4419-6351-2>
- [25] Cramer, C.J. (2004) Essential of Computational Chemistry. Theories and Models. 2nd Edition, Wiley, Hoboken.
- [26] Camproux, A.C. and Tufféry, P. (2005) Hidden Markov Model-Derived Structural Alphabet for Proteins: The Learning of Protein Local Shapes Captures Sequence Specificity. *Biochimica et Biophysica Acta*, **1724**, 394-403. <http://dx.doi.org/10.1016/j.bbagen.2005.05.019>
- [27] Yeo, W.H., Yun, B.S., Kim, Y.S., Lee, S.J., Yoo, I.D., Kim, K.S., Park, E.K., Lee, J.C. and Kim, Y.H. (2002) Antiviral, Antimicrobial, and Cytotoxic Properties of Peptavirins A and B Produced by *Apiocrea* sp. 14T. *The Plant Pathology Journal*, **18**, 18-22. <http://dx.doi.org/10.5423/PPJ.2002.18.1.018>

- [28] Luo, Y., Zhang, D.D., Dong, X.W., Zhao, P.B., Chen, L.L., Song, X.Y., Wang, X.J., Chen, X.L., Shi, M. and Zhang, Y.Z. (2010) Antimicrobial Peptaibols Induce Defense Responses and Systemic Resistance in Tobacco against Tobacco Mosaic Virus. *FEMS Microbiology Letters*, **313**, 120-126. <http://dx.doi.org/10.1111/j.1574-6968.2010.02135.x>
- [29] Locali-Fabris, E.C., Freitas-Astúa, J., Souza, A.A., Takita, M.A., Astúa-Monge, G., Antonioli-Luizon, R., Rodrigues, V., Targon, M.L. and Machado, M.A. (2006) Complete Nucleotide Sequence, Genomic Organization and Phylogenetic Analysis of Citrus Leprosis Virus Cytoplasmic Type. *Journal of General Virology*, **87**, 2721-2199. <http://dx.doi.org/10.1099/vir.0.82038-0>
- [30] Manhy, B.W. and Van Regenmortel, H.V. (2010) Desk Encyclopedia of Plant and Fungal Virology. Academic Press, New York.
- [31] Sastry, K.S. (2013) Plant Virus and Viroid Diseases in the Tropics, Vol. 2: Epidemiology and Management. Springer, Berlin.
- [32] Mandadi, K.K. and Cholthof, K.B.G. (2013) Plant Immune Responses against Viruses: How Does a Virus Cause Disease? *The Plant Cell*, **25**, 1489-1505. <http://dx.doi.org/10.1105/tpc.113.111658>
- [33] Yamaguchi, Y. and Huffaker, A. (2011) Endogenous Peptide Elicitors in Higher Plants. *Current Opinion in Plant Biology*, **14**, 351-357. <http://dx.doi.org/10.1016/j.pbi.2011.05.001>
- [34] Trejo-Saavedra, D.L., García-Neria, M.A. and Rivera-Bustamante, R.F. (2013) Benzothiadiazole (BTH) Induces Resistance to *Pepper golden mosaic virus* (PepGMV) in Pepper (*Capsicum annuum* L.). *Biological Research*, **46**, 333-340. <http://dx.doi.org/10.4067/S0716-97602013000400004>
- [35] Chen, T.Z., Lv, Y.D., Zhao, T.M., Li, N., Yang, Y.W., Yu, W.G., He, X., Liu, T.L. and Zhang, B.L. (2013) Comparative Transcriptome Profiling of a Resistant vs. Susceptible Tomato (*Solanum lycopersicum*) Cultivar in Response to Infection by Tomato Yellow Leaf Curl Virus. *PLoS ONE*, **8**, e80816. <http://dx.doi.org/10.1371/journal.pone.0080816>
- [36] Mase, K., Ishihama, N., Mori, H., Takahashi, H., Kaminaka, H., Kodama, M. and Yoshioka, H. (2013) Ethylene-Responsive AP2/ERF Transcription Factor MACD1 Participates in Phytotoxin-Triggered Programmed Cell Death. *Molecular Plant-Microbe Interactions*, **26**, 868-879. <http://dx.doi.org/10.1094/MPMI-10-12-0253-R>
- [37] Hanley-Bowdoin, L., Bejarano, E.R., Robertson, D. and Mansoor, S. (2013) Geminiviruses: Masters at Redirecting and Reprogramming Plant Processes. *Nature Reviews Microbiology*, **11**, 777-788. <http://dx.doi.org/10.1038/nrmicro3117>
- [38] Ghanim, M., Brumin, M. and Popovski, S. (2009) A Simple, Rapid and Inexpensive Method for Localization of Tomato Yellow Leaf Curl Virus and Potato Leafroll Virus in Plant and Insect Vectors. *Journal of Virological Methods*, **159**, 311-314.
- [39] Zvereva, A.S. and Pooggin, M.M. (2012) Silencing and Innate Immunity in Plant Defense against Viral and Non-Viral Pathogens. *Viruses*, **4**, 2578-2597. <http://dx.doi.org/10.3390/v4112578>
- [40] Lopez-Ochoa, L., Ramirez-Prado, J. and Hanley-Bowdoin, L. (2006) Peptide Aptamers That Bind to a Geminivirus Replication Protein Interfere with Viral Replication in Plant Cells. *Journal of Virology*, **80**, 5841-5853. <http://dx.doi.org/10.1128/JVI.02698-05>
- [41] Reyes, M.I., Nash, T.E., Dallas, M.M., Ascencio-Ibáñez, J.T. and Hanley-Bowdoin, L. (2013) Peptide Aptamers That Bind to Geminivirus Replication Proteins Confer a Resistance Phenotype to Tomato Yellow Leaf Curl Virus and Tomato Mottle Virus Infection in Tomato. *Journal of Virology*, **87**, 9691-9706. <http://dx.doi.org/10.1128/JVI.01095-13>
- [42] Rudolph, C., Schreier, P.H. and Uhrig, J.F. (2003) Peptide-Mediated Broad-Spectrum Plant Resistance to Tosspoviruses. *Proceedings of the National Academy of Sciences of the United States of America*, **100**, 4429-4434.
- [43] Mascini, M., Palchetti, I. and Tombelli, S. (2012) Nucleic Acid and Peptide Aptamers: Fundamentals and Bioanalytical Aspects. *Angewandte Chemie International Edition*, **51**, 1316-1332. <http://dx.doi.org/10.1002/anie.201006630>
- [44] Campos Olivas, R., Louis, J.M., Clerot, D., Gronenborn, B. and Gronenborn, A.M. (2002) The Structure of a Replication Initiator Unites Diverse Aspects of Nucleic Acid Metabolism. *Proceedings of the National Academy of Sciences of the United States of America*, **99**, 1310-1315.
- [45] Kim, Y.H., Yeo, W.H., Kim, Y.S., Chae, S.Y. and Kim, K.S. (2000) Antiviral Activity of Antibiotic Peptaibols, Chrysopeptides B and D, Produced by *Apiocreas*. 14T against TMV Infection. *Journal of Microbiology and Biotechnology*, **10**, 522-528.
- [46] Han, S.H., Lee, S.J., Moon, J.H., Yang, K.Y., Cho, B.H., Kim, K.Y., Kim, Y.W., Lee, M.C., Anderson, A.J. and Kim, Y.C. (2006) GacS-Dependent Production of 2R, 3R-Butanediol by *Pseudomonas chlororaphis* O6 Is a Major Determinants for Eliciting Systemic Resistance against *Erwinia carotovora* but Not against *Pseudomonas syringae* pv. *tabaci* in Tobacco. *Molecular Plant-Microbe Interactions*, **19**, 924-930. <http://dx.doi.org/10.1094/MPMI-19-0924>
- [47] Kang, B.R., Han, S.H., Zdor, R.E., Anderson, A.J., Spensor, M., Yang, K.Y., Kim, Y.H., Lee, M.C., Cho, B.H. and Kim, Y.C. (2007) Inhibition of Seed Germination and Induction of Systemic Disease Resistance by *Pseudomonas chlororaphis* O6 Require Phenazine Production Regulated by the Global Regulator, GacS. *Journal of Microbiology*

*and Biotechnology*, **17**, 586-593.

- [48] Ryu, C., Kang, B.R., Han, S.H., Cho, S.M., Kloepper, J.W., Anderson, A.J. and Kim, Y.C. (2007) Tobacco Cultivars Vary in Induction of Systemic Resistance against *Cucumber mosaic virus* and Growth Promotion by *Pseudomonas chlororaphis* O6 and Its *gacS* Mutant. *European Journal of Plant Pathology*, **119**, 383-390. <http://dx.doi.org/10.1007/s10658-007-9168-y>
- [49] Howell, C.R. (2003) Mechanisms Employed by *Trichoderma* Species in the Biological Control of Plant Diseases: The History and Evolution of Current Concepts. *Plant Disease*, **87**, 4-10. <http://dx.doi.org/10.1094/PDIS.2003.87.1.4>



Scientific Research Publishing (SCIRP) is one of the largest Open Access journal publishers. It is currently publishing more than 200 open access, online, peer-reviewed journals covering a wide range of academic disciplines. SCIRP serves the worldwide academic communities and contributes to the progress and application of science with its publication.

Other selected journals from SCIRP are listed as below. Submit your manuscript to us via either [submit@scirp.org](mailto:submit@scirp.org) or [Online Submission Portal](#).

